

2009

Drying of potable water treatment plant residuals

Ali Mohammad Gharaibeh
University of Wollongong

Recommended Citation

Gharaibeh, Ali Mohammad, Drying of potable water treatment plant residuals, Doctor of Philosophy thesis, School of Civil, Mining and Environmental Engineering, Faculty of Engineering, University of Wollongong, 2009. <http://ro.uow.edu.au/theses/3199>

Research Online is the open access institutional repository for the University of Wollongong. For further information contact Manager Repository Services: morgan@uow.edu.au.

DRYING OF POTABLE WATER TREATMENT PLANT RESIDUALS

A thesis submitted in fulfilment of the
requirements for the award of the degree

DOCTOR OF PHILOSOPHY

from

UNIVERSITY OF WOLLONGONG

by

Ali Mohammad Gharaibeh (B. Chem. Eng., M. Eng. Mgt.)

SCHOOL OF CIVIL, MINING AND ENVIRONMENTAL ENGINEERING

2009

THESIS CERTIFICATION

I, Ali Gharaibeh, declare that this thesis, submitted in fulfilment of the requirements for the award of Doctor of Philosophy, in the School of Civil, Mining and Environmental Engineering, University of Wollongong, is wholly my own work unless otherwise referenced or acknowledged. The document has not been submitted for qualifications at any other academic institution.

Ali Mohammad Gharaibeh

June 2009

LIST OF PUBLICATIONS

The following publications are related to the research work conducted in this study:

Published Papers:

Gharaibeh, A., Sivakumar, M. & Dharmappa, H. B. (2007), *Mathematical Model to Predict Solids Content of Water Treatment Residuals during Drying*, Journal of Environmental Engineering, American Society of Civil Engineers. Volume 133, No. 2, pp. 165-172.

Gharaibeh, A., Sivakumar, M. and Dharmappa, H. (2003), *Drying of Water Treatment Plant Residuals*, 7th Annual Environmental Research Conference, Proceeding of EERE 2003 Conference, The Cumberland, Marysville, VIC, Australia.

Gharaibeh, A., Sivakumar, M., and Dharmappa, H. B. (2001), *The Effect of Meteorological Conditions on Residuals Drying*, The Proceedings of 19th Federal Convention, AWA, Canberra, ACT, Australia.

Journal Papers under preparation:

Gharaibeh, A. and Sivakumar, M. (2009), Variance-Based Sensitivity Analysis of the Meteorological Conditions and their effect on Residuals Drying, to be submitted for *Journal of Environmental Engineering, American society of Civil Engineers*.

Gharaibeh, A. and Sivakumar, M. (2009), Solar Drying of Water Treatment Residuals, to be submitted for *Applied Energy, ELSEVIER*.

Gharaibeh, A. and Sivakumar, M. (2009), Meteorological Effect on Residuals Drying, to be submitted for *Journal of Environmental Management, ELSEVIER*.

ABSTRACT

The need for potable water treatment has become an increasing necessity in modern society. Worldwide, the most widely used water treatment technology remains a combination of coagulation, flocculation, sedimentation and filtration. As a result, water treatment operations not only produce drinking water, they also produce wet residuals as a by-product. These residuals mainly include suspended solids, any organics found in water, and chemicals used in the treatment process such as coagulants, coagulant aids and filter aid polymers. The main objective regarding residuals management continues to be the reduction of residuals for either reuse or disposal. This reduction can be achieved by optimising the treatment processes, whilst also reusing the residuals for such diverse purposes as composting, manufacturing of bricks, coagulant for sewage treatment plants, enriching agricultural lands and construction filling material. When residuals from water treatment operations are mismanaged, the economic impact is considerable, and more importantly, these residuals present a possible threat to public health and safety.

As a result, there is a great need to accurately estimate and accelerate the drying time of residuals, as larger quantities of these are generated, particularly as the demand for high quality drinking water increases. Constraints, such as wet weather and land availability have prolonged the drying time of residuals, which in turn has intensified the need for accelerated drying. Although substantial information is available on drying equipment and its performance, very little information is available relating to the actual drying of residuals. One element of considerable interest continues to be the influence of meteorological conditions on the drying time and rate of residuals. From a practical standpoint, these conditions must also be taken into account during the design and operation of drying beds. Clearly meteorological conditions have a significant effect on the residuals drying time, however extensive investigation into the available literature when researching this thesis revealed that these variables were not thoroughly represented in previous models. Therefore, there is a considerable need to develop a model that incorporates the effect of meteorological conditions on the residuals drying process.

The drying of predominantly ferric chloride residuals has been investigated through a series of experiments performed in a laboratory drying tunnel, as well as field experiments in experimental sand drying beds. In the field experiments, two experimental drying beds were used in order to compare the drying of residuals between normal and passive solar beds. The meteorological parameters were measured using a weather monitoring station. Data collected from the drying tunnel were used to calibrate and validate the model. A new mathematical model was developed, in order to calculate the solids content for a control volume of a given residuals application thickness and area. The model was formulated using a heat balance approach, which incorporated the meteorological parameters and the residuals application area and thickness. The model includes the heat transfer components by radiation, convection, and evaporation. A non-dimensional convective heat transfer coefficient has been formulated using dimensional analysis in order to calculate the convective heat transfer term. Variance-based sensitivity analysis has been used to determine the input variables variances and their influence on the model output. This will reveal a better understanding for future designs of water treatment residuals dryers. Finally, a solar drying bed has been designed in order to accelerate the drying process of residuals.

The field study revealed no significant advantage with the passive solar drying bed, and was therefore concluded that drying time would not be enhanced in comparison to the conventional sand drying bed. However, when the solar drying bed was provided with a fan heater and a ventilator, the drying time was significantly reduced by up to 33%. The mathematical model predicts drying time with good accuracy ($r^2 > 0.93$ for the drying tunnel experiments and $r^2 > 0.8$ for the field experiments) of up to 50% solids content (wet basis) for a given application thickness and prevailing meteorological conditions. The relative importance of the model parameters using the sensitivity analysis revealed that relative humidity had the highest influence on the dependent variable and the application thickness the lowest. The model and methodology presented in this thesis will enable design engineers to predict the drying time of residuals as well as sizing of the residuals drying beds. Successful prediction of residuals drying time will also help water treatment facilities in their day-to-day operation and maintenance. The newly designed solar drying bed proposed in this thesis will provide several environmental benefits including reduction in drying time, transport cost savings that can be passed on to the end user, and perhaps more importantly in contemporary society, the reduction of greenhouse gas emissions, as a direct result of embracing this free, renewable energy source.

ACKNOWLEDGMENTS

I would like to express my sincere gratitude to my supervisor, Associate Professor Muttucumaru Sivakumar for his continuous encouragement, advice, support, enthusiasm and patience towards my part-time research at the University of Wollongong.

Grateful appreciation is also expressed to my co-supervisor, at an early part of this study, Dr Dharma Hagare for his support and advice. I also wish to thank the department of mechanical engineering for providing the drying tunnel. Mr Ian Laird you have provided excellent technical support and many thanks for the excellent work in fabrication of the modified duct. Mr Norm Gal many thanks to you for providing technical assistance in mounting the weather station and the fabrication of the experimental drying beds.

I would like to extend my thanks and appreciation to the management and staff of my full-time employer Veolia Water for making the experimental work possible. Without providing the space and resources, this work would not have happened. I would like to thank all colleagues at the Illawarra Water Treatment Plant for their moral and technical support and input while conducting the experiments.

Finally yet importantly, many thanks for my wife and children for their patience and support. In addition, I would like to thank all my friends for their encouragement and help when needed.

TABLE OF CONTENTS

THESIS CERTIFICATION	i
LIST OF PUBLICATIONS	ii
ABSTRACT	iii
ACKNOWLEDGMENTS	v
TABLE OF CONTENTS	vi
LIST OF FIGURES.....	ix
LIST OF TABLES.....	xi
LIST OF NOTATIONS.....	xii
1 Introduction	1
1.1 Background.....	1
1.2 Justification of Research.....	5
1.3 Objectives.....	8
1.4 Scope of Work.....	9
1.5 Overview of the thesis	11
2 Review of Drying of Water Treatment Plant Residuals.....	14
2.1 Introduction	14
2.2 Estimation of Residuals Quantities.....	14
2.2.1 Calculations of Generated Residuals	15
2.2.2 Coagulant Mass Balance.....	19
2.2.3 Field Determination	19
2.3 Dewatering Screening Methods.....	20
2.3.1 Specific Resistance Test	20
2.3.2 Capillary Suction Time (CST) Test	23
2.4 General Theory of Drying	24
2.4.1 Drying of Solids.....	24
2.4.1.1 <i>Constant Rate Period</i>	25
2.4.1.2 <i>Falling Rate Period</i>	28
2.4.1.3 <i>First Falling Rate Period</i>	29
2.4.1.4 <i>Second Falling Rate Period</i>	29
2.4.1.5 <i>Behaviour of Various Materials During Drying</i>	30
2.4.1.6 <i>Equilibrium Moisture Content</i>	31
2.4.2 Mechanisms of Solids Drying.....	32
2.4.2.1 <i>Classification of Water Removal</i>	33
2.4.2.2 <i>Movement of Water in Porous Materials</i>	35
2.4.2.3 <i>Effect of Weather Conditions on Drying Periods</i>	36
2.4.3 Drying of Residuals	37
2.4.3.1 <i>Classification of the Types of Water Found in Residuals</i>	39
2.4.3.2 <i>Constant Rate Period</i>	41
2.4.3.3 <i>Critical Moisture Content</i>	42
2.4.3.4 <i>Falling Rate Period</i>	43
2.4.3.5 <i>Movement of Water in Residuals</i>	44
2.5 Drying Beds Operational Performance.....	45
2.5.1 Sand Drying Beds	46
2.5.1.1 <i>Factors Affecting Drying on Sand Beds</i>	47
2.5.1.2 <i>Effects of Chemical Conditioning</i>	48
2.6 Summary.....	49
3 Effect of Meteorological Conditions on Residuals Drying	51
3.1 Introduction	51
3.2 Meteorological Conditions	51
3.2.1 Effect of Temperature.....	52
3.2.2 Effect of Relative Humidity.....	53
3.2.3 Effect of Wind Speed.....	55
3.2.4 Effect of Solar Radiation	56
3.2.5 Effect of Rainfall	57
3.2.6 Weather Parameters' Relative Contribution for the Drying Process	58
3.3 Heat Transfer and Drying of Residuals	58

3.3.1	Radiation Heat Transfer	60
3.3.2	Convection Heat Transfer	62
3.3.2.1	<i>Heat transfer coefficient</i>	62
3.3.3	Evaporation Heat Transfer	63
3.3.4	Conduction Heat Transfer	63
3.4	Estimation of Residuals Drying Time	64
3.4.1	Drying Bed Loading	64
3.4.2	Drying Time	65
3.4.3	Design Parameters of Drying Beds	67
3.5	Solar Drying Technologies	68
3.5.1	Types of Solar Radiation	69
3.5.2	Solar Angles	69
3.5.3	Solar Radiation and Drying	71
3.5.3.1	<i>Passive Solar Systems</i>	71
3.5.3.2	<i>Active Solar Systems</i>	72
3.6	Summary	75
4	Mathematical Model for Residuals Drying	77
4.1	Introduction	77
4.2	Basic Heat Balance	78
4.2.1	Radiative Heat Transfer	80
4.2.2	Convective Heat Transfer	83
4.2.3	Evaporative Heat Transfer	83
4.2.4	Heat Stored	84
4.3	Non-dimensional Heat Transfer Coefficient	84
4.4	Estimation of Constants	86
4.5	Solids Content Calculation	87
4.6	Finite Difference Calculation	87
4.7	Summary	89
5	Materials and Methods	90
5.1	Introduction	90
5.2	Ferric Chloride Residuals	92
5.3	Drying Tunnel	94
5.3.1	Drying Duct	95
5.3.2	Residuals Tray	96
5.3.3	Weight Measurement Balance	97
5.3.4	Temperature Measurements	98
5.4	Moisture Content Measurement	99
5.5	Monitoring of Weather Conditions (Weather Station)	100
5.5.1	Ambient Temperature Measurement	101
5.5.2	Leaf Temperature Measurement	101
5.5.3	Relative Humidity Measurement	101
5.5.4	Solar Radiation Measurement	102
5.5.5	Wind Speed Measurement	102
5.5.6	Rainfall Measurement	103
5.6	Field Experiments	103
5.6.1	Experimental Open Sand Drying Bed	103
5.6.2	Experimental Solar Sand Drying Bed	105
5.6.3	Field Experiments without Drainage	105
5.7	Sample Collection and Analysis	107
5.7.1	Moisture Content Analysis	107
5.7.2	Moisture Content Calculation	108
5.8	Summary	109
6	Field Drying Experiments	111
6.1	Introduction	111
6.2	Open (Normal) Bed Field Experiments	111
6.2.1	Single Application Experiments	112
6.2.2	Multiple Application Experiments	113
6.3	Solar Bed Experiments	116
6.3.1	Solar Bed Single Application Experiments	117

6.3.2	Solar Bed Multiple Application Experiments	119
6.4	Comparison of Open and Solar beds Results	121
6.4.1	Single Application Experiments Results	121
6.4.2	Multiple Application Experiments Results	130
6.5	Field Experiments without Drainage and Rain	134
6.6	Summary	135
7	Calibration and Verification of the Mathematical Model	137
7.1	Introduction	137
7.2	Non-dimensional Heat Transfer Coefficient	137
7.3	Discussion of Results	140
7.3.1	Drying Tunnel Experiments	140
7.3.2	Field Experiments	150
7.3.2.1	<i>Single Application Field Experiments</i>	150
7.3.2.2	<i>Multiple Application Field Experiments</i>	151
7.3.2.3	<i>Field Experiments without Drainage and Rain</i>	154
7.4	Summary	155
8	Sensitivity Analysis	156
8.1	Introduction	156
8.2	Selection of Parameters	158
8.2.1	Relative Humidity	159
8.2.2	Wind Speed	160
8.2.3	Ambient Temperature	160
8.2.4	Solar Radiation	161
8.2.5	Application Thickness	162
8.3	The Effect of Model Parameters	162
8.3.1	Effect of Relative Humidity	163
8.3.2	Effect of Wind Speed	164
8.3.3	Effect of Ambient Temperature	165
8.3.4	Effect of Solar Radiation	165
8.3.5	Effect of Application Thickness	166
8.4	Sensitive Parameters	166
8.5	Discussion of Results	168
8.6	Summary	173
9	Solar Drying of Residuals	175
9.1	Introduction	175
9.2	Solar Drying Technologies of Residuals	176
9.3	Theoretical Analysis	177
9.3.1	Orientation of Solar Collector	178
9.3.2	Theoretical Considerations	181
9.4	Solar Dryer Design	189
9.5	Summary	197
10	Conclusions and Recommendations	198
10.1	Introduction	198
10.2	Conclusions	199
10.2.1	Mathematical Modelling of Water Treatment Residuals	199
10.2.2	Results	200
10.2.2.1	<i>Laboratory Drying Tunnel Experiments</i>	200
10.2.2.2	<i>Field Experimental Drying Beds</i>	201
10.2.2.3	<i>Sensitivity Analysis</i>	202
10.2.2.4	<i>New Active Solar Drying Bed Design</i>	202
10.2.3	Benefits	203
10.3	Recommendations for future work	205
	References	207
	Appendices	219
	Appendix A: Drying Tunnel Experiments	220
	Appendix B: Open and Solar Drying Beds Experiments	248
	Appendix C: Field Experiments (Under Perspex Cover) and without Drainage	257

LIST OF FIGURES

Figure 1.1 Schematic diagram showing a detailed presentation of the research undertaken.	13
Figure 2.1 A process diagram of the Illawarra Water Treatment Plant.....	18
Figure 2.2 Illawarra Water Treatment Plant.....	18
Figure 2.3 Buchner funnel apparatus for determining the specific resistance to filtration, (Vesilind et al. 1986)	22
Figure 2.4 Capillary suction time apparatus, (Vesilind et al. 1986).....	23
Figure 2.5 Typical drying curve of wet solids	26
Figure 2.6 Schematic of the proportions of water in residuals (a) Internal water, (b) Adsorption and adhesion water, (c) Interstitial capillary water, (d) Capillary-held water, and (e) Solid particles, (Moller, 1983)	41
Figure 2.7 Water removal from residuals by draining and drying, Moller (1983).....	42
Figure 2.8 Dry residuals removed from a sand drying bed	46
Figure 2.9 Cross sectional area of a sand drying bed.....	47
Figure 3.1 Solar altitude angle ALT and solar azimuth angle AZM, (Kreider et al. 1989)	70
Figure 4.1 Schematic diagram showing a detailed presentation of the model	78
Figure 4.2 Heat balance of a control volume of residuals.....	79
Figure 5.1 A map showing raw water supply from Avon Lake to the Illawarra region (Illawarra water quality report, 1992).....	91
Figure 5.2 Air conditioning laboratory unit	95
Figure 5.3 Schematic of the drying tunnel unit.....	96
Figure 5.4 Drying tunnel experimental set-up	97
Figure 5.5 Sartorius MA 30 Moisture analyser.....	100
Figure 5.6 Schematic diagram of the weather monitoring station.....	101
Figure 5.7 The weather station adjacent to the drying beds.....	102
Figure 5.8 Experimental open sand drying bed	104
Figure 5.9 Experimental solar sand drying bed.....	106
Figure 5.10 MS Excel spreadsheet showing sample calculation of moisture and solids content.....	108
Figure 6.1 Typical curve showing drying time, drainage water, and rainfall	113
Figure 6.2 Residuals cracked at 10% solids content	113
Figure 6.3 The solar bed showing the holes in all sides and the ventilator.....	118
Figure 6.4 The effect of heated air on the temperatures of solar bed cavity and residuals compared to the open bed residuals temperature (Experiment 14).....	119
Figure 6.5 Drying of residuals (Experiment 4)	123
Figure 6.6 Drying of residuals (Experiment 5)	123
Figure 6.7 Drying of residuals (Experiment 6)	124
Figure 6.8 Drying of residuals (Experiment 7)	124
Figure 6.9 Drying of residuals (Experiment 8)	125
Figure 6.10 Drying of residuals (Experiment 9)	126
Figure 6.11 Drying of residuals (Experiment 11)	126
Figure 6.12 Drying of residuals (Experiment 12)	127
Figure 6.13 Drying of residuals (Experiment 13)	127
Figure 6.14 Drying of residuals (Experiment 14)	128
Figure 6.15 Drying of residuals (Experiment 15)	129
Figure 6.16 Drying of residuals (Experiment 16)	129
Figure 6.17 Drying of residuals (Experiment 10)	131
Figure 6.18 Drying of residuals (Experiment 17)	132
Figure 6.19 Drying of residuals (Experiment 18)	132
Figure 6.20 Drying of residuals (Experiment 19)	133
Figure 6.21 Drying of residuals (Experiment 20)	133
Figure 6.22 The setup of the field experiments performed without drainage and rain	135
Figure 7.1 Residuals at four different solids content	144
Figure 7.2 Laboratory drying tunnel experiments (14, 16, 22, 28, 30, 31, 32, 37).....	145
Figure 7.3 Laboratory drying tunnel experiments (39-44).....	146
Figure 7.4 Laboratory drying tunnel experiments (45-50).....	147
Figure 7.5 Laboratory drying tunnel experiments (51-56).....	148
Figure 7.6 Laboratory drying tunnel experiments (57-63).....	149
Figure 7.7 Single application thickness field experiments.....	152

Figure 7.8 Residuals pumped out into the sand drying bed.....	152
Figure 7.9 Multiple application field experiments.....	153
Figure 7.10 Single application field experiments (without drainage and rain).....	154
Figure 8.1 A schematic overview of the procedure for sensitivity analysis	159
Figure 8.2 The effect of relative humidity on drying rate	164
Figure 8.3 Frequency chart for the sensitivity analysis trials	167
Figure 8.4 Input variables measured by rank correlation	171
Figure 8.5 Input variables and their percentage contribution to the target forecast	171
Figure 8.6 Spider plot for the multiple input parameters for the output variable	172
Figure 9.1 Tilted surface facing solar radiation and the corresponding design angles.....	180
Figure 9.2 Monthly average incident solar radiation for Wollongong	180
Figure 9.3 Optimum tilt angles for latitudes (-34.58°) and (34.58°).....	181
Figure 9.4 The optimum solar collector tilt angle for Wollongong area	182
Figure 9.5 A diagram showing the flat plate solar collector and the drying chamber.....	184
Figure 9.6 Heat balances for the residuals surface, airflow and transparent cover	189
Figure 9.7 Drying predictions for different relative humidity values 50%-80% (at 3 m/s and 55°C) ...	194
Figure 9.8 The drying prediction for different air temperature values 40°C - 55°C (at 3 m/s and 80%)	196
Figure 9.9 The drying prediction for different wind speed values 2-5 m/s (at 80% and 55°C).....	196
Figure 9.10 Drying predictions of experiment 20F2 using equations (4.21 and 9.39).....	197

LIST OF TABLES

Table 2.1 Typical comparison of water residuals, soils, and sewage residuals (Elliott et al. 1990)	16
Table 2.2 Typical values for the empirical constants of some materials (Henderson and Perry, 1955) ..	32
Table 4.1 Moisture content calculation	88
Table 5.1 Typical analysis of Avon raw water	92
Table 5.2 Composition of residuals used in this study compared to typical composition of residuals	94
Table 6.1 Single application experiments	114
Table 6.2 Open bed multiple application experiments	115
Table 6.3 Open bed multiple application experiments and their applications initial solids content	115
Table 6.4 Solar bed single application experiments	116
Table 6.5 Solar bed single application experimental conditions	117
Table 6.6 Solar bed multiple application experiments and their applications initial solids content	120
Table 6.7 Weather conditions of the solar bed multiple application experiments	120
Table 6.8 Solar bed multiple application experimental conditions	121
Table 6.9 Comparison of solar and open beds drying rates for single application experiments	122
Table 6.10 Comparison of solar and open beds drying rates for multiple applications experiments	130
Table 6.11 Field experiments without drainage	134
Table 7.1 Model parameters	139
Table 7.2 Regression analysis table	140
Table 7.3 Summary of the laboratory drying tunnel experiments (8-38)	142
Table 7.4 Summary of the laboratory drying tunnel experiments (39-63)	143
Table 8.1 Model variables showing their probability distribution functions	157
Table 8.2 Model parameters showing their lower and upper ranges	160
Table 8.3 Base values of various parameters used in sensitivity analysis and parameter identification	163
Table 8.4 Summary of the statistics report	168
Table 8.5 Percentiles for the evaporated water	169
Table 9.1 Design parameters for the solar dryer and input values used for modelling	193
Table 9.2 Parameters and average daily values used for drying time prediction of experiment 20F2...	195

LIST OF NOTATIONS

A	Area (m^2) or correlation constant (equation 2.13)
AC	Raw water apparent colour (CU)
A_{absorber}	The length of the absorber (m)
$A_{\text{collector}}$	The area of the solar collector (m^2)
A_{tray}	The length of the tray (m)
Al	Alum dose rate as 17.1% Al_2O_3 (mg/L)
B	Correlation constant (equation 2.13)
c	Specific heat of residuals (J/kg.K) (equation 4.19)
c, n	Empirical constants for a particular material (equation 2.12)
c	Weight of solids per unit volume of filtrate (equation 2.5) (kg/m^3)
c_{air}	Specific heat of air (J/kg.K)
c_{light}	The speed of light in vacuum (2.998×10^8 m/s)
c_{solids}	Specific heat of solids (J/kg.K)
$c_{\text{water}(i)}$	Specific heat of water at the initial moisture content (J/kg.K)
C_{factor}	Conversion factor (10.4) (assuming specific gravity of residuals 1.04)
c_1	Coefficient value (0.03 to 0.05)
c_2	Coefficient value (0.1 to 0.4)
CA	Chemicals added (mg/L)
D	Diffusivity of moisture through the solids (m^2/s), duct diameter (m)
D_0	Initial depth of applied residuals layer (cm)
D_t	The height of the gap of the drying chamber (m)
DAY	The number of days of the calculated from January 1
DEC	Solar declination angle (degrees)
dT / dt	Temperature gradient through the material thickness (K/m)
E	Thermal energy (J)
E	Rate of evaporation (equation 3.21) (mm/month)
E_{pan}	Average pan evaporation during time t_d (cm/month)
$E_{\text{pan}, L_{OS}}$	Average pan evaporation during the period L_{OS} (cm/month)
f	The frequency of radiation (s^{-1}), correction factor, friction factor
Fe	Ferric Chloride dose rate (mg/L)
F_{Removal}	The collector heat removal factor (dimensionless)
g	Gravitational acceleration ($9.8 \text{ m}/\text{s}^2$)
G_{add}	The added heat flux (W/m^2)
$G_{\text{convection}}$	The convection heat flux (W/m^2)
G_{diffuse}	Diffuse solar radiation (W/m^2)
G_{direct}	Direct incident solar radiation (W/m^2)
$G_{\text{evaporation}}$	The evaporation heat flux (W/m^2)
G_{incident}	Incident solar radiation (W/m^2)
Gr	Grashof number = $\beta g L^3 \Delta T / \nu^2$

G_{sky}	Sky incident solar radiation (W/m^2)
G_{solar}	Incident solar radiation (W/m^2)
h	Heat transfer coefficient ($W/m^2.K$)
h_1	Overall heat transfer coefficient from flowing air to ambient ($W/m^2.K$)
h_{fg}	Latent heat of vaporisation (J/kg)
h_m	Mass transfer coefficient (m/s)
h_{Sa}	Surface to air convective heat transfer coefficient ($W/m^2.K$)
$HOUR$	Hour angle, number of hours between solar noon and the time of interest multiplied by $15^\circ/hr$ (noon = 0°)
h_{Planck}	Planck's constant ($6.625 \times 10^{-34} J.s$)
$I_{constant}$	Constant drying rate ($kg/m^2.hr$)
k	The thermal conductivity ($W/m.K$)
k_e	Reduction factor for residuals evaporation versus a free water surface, decimal (0.6 a pilot study is recommended to determine this value)
L	The characteristic length (m) or lime dose rate (equation 2.1) (mg/L)
LAT	Latitude of particular site of interest (degrees)
L_{OS}	Length of operating season (months)
m_{dryair}	Mass of dry air (kg)
m_f	The mass flow rate of air through the collector (kg/s)
$m_{residuals}$	Mass of residuals (kg)
m_{solids}	Mass of solids (kg)
m_{water}	Weight of moisture evaporated (kg)
n	Mass flux of the liquid from the surface ($kg/m^2.s$) (equation 3.2)
N	Air molecular weight ($29 kg/kg-mole$) or number of residuals applications (equation 3.24)
Nu	Dimensionless Nusselt number = hL/k
P	Cationic polymer dose rate (mg/L) or the atmospheric pressure (Pa)
Δp	The total pressure difference (pressure drop) (Pa)
p	Actual vapour pressure (kPa)
p_∞	Water vapour partial pressure at ambient temperature (Pa , millibars)
p_{db}	Water vapour partial pressures at dry bulb temperature (kPa)
p_{wb}	Water vapour partial pressures at wet bulb temperature (kPa)
$p_{saturated}$	Saturated water vapour partial pressure at ambient temperature (Pa)
q_{net}	The net heat flux (W/m^2)
Q	Plant flow in ML/day
$Q_{flowrate}$	Volumetric flow rate (m^3/s)
$Q_{conduction}$	Rate of heat transfer by conduction (W)
$Q_{convection}$	Rate of thermal energy by convection (W)
$Q_{evaporation}$	Rate of heat by evaporation of water (W)
Q_{gained}	The rate of heat gained (W)
$Q_{generated}$	Rate of thermal energy generated within the control volume (W)

Q_{in}	Rate of thermal energy input (W)
$Q_{incident}$	The rate of heat incident (W)
Q_{out}	Rate of thermal energy output (W)
Q_{lost}	The rate of heat lost (W)
$Q_{radiation}$	Rate of thermal energy by radiation (W)
Q_{stored}	Rate of thermal energy stored in the control volume (W)
r	Specific resistance (s^2/kg)
r'	Constant of the specific resistance of a non-compressible cake
R	Universal gas constant ($8314 \text{ kg.m}^2/s^2.\text{kg-mole.K}$)
R_1, R_2	Constants
Re	Reynolds number = uL/ν
RH	Relative humidity (decimal)
R_m	Initial resistance of filter media (usually negligible) (s^2/kg)
s	Thickness (m, mm) or coefficient of compressibility (equation 2.11)
s_0	Initial residuals depth applied on the drying bed (cm)
S	Residuals produced (mg/L)
SC	Wet basis solids content (%)
SC_0	Initial dry solids concentration (%)
SC_f	Final dry solids concentration (%)
S_{const}	The solar radiation constant (1353 W/m^2)
S_{gross}	Gross bed loading of solids ($\text{kg/m}^2.\text{day}$)
$S_{loading}$	Solids loading during the period L_{os} (kg/m^2)
S_{net}	Net bed loading of solids ($\text{kg/m}^2.\text{day}$)
SS	Raw water suspended solids (mg/L)
t	Time (seconds)
T	The temperature of air (K) (equation 9.18)
ΔT	Temperature difference between the air and the residuals surface (K)
T_∞	Temperature of the air (K, $^\circ\text{C}$)
$T_{air,0}$	The initial air temperature entering the chamber at $x = 0$ (K)
$T_{air,average}$	The average value of the air (K)
$T_{air,in}$	Temperature of air inlet (K)
$T_{air,out}$	Temperature of air outlet (K)
$T_{ambient}$	The ambient air temperature (K)
$T_{collector}$	The average temperature of the collector (K)
$T_{DryingChamber,in}$	Temperature of drying chamber inlet (K)
t_d	De-watering time for a single application (months)
$TILT$	The tilt angle (degrees)
T_{sky}	Sky temperature (K)
$T_{surface}$	Surface temperature (K)
T_{wet}, T_{dry}	Wet and dry bulb temperatures ($^\circ\text{C}$)
u	Wind speed (m/s)

U_{lost}	The overall heat lost coefficient (W/m ² .K)
u_{ref}	Wind speed and wind speed at reference level (m/s)
V	Volume (m ³)
W	The total power output (W)
$W_{Drainage}$	Fraction of water removed by drainage (decimal)
W_t	The breadth of the drying chamber (m)
x	Distance in direction of diffusion (m)
x_1, x_2	The axial positions (m)
X	Moisture content, dry basis (kg _{water} /kg _{dry solids})
X_0	Moisture content at time zero (kg _{water} / kg _{dry solids})
$X_{average}$	Average total moisture content at time t (dry basis)
$X_{Free(i)}$	Initial free moisture content (dry basis)
X_e	Equilibrium moisture content (dry basis)
$X_{initial}$	Initial moisture content as dry basis (%kg _{water} / kg _{dry solids})
X_n	Moisture content at time n (kg _{water} / kg _{dry solids})
X_t	Moisture content at time t as dry basis (%)
dX / dt	Change of moisture content with respect to time (s ⁻¹)
Y	The fractional year in radians
$Z_{1,2,3,...,n}$	Change of moisture content (dX / dt) at times 1,2,3,..., n (s ⁻¹)
z, z_{ref}	Heights above the ground surface and at reference height (m)

Greek Letters

α	Absorption coefficient of the absorber plate (equation 9.2)
α_s, α_l	Short and long wave solar radiation absorptivities
β	Coefficient of volume expansion = $1 / ((T_\infty + T_{surface}) / 2)$ (K ⁻¹)
γ, a, b, c, d	Empirical constants (equation 4.24)
δ	The boundary layer thickness (m)
$\eta_{collector}$	The efficiency of a solar collector
η_{pump}	The efficiency of the pump (dimensionless)
θ	Angle of incidence (equation 8.1)
ε	Emissivity of the surface
$\varepsilon_{atmospheric}$	Atmospheric emissivity under clear sky
λ_{wave}	The electromagnetic wavelength ($\mu\text{m} = 10^{-6} \text{ m}$)
μ	Filtrate dynamic viscosity (kg/s.m)
ν	Kinematic viscosity of air (m ² /s)
$\rho_{Density}$	The air density (kg/m ³)
τ	Transmission coefficient of glazing
σ	Stefan-Blotzmann constant ($5.6697 \times 10^{-8} \text{ W/m}^2\text{K}^4$)

1 Introduction

1.1 Background

World population has increased dramatically in the second half of the twentieth century. As a result, the demand for clean drinking water has increased and the need for effective water treatment has become an important issue. Fresh water is a very critical resource, not only for households but also for successful development of industry and agriculture. Around 75% of our planet's surface is covered with water; only 2.5 % is fresh and nearly 70% of this water forms the ice caps of the north and south poles and Greenland. Fresh water occurs naturally through evaporation from the oceans, at a rate of more than half a million cubic kilometres a year, nearly 90% of which, falls back into the oceans as rain (UNESCO, 2003). It is interesting to note, that an estimated 20% of the world population (more than 1.2 billion people) have no access to a continuous source of improved drinking water. The World Health Organisation (WHO, 2005) and UNICEF (2005) believe that an additional 1.8 billion people will require access to some form of improved water supply by 2015. Therefore, innovative processes for the treatment of drinking water need to be developed in a sustainable manner, to ensure future generations have access to safe drinking water and cleaner environment.

Australia, whilst being the driest inhabited continent in the world, uses 67% of its water resources for irrigation. Only 12% of the annual rainfall over Australia results in runoff into streams and rivers or soaks into and is retained in the ground, the rest is returned to the atmosphere by evaporation or through transpiration from vegetation (A consumer's guide to drinking water, 2006). Climate change and the rise of temperature will have dramatic effect on the global water resources and more specifically on Australia. According to CSIRO's latest climate change estimates, Australia will become

hotter and drier in coming decades (Water in the Future, 2006), which could cause longer and more frequent droughts.

Water is naturally pure; however it is exposed to various types of pollutants and sediments in its natural storage and therefore requires treatment. Natural contaminants present in water are organic matter washed from soil and vegetation, bacteria, viruses, plankton, and suspended matter. Urban water supply has to be treated to make it safe to drink and to improve its colour, taste, and odour. Traditionally, sedimentation is a treatment process where large particles separate from the water. Another water treatment method is slow sand filtration, a process that is very effective in removing small particles but requires large areas of land. However, a process of rapid sand filtration uses coagulants such as aluminium sulphate or ferric chloride to form larger particles (flocs), thereby requiring less land. The widely used high rate, direct filtration process involves raw water, with low suspended solids. New filtration technologies for the treatment of water have been adopted with the development of plastic materials. Micro, ultra, and nano filtration as well as reverse osmosis, are the latest membrane technologies used for the removal of particles and microorganisms as small as 0.0001 micron (A consumer's guide to drinking water, 2006).

Environmental problems involving air, noise and water pollution have increased the pressure to utilise a cleaner and cheaper energy source. The environmental impact of renewable energy sources, are much lower than conventional sources, however the current costs of using renewable sources are, in many cases higher than conventional ones (Dicorato et al. 2008). Rising energy prices since the beginning of the 21st century have been attributed to the increased demand on energy resources and the fragility of the world's energy supply; particularly oil (Survey of Energy Resources, 2004). Current world energy sources are largely dependent on fossil fuels, 77.6% of sources are fossil

fuels (oil, natural gas and coal), 8.9% nuclear and hydro, 11.3% biomass and only 2.2% new renewables (Boyle et al. 2003). The annual solar energy striking the surface of the earth is 2,895,000 Exa Joules compared to 325,300 Exa Joules of the total non-renewable energy sources available on earth (Survey of Energy Resources, 2004). Therefore, the free solar energy is almost 90% more available than any other energy source on the surface of earth.

Solar energy is a constant, free, and clean energy, which mankind has used for centuries, for example in the drying of food. In modern society however, solar energy remains under utilised in favour of cheaper fossil fuels, despite the negative environmental impact. Solar energy technologies including, photovoltaic, solar thermal-electric and solar heating and cooling systems are expensive, but have nominal impact on the environment. The first large scale thermal application of solar energy is the supply of hot water, followed by heating and cooling of commercial and residential buildings (Kreider et al. 1989). Renewable energy sources, such as solar energy, indirect solar energy (wind, wave power and biomass), non-solar renewables (tidal, geothermal, biomass and hydro energy) appear to be the most environmentally sustainable solution to the vastly growing demand for energy. In the past few decades, researchers have utilised active solar energy systems in the drying of sewage treatment plant residuals (El-Ariny and Miller, 1984), (Marklund, 1990), (Hossam et al. 1990), (Luboschik, 1999), (Shannon et al. 2004), (Seginer and Bux, 2006), (Seginer et al. 2007), and (Salihoglu et al. 2007).

As well as its high-energy requirements, water treatment also leads to waste disposal problems, which in turn have their own associated environmental issues. The residuals produced in the treatment of drinking water are generated in the settling stage, where applicable, or in the washing of the filters. Residuals are composed of the

contaminants present in the water, along with additional chemicals added in the treatment processes, and the metallic hydroxides from coagulants. Increased demands on clean and safe drinking water have increased the amount of residuals. Therefore, another problem has surfaced; that being the disposal or the re-use of these residuals. A primary environmental aspect refers to the disposal of residuals into waterways, which may impact the environment by increasing suspended sediments. Additional aspects include metals and chemical residuals that are attached to the solids. Residuals in a landfill or applied to land, have minimal environmental impact. However, excessive land application can lead to residual runoff into waterways during rain events, which may result in increased sedimentation in water bodies. Residuals that are disposed of in sewage treatment plants may increase the solids in the system excessively.

Economically, the quantity of residuals should be reduced before final disposal or reuse in order to minimise labour and transport costs. Sand drying beds are commonly used in water treatment operations, providing land is available, allowing residuals to dry naturally by solar energy. The use of sand drying beds may be limited by high capital cost, as well as land availability. Removal of dry residuals is normally accomplished by a front-end loader, which inevitably removes a substantial layer of the sand bed. While drying bed performance is highly dependent on climatic conditions, improvement can be made by the following factors:

- *The nature of the residuals.* For example, conditioning the residuals with polyelectrolyte can enhance its drainage ability.
- *Initial solids content of residuals.* The higher the solids content of the residuals the faster it dries.
- *The depth of residuals application.* Small depths dry faster.

- *The condition of the drainage medium.* The sand condition and grading can improve the effectiveness of the drainage system.
- *Weather conditions.* Rainfall has great effect on the drying of residuals. Cloudy or humid days can increase the drying period while high wind speed and prolonged sunshine hours improve the drying process.

Unexpected wet days contribute to further delays in the disposal process of residuals. The drying time of water treatment plant residuals, on drying beds, ranges from several days to several months and depends upon weather conditions as well as other handling problems. On the other hand, ferric chloride residuals do not dewater easily, and extensive delays of disposal or reuse will occur. Hence, a better and thorough understanding of the drying process of ferric chloride residuals under natural and controlled drying conditions may lead to a long-term solution to this problem.

1.2 Justification of Research

The treatment of drinking water is extremely important in daily life. Increased demand on clean drinking water has produced large quantities of residuals, which require fast and effective drying techniques before reuse or final disposal. These residuals mainly include suspended solids, any organics found in water and chemicals used in the treatment process such as coagulants, coagulant aids, and filter aid polymers. Residuals are conventionally dried in lagoons and sand drying beds that are open to the atmosphere (A consumer's guide to drinking water, 2006). Residuals can be removed when dried, or stored for a prolonged period in these lagoons.

Conventional or traditional water treatment processes have been widely used in Australia in addition to new and innovative technologies. In New South Wales, sand drying beds are the most widely used form of residuals dewatering in water treatment

plants (Anen and Dharmappa, 1997). However, the use of lagoons and sand drying beds are limited by the availability of land and the associated costs. Weather is also a major factor in the drying of residuals, which, depending upon the conditions, may take from days to a few months. The dried residuals are easy to handle if the solids content is approximately 30-50% (wet basis).

The quantity of residuals produced in any water treatment plant is a function of raw water turbidity and the quality of the treatment process. The chemicals added in the treatment process of the ferric chloride coagulation include the iron salts, polyelectrolytes, lime, fluoride, and chlorine. The volume of residuals is reduced by the following means:

- Thickening - this produces residuals with high water content (up to 98% water).
- Dewatering - this is natural drainage by gravity and drying or separation by mechanical means (98% - 95% water).
- Thermal drying - by either natural drying or other thermal processes such as thermal dryers (below 95% water).

Drying is one of the largest energy consuming unit operation. It is estimated that 10-15% of the total energy required for industry, is consumed in drying operations (Kerkhof and Coumans, 2002). The use of sand drying beds does not require high-energy demand dewatering equipment. However, in communities where land availability is scarce, mechanical dewatering techniques are a preferred option. Management and disposal of water treatment plant residuals have become more expensive because of numerous federal and state guidelines and regulations (Aldeeb et al. 2003). In Australia, specifically in New South Wales, water treatment plants rely mainly on drying lagoons and drying beds for dewatering of residuals (Anen and Dharmappa, 1997).

Drying of water treatment plant residuals is a process involving the simultaneous transfer of heat and mass. Drying of wet solids has been studied extensively and the phases of drying were identified as constant and falling rate periods. Fresh residuals applied on sand drying beds normally have a concentration of 1% to 4% solids content (wet basis). Most of the free water in the residuals can be drained easily (Tsang and Vesilind 1990), and a portion evaporates into the atmosphere. The two distinct drying periods were clearly identified in a previous study (Gharaibeh et al. 2001), the first period is below 15% solids content and the second period is above 15%.

Although there were some attempts to model drying of sewage residuals (Vaxelaire and Puiggali, 2002) (Reyes et al. 2004) (Leonard et al. 2005), limited research has been previously published involving the use of models of drying water treatment plant residuals. The sewage treatment residuals drying models were focussed on industrial dryers. Two previous attempts to develop mathematical models for the alum water treatment residuals on sand drying beds were based on the preliminary work of researchers such as Quon and Tamblyn (1965) and Nebiker (1967). Firstly, Clark (1970) developed mathematical equations allowing the design engineer to predict the area of drying bed. An equation was developed to predict the drainage time on sand beds. Another equation predicted the evaporation component using the knowledge of the critical moisture content. The critical moisture content is dependent on the nature of the material under investigation and not on the weather conditions. Secondly, Lo (1971), studied the effect of rain on the rate of drainage of water treatment residuals on the sand drying beds; the constant rate period was approximated by the drying rate of a free water surface. For the falling rate period, the drying equations developed by Nebiker (1967) and Clark (1970) were used by Lo (1971). The drying rate of the falling rate period depends upon the equilibrium moisture content. However, this equilibrium

moisture content of a material varies as it dries (Henderson 1952), making it difficult to predict. The critical moisture content, which is the main feature of the above-mentioned models, varies with the thickness of the material and with the rate of drying as reported by McCabe and Smith (2000). In practice, residuals are removed (around 30-50% solids content) from the drying beds before reaching the equilibrium moisture content.

Rolan (1980) developed a series of empirical equations in order to determine the design criteria for sand drying beds as well as the determination of their optimum operation. Cornwell and Vandermeiden (1999) developed three empirical models, which allow the sizing of water treatment sand drying beds. Meteorological conditions have great effect on the residuals drying time. The above-mentioned models however, did not consider the meteorological conditions in their predictions of the residuals drying time. Therefore, there is a need to develop a model that combines an understanding of the residuals drying process, together with the prediction of meteorological conditions. This will enable the design of a drying system that reduces the total drying time.

1.3 Objectives

The aim of this project was to investigate the drying process of ferric chloride water treatment plant residuals and determine the effect of weather conditions. The objective of residuals management is to minimise the drying time and handling of residuals with minimal cost and land usage. The ultimate objective was to design a solar based drying system for water treatment plant residuals. The targeted objectives in this research are:

- To critically review existing literature regarding the drying process of water treatment plant residuals and the effect of meteorological conditions on the drying of residuals.

- To design, construct and conduct experiments in a laboratory drying tunnel as well as in sand drying beds for varying weather conditions.
- To develop a new mathematical model using a heat balance approach for the drying process of water treatment plant residuals.
- To calibrate the mathematical model using the experimental data and to determine model parameters and coefficients.
- To carry out sensitivity analysis under different weather conditions such as ambient temperature, relative humidity, wind speed, solar radiation, and application thickness.
- To design a solar drying system for the drying of water treatment plant residuals using theoretical and experimental data.

1.4 Scope of Work

To achieve the objectives of this thesis, it is important to have a planned scope of work. The following research programs have been followed:

- The literature has been critically reviewed regarding the drying of solids as well the drying of residuals. The effect of the meteorological conditions on the drying of residuals has been reviewed as well as the effect of heat transfer. The solar drying technologies (passive and active) in the field of residuals drying have been reviewed. The literature reviewed includes physical and chemical properties used to characterise water and wastewater residuals, drying and management of residuals, drying of solids, heat and mass transfer and their effect on the drying process and solar drying technologies. Various electronic databases have been used in the literature review process, such as Science

Direct, ADT, UOW Digital Theses, Australian Universities Catalogues, InformaWorld.

- New experimental equipment has been designed to study the drying of water treatment plant residuals in the lab. In addition to this, equipment for field experiments of normal and solar sand drying beds has also been developed. The design included the set-up of the field experimental drying beds and a weather monitoring station. The meteorological parameters were measured including, wind speed, air temperature, relative humidity, and solar radiation using the weather monitoring station.
- Indoor drying experiments were performed in the drying tunnel unit in order to control the wind speed. Despite this, relative humidity, and air temperature varied, as they could not be controlled. A rectangular-shaped test section was fabricated from Perspex and assembled at the exit of the drying tunnel in the direction of the wind flow. Meteorological conditions and weight of residuals were logged continuously in a data logger and the treatment plant Supervisory Control and Data Acquisition System (SCADA).
- A mathematical model for the drying of water treatment plant residuals was developed. Steady-state heat balance equation was applied for a control volume of residuals that takes into account the heat transfer by radiation, convection, and evaporation. A heat transfer coefficient correlation was developed using dimensional analysis. An empirical relationship using the Buckingham Pi theorem was used to predict the heat transfer coefficient. Meteorological parameters, such as wind speed, ambient temperature, relative humidity, and residuals surface temperature were taken into consideration in the model. The

model predicted the drying time of water treatment plant residuals based on the knowledge of weather parameters.

- The model was calibrated using the experimental data. The model coefficients values were assumed, as well as the use of design parameters, which include solids/water content and drying period.
- Sensitivity analysis was carried out under different weather conditions. The model was evaluated by generating input parameters such as wind speed, relative humidity, ambient temperature, and application thickness with ranges of variation to each input parameter. Assessment of the influences and the relative importance of each independent variable on the dependent variable (i.e. solids content) have been evaluated.
- A solar dryer has been designed in order to accelerate the residuals drying process. The optimum design was achieved by optimising the tilt angle and the collector size for the weather conditions of Wollongong, Australia.

1.5 Overview of the thesis

The work presented in this thesis is divided into the following:

Chapter 1 provides a background to the problem, justification of the research, the research objectives, the scope of work and an overview of the whole thesis.

In chapters 2 and 3, the general description of residuals and the estimation of their quantities are introduced. The theory of drying and the description of meteorological conditions have been reviewed. Attempts of relevant residuals drying research have also been reviewed.

In chapter 4, detailed mathematical and numerical modelling are presented beginning with basic heat balance. Formulations of radiative, convective, and

evaporative heat transfer equations, as well as complete model formulation have been detailed.

Chapter 5 shows detailed set-up of the experimental sand drying bed, the measurements, and the data logging of the weather station. The methods of analysis and measurements are detailed.

Experimental data gathered from the weather station, as well as solids contents measurements are presented in chapter 6. A detailed discussion of all experiments of both open and solar drying beds results is presented.

The calibration of the mathematical model is presented in chapter 7. Data from field experiments with and without drainage are used to calibrate the model.

A sensitivity analysis study under different weather conditions is presented in chapter 8.

In chapter 9, a solar dryer design is presented for the optimum tilt angle and collector size for the local weather conditions of Wollongong, Australia.

Finally, chapter 10 concludes the results and findings of the study presented in this thesis. Recommendations for future work are given at the end of this chapter.

Figure 1.1 shows a detailed overview of presentation of the research that has been undertaken, highlighting both the methodology and the published papers.

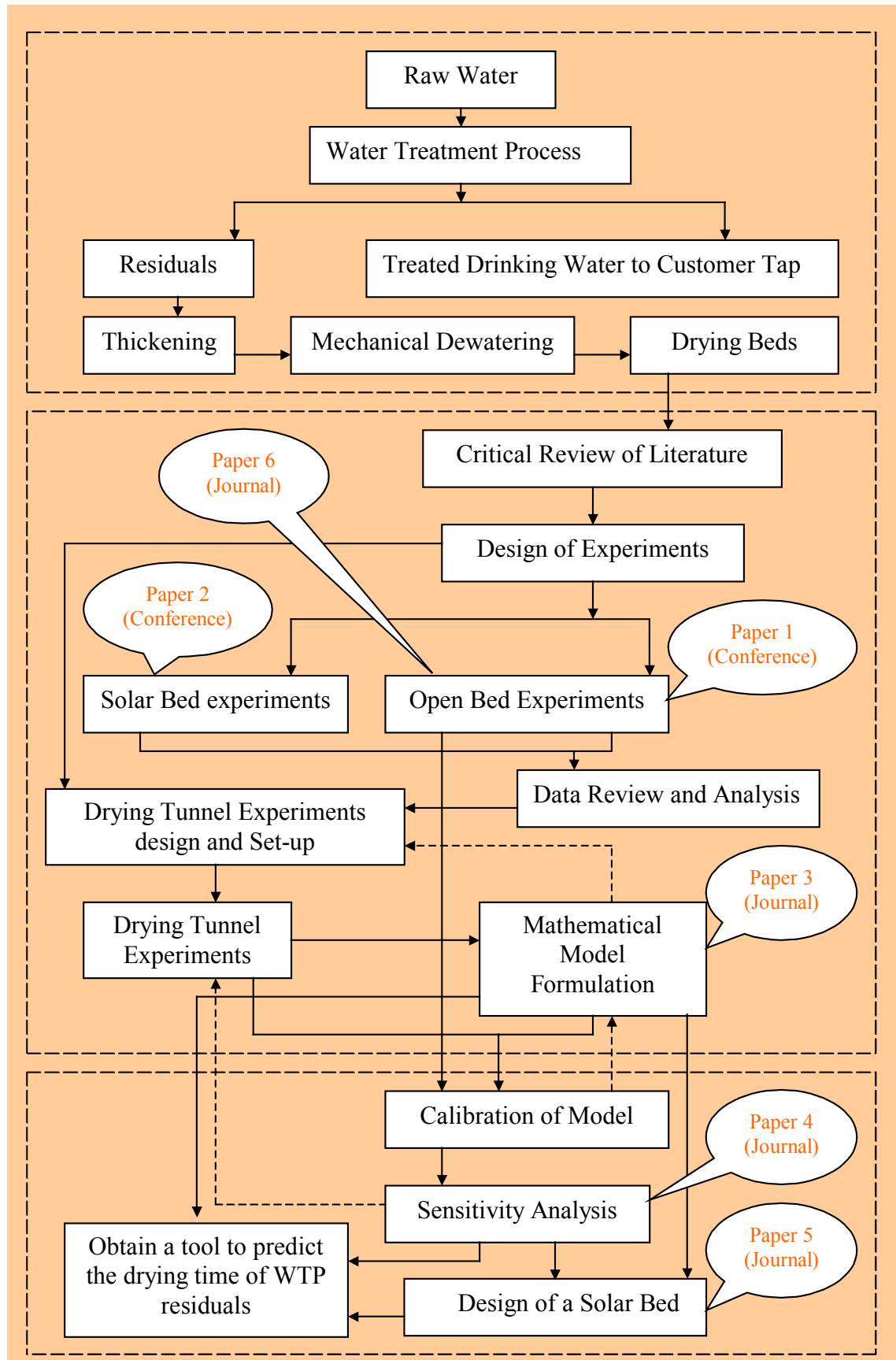


Figure 1.1 Schematic diagram showing a detailed presentation of the research undertaken.

2 Review of Drying of Water Treatment Plant Residuals

2.1 Introduction

The need for potable water treatment has become an increasing necessity in modern society. Water treatment operations not only produce drinking water, they also produce wet residuals as a by-product. There is a great need to understand the drying mechanisms of residuals, as larger quantities are generated, particularly as the demand for high quality drinking water increases. The main objective regarding residuals management continues to be the reduction of residuals for either reuse or disposal. Current literature dealing with the drying of water treatment plant residuals is relatively limited.

The objective of this chapter is to critically review and understand the drying mechanisms of the solids residuals as well as the factors affecting this process. In this chapter, a critical literature review of solids and residuals drying are presented. Estimation of residuals quantities will be categorised (Section 2.2). Dewatering screening methods of residuals will be discussed (Section 2.3). The theory behind residuals drying will be reviewed, including the mechanisms of solids drying (Section 2.4). Finally, the drying operational performance of sand drying beds will be presented discussing the factors affecting the drying on sand beds as well as the effects of chemical conditioning on residuals drying (Section 2.5).

2.2 Estimation of Residuals Quantities

The major components of water treatment residuals are aluminium and iron hydroxides, clays and other contaminants, and organic materials (Elliott et al. 1990). However, the quantity of residuals generated by water treatment operations depend

upon raw water quality, dose rates of chemicals used, and performance of the treatment process and the method of residuals' removal. Residuals quantity is a function of flow projections of the treatment plant. The backwash water normally comprises 2 to 5% of the treatment plant flow. Solid/liquid wastes normally come from iron/aluminium residuals, polymeric residuals, lime residuals, and backwash waste. Table 2.1 shows the typical constituents of water treatment plant residuals compared to soils and sewage residuals. The water treatment plant residuals values in Table 2.1 were calculated from 71 samples taken at four plants using ferric chloride and three plants using alum.

Estimation of residuals quantities is difficult and unpredictable; therefore, no single method can calculate their quantity accurately. There are three methods to predict the residuals quantities and in the following subsections, these methods will be discussed.

2.2.1 Calculations of Generated Residuals

For the estimation of ferric chloride residuals, the following formula can be used, Fabrou (1998):

$$S = Q(SS + 0.07AC + c_1L + 0.25Fe + c_2P) \quad (2.1)$$

Where,

S	Residuals produced (mg/L)
Q	Plant flow (ML/day)
AC	Raw water apparent colour (CU)
L	Lime dose rate (mg/L)
Fe	Ferric Chloride dose rate (mg/L)
SS	Raw water suspended solids (mg/L)
P	Cationic polymer dose rate (mg/L)
c_1	Coefficient value (0.03 to 0.05)

c_2 Coefficient value (0.1 to 0.4)

Table 2.1 Typical comparison of water treatment residuals, soils, and sewage residuals (Elliott et al. 1990)

Parameter	Water Treatment Residuals	Soils	Digested Sewage Residuals
% Solids	6.6	75	-
LOI %	33	5	70
TOC %	3	3	40
TKN %	0.6	0.5	4
C/N ratios	7:1	10:1	10:1
NH ₃ -N %	0.05	0.1	0.1
Total P %	0.2	0.1	2.5
Al %	7.1	7.1	0.5
Fe %	6.9	4	1.5
pH	6.8	6-9	6.9-7.5
CaCO ₃ Equivalence %	10-25	-	-
Coliforms (Counts/gm)	<20	-	10 ⁶
Total Cd (ppm)	1.5	0.4	15
Total Cu (ppm)	134	12	800
Total Ni (ppm)	55	25	80
Total Pb (ppm)	88	15	500
Total Zn (ppm)	308	40	1700

Other prediction equations are also found in Cornwell et al (1987) as shown in the following equation:

$$S = Q(2.9Fe + SS + CA) \quad (2.2)$$

Where,

S Residuals produced (kg/day)

Q Plant flow (ML/day)

CA Chemicals added (mg/L)

There is another similar equation for the alum residuals, which is shown as follows:

$$S = Q(0.44Al + SS + CA) \quad (2.3)$$

Where,

Al Alum dose rate as 17.1% Al_2O_3 (mg/L)

The suspended solids of raw water are not calculated all the time in the water treatment plants. Therefore, correlations can be used to calculate the suspended solids from the raw water turbidity. The correlations are not necessarily linear and the utility has to develop its own correlation. Equations (2.2) and (2.3) have a single term for the various chemicals added to the treatment process. Whereas, equation (2.1) provides separate terms for the chemicals added in the treatment process as well as the true colour of raw water, which probably makes it more accurate.

In order to compare equations (2.1) and (2.2), ferric chloride residuals produced from the Illawarra water treatment plant (Wollongong, Australia) (Figures 2.1 and 2.2), can be estimated fairly accurately by calculation of the residuals pumped into the drying beds from the thickeners. The residuals pumps run on average (3.4 hr/day), and the pumps flow rate (3 L/s), which gives total flow rate of (36720 L/day) of an average (0.5%) solids content. The amount of residuals produced per day as dry solids, based on this estimation, is (183.6 kg/day). A plant flow rate of 76.76 ML/day, and chemical dosages of 3.1 mg/L ferric chloride, 24.55 mg/L lime, 22 colour units, and 1.42 mg/L cationic polymer were used to calculate the amount of residuals using equations (2.1) and (2.2). Noting that ferric chloride is 43% active and cationic polymer is 40% active, equation 2.1 gives (281.4 kg/day) and (332.2 kg/day) for lower and upper ranges of the coefficients. Equation (2.2) gives (1985 kg/day); therefore it is excessively over predicting the quantities of residuals. Although equation (2.1) is more favourable, it is

clearly shown that both equations over predict the quantities of residuals since actual dry solids removed from the Illawarra beds ranges from 70 to 80 tonnes per annum.

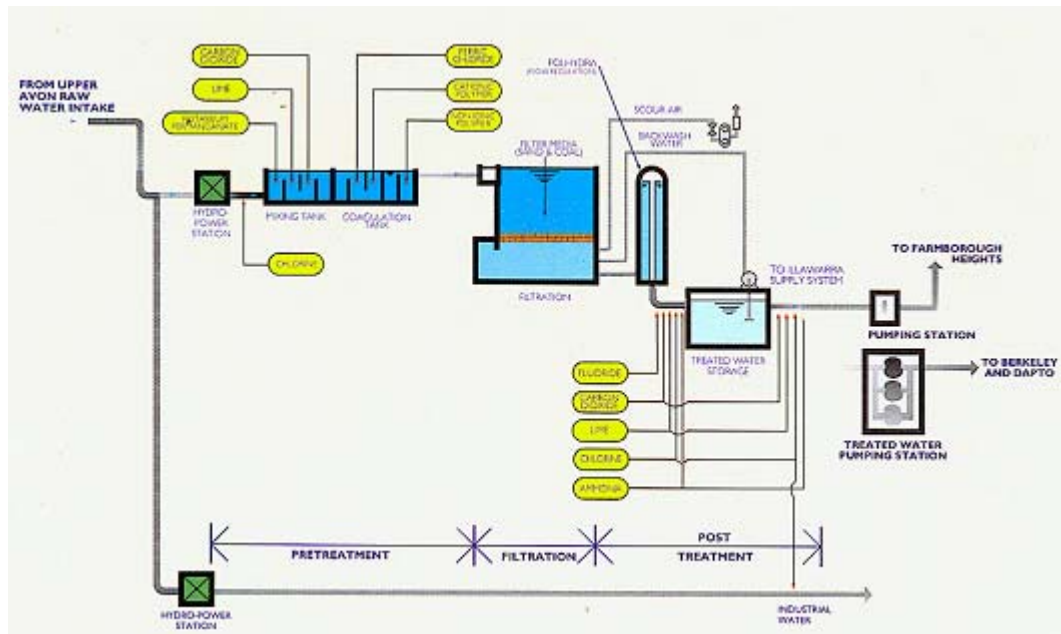


Figure 2.1 A process diagram of the Illawarra Water Treatment Plant

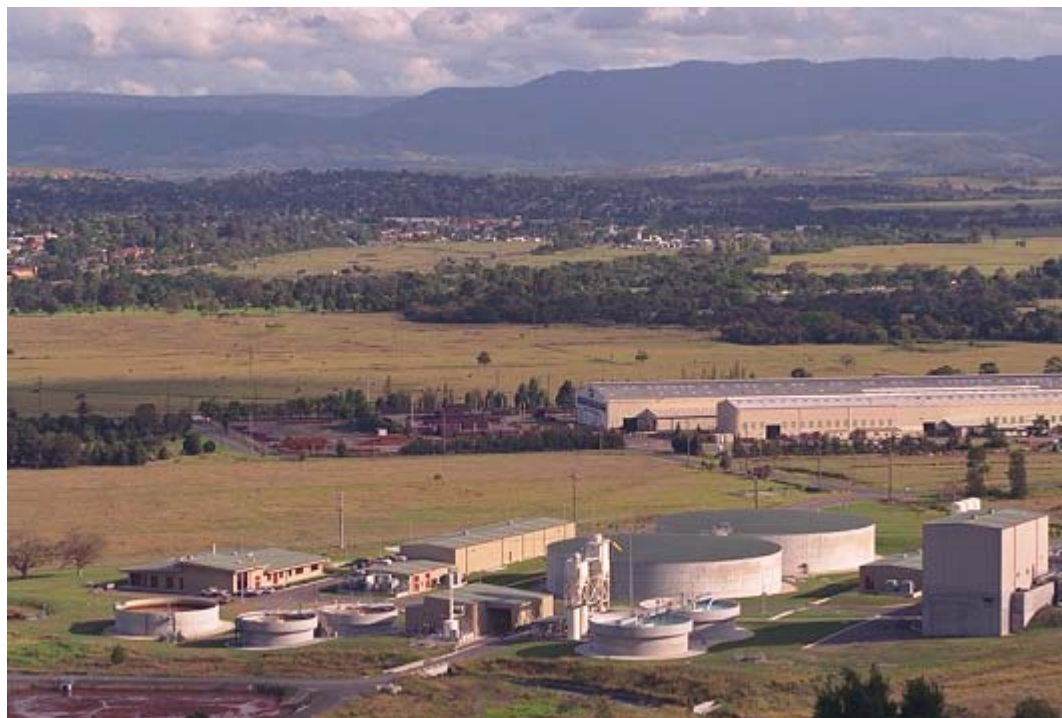


Figure 2.2 Illawarra Water Treatment Plant

2.2.2 Coagulant Mass Balance

The iron added in the coagulation process plus the iron present in the raw water has to end up in the sedimentation basin, backwash water, and the finished product. Conducting a conservation of coagulant mass balance analysis by collection of a sample for iron content from residuals, backwash solids and finished water then applying this formula (Cornwell et al. 1987) gives us:

$$\text{Total Iron Added (kg/d)} = \text{Plant Flow (ML/d)} * \text{percentage of Iron present in dry weight of Ferric Chloride} * \text{Dose rate of ferric chloride (mg/L)} \quad (2.4)$$

The amount of residuals can then be estimated by dividing the result from equation (2.4) by the amount of iron present in the residuals when analysed, and finally multiplying the result by the solids concentration of residuals to get the dry weight of residuals produced per day. A similar equation can be used for alum residuals. The coagulant mass balance method is reasonably more accurate, since it depends on actual analysis of the input and output parameters of the process.

2.2.3 Field Determination

Field determination is a method requiring continuous residuals collection equipment with monitoring systems. Volumes and suspended solids concentrations of residuals leaving the sedimentation basins or clarifiers are a function of raw water quality and the treatment method. Data on filter run-times, number of backwashes per day, and sequencing of backwashes should be periodically reviewed. These parameters are extremely important in the determination process, since the number of backwashes can vary from one day to another. The variations arise from the build up of solids while pumping of backwash water. This operational problem leads to reduced flow-rate of the

backwash water to the residuals thickeners, hence to less number of backwashes per day in the water treatment facility.

2.3 Dewatering Screening Methods

2.3.1 Specific Resistance Test

The use of chemical conditioners can improve the residuals dewater-ability. Until the early 1960s, lime, in conjunction with iron salts, was used as a chemical conditioner for residuals. In the early 1950s, aluminium chlorohydrate was introduced and in the late 1960s, polyelectrolytes had a profound effect upon the development of alternative dewatering equipment (The Manuals of British Practice in Water Pollution Control, 1981). The rate of filtration of residuals has been formulated using Darcy's law and the Carmen-Kozeny equations:

$$\frac{dV}{dt} = \frac{PA^2}{\mu(rcV + R_m A)} \quad (2.5)$$

Where,

V	Volume of filtrate (m ³)
t	Time of filtration (seconds)
P	Vacuum applied (Pa)
A	Filtration area (m ²)
μ	Filtrate dynamic viscosity (kg/s.m)
r	Specific resistance (s ² /kg)
c	Weight of solids per unit volume of filtrate (kg/m ³)
R_m	Initial resistance of filter media (usually negligible) (s ² /kg)

Integration and rearrangement of this equation permits the calculation of specific resistance, which is a measure of the filter-ability of a given type of residuals.

Integration of this equation gives:

$$\frac{t}{V} = \frac{\mu rc}{2PA^2} V + \frac{\mu R_m}{PA} \quad (2.6)$$

A plot of t/V versus V will generate a linear relationship with a slope equal to $\frac{\mu rc}{2PA^2}$

and with intercept $\frac{\mu R_m}{PA}$. If we define b as the slope of the line, then:

$$b = \frac{\mu rc}{2PA^2} \quad (2.7)$$

Moreover, the specific resistance is therefore:

$$r = \frac{2PA^2 b}{\mu c} \quad (2.8)$$

Specific resistance measurement is useful to compare the filtration characteristics of different residuals and to determine the optimum coagulant requirements for specific residuals. To determine t/V versus V relationship and, subsequently, specific resistance the Buchner funnel apparatus can be used. The laboratory evaluation of various residuals conditioners is accomplished by filtering the residuals through a filter paper using Buchner funnel as shown in Figure 2.1 and measuring both the rate of filtration and the time required for the residuals cake to begin to crack. Typical values of specific resistance vary from 2×10^{10} to 3×10^{13} s²/kg for conditioned residuals with higher values indicating poor dewater-ability. Aldeeb et al. (2003) determined the specific resistance for two alum plant residuals; the results were 2.99×10^{12} s²/kg and 3.42×10^{12} s²/kg.

Most water and wastewater residuals are compressible, their solids deforming at high vacuum or pressure levels. Consequently, resistance to filtration increases with

higher vacuum due to a packing effect. The effect of pressure differential across the cake of given residuals on its permeability can be expressed as:

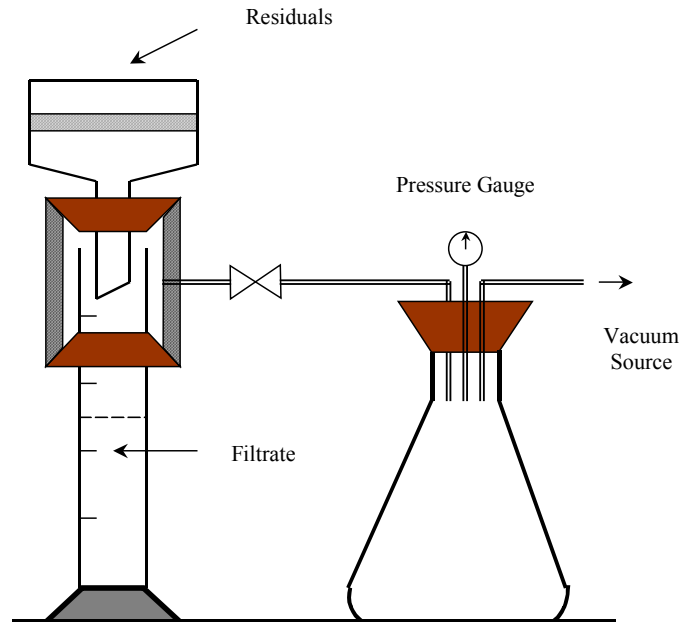


Figure 2.3 Buchner funnel apparatus for determining the specific resistance to filtration, (Vesilind et al. 1986)

$$r = r' p^s \quad (2.11)$$

Where,

r' Constant of the specific resistance of a non-compressible cake

s Coefficient of compressibility

p Vacuum applied (Pa)

The coefficient of compressibility is determined from Buchner funnel results. The coefficient (s) varies from zero for an incompressible cake to greater than one for highly compressible cakes. Cornwell et al (1987) specified some typical values for the coefficient of compressibility, (0.71 - 0.83) for ferric hydroxide residuals, and (0.6 – 0.8) for aluminium hydroxide residuals. However, the domestic wastewater residuals

coefficient of compressibility values ranges from 0.4 to 1.2, (Reimers and Englande, 1983).

2.3.2 Capillary Suction Time (CST) Test

Capillary suction time test is an evaluation technique of characterising the dewaterability of a given type of residuals. The filtrate is withdrawn from the residuals sample by capillary action of absorbent filter paper. Filterability is measured by observing the time a given area of paper takes to become wetted (Figure 2.2). The lower the CST, the more filterable the residuals become. The CST test makes it possible to compare the effectiveness of the conditioning process whether it is mineral or thermal. The CST can be correlated with the specific resistance. The optimum coagulant and its respective dosage can be determined by a plot and is taken at the point of minimum specific resistance and minimum CST. Letterman (1991) mentioned some typical CST values, for alum residuals (194.1) seconds and for ferric chloride residuals (103) seconds.

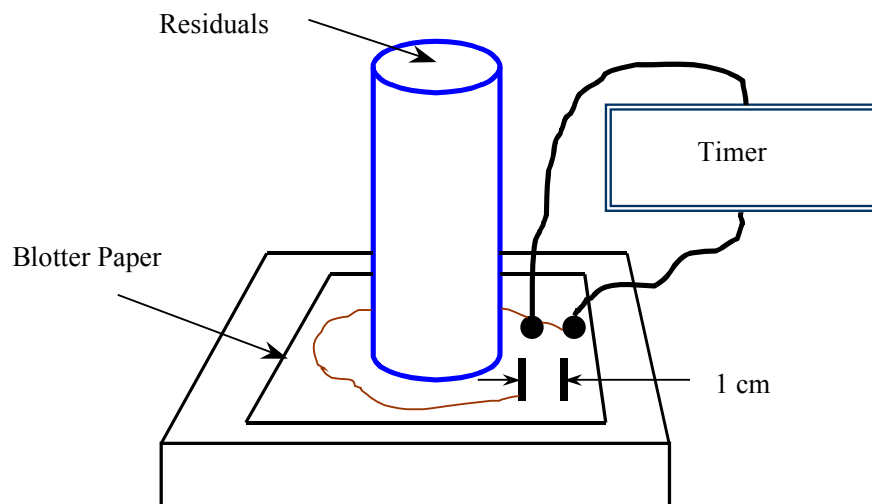


Figure 2.4 Capillary suction time apparatus, (Vesilind et al. 1986)

2.4 General Theory of Drying

A fundamental theory of drying depends on knowledge of the forces governing the flow of liquids within solids. The movement mechanisms of liquids within the solids could result from a combination of forces. These forces may include capillarity, internal pressure gradients caused by shrinkage (Tao et al. 2005), vapour-liquid flow sequence caused by temperature gradients, diffusion, and osmosis. Drying of food is one of the oldest unit operations used by mankind; nowadays it is used in various industries, such as paper, pharmaceutical, textile, etc. Drying is an energy intensive process, since heat is required to evaporate moisture from a material that yields dry solids. The benefits of drying include, preserving foodstuffs for ease of handling, reduction of materials quantity or size in order to minimise storage area and transport costs ((Swami et al. 2007), (Doymaz, 2004), (Doymaz et al. 2006), (Inazu et al. 2003) and (Leite et al. 2007)). A review of the drying of solids and their mechanisms as well as the mechanisms of the residuals drying will be discussed in this section.

2.4.1 Drying of Solids

The drying of any wet material involves the movement of water to the surface, thereby allowing the water to be evaporated. Wet materials are either hygroscopic or non-hygroscopic; whereas residual moisture content will be found within a hygroscopic material, non-hygroscopic materials, such as textiles, can be dried to zero moisture content. The moisture in hygroscopic materials may be bound moisture (Vaxelaire and Puiggali, 2002) an example occurring in fruits, grains, and residuals. On the other hand, macro-porous materials are partially hygroscopic, having bound moisture, which exerts a vapour pressure that is slightly lower than that of a free water surface (Keey, 1972).

During drying, it is necessary to remove free moisture from the surface and from the interior of the material. When hot air is blown over a wet surface, heat is transferred to the surface and the latent heat of vaporisation causes water to evaporate. Water vapour is diffused through a boundary film of air and is carried away by the movement of air. This creates a region of lower water vapour pressure at the surface of the drying material and establishes a water vapour pressure gradient from the moist interior of the material, to the drying air. This gradient provides the driving force for the removal of water from the material. Water moves to the surface by the following mechanisms:

1. Water movement by capillary forces.
2. Diffusion of water, caused by differences in the concentration of moisture in different regions of the material.
3. Diffusion of water, which is adsorbed in layers at the surfaces of solid components of the material.
4. Water vapour diffusion in air spaces within the material caused by vapour pressure gradients.

The drying rates for different materials will have a wide range of variation, but a typical curve is shown in Figure 2.3 (Perry and Green 1997).

2.4.1.1 Constant Rate Period

The surface heats up to the wet bulb temperature (region AB), then drying commences along BC and if water moves from the interior of the material at the same rate as it evaporates from the surface, the surface remains wet. This period is known as the constant rate period. It can be seen from the drying curve, the drying rate remains constant over the period BC for constant drying conditions. The constant rate period continues until the critical moisture content is reached. Broughton (1945) developed a relation assuming that the surface moisture concentration at the critical moisture content

is a function only of the nature of the material. Thus, the critical moisture content is not fixed for a given material and it depends on the amount of the drying material and the rate of drying. Swami et al. (2007) found that the critical moisture content occurs earlier with higher air temperature and larger air velocity.

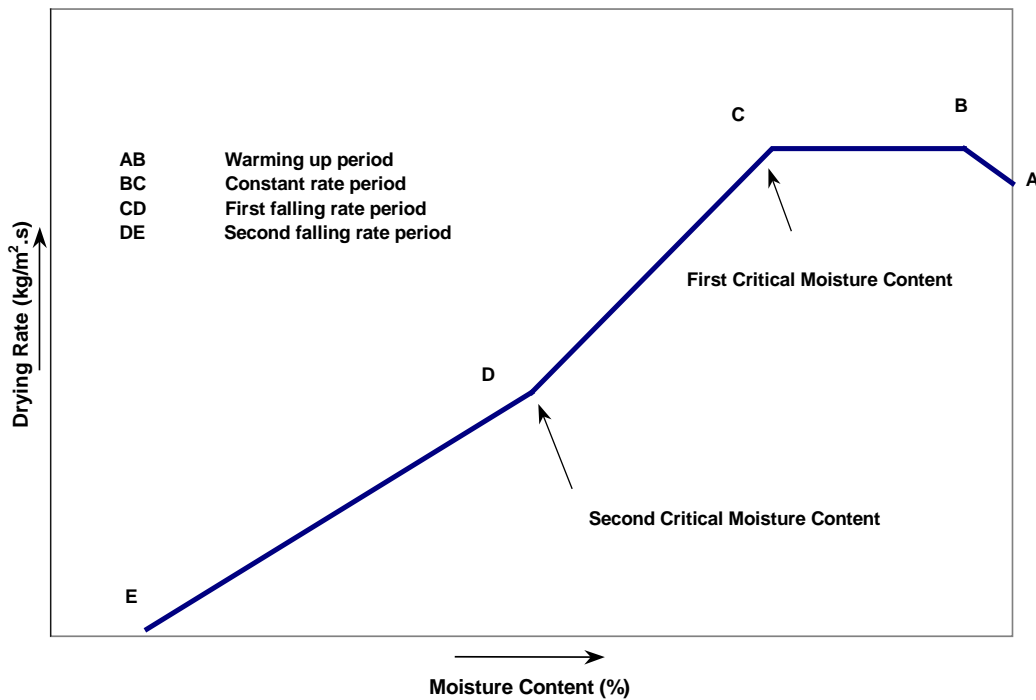


Figure 2.5 Typical drying curve of wet solids

The rate of drying may decline gradually during the constant rate period. In some cases, it is also accepted that the constant rate period does not exist, since the drying rate starts to fall after the warming up period (Strumillo and Kudra, 1986). Shin et al. (2000) found that the constant drying period does not exist in the drying curve of water treatment residuals using a fluidised bed dryer at elevated temperatures (more than 50°C). By increasing the drying potential (high temperatures and reduced relative humidity), the constant rate period disappears in the drying of activated sewage residuals (Vaxelaire et al. 2000b). It is noted from previous research that when drying

under elevated temperatures, the constant drying period tends to disappear. The constant drying period also cease to exist when the diffusion is the dominant physical mechanism governing the movement of moisture in the drying material ((Kadam and Samuel, 2006) and (Gogus and Maskan, 2006)). Moreover, the shape of the drying curve depends on moisture transfer within the material. Thereby, determines the length of the constant rate period.

The three characteristics of air that are necessary for successful drying in the constant rate period are:

1. Moderately high dry bulb temperature.
2. Low relative humidity.
3. High air velocity.

The boundary film of air above the drying material acts as a barrier to the transfer of both heat and water vapour during drying (Incropera and DeWitt, 1996). The thickness of the film is determined primarily by air velocity. If air velocity is too low, water vapour leaves the surface of the material and increases the humidity of the surrounding air, causing a reduction in the water vapour pressure gradient and hence the rate of drying.

In the constant rate-drying period, the drying conditions are not necessarily constant. The constant rate-drying period is characterised by a rate of drying independent of moisture content (McCabe and Smith, 2000). In other words, the moisture does not face any resistance in its movement through the solid material and moisture evaporation happens as of free water surface. To calculate the rate of drying in the constant rate period, a simple mass transfer equation can be used:

$$\frac{dm_{water}}{dt} = \frac{A}{h_m} (p_{saturated} - p_{\infty}) \quad (2.10)$$

Where,

m_{water}	Weight of moisture evaporated (kg)
$p_{saturated}$	Saturated water vapour pressure (Pa)
p_{∞}	Vapour pressure of water of the air (Pa)
A	Area of the drying surface (m ²)
t	Time (seconds)
h_m	Mass transfer coefficient (m/s)

In terms of heat transfer the moisture loss can be expressed in the following equation:

$$\frac{dm_{water}}{dt} = \frac{hA(T_{\infty} - T_{surface})}{h_{fg}} \quad (2.11)$$

Where,

h	Heat transfer coefficient from air to the wet surface (W/m ² .K)
T_{∞}	Temperature of the air (K)
$T_{surface}$	Temperature of the surface (K)
h_{fg}	Latent heat of vaporisation (J/kg)

In order to calculate the rate of moisture loss using either method, the mass or heat transfer coefficients have to be determined by experimental methods.

2.4.1.2 Falling Rate Period

The falling rate period starts at the end of the constant rate period. The point where the drying rate changes is called the critical moisture content. The falling rate period of a drying material, means that the rate of drying is falling and is no longer maintained at the same rate. Non-hygroscopic materials such as textiles have a single falling rate period, whereas hygroscopic materials such as food and residuals have two falling rate

periods. The single falling rate period indicates that the material does not have bound moisture; the two falling rate periods indicate the presence of bound moisture. The two periods will be discussed in the following subsections.

2.4.1.3 First Falling Rate Period

In this period, the plane of evaporation moves inside the material being dried and water diffuses through the dry solids to the drying air. It represents a condition whereby the surface is no longer capable of supplying sufficient free moisture to saturate the air in contact with the surface. Under these conditions, the rate of drying depends very much on the mechanism by which moisture from inside the material is transferred to the surface. These mechanisms are either the resistance to water removal at the surface of the solid or the resistance to moisture movement within the solid. The shape of the drying rate curve depends upon the type of the material, the drying rate in the constant rate period and the critical moisture content (Strumillo and Kudra, 1986). Gardner and Hillel (1962) found that the rate of water evaporation from soil surface depends upon the water content of the soil in the falling rate period. This appears to be correct, since the quantity of moisture dictates the movement of water in the body of the solid. With less moisture content, the water will face more resistance in its movement.

2.4.1.4 Second Falling Rate Period

At the end of the first falling rate period, it may be assumed that the surface is dry and that the plane of separation is moving into the solid. The vapour then reaches the surface, by molecular diffusion through the material. The forces controlling the vapour diffusion will determine the final rate of drying and will be largely independent of the conditions outside the material. During the falling rate period, the factors that control the rate of drying change. Initially the important factors are similar to those in the constant rate period, but gradually the rate of mass transfer becomes the controlling

factor. This depends mostly on the thickness of the material. The drying rate is unaffected by both the relative humidity of the air (except in determining the equilibrium moisture content) and the velocity of the air.

The surface temperature of the drying material remains close to the wet bulb temperature of the drying air, until the end of the constant rate period due to the cooling effect of the evaporating water. During the falling rate period, the amount of water evaporating from the surface gradually decreases. The same amount of heat is being supplied by the air, which elevates the surface temperature until it reaches the dry bulb temperature of the drying air at the end of the second falling rate period.

2.4.1.5 Behaviour of Various Materials During Drying

The drying of wet materials in general behaves according to the typical drying curve (Figure 2.3). Chen et al (2002) indicated that thermal drying of wastewater residuals would normally undergo the three drying periods shown in the typical drying curve. Reyes et al (2004) noted that the constant drying period was relatively longer for diluted organic suspensions. Youngman et al (1999) used a combined constant rate and diffusion model for the two constant and falling rate drying periods of timber. Chen and Pei (1989) presented a drying model to simulate the drying process of brick, wool and corn kernels, where they all follow the typical drying curve.

The drying of the wide range of materials presented in this section shows that they follow the typical drying curve of constant and falling rate periods. The length of the constant rate period depends on the characteristics of the material, the drying conditions and the initial moisture content. The shape of the falling rate period varies from one material to another as explained in section 2.4.1.3. The shape of the drying curve in the falling rate period, depends mainly on the type of the material and hence the movement of moisture inside the material. The particle shape and size affects the pore size of the

material and hence the movement of moisture; large pores hold water loosely while small pores hold water very tightly (Ashman and Puri, 2002). Therefore, the shape of the falling rate period curves whether it is straight, concave, or convex line, will be determined according to the moisture movement within the material pores. The shape of the curve will be shown in section (2.4.3) when the drying of residuals is discussed.

2.4.1.6 Equilibrium Moisture Content

When the air is more humid than the solid in equilibrium with it, the solid absorbs moisture from the humid air until equilibrium is achieved. The residual moisture in a wet solid, which cannot be removed by air, is called the equilibrium moisture content. The rate of moisture removal, in a drying material, is proportional to the difference between the moisture content of the material at any time and the equilibrium moisture content. Therefore, if the equilibrium moisture content value is close to the moisture content at any instant, the drying rate drops sharply. This explains the falling rate drying period behaviour.

Henderson (1952) expressed a relationship between the equilibrium moisture content and the relative humidity at a given temperature in a semi-theoretical model:

$$1 - RH = e^{-cT} X_e^n \quad (2.12)$$

Where,

RH	Relative humidity of air, fraction
T	Temperature of the drying material (K)
X_e	Equilibrium moisture content, dry basis (%)
c, n	Empirical constants for a particular material

The empirical constants can be determined from experimental results; Table 2.2 shows some typical values for c and n . This model is useful when drying of a material is

required for very low moisture contents especially in industrial dryers. McKenzie (1992) developed a relationship to calculate the equilibrium moisture content:

$$X_e = \exp\left(\frac{RT \ln(1/RH) + A}{B}\right) \quad (2.13)$$

Where,

R The universal gas constant, $8314 \text{ kg.m}^2/\text{s}^2.\text{kg-mole}^0\text{K}$

A, B Correlation constants

Equation (2.13) was developed by correlating X_e and $RT \ln(1/RH)$ for ion exchange resin and it can be used in the dryer design procedures.

Table 2.2 Typical values for the empirical constants of some materials (Henderson and Perry, 1955)

Material	c	n
Wheat	5.59×10^{-7}	3.03
Cotton	4.91×10^{-5}	1.7
Wood	5.34×10^{-5}	1.41
Natural Clay	7.53×10^{-5}	1.72

2.4.2 Mechanisms of Solids Drying

The most comprehensive studies of the drying of solids are illustrated in a series of research publications by Professor T. K. Sherwood in the Massachusetts Institute of Technology, from 1928 until 1936. Sherwood (Jan. 1929, Oct. 1929, 1930, 1932), Sherwood and Comings (1933), Gilliland and Sherwood (1933) and Sherwood (1936) studied the mechanisms of drying solids in general. These studies classified the drying mechanisms in terms of evaporation and resistance to evaporation at the surface and inside the solids body, the different periods of solids drying, the effect of weather

conditions on the drying of solids and the diffusion of moisture as well as the diffusion equation through various wet solids.

2.4.2.1 Classification of Water Removal

Drying involves the vaporisation of water and the removal of this vapour away from the surface of the drying solids. The rate of removal of moisture from solids depends upon external factors. These factors involve temperature, relative humidity and air velocity. Another set of factors relate to the internal conditions, such as the chemical and physical nature of the material being dried and the changes occurring in these properties, during the drying process. Lee (1996) interpreted a classification scheme of water removal in activated residuals as interstitial, surface and internal water. However, Sherwood (1928) classified the water removal from drying solids and how it occurs in the following four cases:

1. Evaporation at the solid surface, where the resistance to internal diffusion of liquid is small compared to the resistance of vapour removal from the surface.
2. Evaporation at the solid surface, where the resistance to the internal diffusion of liquid is great compared to the resistance of vapour removal from the surface.
3. Evaporation in the interior of the solid, where the resistance to the internal diffusion of liquid is small compared to the resistance of vapour removal.
4. Evaporation in the interior of the solid, where the resistance to the internal diffusion of liquid is great, compared to the resistance of vapour removal.

Sherwood (1929) explained the drying mechanisms of solids where water evaporation occurs at the surface of the solids and beneath the surface. The water as a liquid or as a vapour travels to the surface by diffusion then water vapour diffuses into the main body of the air. Diffusion in solids is governed by the famous diffusion equation:

$$\frac{\partial X}{\partial t} = D \frac{\partial^2 X}{\partial x^2} \quad (2.14)$$

Where,

X	Moisture concentration within the solid, dry basis
D	Diffusivity of moisture through the solids (m ² /s)
t	Time (seconds)
x	Distance in direction of diffusion (m)

The solutions of equation (2.14) for the boundary and initial conditions have been presented by several researchers such as Carslaw and Jaeger (1986) and Crank (1975).

Equation (2.14) can be integrated for drying to obtain the following formula:

$$\frac{X_{average} - X_e}{X_{initial} - X_e} = \frac{X}{X_{Free(i)}} = \frac{8}{\pi^2} \left(e^{-\left(\frac{\pi^2}{4}\right)\eta} + \frac{1}{9} e^{-9\left(\frac{\pi^2}{4}\right)\eta} + \frac{1}{25} e^{-25\left(\frac{\pi^2}{4}\right)\eta} + \dots \right) \quad (2.15)$$

Where,

$$\eta = Dt / s^2$$

s	One-half slab thickness (m)
$X_{average}$	Average total moisture content at time t (dry basis)
X	Average free moisture content at time t (dry basis)
X_e	Equilibrium moisture content (dry basis)
$X_{initial}$	Initial moisture content at start of drying (dry basis)
$X_{Free(i)}$	Initial free moisture content (dry basis)

Diffusivity usually is not constant, varying with moisture content and sensitivity to shrinkage (McCabe and Smith, 2000). Diffusivity is less at low moisture contents rather than at high and may be very small near the drying surface. In practice, an average value of diffusivity established experimentally on the material to be dried is used. When

η is greater than 0.1, only the first term on the right-hand side of equation (2.15) is significant and the other terms can be dropped. Solving equation (2.15) for the drying time gives:

$$t = \frac{4s^2}{\pi^2 D} \ln \frac{8X_{Free(i)}}{\pi^2 X} \quad (2.16)$$

Differentiating the above equation with respect to time and rearranging gives

$$-\frac{dX}{dt} = \left(\frac{\pi}{2}\right)^2 \frac{D}{s^2} X \quad (2.17)$$

The above equation shows that when diffusion controls, the rate of drying is inversely proportional to the square of the thickness. The limitations of the diffusion model are the assumptions of constant diffusivity and negligible shrinkage. It was found that the diffusivity varies with moisture content (Hougen et al. 1940) (Ceaglske and Hougen 1937); therefore, the diffusivity is a function of moisture content. Boudhrioua et al. (2003) observed significant proportional effect of temperature on moisture diffusivity. The falling rate curve explained by equation (2.17) is concaved upwards for nonporous materials, whereas the typical drying curve Figure 2.3 can vary depending on the nature of material.

2.4.2.2 Movement of Water in Porous Materials

Moller (1983) explained the mechanism of capillary forces that govern the movement of moisture in porous materials, which will be presented here. Drying by evaporation allows the water surface to be lowered into the branched passages among the particles, creating a slight curvature of the menisci. This exerts sufficient pull to draw water to the surface. Water continues to rise in the passage until the curvature of the lower end meniscus of the water column is the same as the curvature of the surface meniscus. At this stage, the surface meniscus retreats due to the further evaporation of

moisture. This in turn, decreases the surface curvature of the water and causes the lift of additional moisture. This process continues until all the menisci of all the passages are about the same, when the water cannot be drawn to the surface and evaporation results in a continuous retreat of the menisci. At this point, the resistance to drying will increase, as the vapour will have to diffuse through the stagnant column of air in the voids before reaching the surface.

The movement of moisture among the particles of a solid, as explained by Moller (1983), and the resistance to drying explains the behaviour of the drying of solids in the falling rate period, where the rate of drying starts to decrease. Understanding moisture movement in solids would lead to develop new dewatering techniques. As an example, an electrokinetic process for moisture removal was used in sewage residuals dewatering (Yuan and Weng, 2003).

2.4.2.3 Effect of Weather Conditions on Drying Periods

Sherwood (1936) discussed the effect of weather conditions on the two drying periods where the rate of drying is greatly influenced by air velocity. The effect is analogous to the influence of fluid velocity on the dissipation of heat from a hot surface, placed in contact with a fluid stream. The effect of air velocity on vaporisation is analogous to the effect on heat transfer, which assumes that the curves would not be linear. Sherwood (1936) explained how the rate of drying is affected by air temperature and humidity, since the rate of vaporisation is proportional to the difference between the vapour pressure at the surface temperature and the partial pressure of water vapour in the air as it was explained in section (2.4.1.1). However, Penman (1948) used the difference between the vapour pressure as well as net radiation and wind speed in a simple physical way in his evaporation model. Wright et al. (2001) described grass drying in an empirical model that incorporated a single evaporation parameter (solar

radiation) was shown to describe the drying pattern as accurately as a model based on Penman equation.

Sherwood (1930) categorised the most important manner in which heat may be supplied to a drying material. The heat transferred by radiation to a wet material can increase the temperature above the wet bulb temperature, hence increasing the rate of evaporation. It is important to note that the effect of weather conditions on the rate of drying was studied by Sherwood (1936) in an industrial dryer. It is evident from the previous studies mentioned in section (2.4.2) that the drying of wet solid materials behave differently. The internal factors, which govern the drying behaviour, are different for any given material. When exposing different materials to the same weather drying conditions, they will behave differently. The weather conditions are considered the external factors in any drying process. Weather parameters were used by researchers to describe the drying process successfully.

2.4.3 Drying of Residuals

The oldest and simplest treatment processes involves passing water through a bed of fine particles, usually sand (A consumer's guide to drinking water, 2006). Water treatment has developed from slow to rapid sand filtration in the conventional processes; to the development of the membrane filtration processes. The development of plastic materials has led to new membrane filtration processes, including micro-filtration, ultra-filtration, nano-filtration, and reverse osmosis. The need for water treatment has become an increasing necessity in modern society. As a result, water treatment plants produce increased quantities of residuals. These residuals consist of raw water suspended solids, any organics found in water, the coagulants used in the process of treatment as well as polymers. Water is treated in conventional treatment plants, which include the sedimentation of large particles as well as coagulation and

flocculation for smaller particles. Crittenden et al. (2005) classified the residuals generated from the treatment of potable water as:

1. Residuals from water treatment processes.
2. Liquid wastes from water treatment processes.
3. Liquid wastes resulting from processes used to thicken process residuals and to treat liquid wastes.
4. Gaseous wastes from specialised water treatment processes.

Improper management and disposal of residuals, contributes to air and water pollution and presents a potential risk to public health and safety. In economic terms, an important consideration in the management of residuals, involves minimising transport costs. The environmental impact of residuals also demands further consideration. The reduction of residuals in landfills can be achieved by reuse options such as composting, manufacturing of bricks, coagulant for sewage treatment plants, application to agricultural lands, reuse in building materials and as filling materials. In order to allow the residuals containing high metal hydroxides to be more easily dewatered, it must be conditioned with lime or polymers. The options of either disposal or reuse of the residuals, depends on the types of chemicals used through the whole treatment process, from raw water quality, thickening, and the de-watering processes. To achieve the optimum long-term management of residuals, the drying process must be understood and modified to enable the acceleration of the drying process. The key, to understanding how residuals dry, is found by examination of the drying characteristics of the material in hand. Although substantial information is found on drying equipment and its performance, very little information relates to the drying of potable water residuals. Environmental regulations (EPA, 2003), limited land fills sites and reuse options (Reardon, 2005), have compounded the need for more research regarding minimising

the quantities of residuals therefore innovative reuse options, and better drying techniques need to be developed.

Drying of residuals begins when ample moisture is present at the surface. The surface then begins to crack as it dries and moisture ceases to be visible. The cracks become more evident, forming towards the bottom of the cake. Small fragments of dry solids then become isolated when most of the moisture is evaporated. In order to explain these phenomena, the moisture found in residuals will be classified and the drying period will be explained in the following subsections.

2.4.3.1 Classification of the Types of Water Found in Residuals

Types of water within the residuals and water bound to the solids are categorised as internal and external water. The internal water is included in the particles of the residuals, in other words it is chemically bound water. The chemically bound water increases the residuals quantity and volume, making its removal difficult (Cornwell et al. 1987). The external water in the residuals can be removed only by destroying the membrane of particles and by transforming the internal water into external water, by thermal forces. Free water, which is the water bound by such minute forces that its vapour pressure is equal to the vapour pressure of pure water, can be found in cavities and wide capillaries. The heat of adsorption of this moisture is equal to the normal heat of vaporisation of water, at the same temperature.

The adsorption water forming the protective layer around the particles of the residuals is small compared to the whole water content. The binding forces are very intense, thus, the water can only be removed by thermal forces. The binding forces of the adsorption water are more intensive than the forces binding the adhesion water. The capillary forces are such, that the water fills the branched passages among the particles.

The free water has only a small binding to the solids; therefore, this water is drainable by gravity.

Water comprises most of the thickened residuals. Tsang and Vesilind (1990) categorised moisture present in residuals as follows (Figure 2.3):

1. Free moisture is the moisture, which mostly can be removed by drainage.
2. Interstitial moisture is the moisture removed during the first falling rate period of a drying curve.
3. Surface moisture is the moisture removed during the second falling rate period of a drying curve.
4. Bound moisture is the moisture that cannot be removed by the drying process; it is chemically bound by the solid particles.

Tsang and Vesilind (1990) found that free moisture accounts for about 90% of the total water present in residuals, which can be removed by drainage. The other remaining 10% of the water can be removed by drying or mechanical dewatering, and consists of about 5% free moisture, 3% interstitial moisture, 0.5% surface moisture and 0.2% bound moisture. Chen et al. (2002) explained the water removal in sewage residuals during various drying periods. The free water is removed in the constant rate period, the interstitial water is removed in the first falling rate period and the second falling rate period removes the surface water. The final moisture content retained within the residuals is mostly bound water.

The measure of water present in the residuals can be expressed as a wet basis or dry basis. The moisture content can also be expressed as decimal or percentage. Moisture content on a wet basis can be defined as follows:

$$X_{wet} = \frac{m_{residuals} - m_{solid}}{m_{residuals}} \quad (2.18)$$

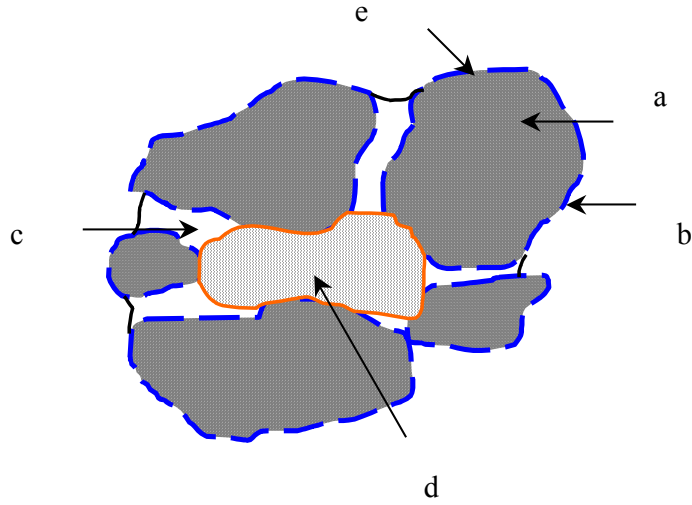


Figure 2.6 Schematic of the proportions of water in residuals (a) Internal water, (b) Adsorption and adhesion water, (c) Interstitial capillary water, (d) Capillary-held water, and (e) Solid particles, (Moller, 1983)

Where,

$m_{residuals}$ Mass of residuals (kg)

W_{solid} Mass of dry solids in residuals (kg)

Moisture content as dry basis can be defined as follows:

$$X_{dry} = \frac{m_{residuals} - m_{solid}}{m_{solid}} \quad (2.19)$$

2.4.3.2 Constant Rate Period

Figure 2.4 represents the drying process of the water treatment residuals as presented by Moller (1983). The drying process curve is divided into a constant rate period and a falling rate period. However, the drying conditions are not necessarily constant during the constant drying period. The drying rate is constant when there is an abundance of moisture on the surface of the residuals. In this period, water evaporates and drains simultaneously on the sand drying bed. Drying takes place at the exposed

surface of the residuals, by diffusion of the vapour through a stationary air film. During the constant drying period, when the surface is completely wet and as soon as the water film on the surface evaporates, water diffuses from the interior of the residuals at a rate similar to that for evaporation. It is estimated that 80% of initial water content is eliminated during the constant rate period (Ruiz et al. 2006).

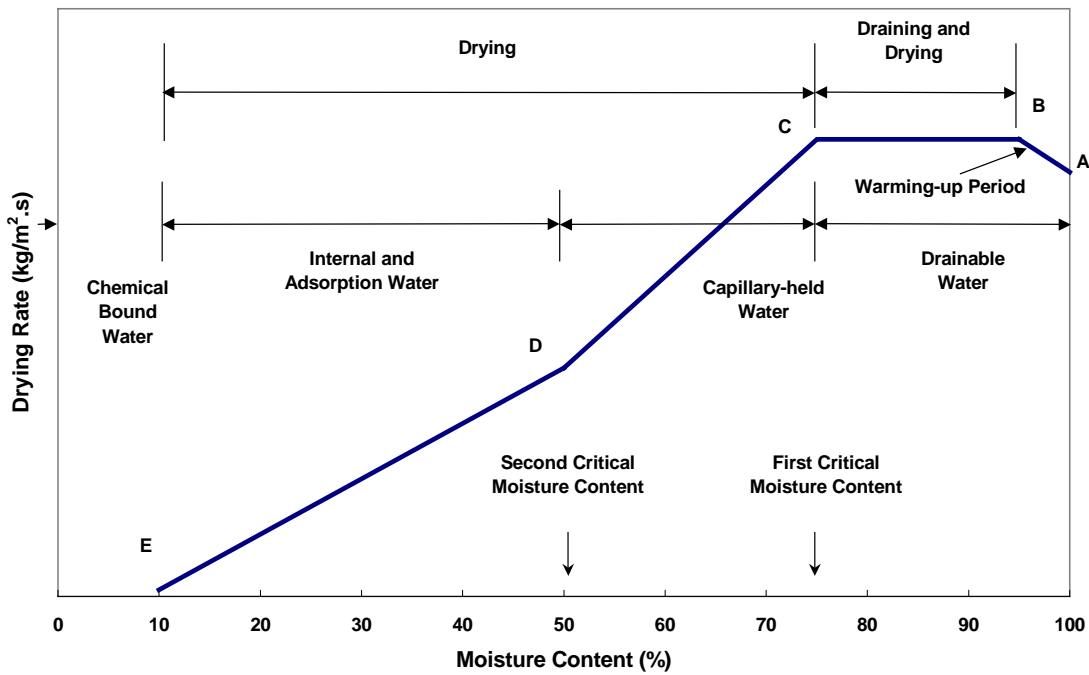


Figure 2.7 Water removal from residuals by draining and drying, Moller (1983)

2.4.3.3 Critical Moisture Content

The constant rate period continues, until certain moisture content is reached. This is the first critical moisture content. At this point, the rate of loss of moisture begins to decrease and the rate of drying drops linearly with a certain slope. The critical moisture content depends upon several factors: the rate of drying, the thickness of the material, and the factors influencing moisture movement and resulting gradients within the solids (Perry and Green, 1997). Therefore, the critical moisture content increases with increased drying rate and with increased thickness of the material being dried. When the

drying material is subjected to severe drying conditions, the critical moisture content happens at a higher level, whereas, it happens at a lower moisture level when the depth of the material is small (Sherwood 1929). On the other hand, Nebiker (1967) in his study on sewage residuals, outlined that the critical moisture content is an average value, calculated from the entire volume of the residuals. Therefore, the greater the depth of the residuals application, the higher the first critical moisture content becomes.

Moller (1983) pointed out that nearly 75% moisture content is the first critical moisture content for all residuals. Around 50% moisture is the second critical moisture content. Gharaibeh et al (2001) found that the change of the drying slope in the drying of water treatment residuals happens at about 15% solids content. The drying slope is the plot of the solids content (wet basis) versus time. Marklund (1990) studied the drying of sewage residuals using two pilot drying beds in an open-air bed and one similar bed in a controlled environment and compared the results with evaporation from a free water surface. The study found that the rate of evaporation above the critical moisture content of residuals (8-14% solids content) equals that from the free water surface. Below this critical moisture level, the rate decreases rapidly. These findings show that the internal resistance to evaporation is dominant in the falling rate period when no moisture is available at the surface of residuals.

2.4.3.4 Falling Rate Period

According to Moller (1983), the factors affecting the rate of drying in the falling rate period are determined by the controlling mechanism. If the graph in the falling rate period is a straight line or is convex upwards, it indicates that the resistance to vapour removal controls the rate of drying. If the graph is concave upwards, it indicates that the internal diffusion of the moisture is the controlling factor and evaporation occurs at points within the solids structure. The external conditions, such as temperature,

humidity and air velocity, affect the rate of moisture removal in the first falling rate stage as shown by Sherwood (1936). Further, Moller (1983) explained that after the second critical moisture content, the rate of arrival of water at the surface is less than the rate of evaporation; this results in the plane of evaporation retreating from the surface. In this period, the resistance to internal diffusion of moisture is greater than the surface resistance to vapour removal. The factors affecting the rate in this period are those affecting the moisture movement within the material, such as the physical and chemical nature of the residuals. Evaporation will continue until certain moisture content, when there will be no further evaporation.

2.4.3.5 Movement of Water in Residuals

Most of the moisture removed in the constant rate period can be removed by drainage. This water could be considered as the interspace water, as free water, or water with only a small binding to the solids. The first critical moisture content gives a measure of this water, below that the moisture content represents moisture, which cannot be drained due to the resistance of capillary forces. Between the first and second critical moisture content the material is drying internally, the second critical moisture content may be a measure of the quantity of water held within the residuals flocs or particles.

The methods used to estimate or predict the drying rate and drying time, in the falling rate period depend on whether the solid is porous or non-porous. Water treatment residuals can be considered having both hygroscopic-porous media and colloidal (non-porous) media (Mujumdar, 1987). Residuals can be identified as having a clear pore space since there is a large amount of physically bound water and shrinkage often occurs in the initial stages of drying. Water treatment residuals contain considerable amounts of polymers, which are considered colloidal (non-porous) media.

Swamy (2006), while studying the water treatment residuals characteristics, found that the particle size increases due to drying; therefore, the residuals should have larger pore space with reduced moisture content.

2.5 Drying Beds Operational Performance

Residuals drying process has two major effective factors drainage and evaporation. Drainage in a conventional sand drying bed might last a few days until the sand is clogged with the fine particles and/or all of the free water has drained away. Further dewatering occurs by evaporation, which depends on unpredictable weather conditions.

The aim is to dry the water treatment residuals to a manageable level with due consideration to environmental protection. The boundary conditions of a drying design are determined by the quantity of residuals produced, the local meteorological conditions and the other available sources of energy. Unexpected wet days contribute to extensive delays in the drying process. From an economical and handling point of view, it is important to dry the residuals to 30%-45% solids content, before final disposal or reuse as quickly as possible. In order to sustain this process as a long term solution, the drying technique should be modified to improve the drying process.

Cheremisinoff (1994) reported that residuals formed from ferric and ferrous compounds are surprisingly soft, fluffy and difficult to dewater to more than 10% or 12% solids content. In addition, Miller (1999) reported that conventional dewatering produces cakes with solids contents of 10-20% by weight. This means between 80-90% of the weight of the cake is water. This contributes significantly to the cost of reuse, particularly the cost of transport and storage. These costs provide an incentive to reduce the amount of water remaining in de-watered cakes.

2.5.1 Sand Drying Beds

In early years of the twentieth century, the use of drying beds was wide spread as a dewatering technique (Spellman, 1997). The increased in demand for high quality drinking water would result in increased quantities of residuals. Land constraints have made the use of drying beds less economical; however, other dewatering technologies have become increasingly attractive. In humid areas, the weather conditions have made the use of drying beds less efficient in residuals drying. The area of the drying bed depends on the land availability, drying time, and bed loading. Drying beds require less labour attention but residuals removal from the bed might result in excessive sand loss, which could be more costly (Figure 2.8). The drying beds are constructed by having a drainage tile system, a layer of drainage gravel and another layer of sand. Drying beds can be either covered in areas of high average rainfall or uncovered in relatively dry areas (Figure 2.9).



Figure 2.8 Dry residuals removed from a sand drying bed

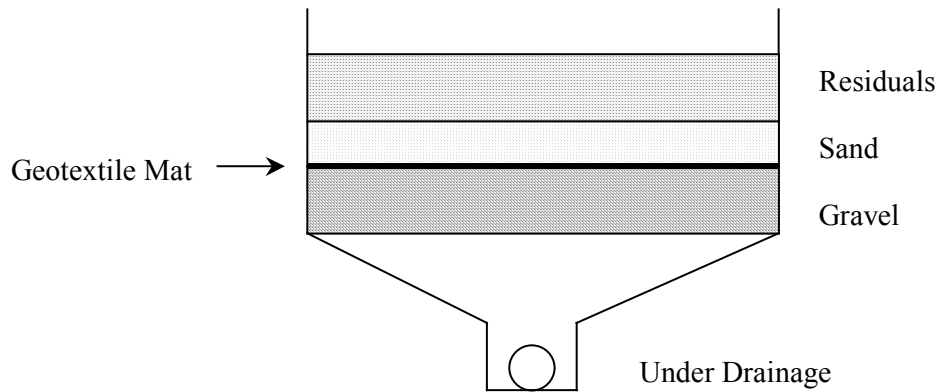


Figure 2.9 Cross sectional area of a sand drying bed

2.5.1.1 Factors Affecting Drying on Sand Beds

A key variable in minimising the size of the required drying area is to maximise the water release from residuals (Cornwell and Vandermeiden, 1999). The drying of residuals on sand beds is governed by operational, chemical, and meteorological factors. The Manuals of British Practice in Water Pollution Control (1981) listed the following factors in which water removal in drying beds depend upon:

1. The type of residuals applied: Some residuals release water faster than others and chemically conditioned residuals are easier to dewater.
2. The initial solids content: The higher the solids content the faster the dewatering and the drying becomes.
3. The depth of the application: Shallow applications release their water easier and faster, and optimising of the bed application depth has to be studied.
4. The porosity of the sand bed: The size of sand particles impacts significantly upon the dewatering time.
5. The time required for drying: The frequency of the application of residuals and the bed loading over a set period of time, is one of the most important factors involved in drying on sand beds.

6. The meteorological conditions: Wind speed, ambient temperature and relative humidity play an important role. These together with the average annual rainfall can affect the drying process greatly.

2.5.1.2 *Effects of Chemical Conditioning*

Many researchers have investigated the effects of chemical conditioning, on enhancing water treatment plant residuals' ability to drain. Novak and Montgomery (1975) concluded from their study of chemical residuals (water treatment plant) dewatering on sand drying beds, that the drainage of these residuals depend on the specific resistance and the initial solids concentration. Smollen (1990) discovered that the addition of polyelectrolyte increases the rate of filtration by releasing some of the immobilised water. Tsang and Vesilind (1990) also found that chemical conditioning by cationic polymer enhances the residuals dewatering process. Dewatering can be enhanced of up to 6% using polymers as conditioners for water treatment residuals (Cornwell and Vandermeiden, 1999).

Dharmappa et al (1997) conducted a study, investigating the performance and design of sand drying beds when treating chemically conditioned water treatment plant residuals. Synthetic organic polymers are found to be highly effective conditioners for de-watering water treatment plant residuals on sand drying beds. This leads to a substantial increase in the average drainage rates, indicating the possibility of reducing the land area required for the sand drying beds. Chu and Lee (1999) studied the effect of polymer conditioning on moisture distribution in residuals, finding that by increasing the cationic polymer dose rate, the water-solid bond strength decreases at specific moisture content after it reaches a charge neutralisation point; however, the strength increases in the overdose regime.

The abovementioned studies show that sand drying bed's performance could be improved by either conditioning the residuals or by altering the operational conditions of the beds. Operational fine-tuning is important when dealing with sand drying beds; the frequency of applications as well as thickness and rotating beds improve the drying performance dramatically.

2.6 Summary

This chapter has examined the various aspects of the drying of water treatment residuals. Three methods have been reviewed to estimate the quantities of residuals generated in any water treatment plant. Two methods are mainly projections based on the treatment plant flows and chemical dose rates. The coagulation mass balance (Cornwell method) has been found to be the most reliable method since it depends on actual analysis of the input and output parameters of the process. The dewatering screening methods were reviewed showing typical values for the coefficient of compressibility, using the Buchner funnel and some typical values of the capillary suction time for alum and ferric chloride residuals.

The general theory of drying was reviewed, in an effort to outline past research in this field. The drying periods, as well as the critical and equilibrium moisture contents were identified. The drying of solids involves mass transfer of moisture and the transfer of heat simultaneously. Mass transfer relates the moisture loss with time with the vapour pressure gradient. Heat transfer relates the moisture loss with the temperature gradient. The heat and mass transfer coefficients have to be determined experimentally. The constant rate period could be long, short, or non-existent; it was found that drying under elevated temperatures leads to the elimination of the constant drying period. The single falling rate period indicates that the material is non-hygroscopic. For hygroscopic

materials the falling rate period multiples to two. The falling rate period curve varies with the type and porosity of the material.

The drying of residuals has been reviewed through the classification of the types of water found in residuals. Moller (1983) pointed out the mechanisms of the drying of residuals and explained the residuals drying curve. In the constant drying period, drainage and drying occur, while only drying occurs during the falling rate period. The critical moisture content varies with the residuals cake thickness and the variations of weather conditions.

Finally, the drying beds operational performance, together with the major factors affecting their operation, concludes this chapter. The major factors are the type of residuals, the initial solids content, depth of application, porosity of sand bed, time required for drying and meteorological conditions. Managing the drying of residuals is important from an environmental and economical point of view. Considering this, the favourable drying technique of residuals involves the use of sand drying beds. However, the factors affecting sand drying beds' operational techniques including chemical conditioning and external weather conditions must also be taken into account. In the following chapter, the effect of meteorological conditions will be reviewed in more detail.

3 Effect of Meteorological Conditions on Residuals Drying

3.1 Introduction

The influence of meteorological conditions on the drying time and rate of residuals is of considerable interest and practical importance. Weather parameters relevant to the residuals drying process include temperature, wind speed, relative humidity, solar radiation, and rainfall. In contemporary society, there is a great need to estimate and accelerate the drying time of residuals as the demand for high quality drinking water continues to increase. Wet weather prolongs the drying period of residuals. This coupled with land availability constraints, has intensified the need for accelerated residuals drying, hence the application of solar energy should become highly desirable. In this chapter, the relationship between heat transfer and residuals drying will be reviewed, as well as the effect of meteorological conditions on residuals drying. Finally, the estimation of residuals drying time and the various drying technologies will be reviewed.

3.2 Meteorological Conditions

The transport mechanisms in the boundary layer of the drying material dominate the constant rate-drying period. The drying rate is affected by external drying conditions (Walker et al. 1993) and (Keey et al. 2000). The transport mechanisms are affected by the weather conditions including wind speed, ambient temperature, solar radiation, rainfall, and relative humidity. The effect of the internal structure of the drying material becomes dominant in the falling rate-drying period; therefore, weather conditions such as high ambient temperature increases the viscosity of water, hence increasing the drying rate. Clark (1970) found that most of the moisture removal (80-85%) during the

drying process happens in the constant rate period; the same value (80%) was found by Ruiz et al. (2006). Weather conditions can favour the use of certain drying processes or technology. In arid areas, drying beds or drying lagoons are more favourable, whereas, covered beds and active drying technologies are used in cold or wet areas. For example, an average drying rate of 8 kg/m²/day, for sewage residuals in Queensland Australia, was achieved, while only 2-3 kg/m²/day occurred in Germany (Shannon et al. 2004). In the following subsections, the effect of various meteorological conditions on the drying rate will be discussed.

3.2.1 Effect of Temperature

The surface of the earth is heated by the incident solar energy, hence heating the air in contact with that surface. The higher the air temperature, the more moisture it can absorb providing the absolute humidity is kept constant therefore increasing the drying rate of the material. Temperature influences the drying rate by increasing the moisture holding capacity of the air, as well as accelerating the diffusion rate of moisture through the drying material.

The effect of temperature on the drying process can be observed in the application of the heat and mass transfer analogy in the process of evaporative cooling. When air flows over the surface of water, evaporation occurs from that surface. The energy used by the phase change is the latent heat of vaporisation of the water. The energy required for evaporation must come from the internal energy of the water, hence creating a reduction in temperature. Applying the conservation of energy to a control surface about the water for a unit surface is given in the following equation:

$$G_{convection} + G_{add} = G_{evaporation} \quad (3.1)$$

Where,

$G_{convection}$ The convection heat flux (W/m²)

G_{add} The added heat flux (W/m²)

$G_{evaporation}$ The evaporation heat flux (W/m²)

Neglecting the added radiation effects or any other heat source, and expanding equation (3.1), the following equation is achieved:

$$h(T_{\infty} - T_{surface}) = nh_{fg} \quad (3.2)$$

Where,

h Heat transfer coefficient (W/m².K)

T_{∞} Ambient air temperature (K)

$T_{surface}$ Surface temperature (K)

n Mass flux of the liquid from the surface (kg/m².s)

h_{fg} Latent heat of vaporization (J/kg)

From equation (3.2) it follows that the drying rate increases with the increase of air temperature as well as the heating rate, which is determined by the heat transfer coefficient.

3.2.2 Effect of Relative Humidity

The relative humidity of air is defined as the partial pressure of water vapour divided by the saturated vapour pressure at the same temperature and total pressure. Mathematically, relative humidity can be expressed:

$$RH = \frac{P_{\infty}}{P_{saturated}} \quad (3.3)$$

Where,

RH Relative humidity (decimal)

P_{∞} Water vapour partial pressure at ambient temperature (kg/m.s²)

$P_{saturated}$ Saturated water vapour partial pressure at ambient temperature (kg/m.s^2)

However, relative humidity is usually expressed as percentage.

If the temperature is kept constant, lower relative humidity results in higher drying rates, due to the increased moisture gradient in the drying material. This stems from the reduction of the moisture content in the surface layers when the relative humidity of air is reduced. For drying, the other essential parameter related to relative humidity is absolute humidity, which is the mass of water vapour per unit mass of dry air ($\text{kg}_{\text{water}} / \text{kg}_{\text{dry air}}$). The capacity of air for moisture removal depends on its humidity and its temperature.

The study of relationships between air and its associated water is called psychrometry. A useful concept in psychrometry is the wet-bulb temperature, as compared with the ordinary temperature, which is called the dry-bulb temperature. The wet-bulb temperature is the temperature reached by the water's surface, as registered by a thermometer bulb surrounded by a wet porous cloth, when exposed to a stream of air. The temperature of the wet porous cloth and the thermometer bulb drops below the dry-bulb temperature; therefore the rate of heat transfer from the warmer air to the wet porous cloth is equal to the rate of heat transfer required for the evaporation of water from the wet porous cloth into the air stream.

The psychrometric chart, which can be found in any standard text (Cengel and Boles, 2006) gives illustrates the relationship between the temperature and the humidity. For example, if the temperature is raised from 20°C to 30°C by keeping the relative humidity constant at 60%, the absolute humidity increases from 0.008 to 0.016 $\text{kg moisture/kg air}$ in other words, the air moisture holding capability doubles.

3.2.3 Effect of Wind Speed

Variations of atmospheric pressure and temperature on the earth's surface cause the movement of air, which produces wind. Drying time depends on the air velocity; at constant temperature and relative humidity, the highest possible drying rate is obtained by higher wind speed across the surface of the drying material. With increased wind speed, the boundary layer over the drying surface becomes small, which improves the heat transfer which in turn increases the evaporation rate of water vapour away from the surface.

The effect of wind speed is shown in convective drying, which is explained by the convective heat transfer (section 3.3). The heat transfer coefficient is a strong function of wind speed; some researchers developed dimensional relationships for the heat transfer coefficient. McAdams (1954) reported a dimensional equation, which relates the heat transfer coefficient with the wind speed:

$$h = 5.7 + 3.8u \quad (3.4)$$

Where,

u The wind speed (m/s)

It is probable that the effects of free convection and radiation are included in this equation, so Watmuff et al. (1977) reported that equation (3.5) should be:

$$h = 2.8 + 3.0u \quad (3.5)$$

Since it is not possible to obtain analytical solutions to convection problems, experimental data can be used from the drying process to obtain values of constants or exponents for certain significant dimensionless parameters, such as the Reynolds number. A dimensionless group known as Nusselt number (after Wilhelm Nusselt), is interpreted as the dimensionless temperature gradient at the drying surface and is related to the heat transfer coefficient in the following equation:

$$Nu = \frac{hL}{k} \quad (3.6)$$

Where,

L The characteristic length (m)

k The thermal conductivity (W/m. K)

A velocity boundary layer develops when there is a fluid flow over a surface; a thermal boundary layer must also develop if the fluid free stream and surface temperatures differ. The thickness of the boundary layer is a function of wind speed, hence the higher the wind speed, the smaller the boundary layer thickness. Therefore, wind speed is considered one of the major meteorological conditions affecting the drying process.

3.2.4 Effect of Solar Radiation

Solar radiation is the main source of energy on the surface of this planet. In a vacuum, all radiant energy travels with the speed of light. The wavelength characterising the electromagnetic wave is related to its frequency by the equation:

$$\lambda_{wave} = \frac{c_{light}}{f} \quad (3.7)$$

Where,

λ_{wave} The electromagnetic wavelength ($\mu\text{m} = 10^{-6} \text{ m}$)

c_{light} The speed of light in vacuum ($2.998 \times 10^8 \text{ m/s}$)

f The frequency of radiation (s^{-1})

The thermal radiation is a small portion ($0.1 - 100 \mu\text{m}$) of the broad electromagnetic spectrum. The propagation of thermal radiation takes place in the form of a photon and each photon having energy of:

$$E = h_{Planck} f \quad (3.8)$$

Where,

E Thermal energy (J)

h_{Planck} Planck's constant (6.625×10^{-34} J.s)

The Stefan-Boltzmann law enables calculation of the amount of radiation emitted in all directions and over all wavelengths, simply from the knowledge of the temperature of the black body (perfect emitter). A mathematical presentation of the law will be presented in section (3.3.1). Solar radiation increases the temperature of the drying material surface; the surface temperature will increase above the wet-bulb temperature, thus increasing the rate of drying (Sherwood, 1929). Increasing the surface temperature of the drying material amplifies the energy of the water molecules, thus allowing the molecules to escape from the surface of the material during the drying process.

Different surfaces absorb or emit solar radiation differently. Absorptivity is a property of the body surface and is dependent on the temperature of the body and the wavelength of the incident radiation. It is a dimensionless value and measured as the fraction of incident radiation that is absorbed by the body. Emissivity is the ratio of radiation emitted by a blackbody or a surface and the theoretical radiation predicted by Planck's law.

3.2.5 Effect of Rainfall

Rainfall has a profound influence upon the total behaviour of the dewatering system of the residuals (Lo, 1971). Precipitation prolongs the drying of residuals, especially when open drying beds or lagoons are used. In countries where wet weather prevails, covered beds, mechanical dewatering equipment and passive or active solar drying systems are used. El-Ariny and Miller (1984), Hossam et al. (1990), and

Luboschik (1999) found that covered solar drying beds improve the drying process by up to 50% in wet climates. On the other hand, in countries where dry weather is dominant, and if land is available, drying lagoons and open sand drying beds are preferred.

During the constant rate period the moisture content is high; rainwater dilutes the residuals, increasing the moisture content. During the falling rate period, when the moisture content is low, rain is partially absorbed by residuals, however most of it drains through the cracks. The most significant work on the effect of rain on the residuals dewatering was performed by Lo (1971), Lo found that the moisture content of residuals after rain, was found to be a function of the moisture content before rain.

3.2.6 Weather Parameters' Relative Contribution for the Drying Process

It is of particular interest to understand the most sensitive weather parameters to the drying process of the water treatment residuals. Shin et al. (2000) found that the moisture content of water treatment residuals was more highly influenced by relative humidity than the temperature of the drying air. Liu et al. (1997) concluded that with regards to food, the drying air humidity, more than any other weather parameters, resulted in the largest change to the overall drying time of food. Vaxelaire et al. (2000b) introduced the drying potential term, which compiles the ambient temperature, relative humidity, and wind speed. The single value gives a good characterisation of the drying kinetics of residuals; however it is difficult to know the single effect of each parameter separately.

3.3 Heat Transfer and Drying of Residuals

In order to dry residuals, heat is required to evaporate water from the bulk of residuals through the drying surface. Energy is transferred to a drying material due to

convection from the atmospheric air, direct solar radiation and heat conduction (Welty et al. 1984). The heat received by a bulk of residuals is transferred by radiation, convection from the bulk of air above the residuals surface and by conduction from its surroundings (i.e. ground). The heat can be lost from the bulk of residuals to the surroundings by convection, radiation, evaporation, and conduction.

When hot air supplies the heat for evaporation in the constant rate period, a dynamic equilibrium establishes the rates of heat transfer to the material, as well as the vapour removal from the surface (McCabe and Smith, 2000). The magnitude of the constant rate evaporation depends upon three factors:

1. The heat or mass transfer coefficient, which is a function of wind speed.
2. The area exposed to the drying medium.
3. The difference in temperature or humidity between the air stream and the wet surface of the solid.

Instrumental to the drying force, is the change of partial pressure between the drying medium, which is air and the surface of the residuals. The temperature of air and its relative humidity at constant pressure, determine its ability to absorb moisture. This is known as the drying potential of air (Strumillo and Kudra, 1986). Shin et al. (2000) performed a study on water treatment plant residuals using a fluidised bed dryer. The results of moisture content versus relative humidity at different temperatures indicated that if residuals were dried at a temperature below the boiling point of water, it is more important to control the relative humidity of the drying air below 30%, rather than increase the temperature of drying air.

Drying of residuals is a complicated process, where moisture is removed from the wet solids on sand drying beds by gravity drainage and by evaporation. The meteorological conditions and the material characteristics affect evaporation. Quon and

Tamblyn (1965) conducted an experiment to calculate the rate of evaporation from sewage residuals surface, finding that it was $(1.5 \times 10^{-4} \text{ Kg/m}^2.\text{s})$ with a radiant intensity of $(767.1 \text{ J/m}^2.\text{s})$. In order to maintain steady state conditions, energy transfer to the water from the surroundings must replenish the latent energy lost by the evaporation of water.

Heat transfer is so important because it gives a clear indication of the rate of heat transferred per unit time, in order to analyse and design a drying system. The time required for a system to be heated or cooled, depends on the difference in temperatures between the system and the surroundings. The rate of heat transferred also depends on the structure, nature, and colour of the material in question. The transport phenomena of heat will be examined in the following subsections.

3.3.1 Radiation Heat Transfer

One of the transport phenomena of heat is radiation. The rate of radiative heat absorbed by a surface can be written as follows:

$$Q_{\text{radiation}} = A \times G_{\text{incident}} \quad (3.9)$$

Where,

$Q_{\text{radiation}}$ Rate of thermal energy by radiation (W)

G_{incident} Incident solar radiation (W/m^2)

A Surface area (m^2)

Cengel (1997) expanded equation (3.10) in the following form:

$$Q_{\text{radiation}} = \alpha_s A (G_{\text{direct}} \cos \theta + G_{\text{diffuse}}) + \alpha_l A G_{\text{sky}} \quad (3.10)$$

Where,

G_{direct} Direct solar radiation (W/m^2)

G_{diffuse} Diffuse solar radiation (W/m^2)

G_{sky}	Sky incident solar radiation (W/m ²)
α_s, α_l	Short and long wave solar radiation absorptivities
θ	Angle of incidence

In addition, equation (3.11) can be further expanded to:

$$Q_{radiation} = \alpha_s (G_{direct} \cos \theta + G_{diffuse}) + A \alpha_l \varepsilon_{atmospheric} \sigma T_{sky}^4 \quad (3.11)$$

Where,

$\varepsilon_{atmospheric}$	Atmospheric emissivity under clear sky
σ	Stefan-Boltzmann constant (5.6697x10 ⁻⁸ W/m ² K ⁴)
T_{sky}	Sky temperature (K)

The rate of the heat emitted by radiation from any drying surface can be written:

$$Q_{radiation} = A \varepsilon \sigma T_{surface}^4 \quad (3.12)$$

Where,

$T_{surface}$	Surface temperature (K)
ε	Emissivity of the surface

Heat transferred by radiation can be categorised as long wave and short wave.

Short wave thermal radiation is limited to the visible light region of the spectrum (0.4 and 0.76 μm) and the part of the ultra-violet radiation, which lies between 0.1 and 0.4 μm . The long wave thermal radiation is in the infrared region of the electromagnetic spectrum (from 0.76 to 100 μm) (Cengel, 1997). The short wave solar radiation can pass through a glass surface, however infrared radiation cannot. This is known as the greenhouse effect, inspiring researchers in the design of passive and active solar systems.

3.3.2 Convection Heat Transfer

Heat transfer by convection occurs between a solid material and an adjacent fluid (gas or liquid) that is in motion. Heat is supplied or lost to the drying material by convection, according to Newton's law of cooling:

$$Q_{convection} = hA(T_{\infty} - T_{surface}) \quad (3.13)$$

The difference between the ambient temperature and the drying surface of the material is the driving force in the transfer of heat by convection. The convection heat transfer can be natural (free) or forced. Buoyancy forces, cause free convection, and external forces, such as blowing air over the drying surface, cause forced convection. The heat transfer coefficient can be expressed in terms of dimensionless parameters to best suit the system conditions.

3.3.2.1 Heat transfer coefficient

The heat transfer coefficient is defined as the rate of energy transferred per unit area per unit temperature difference. The heat transfer coefficient is the proportionality constant in equation (3.14) and is dependant on the conditions in the boundary layer; these are affected by the nature of the fluid motion, surface geometry, and fluid thermodynamics transport properties. The heat transfer coefficient is difficult to calculate and therefore must be estimated experimentally. In convection heat transfer analysis, it is common to use the non-dimensional heat transfer coefficient with the Nusselt number.

Since the Nusselt number is the ratio of the convection heat transfer to the conduction heat transfer, it is a measure of the convection heat transfer effectiveness. Heat transfer between a drying material and a drying agent depends on the influence of the external parameters in which they could be included in dimensionless numbers. One of the dimensionless numbers used in the forced convection analysis is the Reynolds

number, which depends on the wind speed. Another, used in free convection analysis is the Grashof number, which depends on the temperature difference between the material and the drying agent.

3.3.3 Evaporation Heat Transfer

Heat can be released from the drying surface by the change in phase of liquid water into water vapour. Heat transfer rate by evaporation can be expressed by the following equation (Mujumdar, 1987) and (Vaxelaire et al. 1999):

$$Q_{evaporation} = h_{fg} m_{solids} \frac{dX}{dt} \quad (3.14)$$

Where,

$Q_{evaporation}$ Rate of heat transfer by evaporation of water (W)

m_{solids} Mass of solids in the drying material (kg)

dX / dt Change of moisture content with respect to time (s^{-1})

3.3.4 Conduction Heat Transfer

Conduction is the energy transferred from energetic particles of a material to less energetic ones. This type of heat transfer happens in solids, liquids or gases. Heat conduction can be expressed in the differential form:

$$Q_{conduction} = -kA \frac{dT}{dx} \quad (3.15)$$

Where,

$Q_{conduction}$ Rate of heat transfer by conduction (W)

dT / dx Temperature gradient through the material thickness (K/m)

A drying material can gain or lose energy by conduction through the ground or surroundings.

3.4 Estimation of Residuals Drying Time

It is important to estimate the residuals drying time in any water treatment plant. In order to achieve this, the estimation of land and availability of energy sources are important factors to be considered, when designing a suitable drying facility for water treatment plant residuals. There have been few attempts by researchers to develop empirical mathematical models describing the drying time of residuals on sand drying beds.

3.4.1 Drying Bed Loading

Haseltine (1951) developed one of the first empirical relationships describing the time required for residuals to dewater on sand drying beds. This relates the gross bed loading of solids with the initial solids content of the applied residuals. The following equation shows that relationship:

$$S_{gross} = 0.157SC - 0.286 \quad (3.16)$$

Where,

S_{gross} Gross bed loading of solids (kg/m².day)

SC Solids content wet basis (%)

The gross bed loading did not consider the solids content at removal; therefore Haseltine (1951) defined another term, which is the net bed loading depending on his observations that there was a relationship between the solids content and the bed loadings as shown in the following equation:

$$S_{net} = 0.057SC - 0.082 \quad (3.17)$$

Where,

S_{net} Net bed loading of solids (kg/m².day)

3.4.2 Drying Time

Clark (1969) found that the first critical moisture content was inversely proportional to the initial moisture content and the initial depth of the applied water treatment plant residuals, which was expressed by the following empirical relation:

$$X_{critical} = 4000SC_0^{0.32} s_0^{0.2} I_{constant}^{0.5} \quad (3.18)$$

Where,

SC_0 Initial dry solids concentration (%)

s_0 Initial residuals depth applied on the drying bed (cm)

$I_{constant}$ Constant drying rate (kg/m².hr)

Lo (1971) calculated the drying time in the falling rate period as shown in the following empirical equation:

$$T_{Falling} = \frac{2m_{solid} X_{critical}^{0.5}}{100AI_{constant}} (X_{initial}^{0.5} - X_t^{0.5}) \quad (3.19)$$

Where,

$X_{initial}$ Initial moisture content as dry basis (%)

X_t Moisture content at time t as dry basis (%)

Another attempt was done by Rolan (1980) to determine the drying time of residuals on sand drying beds, ignoring the first one or two days of drainage and assuming both the evaporation rate and the resultant changes in depth to be linear. Rolan (1980) expressed the drying time in months to be as follows:

$$T = \frac{s}{E} \quad (3.20)$$

Where,

s Change in depth due to water loss by evaporation (mm)

E Rate of evaporation (mm/month)

Albertson et al. (1991) estimated the drying time for a single residuals application using the following empirical equation:

$$t_d = \frac{D_0 (1 - SC_0 / SC_f) (1 - W_{Drainage})}{k_e E_{pan}} \quad (3.21)$$

Where,

- t_d De-watering time for a single application (months)
- D_0 Initial depth of applied residuals layer (cm)
- SC_0 Initial dry solids concentration (%)
- SC_f Final dry solids concentration (%)
- $W_{Drainage}$ Fraction of water removed by drainage (decimal)
- k_e Reduction factor for residuals evaporation versus a free water surface, decimal (0.6 a pilot study is recommended to determine this value)
- E_{pan} Average pan evaporation during time t_d (cm/month)

The final depth of the dewatered residuals can be estimated by the following formula:

$$D_f = D_0 \frac{SC_0}{SC_f} \quad (3.22)$$

Where,

- D_f Final depth of dewatered residuals cake (cm)

Cornwell and Vandermeiden (1999) developed three empirical models, based on the previous work of Rolan (1980), which used data from a pilot test program to determine the optimal size of non-mechanical dewatering systems.

The previously mentioned studies did not consider the meteorological conditions in their predictions of the residuals drying time. However, Cornwell and Vandermeiden (1999) concluded that any model used to determine a drying bed design should consider

local climate factors. The critical moisture content, which is the main feature of Clark (1969) and Lo (1971), varies with the thickness of the material and with the rate of drying as reported by McCabe and Smith (2000). In practice, residuals are removed (around 30-50% solids content) from the drying beds before reaching the equilibrium moisture content.

3.4.3 Design Parameters of Drying Beds

Albertson et al. (1991) estimated the number of applications during the operating season by:

$$N = \frac{L_{OS} E_{pan, L_{OS}} k_e}{D_0 (1 - SC_0 / SC_f) (1 - W_{Drainage})} \quad (3.23)$$

Where,

N Number of residuals applications

L_{OS} Length of operating season (months)

$E_{pan, L_{OS}}$ Average pan evaporation during the period L_{OS} (cm/month)

Albertson et al. (1991) estimated the solids loading by the following equation:

$$S_{loading} = C_{factor} SC_0 \frac{L_{OS} E_{pan, L_{OS}} k_e}{(1 - SC_0 / SC_f) (1 - W_{Drainage})} \quad (3.24)$$

Where,

$S_{loading}$ Solids loading during the period L_{OS} (kg/m²)

C_{factor} Conversion factor (10.4) (assuming specific gravity of residuals 1.04)

Researchers were trying to estimate the dewatering and drying time of residuals on sand drying beds, using experimental techniques by making assumptions in order to simplify their empirical relationships. The knowledge of constant drying rate or the average pan evaporation, as seen in the previously mentioned empirical models,

requires monitoring of weather conditions. However, weather conditions vary all the time and the need arises to develop a model, which takes into account these variations with respect to time. Increased demand on energy resources, and the related increase of energy costs, has lead to high operation costs of the various drying processes. The use of fossil fuel energy supplies increases the pollution of the environment. Many researchers have estimated the drying process in an attempt to save energy and transport costs underlining the importance to accelerate the process using renewable technologies.

3.5 Solar Drying Technologies

Solar energy is the origin of all sources of energy available on the surface of the Earth. Therefore, solar energy is being used in one form or another in daily life; it is a constant, free, and clean energy. For example, solar technologies can be employed cheaply during simple passive drying techniques, such as foods. On the other hand, when using solar collectors or photovoltaic cells, solar technology is relatively expensive. The rising issue of environmental problems, including air, noise and water pollution have placed enormous pressure to optimise clean and cheap renewable energy sources. Solar drying is a technology suitable for producing dry material of particular water content, at an economical price.

Applying solar drying techniques in order to achieve an efficient drying process of residuals can be effective. The drying processes can be improved by using some form of heat storage for when sunlight is less available, as this ensures the drying period can be extended, using surplus energy. Efforts to improve the solar drying process have included the use of forced air circulation, in combination with other drying processes, such as conventional drying processes.

3.5.1 Types of Solar Radiation

The major factor of the drying process is the solar radiation, which supplies the required energy to evaporate water from any drying surface. There are three types of solar radiation; the first type is called the beam or direct radiation, which travels from the sun to a point on the earth with negligible change in direction. This type casts a sharp shadow and on a sunny day, it can be as much as 80% of the total sunlight striking a surface. The second type is diffused or scattered sunlight, which comes from all directions in the sky-dome, rather than the direction of the sun. Scattering of sunlight produces this type of radiation by atmospheric components such as particles or water vapour. On a cloudy day, the sunlight is 100% diffused. The third type of radiation, sometimes present at the glazing of a solar collector or a window, is known as reflected radiation. Reflected radiation is either diffused or direct radiation reflected from the foreground onto the solar aperture.

3.5.2 Solar Angles

In solar design, it is important to locate the sun in the celestial sphere at any time of the day. The Solar Altitude Angle (*ALT*) is measured upward from the local horizontal plane to a line between the observer and the sun. The Azimuth Angle (*AZM*) is measured in the horizontal plane between the due-north (due-south) direction and the projection of the sun-earth line onto the horizontal plane, as shown in Figure 3.1 Solar altitude and azimuth angles can be calculated from the following spherical trigonometry equations:

$$ALT = \sin^{-1}[\cos(DEC)\cos(LAT)\cos(HOUR) + \sin(DEC)\sin(LAT)] \quad (3.25)$$

Where,

DEC Solar declination angle (degrees)

LAT Latitude of particular site of interest (degrees)

HOURL Hour angle, number of hours between solar noon and the time of interest
multiplied by $15^\circ/\text{hr}$ (noon = 0°)

$$AZM = \sin^{-1}[\cos(DEC)\sin(HOUR)/\cos(LAT)] \quad (3.26)$$

$$DEC = -23.45^\circ \times \cos[0.986(DAY + 10.5)] \quad (3.27)$$

Where,

DAY Day number counted from January 1

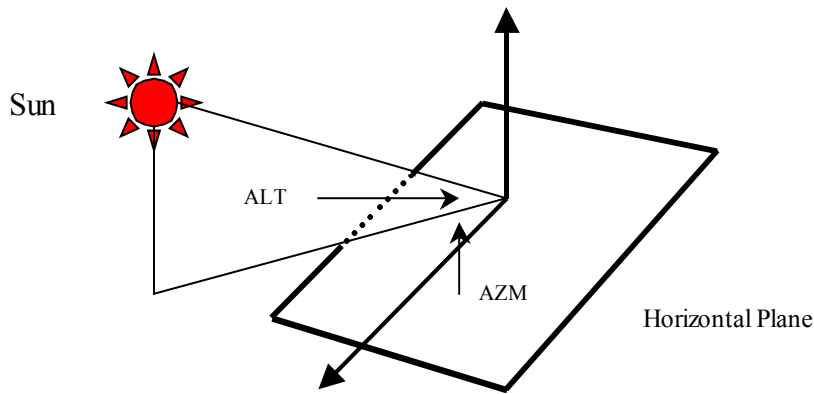


Figure 3.1 Solar altitude angle ALT and solar azimuth angle AZM, (Kreider et al. 1989)

The other angle that is useful in solar design is the incident angle *INC*. This is the angle between beam radiation from the sun and a line constructed perpendicular to an irradiated surface. In the northern hemisphere the incident angle is calculated from the following equation:

$$INC = \cos^{-1} \left[\frac{\cos(DEC)\cos(LAT - TILT)\cos(HOUR) + \sin(DEC)\sin(LAT - TILT)}{\sin(LAT - TILT)} \right] \quad (3.28)$$

Where,

TILT The tilt angle (degrees)

It is important to optimise the tilt angle of the solar collector; therefore, Equations (3.26) through (3.29) are useful in solar design in both the passive and active solar equipment.

3.5.3 Solar Radiation and Drying

Solar radiation can be utilised in the applications of different solar systems to improve the drying process. Radiation is effective in increasing the constant rate period by augmenting the convection heat transfer and raising the surface temperature above the wet-bulb temperature (Perry and Green, 1997). This fact has encouraged researchers to use solar radiation in the drying process, thus maximising the efficiencies of the solar drying equipment.

3.5.3.1 *Passive Solar Systems*

The application of passive solar systems in the drying of residuals has not been found in any relevant literature. Researchers applied passive solar systems mainly in the field of solar distillation. The first application of solar distillation was in 1872 in Chile (Duffie and Beckman, 1991), when a still was used to provide drinking water for animals used in nitrate mining. Since that time, most stills have been based on the same concept. It has been observed that most of the research conducted in this field, was done in the last decade of the twentieth century, mainly in Middle Eastern countries and India. Mohammad et al. (1995) conducted an experimental and financial investigation of three asymmetric solar stills. The stills have the same dimensions, with (20°) cover inclination angle. The bottom and sides of the stills are insulated with 50 mm thick polyurethane rigid foam, glass wool and sawdust. The annual production of distillate was higher using the polyurethane insulation, but with higher annual total cost. Porta et al. (1997) performed an experiment on a shallow solar still of an average distance

between the bottom tray and glazing 0.072 m. The cover tilt is 4° with respect to the horizontal. The average production is $4.9 \text{ L/m}^2\text{-day}$.

An attempt to study the drying of residuals in an experimental passive solar drying bed was performed by Gharaibeh et al. (2003). The solar bed was a distillation type still shape, with a glass sloped cover. It was found that there was no significant advantage in using the passive solar bed.

3.5.3.2 Active Solar Systems

Active solar systems were mainly used in the field of distillation. El-Haggag and Awn (1993) mounted the solar still unit on a greenhouse; it was found that the distilled water output was adequate for both greenhouse agriculture and drinking water. Zaki et al. (1993) performed a study on a solar still coupled to an external assisting solar collector. It has been found that by increasing the solar flux, the yield increases. An inclined flat-plate, wick-type solar still has been equipped with a V-trough solar concentrator. The performance of this combination has been investigated by Mahdi and Smith (1994). It has been observed that this combination can lead to an increase in still efficiency on clear days in winter, rather than on clear days in summer.

A double effect active solar distillation unit has been analysed by Prasad and Tiwari (1996). The unit has two basins; the bottom basin receives thermal energy from the solar radiation through the glass covers and the water mass in the upper basin, as well as the compound parabolic concentration collector. A substantial yield (up to 12 kg/day) has been achieved.

To achieve maximum yield from a solar still, Tiwari et al. (1997) used a double glass- cover solar still to maintain higher water temperatures, similar to the case of a flat plate collector. Upward heat loss is reduced, in contrast to the single glass cover solar still. This still has also a double-condensing chamber where the enclosure is separated

by a partial wall. The solar radiation is reflected to the water mass in the still by a mirror in the first chamber, which is fitted on the partition wall. The performance of the double-condensing chamber still gives a higher daily output of about 35-77% over the conventional solar still.

Ghoneym and Ileri (1997) have designed, constructed, and tested four single-effect basin type solar stills. The first three had glass covers; the thicknesses being 3, 5, and 6 mm, the fourth had a plastic cover. The effect of the glass thickness was considerable, still 1 (3 mm) production rate was about 0.03 Kg higher than that of still 2 (5 mm) and 0.04 Kg higher than that of still 3 (6 mm). The fourth still with the plastic cover had a reduced output, due to fogging and dripping from the cover back to the water mass. For the maximum radiation intensity $29 \text{ MJ/m}^2\cdot\text{day}$, the average daily outputs were 3.3, 2.7, and 2.6 $\text{Kg/m}^2\cdot\text{day}$ for stills 1, 2, and 3, respectively. For the maximum ambient temperature (37°C), the productivity of the three stills were 3.4, 2.75 and 2.6 $\text{Kg/m}^2\cdot\text{day}$, respectively.

A parametric study of an inverted absorber double-effect solar distillation system was conducted by Suneja et al. (1997). They have observed that an inverted absorber solar still gives a higher output than the conventional double-effect.

In the field of residuals drying, an experiment was conducted by El-Ariny and Miller (1984) using solar heated residuals drying beds together with a normal drying bed. The solar experimental bed was a greenhouse type bed with a sloping roof; the bed enclosure was covered with translucent acrylite sheets. These sheets were clear and colourless with light transmission of 92 %. The bed was equipped with five air outlet louvers, opposite the hot air inlet nozzles. Hot air was forced through an array of 16 flat-plate, air-type solar collectors and into the drying bed. In this experiment, it was found that a reduction of 45 percent in the size of covered residuals drying bed area

could be achieved. Accordingly, the land and construction costs are also reduced. For the sewage residuals, El-Ariny and Miller (1984) found that the related odour disappears after few days in the solar drying beds. This indicates that heat destroys the microorganisms in these residuals.

More recently, new techniques using solar energy have been used in the drying of residuals. These techniques include covered beds, air-heated beds and beds having active solar energy collectors. Marklund (1990) recommended further studies should be directed towards full-scale tests with covered drying beds, the action of airflow, humidity and factors affecting the falling rate period, as major points of interest.

An experimental study was conducted by Hossam et al. (1990) to use solar air heated drying beds in comparison with conventional sand drying beds. It was concluded that solar heated drying beds save about 35% of the conventional bed area. Solar air heated drying beds cut the drying time; from 18 days to 8 days and the costs of the solar air heated drying beds are less than those of the conventional sand drying beds. The climatic conditions in Alexandria (Egypt), where the experiment was conducted, were generally favourable for de-watering residuals on sand drying beds except when there was heavy rainfall during the wet season, which prolonged the drying time. The covered bed loading was 248 Kg (solids)/m²/year compared to 147 Kg (solids)/m²/year for conventional sand drying beds.

Luboschik (1999) developed a process as part of a research project in Germany. This process is a greenhouse type solar drying bed equipped with an air exhaust duct. Air in the duct is exhausted by gravitational circulation, and to accelerate transport of moist air, ventilators are activated when required. In this drying process, it was found that drying time was dependent on the initial moisture content and the natural radiation.

Shannon et al. (2004) published their operational experience using the “Solar Mix” facility, which was supplied by Mixwell Pty. Ltd. The solar residuals greenhouse dryer hall was installed in Burpengary East Sewage Treatment Plant, north of Brisbane, Australia. This technology is successfully used in Germany and some other European countries, obviously utilising the same principal as that of the Luboschik project (1999). In areas where temperatures reached up to 65 °C, average drying rates of eight kg/m²/day were achieved. On the other hand, in Germany and mid Europe 2-3 kg/m²/day were achieved.

In the previous studies, experiments were performed on sewage residuals, with only one study reported on solar drying of water treatment plant residuals. Gharaibeh et al. (2003) performed this study using an experimental covered sand bed. A fan heater was designed to supply hot air through holes at the front of the bed, the air then leaving via an opening at the back of the bed. It was found that the drying time could be reduced by 33% of that of the normal drying bed.

The previous studies on residuals drying predominantly overlook the effect of weather conditions when modelling the water treatment plant residuals drying process. Weather condition will be always the decisive factor on the drying process of residuals and other materials.

3.6 Summary

The effect of meteorological conditions on the drying of water treatment plant residuals was critically reviewed. The meteorological parameters that influence the drying process were relative humidity, wind speed, ambient temperature, rainfall, and solar radiation. The most influential parameters on the drying process of residuals were rainfall, relative humidity, and wind speed. The supply of heat to evaporate the moisture

from residuals, through heat transfer, is an important phenomenon in the process of drying. Heat is transferred to and from the residuals by convection, conduction, radiation, and evaporation. Researchers made many attempts to estimate the water treatment residuals drying time by developing empirical models. The most important work to determine the drying time of residuals on sand drying beds has been performed by Clark (1969) and Lo (1971), however, another attempt has been done by Rolan (1980). Based on the work of Rolan (1980), Cornwell and Vandermeiden (1999) developed three empirical models to determine the size of non-mechanical dewatering systems.

Solar drying technologies can be applied to achieve efficient solar dryers for the drying of residuals. The solar design depends on the knowledge of the spherical trigonometric equations to calculate the position of the sun at any time of the day; some basic design equations were identified. Passive and active solar drying technologies were reviewed, no passive solar drying residuals systems were reported in the literature; however, many active solar systems were reported. The theory presented in this chapter can be applied in the development of the mathematical drying model of the water treatment residuals in chapter 4.

4 Mathematical Model for Residuals Drying

4.1 Introduction

Dewatering and drying of residuals are extremely energy intensive processes, which are necessary to reduce the quantity of wet residuals produced from the water and wastewater treatment operations. Meteorological conditions are a major factor in the drying of residuals, which can greatly affect the drying period.

A mathematical model is developed for the process of drying of water treatment residuals. A steady-state heat balance equation is applied for a control volume of residuals that takes into account the heat transfer by radiation, convection and evaporation. The model can be used to predict the drying time of a given application of water treatment residuals with the knowledge of meteorological conditions. A heat balance approach can be utilised to predict the drying process of residuals reasonably well.

This chapter is dedicated to predicting the drying time of water treatment plant residuals. In order to achieve this, a steady-state heat balance approach has been applied to a control volume of residuals, taking into account the heat transfer by radiation, convection and evaporation. A non-dimensional heat transfer relationship has been developed to predict the convective heat transfer for a given control volume of residuals. Since drying rates vary with changing weather conditions, in this case, the drying process will not be effectively represented with regards to moisture content. The developed model predicts the change of moisture content with respect to time. Moisture content can then be transformed into solids content versus time, therefore allowing for easier graphical representation. A finite difference technique has been used in the cumulative moisture content calculation of time intervals, in order to achieve the

desired moisture content with the knowledge of weather parameters. A schematic diagram shows a detailed presentation of this chapter in Figure 4.1.

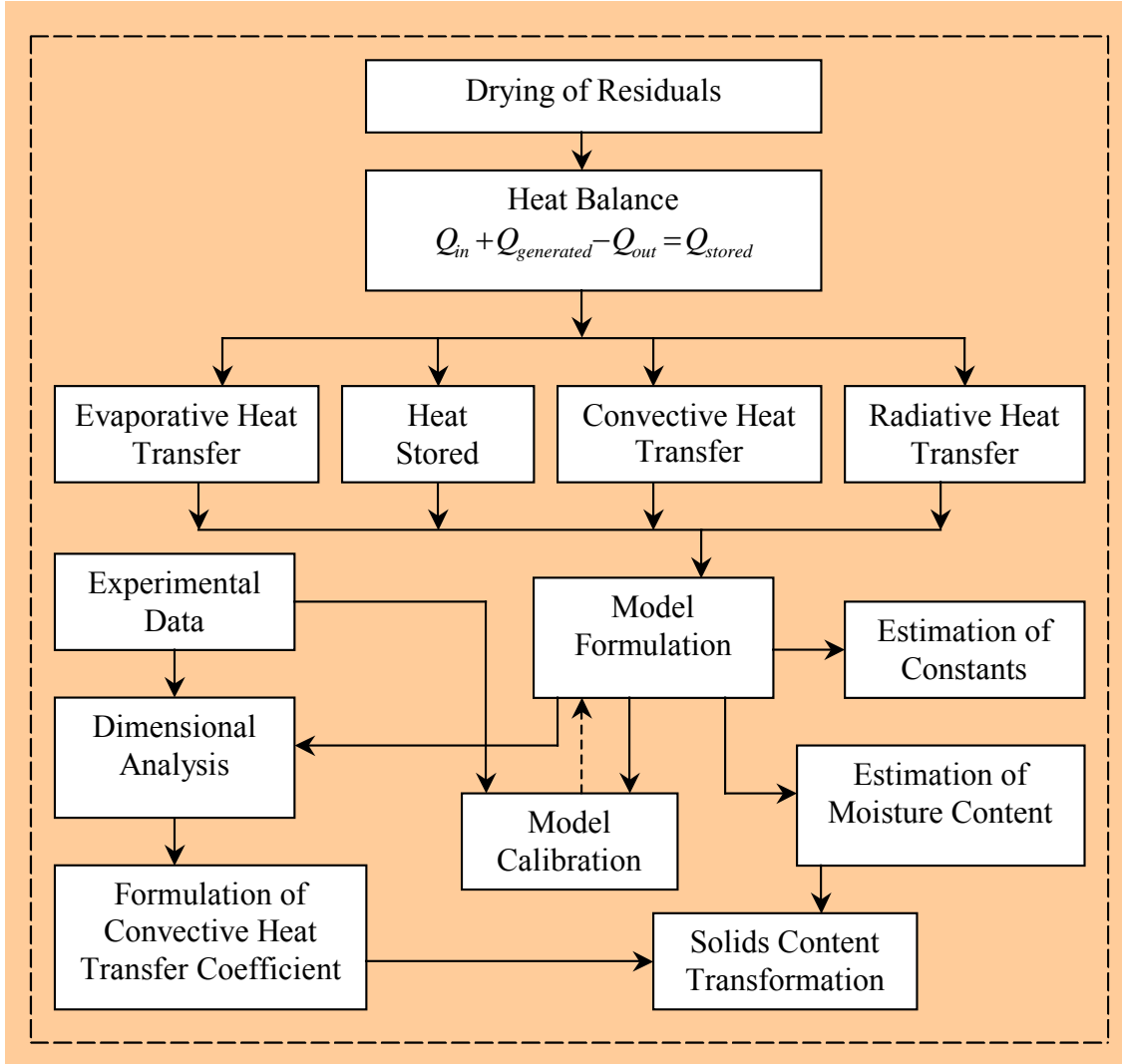


Figure 4.1 Schematic diagram showing a detailed presentation of the model

4.2 Basic Heat Balance

Consider a rectangular control volume (open system) of residuals having an area A and a small thickness s as shown in Figure 4.2. Since the residuals are exposed to air, water will evaporate from the control volume through the control surface A to the open atmospheric bulk of air above the residuals volume. The water evaporates and the solids remain within the control volume, so the moisture content X becomes less with time t .

The temperature is assumed uniform throughout. Heat can be transferred in and out of the control volume via convection, radiation, evaporation and conduction. Water vapour leaves the control volume through the control surface A .

At any time t , rate of thermal energy Q enters the control volume by convection from the bulk of air above it and/or by direct and diffuse solar radiation. The thermal energy also leaves the control volume by convection, radiation, evaporation and conduction. At any time t , there will be some rate of thermal energy stored Q_{stored} in the control volume. However, there will be no energy generated in this control volume.

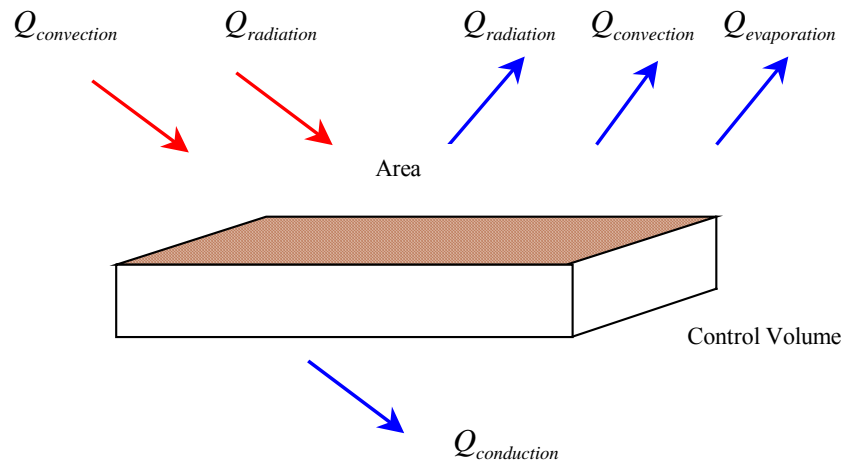


Figure 4.2 Heat balance of a control volume of residuals

The aim is to find the moisture content X ($\text{kg}_{\text{water}} / \text{kg}_{\text{dry solids}}$) of the residuals at any time t (s) under the effect of various weather conditions. To achieve this goal, the basic heat balance equation can be written over the control volume in the general form as:

$$Q_{in} + Q_{generated} - Q_{out} = Q_{stored} \quad (4.1)$$

Where,

Q_{in} Rate of thermal energy input (W)

Q_{out} Rate of thermal energy output (W)

Q_{stored} Rate of thermal energy stored in the control volume (W)

$Q_{generated}$ Rate of thermal energy generated within the control volume (W)

Expanding equation (4.1) gives us the following equations:

$$Q_{in} = Q_{radiation} + Q_{convection} \quad (4.2)$$

$$Q_{out} = Q_{radiation} + Q_{convection} + Q_{conduction} + Q_{evaporation} + Q_{conduction} \quad (4.3)$$

Where,

$Q_{radiation}$ Rate of thermal energy by radiation (W)

$Q_{convection}$ Rate of thermal energy by convection (W)

$Q_{conduction}$ Rate of thermal energy by conduction (W)

$Q_{evaporation}$ Rate of thermal energy by evaporation (W)

Substituting equations (4.2) and (4.3) in equation (4.1) and assuming no heat generation within the control volume and arranging gives:

$$(Q_{radiation} + Q_{convection})_{in} = (Q_{radiation} + Q_{convection} + Q_{conduction} + Q_{evaporation} + Q_{conduction})_{out} + Q_{stored} \quad (4.4)$$

The rate of heat lost by conduction to the ground can be considered negligible if the control volume is well insulated. Equation (4.4) can be reduced into the following form:

$$(Q_{radiation} + Q_{convection})_{in} = (Q_{radiation} + Q_{convection} + Q_{evaporation})_{out} + Q_{stored} \quad (4.5)$$

4.2.1 Radiative Heat Transfer

The rate of radiative heat absorbed by the control surface in the left hand side of equation (4.5) can be written as follows:

$$(Q_{radiation})_{in} = A \times G_{incident} \quad (4.6)$$

Where, $G_{incident}$ is the incident solar radiation on the residuals surface.

Cengel (1997) expanded equation (4.6) in the following form:

$$(Q_{radiation})_{in} = \alpha_s A (G_{direct} \cos \theta + G_{diffuse}) + \alpha_l A G_{sky} \quad (4.7)$$

Where,

G_{direct}	Direct incident solar radiation (W/m ²)
$G_{diffuse}$	Diffuse incident solar radiation (W/m ²)
G_{sky}	Sky incident solar radiation (W/m ²)
α_s	Short wave solar radiation absorptivities of residuals surface
α_l	Long wave solar radiation absorptivities of residuals surface
θ	Angle of incidence

In addition, equation (4.7) can be further expanded to:

$$(Q_{radiation})_{in} = \alpha_s (G_{direct} \cos \theta + G_{diffuse}) + A \alpha_l \varepsilon_{atmospheric} \sigma T_{sky}^4 \quad (4.8)$$

Where,

$\varepsilon_{atmospheric}$	Atmospheric emissivity under clear sky
σ	Stefan-Boltzmann constant (5.6697x10 ⁻⁸ W/m ² K ⁴)
T_{sky}	Sky temperature (K)

The rate of the heat emitted by radiation from the control surface in the right hand side of equation (4.5) can be written:

$$(Q_{radiation})_{out} = A \varepsilon \sigma T_{surface}^4 \quad (4.9)$$

Where,

$T_{surface}$	Surface temperature of residuals (K)
ε	Emissivity of the residuals surface

The sky temperature is measured by an empirical relation found by Berdahl and Martin (1984), which can be related to the dew temperature T_{dew} ($^{\circ}\text{C}$), the ambient temperature T_{∞} (K), and the time t (hours) is measured from midnight as the starting point, by the following equation:

$$T_{sky} = T_{\infty} \left(0.711 + 0.0056T_{dew} + 0.000073T_{dew}^2 + 0.013 \cos(15t) \right)^{0.25} \quad (4.10)$$

The dew temperature can be estimated using the following equation (Palanz, 1984):

$$T_{dew} = \frac{237.7 \ln(p_{\infty}) - 430.22}{19.08 - \ln(p_{\infty})} \quad (4.11)$$

Where,

p_{∞} Water vapour partial pressure at the ambient temperature (kg/m.s^2)

The water vapour partial pressure can be expressed in the following equation:

$$p_{\infty} = RH \times p_{saturated} \quad (4.12)$$

The saturated partial pressure $p_{saturated}$ can be calculated from the following expression (Murray 1967):

$$p_{saturated} = 611 \times 10^{\left(\frac{7.5T_{\infty}}{237.7 + T_{\infty}} \right)} \quad (4.13)$$

Where,

T_{∞} Ambient temperature in degrees ($^{\circ}\text{C}$)

Brutsaert (1982) expressed the atmospheric emissivity under clear skies in the following formula:

$$\epsilon_{atmospheric} = 1.24 \left(\frac{p_{\infty}}{T_{\infty}} \right)^{1/7} \quad (4.14)$$

Where,

p_{∞} Water vapour partial pressure (millibars)

When drying occurs in an enclosure, the ambient temperature replaces the sky temperature as expressed by Cengel (1997), in the following equation:

$$(Q_{\text{radiation}})_{\text{in}} = \alpha_s A (G_{\text{direct}} \cos \theta + G_{\text{diffuse}}) + A \alpha_l \sigma T_{\infty}^4 \quad (4.15)$$

Where,

T_{∞} Ambient temperature in degrees (K)

4.2.2 Convective Heat Transfer

In the right hand side of equation (4.5), the heat lost by convection can be expressed by:

$$(Q_{\text{convection}})_{\text{out}} = hA(T_{\text{surface}} - T_{\infty}) \quad (4.16)$$

Where,

h Heat transfer coefficient ($\text{W}/\text{m}^2 \cdot \text{K}$)

T_{∞} Ambient temperature (K)

In the left hand side of equation (4.5) and in the same way heat is supplied to the control volume by convection according to Newton's law of cooling:

$$(Q_{\text{convection}})_{\text{in}} = hA(T_{\infty} - T_{\text{surface}}) \quad (4.17)$$

4.2.3 Evaporative Heat Transfer

Heat can be released from the control surface of the residuals by the change in phase of liquid water into water vapour. Heat rate by evaporation can be expressed by the following equation (Mujumdar, 1987) and (Vaxelaire et al. 1999):

$$Q_{\text{evaporation}} = h_{fg} m_{\text{solids}} \frac{dX}{dt} \quad (4.18)$$

Where,

$Q_{\text{evaporation}}$ Rate of heat by evaporation of water (W)

h_{fg} Latent heat of vaporization (J/kg)

m_{solids} Mass of solids in the residuals application (kg)

4.2.4 Heat Stored

The heat stored within the control volume of the residuals can be estimated from the following equation:

$$Q_{stored} = m_{residuals} c \frac{dT_{surface}}{dt} \quad (4.19)$$

Where,

$m_{residuals}$ Mass of residuals (kg)

c Specific heat of residuals (J/kg.K)

Strumillo and Kudra (1986) expanded equation (4.19) in the following form:

$$Q_{stored} = \frac{d}{dt} [(m_{solids} c_{solids} + m_{water(i)} c_{water}) T_{surface}] \quad (4.20)$$

Where,

c_{solids} Specific heat of solids (J/kg.K)

$c_{water(i)}$ Specific heat of water at the initial moisture content (J/kg.K)

Substituting equations (4.8), (4.9), (4.17), (4.18) and (4.20) in equation (4.5) gives us:

$$\alpha_s A (G_{direct} \cos \theta + G_{diffuse}) + A \alpha_l \varepsilon_{atmospheric} \sigma T_{sky}^4 + A h (T_{\infty} - T_{surface}) - A \varepsilon \sigma T_{surface}^4 - h_{fg} m_{solids} \frac{dX}{dt} = \frac{d}{dt} [(m_{solids} c_{solids} + m_{water(i)} c_{water}) T_{surface}] \quad (4.21)$$

4.3 Non-dimensional Heat Transfer Coefficient

In order to predict the moisture content using equation (4.21), all the variables are either measured or obtained from the literature. The measured variables are the ambient temperature, surface temperature, and weight of residuals. The constants found in the

literature include absorptivity, emissivity and latent heat of vaporization. In this study, an attempt was made to predict the heat transfer coefficient for the water treatment plant residuals. If drying occurs in the absence of short wave heat radiation and the heat stored term is considered negligible in equation (4.21), the equation becomes:

$$A\alpha_l\sigma T_\infty^4 + Ah(T_\infty - T_{surface}) - A\varepsilon\sigma T_{surface}^4 - h_{fg}m_{solids}\frac{dX}{dt} = 0 \quad (4.22)$$

Solving for the heat transfer coefficient h , equation (4.21) becomes:

$$h = \frac{(\varepsilon\sigma T_{surface}^4 - \alpha_l\sigma T_\infty^4 + h_{fg}m_{solids}(dX/dt))}{A(T_\infty - T_{surface})} \quad (4.23)$$

Equation (4.23) predicts the experimental values of the heat transfer coefficient assuming the emissivity and absorptivity values (0.9) and by substituting the experimentally measured values of the evaporated water term.

In practice, heat transfer coefficient is expressed as a non-dimensional quantity and is usually related to other known non-dimensional numbers. This relationship can be obtained from dimensional analysis. The convective heat transfer coefficient is a strong function of wind speed. Other factors, which have influence on the heat transfer coefficient, could be the difference of temperature between the residuals and the drying medium (air), relative humidity, the surface area and the thickness of the application.

Using the Buckingham Pi theorem (Munson et al, 1994) a relationship was formulated to predict the heat transfer coefficient in the following form:

$$Nu = \frac{hL}{k} = \gamma Re^a Gr^b \left(\frac{L}{s}\right)^c RH^d \quad (4.24)$$

Where,

γ, a, b, c, d Empirical constants

k Thermal conductivity of humid air (J/m².K)

L Characteristic length of the application of residuals (m)

Nu	Dimensionless Nusselt number = hL/k
Re	Reynolds number = uL/ν
u	Wind speed (m/s)
ν	Kinematic viscosity of air (m^2/s)
Gr	Grashof number = $\beta g L^3 \Delta T / \nu^2$
β	Coefficient of volume expansion = $1/((T_{\infty} + T_{surface})/2)$ (K^{-1})
g	Gravitational acceleration ($9.8 m/s^2$)
ΔT	Temperature difference between the air and the residuals surface (K)
s	Application thickness (m)
RH	Relative humidity of air (decimal)

Performing linear regression analysis of the logarithmically transformed data obtained from 23 drying tunnel experiments ($R^2=0.968$), the coefficients of equation (4.24) were determined and given as:

$$\frac{hL}{k} = 890.36(Re^{1.192}) (Gr^{-0.927}) \left(\frac{L}{s}\right)^{0.0628} (RH^{-1.997}) \quad (4.25)$$

The heat transfer coefficient calculated from equation (4.25) is then inserted in equation (4.21) where moisture content can be calculated with respect to time.

4.4 Estimation of Constants

Equation (4.21), including the heat transfer coefficient term, requires the use of some constants from the thermo-physical properties tables of air and saturated water, which were adapted from Incropera and Dewitt (1996). These constants change with changing temperature. For continuous calculation, using an Excel spreadsheet it is convenient to correlate these constants with temperature. The latent heat of vaporisation for saturated water can be estimated by the following equation:

$$h_{fg} = (2502.2 - (2.386 \times T_{\infty})) \times 1000 \quad (4.26)$$

Where,

h_{fg} Latent heat of vaporization (J/kg)

T_{∞} Ambient temperature in degrees ($^{\circ}\text{C}$)

The kinematic viscosity and thermal conductivity of air can be estimated from the following equations:

$$\nu = (9 \times 10^{-11}) T_{\infty}^2 + (4 \times 10^{-8}) T_{\infty} - (5 \times 10^{-6}) \quad (4.27)$$

$$k = (-3 \times 10^{-8}) T_{\infty}^2 + (9 \times 10^{-5}) T_{\infty} + 0.0008 \quad (4.28)$$

Where,

T_{∞} Ambient temperature in degrees (K)

4.5 Solids Content Calculation

The estimation of moisture content using equation (4.21) can be transformed to solids content using the following equation:

$$SC = \frac{100}{1 + X} \quad (4.29)$$

The results of moisture content can then be plotted against time to show the drying time of a given mass of residuals.

4.6 Finite Difference Calculation

Equation (4.21) has been used to calculate the moisture content. The calculation begins with the initial moisture content, which is measured using the moisture analyser or any other technique. The moisture content calculation has been performed in a specific time frame; the value can then be deducted from the initial moisture content,

until the final moisture content has been achieved. The calculation is shown in the following equation:

$$X_n = X_0 - Z_1 - Z_2 - Z_3 - \dots - Z_n \quad (4.30)$$

Where,

X_n Moisture content at time n (kg_{water} / kg_{dry solids})

X_0 Moisture content at time zero (kg_{water} / kg_{dry solids})

$Z_{1,2,3,\dots,n}$ Change of moisture content (dX / dt) at times 1,2,3,..., n (s⁻¹)

Whereas,

$$Z_{1,2,3,\dots,n} = X_{0,1,2,\dots,n-1} - X_{1,2,3,\dots,n} \quad (4.31)$$

The calculation of equations (4.30) and (4.31) is explained in Table 4.1.

Table 4.1 Moisture content calculation

Time Interval	Moisture Content/Time (dX/dt)	Moisture Content
-	-	X_0
t_1	$Z_1=(dX/dt)_1$	X_1
t_2	$Z_2=(dX/dt)_2$	X_2
t_3	$Z_3=(dX/dt)_3$	X_3
-	-	-
-	-	-
-	-	-
-	-	X_{n-1}
t_n	$Z_n=(dX/dt)_n$	X_n

4.7 Summary

In this chapter, a new drying model has been developed in order to predict the drying time of water treatment plant residuals with the knowledge of meteorological conditions. A steady state heat balance equation was formulated over a control volume of residuals application thickness in order to predict the moisture content of residuals for a given time. The heat balance takes into account heat transmission by radiation, convection and evaporation. A convective heat transfer coefficient was formulated using dimensional analysis (Buckingham Pi theorem). Performing linear regression analysis of the logarithmically transformed data obtained from 23 drying tunnel experiments ($R^2=0.968$), the coefficients of the heat transfer coefficient relationship were determined. Correlations to estimate kinematic viscosity, thermal conductivity and the latent heat of vaporisation constants used in the model, has been shown as well as the calculation of solids content and prediction of the model using the finite difference technique.

5 Materials and Methods

5.1 Introduction

The residuals used in this study originated from Illawarra Water Treatment Plant located in Kembla Grange, on the eastern coast of New South Wales. Raw water is sourced from Avon reservoir. Avon reservoir is situated west of the Illawarra region in a plateau 300 metres above sea level (Figure 5.1). Equipment for the field experiments includes the experimental sand drying beds and the meteorological monitoring station in order to measure weather parameters. An air conditioning unit, which is capable of controlling the wind speed, has been used in the drying tunnel experiments. The air conditioning unit has provisions to control the temperature and relative humidity of air within reasonable tolerances. The modified duct was attached at the air exit of the air conditioning unit. The top loading balance was used to continuously weigh the residuals tray, and the data logger to store the various weather parameters. The moisture content measurement was obtained using a moisture analyser.

The objective of this chapter is to describe the nature of the ferric chloride residuals, together with the equipment and instruments used in this study. The equipment includes experimental drying beds, drying tunnel, weather monitoring station, moisture analyser and measuring instruments. Finally, sample collection and analysis techniques will be discussed.

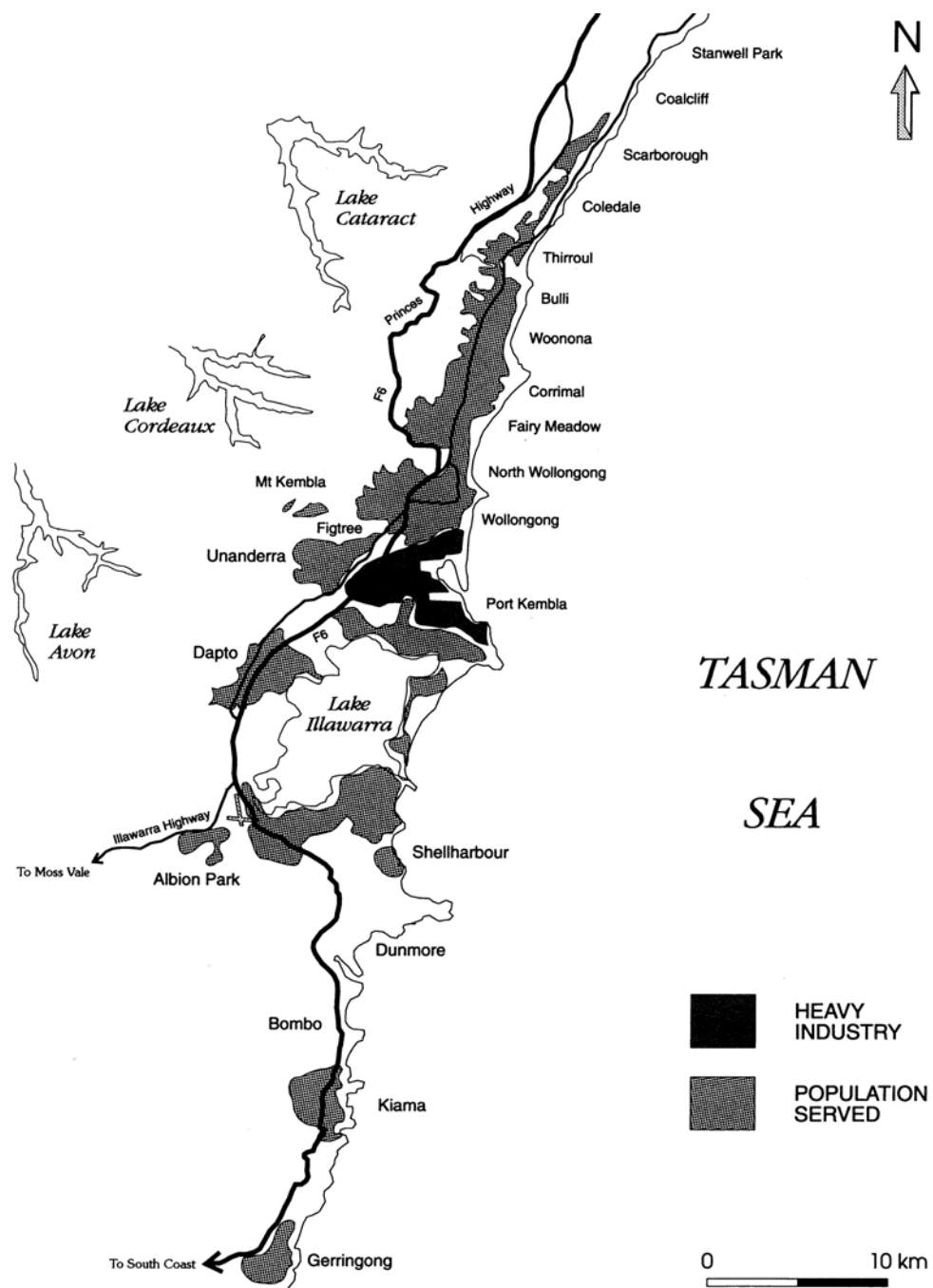


Figure 5.1 A map showing raw water supply from Avon Lake to the Illawarra region (Illawarra water quality report, 1992)

5.2 Ferric Chloride Residuals

The water treatment plant residuals studied in this investigation originated Ferric Chloride coagulation with the aid of the Cationic Polymer (LT 425), and Non Ionic Polymer (LT 20) was used as a filter aid conditioner. The normal treatment plant dose rate range is (3–5 mg/L) Ferric Chloride, (1.6-3 mg/L) Cationic Polymer, and (0.05-0.1 mg/L) Non-Ionic Polymer, however dose rates could be much higher in the event of heavy rainfall in the catchment.

Table 5.1 Typical analysis of Avon raw water

Parameter	Units	Minimum	Maximum
Turbidity	NTU	0.55	10
Apparent Colour	CU	7	48
Iron	mg/L	0.11	1.12
Manganese	mg/L	0.002	0.37
Aluminum	mg/L	0.003	1.401
Hardness	mg/L as CaCO ₃	5.2	23
Alkalinity	mg/L as CaCO ₃	0.6	7.6
pH	-	6.15	7.2
Temperature	⁰ C	10	25
Algae	Cell/mL	0	5000

Avon raw water is soft and its typical characteristics are shown in Table 5.1. The treatment plant is a direct filtration process using dual media of gravel, sand and anthracite. The water is buffered with hydrated lime Ca (OH)₂ with a dose rate of 16 mg/L; coagulation pH is 9.5 in order to oxidise the iron and manganese present in raw water (Gharaibeh and Craig, 1999).

The main constituent of the residuals is ferric hydroxide, which is formed according to the following chemical reaction:



Table 2 shows the typical composition of water treatment plant residuals compared to the Illawarra residuals used in this study. The data shown from Elliott et al (1990) in Table 5.2 were used from a mixture of plants using alum and ferric coagulants. Therefore, Aluminium content is higher and Iron content is lower. The other constituents vary depending on the raw water quality and environmental pollutants. The concentrations of total Kjeldahl nitrogen (TKN) and phosphorous are influenced by plant and algal growth in raw water supply, however, the lower values of TKN and phosphorous in the Illawarra residuals indicate lower microbial activity. Low phosphorous in Avon water supply is driven by its low presence in catchment soils and sediments. However, the use of residuals as soil conditioner is more desirable, since many Australian native plants are very sensitive to phosphorus (Scotts Australia, 2007).

Backwashing of filters removes the trapped flocs from the filter media where backwash water of about 0.5% solids content (wet basis) is generated. Backwash water is thickened in two thickeners (capacity of 450 m³ each) where Anionic Polymer (LT 30) is dosed (0.04 mg/L). Two pumps remove the residuals from the bottom of the thickeners to the sand drying beds. The sand drying beds dewater the residuals by gravity drainage as well as natural atmospheric drying. Residuals for drying tunnel experiments were collected from the sand drying beds after most drainage water had been removed. Residuals used for the experimental sand drying beds were collected directly from a sampling point at the discharge of the residuals pumps.

Table 5.2 Composition of residuals used in this study compared to typical composition of residuals

Parameter	Units	Illawarra Residuals	Typical Residuals*
Aluminium	ppm	8000	71000
Iron	ppm	120000	68000
Manganese	ppm	3600	-
Zinc	ppm	200	308
Lead	ppm	16	88
Copper	ppm	35	134
Nickel	ppm	40	55
Chromium	ppm	32	-
Barium	ppm	236	-
Cadmium	ppm	< 2	1.5
Cobalt	ppm	15	-
Boron	ppm	< 2	-
TKN	ppm	36	6000
Phosphorus	ppm	1	2000

* Data from (Elliot et al. 1990)

5.3 Drying Tunnel

The drying tunnel is an air conditioning laboratory unit (Model A572, manufactured by P. A. Hilton Ltd. UK) (Figure 5.2). This compact and mobile unit heats, cools, humidifies and dehumidifies an air stream. The air conditioning laboratory unit is mounted on a mobile frame, which houses a refrigeration unit and steam generator as shown in Figure 5.3. Air entering the duct passes in series through:

1. Centrifugal fan with variable speed controller.
2. Air heating element.
3. Steam diffusers.
4. Air straightener.
5. Cooler/dehumidifier with precipitate water content.
6. Air heating element.

The drying tunnel is equipped with a variable speed fan in order to control the wind speed. The variable speed control in the drying tunnel allows an exact adjustment of wind speed. However, the wind speed is measured using a Pitot tube by taking a profile measurement across the height of the duct.

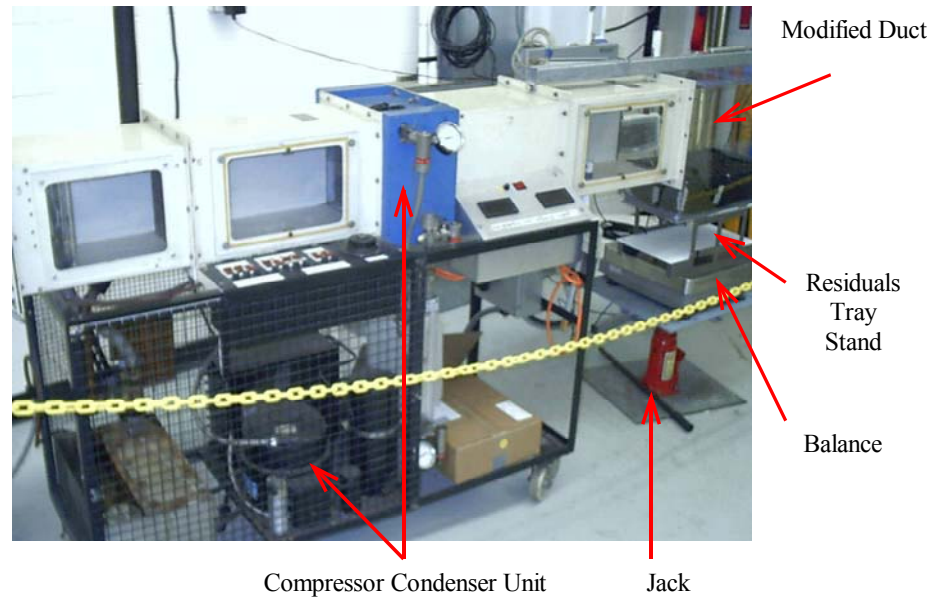


Figure 5.2 Air conditioning laboratory unit

5.3.1 Drying Duct

Drying experiments were performed in a rectangular duct attached to the drying tunnel. A duct fabricated from Perspex sheets 5 mm thick, 254 mm wide and 254 mm high, is attached to the exit frame of the drying tunnel. The duct is open from the bottom, as shown in Figure 5.4, situated above the tray and forming part of the duct lies an easy-access cover. This allows the tray surface area of residuals to align with the direction of the wind.

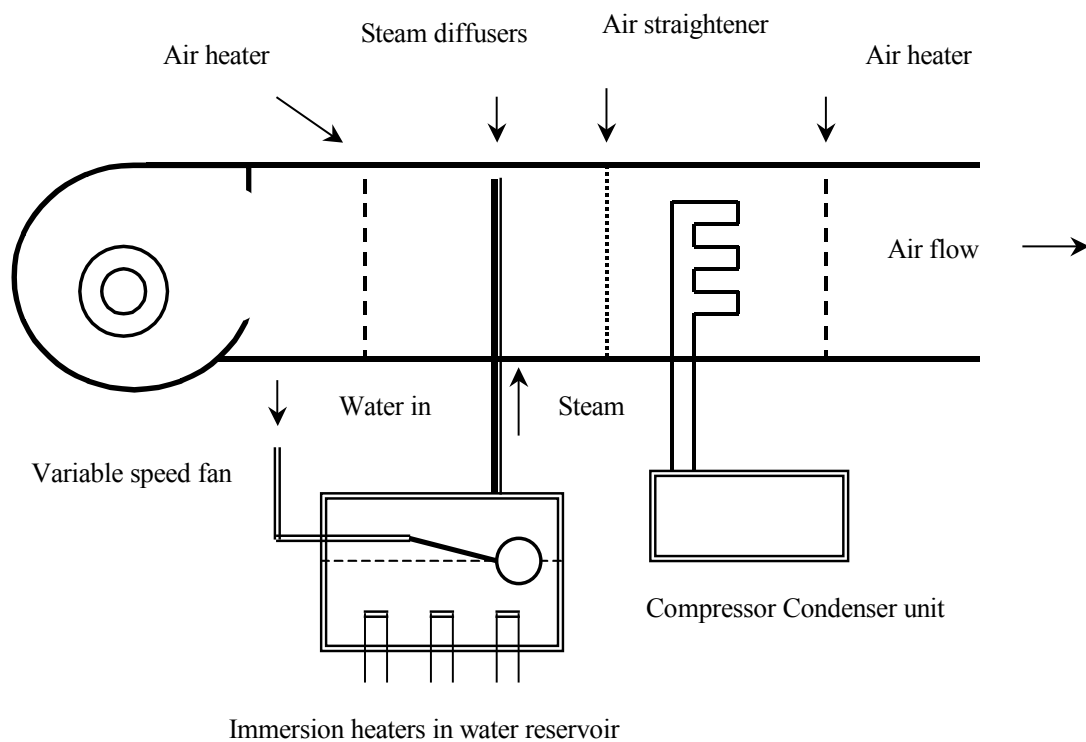


Figure 5.3 Schematic of the drying tunnel unit

5.3.2 Residuals Tray

Residuals to be dried are placed in an aluminium foil tray 330 mm long, 220 mm wide and 90 mm deep. The tray is placed on a stand made of an aluminium plate, which is supported by two wooden legs. This allows the tray to be set above the top loading balance. Both the aluminium plate and the foil tray are separated by a sheet of polystyrene foam 25mm thick, for insulation. The foil tray can be easily folded down from both sides, according to the direction of wind flow. As the drying process progresses, the residuals applied thickness becomes less, thereby the surface of the residuals can be kept at the same level of the duct by using the jack to elevate it, thus minimising the turbulence on the surface.

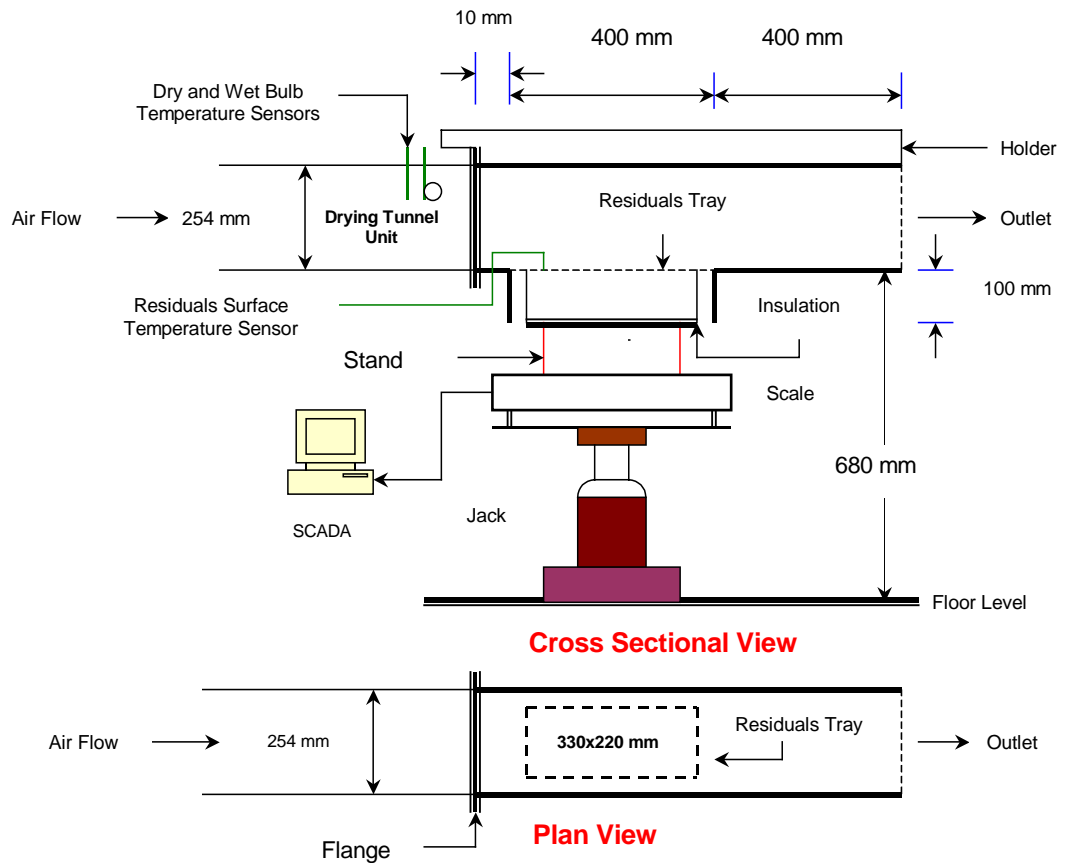


Figure 5.4 Drying tunnel experimental set-up

5.3.3 Weight Measurement Balance

A top loading balance (AND HP-22K) was used to weigh the moisture loss of the residuals in the residuals tray; the balance weighs up to 21 kg to an accuracy of 0.1 g. The weight is logged continuously via a RS-232-C interface into the Supervisory Control and Data Acquisition (SCADA) System of the water treatment plant. The weight is recorded into (SCADA) in six-minute intervals; this trend can then be exported onto an MS Excel spreadsheet. This facilitates continuous recording of weight loss, which gives an exact logging of the drying rate of residuals as a function of time.

5.3.4 Temperature Measurements

The residuals surface temperature, the wet bulb, and dry bulb temperatures were measured in the drying tunnel. Relative humidity is then calculated from the wet and dry bulb temperatures using the psychrometric chart. Alternatively, and in this particular case, relative humidity can be easily calculated using the following formulae (Smith et al 1996), found in any standard thermodynamics book.

$$p_{wb} = \text{Exp} \left[\frac{(16.78 \times T_{wet}) - 116.9}{T_{wet} + 237.3} \right] \quad (5.2)$$

$$p = p_{wb} - (0.00066 \times (1 + (0.00115 \times T_{wet})) \times 101.325 \times (T_{dry} - T_{wet})) \quad (5.3)$$

$$p_{db} = \text{Exp} \left[\frac{(16.78 \times T_{dry}) - 116.9}{T_{dry} + 237.3} \right] \quad (5.4)$$

$$RH = \frac{p}{p_{db}} \quad (5.5)$$

Where,

p_{wb}, p_{db} Water vapour partial pressures at wet and dry bulb temperatures (kPa)

T_{wet}, T_{dry} Wet and dry bulb temperatures ($^{\circ}\text{C}$)

p Actual vapour pressure (kPa)

RH Relative humidity (decimal)

The leaf temperature sensors were used to measure the surface, wet bulb, and dry bulb temperatures. The leaf temperature sensors (TL1) (accuracy $\pm 0.1^{\circ}\text{C}$, range -20°C to 60°C) were connected to an eight-channel data logger; data was logged at six-minute intervals. Data can be downloaded via a laptop using software that is compatible with MS Excel. The data logger is able to store data up to eighty days of information depending on the number of sensors used and the frequency of measurements. The wet bulb temperature is measured by immersing one of the leaf sensors in a small water

reservoir. The sensor is wrapped with a porous cloth, which is kept wet in the water reservoir. The small water reservoir is kept full of water via its connection with a larger water reservoir outside the cavity of the drying tunnel duct, by the use of a small tube.

5.4 Moisture Content Measurement

The apparatus used in measuring the moisture content is a Sartorius MA 30 moisture analyser as shown in Figure 5.5. The analyser is regularly checked on a monthly basis for calibration. The accuracy of the weight measurement of the analyser is ± 0.001 g. The heating element is set at 105°C for the drying of the residuals samples (Eaton et al. 1995). Residuals were collected in a large container (60 Litre) and mixed thoroughly in order to ensure uniformity. Drying samples were then taken from the container to be tested for initial solids content in the moisture analyser. The samples were taken in duplicates and measured in the analyser. Five grams of residuals were taken, in order to measure the moisture content; these were then spread evenly in the tray of the moisture analyser in order to ensure accurate measurement.

The moisture analyser gives the results in wet or dry basis according to the following equations:

$$SC = 1 - \left[\frac{m_{residuals} - m_{solids}}{m_{residuals}} \right] \quad (5.6)$$

$$X = \frac{m_{residuals} - m_{solids}}{m_{solids}} \quad (5.7)$$

Where,

$m_{residuals}$ Mass of residuals (kg)

m_{solids} Mass of solids (kg)

SC Wet basis solids content (percentage)

X Dry basis moisture content ($\text{kg}_{\text{water}} / \text{kg}_{\text{dry solids}}$)



Figure 5.5 Sartorius MA 30 Moisture analyser

5.5 Monitoring of Weather Conditions (Weather Station)

A weather station is used to monitor the weather conditions and is mounted next to the experimental sand drying beds. The weather parameters measured ambient temperature, wind speed, solar radiation, relative humidity and rainfall (Figure 5.6). Relative humidity, wind speed and solar radiation are logged in the data logger on an hourly basis. Ambient temperature, residuals surface temperature and rainfall are logged on a 6-minute basis.

The weather parameters are stored in the data logger (*MONITOR LOGGER 40*) and later downloaded via a laptop computer equipped with software compatible with MS Excel. The data logger's communication software calculates maximum, minimum and daily averages of the temperatures, relative humidity, rainfall, and wind speed. The software also calculates daily total solar radiation and the number of sun-hours of the day. The data logger is powered by a built-in rechargeable battery, charged by a solar panel mounted on a 5 m mast on top of the weather station as shown in Figure 5.7.

5.5.1 Ambient Temperature Measurement

Ambient temperature was measured using an air temperature sensor (TA1) mounted upwards, on top of the data logger box inside a sensor shelter (Figure 5.7). The temperature range is (-20 °C to 60 °C) with measurement accuracy of (± 0.1 °C).

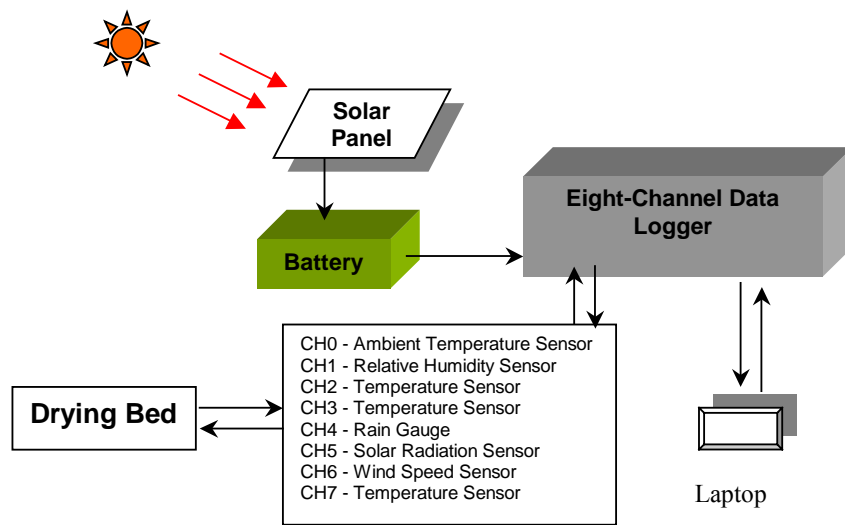


Figure 5.6 Schematic diagram of the weather monitoring station

5.5.2 Leaf Temperature Measurement

Surface temperature of the residuals was measured using a leaf temperature sensor (TL1) connected to the data logger. The temperature range is (-20 °C to 60 °C) with measurement accuracy of (± 0.1 °C).

5.5.3 Relative Humidity Measurement

Relative humidity was measured using a relative humidity sensor (HU1) mounted upwards on top of the data logger box inside a sensor shelter (Figure 5.7). The sensor range is 0 to 100% with accuracy of $\pm 2\%$ (over the full range) and operating over a temperature range of -30 °C to 80 °C.

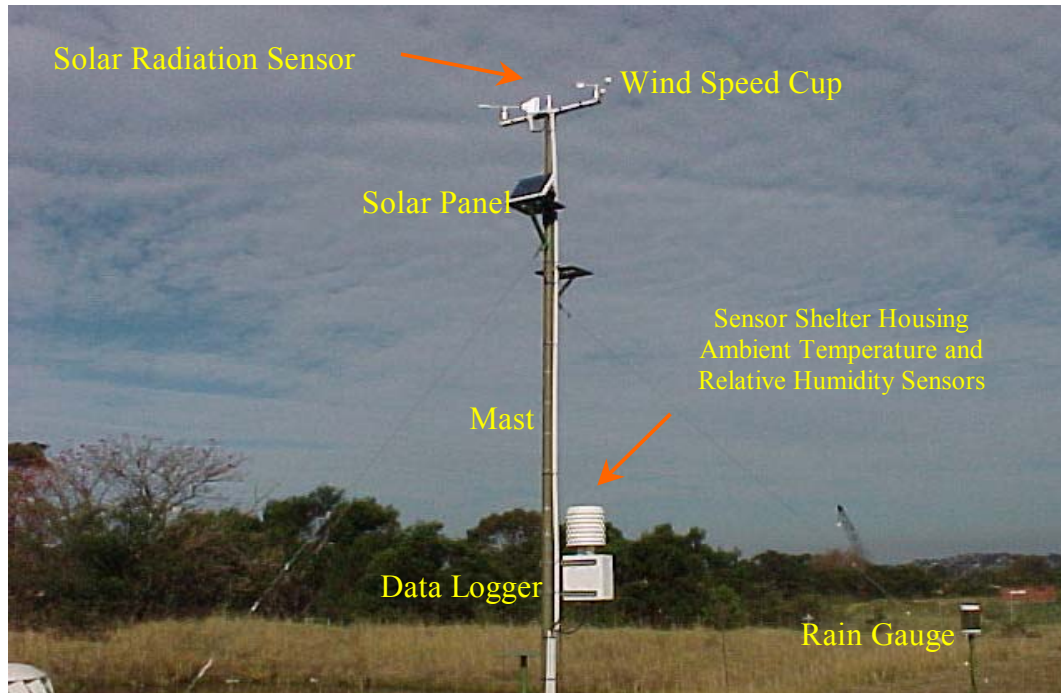


Figure 5.7 The weather station adjacent to the drying beds

5.5.4 Solar Radiation Measurement

The Solar Radiation short-wave (global) spectrum sensor (SR2) has a spectral response from 400 to 1100 nanometres. The SR2 uses a photovoltaic sensor housed under a shaped Teflon diffuser to measure the global radiation. The solar radiation sensor was mounted on top of the mast. The sensor range is 0 to 2000 W/m², with accuracy of $\pm 5\%$ (over the full range) and operating over a temperature range of -20 °C to 50 °C.

5.5.5 Wind Speed Measurement

A three-cup Anemometer (AN3) was mounted on top of the mast to measure the wind speed. The sensor range is 0 to 55 m/s with accuracy of $<\pm 2\%$ (over the full range) and operating over a temperature range of -20 °C to 60 °C.

5.5.6 Rainfall Measurement

A tipping bucket rain gauge was used to measure rainfall and mounted next to the mast. The rain gauge range is 0 to 720 mm/hr, with accuracy of $\pm 2\%$ over 0 to 720 mm/hr range and operating over a temperature range (1 to 60 °C).

5.6 Field Experiments

A series of experiments were performed in the field next to the weather monitoring station. Two identical experimental sand drying beds were fabricated from a 2 millimetre thick galvanised metal sheets. One of the beds was left open, whilst the other was covered with a glass cover.

5.6.1 Experimental Open Sand Drying Bed

The open experimental sand drying bed has dimensions of 500 mm long, 500 mm wide and 600 mm deep. It is supported on the ground with four legs (400 mm high), and it is fitted with a drainage tap, filling a 20-litre container via a hose. Large gravel (10 mm Diameter) was placed at the bottom triangular section for drainage and supporting the sand area, the sand (0.7 mm effective size with a uniformity coefficient of 1.3) was placed on the top 200 mm section of both beds, which were separated by a Geo-textile mat. The upper 200 mm section is left for the residuals applications (Figure 5.8). The bed's residuals temperature is continuously measured using a temperature sensor supported with a piece of polystyrene on top of the residuals surface to keep it afloat. The tip of the leaf temperature sensor was immersed 3 to 5 mm beneath the residuals surface and placed roughly in the centre of the residuals surface.

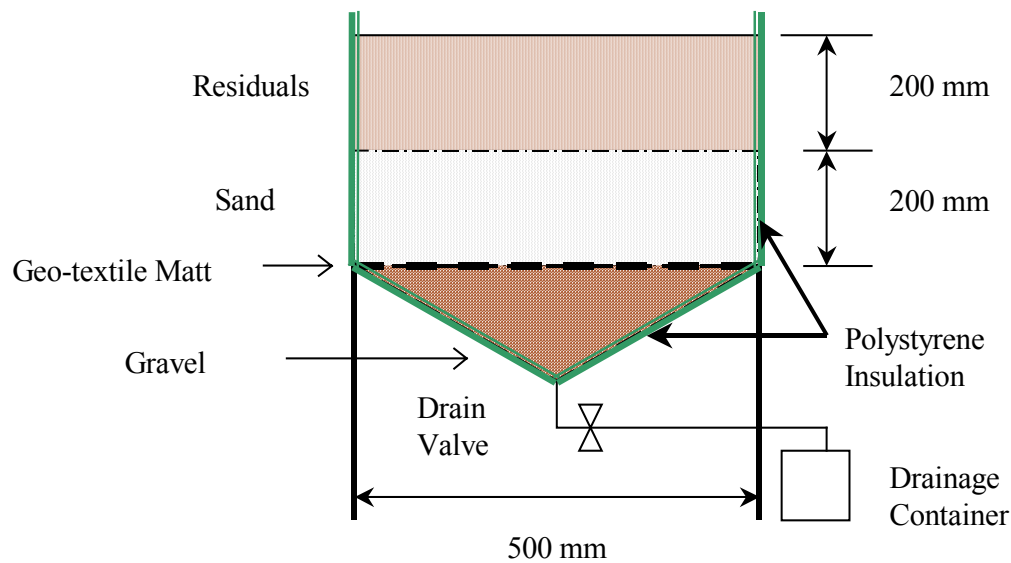


Figure 5.8 Experimental open sand drying bed

The residuals are pumped regularly from the thickeners into the treatment plant sand drying beds. The residuals pump is equipped with a sampling tap. The residuals were collected from the sampling tap into a large container, as mentioned in section 5.4, and then thoroughly mixed before being applied in the experimental drying bed. The solids content of the thickened residuals ranges from 1.0% to 3.5%. During the experiments, samples were taken on a daily basis, at 8:00 am, from the experimental beds in order to measure the moisture content using a moisture analyser (Sartorius MA 30). Five samples were taken each day from five different locations from the residuals application; samples were mixed together, then duplicate measurements were performed in order to measure the solids content. The under-drained water is collected and measured daily in a 20-litre container. When the solids content reaches nearly 50%, most experiments are halted, and residuals are removed from the bed.

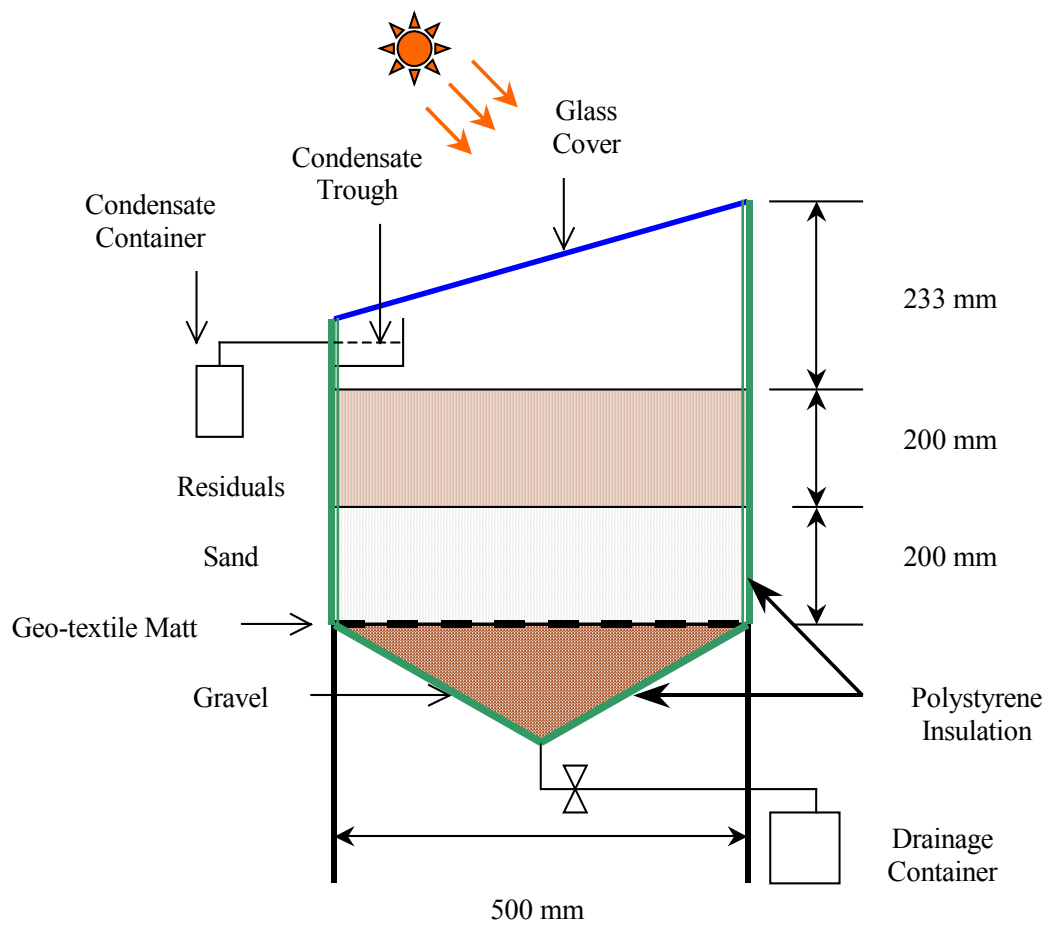
5.6.2 Experimental Solar Sand Drying Bed

The solar bed dimensions were 500 mm wide, 500 mm long, 400 mm high from all three sides and 633 mm high from the rear side; the tilt angle of the cover was 25° with respect to the horizontal (Figure 5.9). Under the glass cover, from all sides, a condensate trough was fitted and condensed water was collected via a drainage tube at the front left hand side of the trough into a one litre plastic container.

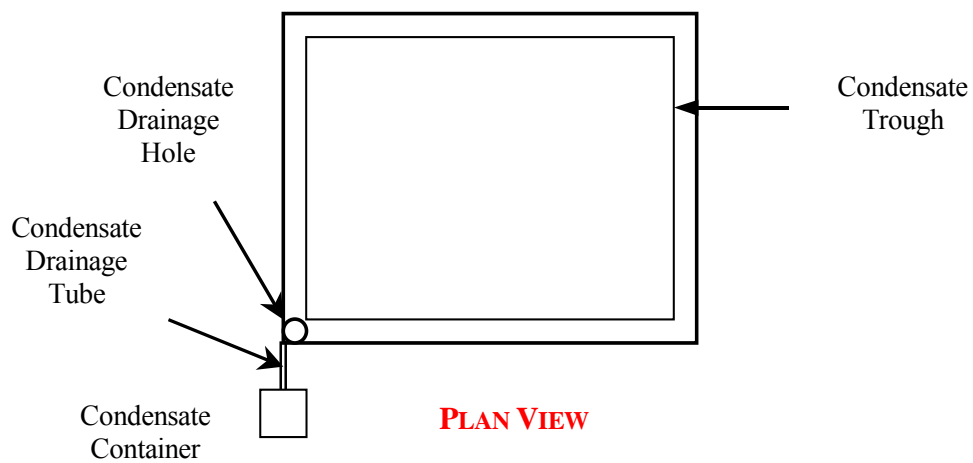
Another plastic container was used for the collection of the drained water from the lower end of the triangular bottom section. Large gravel of about 10 mm diameter was placed at the bottom triangular section for both drainage and for supporting the sand area. The sand (0.7 mm effective size with a uniformity coefficient of 1.3) was placed on the top 200 mm section of both beds, which were separated by a Geo-textile mat. The upper 200 mm section is left for the residuals applications. Both beds were thermally insulated with polystyrene foam.

5.6.3 Field Experiments without Drainage

Four experiments were performed in the field next to the weather monitoring station in order to study the evaporation part without the drainage part. A plastic tray with dimensions of 495 mm long and 335 mm wide was used for the experiments, which was placed under a cover sheet of Perspex (800 mm above the tray). The Perspex cover allows solar radiation penetration and prevents the rain from filling up the tray. The tray was weighed on a daily basis at an exact time (8:00 am) to calculate the daily water evaporation from the residuals and subsequently to calculate the solids content of the residuals using equation (5.6).



CROSS SECTIONAL VIEW



PLAN VIEW

Figure 5.9 Experimental solar sand drying bed

5.7 Sample Collection and Analysis

Samples of residuals were collected and analysed for all field experiments from the solar and normal drying beds on a daily basis. The samples were collected from the start of each experiment until the final solids content of 50%. Samples were collected at the start of each drying tunnel experiment, and then solids content measurements were then calculated continuously, by calculating the of weight loss of residuals.

5.7.1 Moisture Content Analysis

Samples were taken on a daily basis from both beds, in order to check the solids content using the moisture analyser. The samples were taken from each bed initially using a 2.5 mL syringe until the residuals reached approximately 15% solids content. The sample was usually taken from at least 4 separate areas and then it was mixed before analysis. To analyse the moisture content, the sample was split into two identical samples and two analyses were performed. An average result is then taken. When the solids content of the residuals in the drying bed is above 15%, samples were taken with the use of a spatula from at least 4 separate areas. In each sample area, a percentage of the sample was taken from the top, whilst another is taken deeper within the cake; great care is taken, to avoid reaching the sand. The samples were mixed and analysed using the same method explained previously.

In order to measure the solids content of the residuals samples, 5 grams of the sample was spread evenly into the measurement tray, this was then placed into the moisture analyser. After taring the tray, and closing the cover of the analyser, the heater element starts automatically, heating the sample at 105 °C. The heater shuts off automatically when the balance of the moisture analyser detects no further moisture loss

and the reading is then shown on the display. Equations (5.6) and (5.7) are the basis of the theoretical calculation of the solids and moisture contents in the moisture analyser.

5.7.2 Moisture Content Calculation

Another approach when calculating the moisture content of residuals in the drying tunnel experiments was performed by continuously logging the residuals' weight loss using the top loading balance (AND HP-22K). Residuals are composed of water and solids, the water evaporates and the solids remain in the drying tray. The initial solids content of the residuals was measured using the moisture analyser. However, the weight of solids in the tray can be calculated using equation (5.6) with the knowledge of initial weight of residuals and the initial solids content. The following calculation was performed using this formula to achieve the solids content as a percentage:

$$SC = \frac{100}{1 + X} \quad (5.8)$$

Figure 5.10 shows a sample calculation of moisture content in column C (equation 5.7) and solids content in column D (equation 5.8). Row 3 shows the beginning of the experiment where the initial weight, moisture content and the solids content in columns B, C and D respectively.

	A	B	C	D
1	Date/Time	Weight (g)	Moisture Content (kg _{water} /kg _{solids})	Solids Content %
2	d/mm/yyyy h:mm	m _{residuals}	$X = (m_{\text{residuals}} - m_{\text{solids}})/m_{\text{solids}}$	$SC = 100/(1+X)$
3	21/03/2006 9:00	1613	12.39	7.47
4	21/03/2006 9:06	1593	12.22	7.56
5	21/03/2006 9:12	1578	12.10	7.64
6	21/03/2006 9:18	1553	11.89	7.76
7	21/03/2006 9:24	1542	11.80	7.81
8	21/03/2006 9:30	1533	11.72	7.86
9	21/03/2006 9:36	1519	11.61	7.93

Figure 5.10 MS Excel spreadsheet showing sample calculation of moisture and solids content

The weight of residuals was logged in six-minute intervals, subsequently the moisture and solids content has been calculated in the adjacent columns. As time progresses the weight of residuals is reduced, hence the solids content increased. The logging of weight loss continues during the experiment until the final solids content (50%) has been achieved. The drying curves for any given experiment can then be plotted on a graph.

5.8 Summary

This chapter provides a description of the residuals used in the drying experiments, the equipment and instruments used in this study. Ferric chloride residuals were used from the Illawarra water treatment plant. Indoor experiments were performed using an air conditioning (drying tunnel) unit. The various components of the drying tunnel were discussed. A drying duct was fabricated from perspex and attached at front end of the drying tunnel in order to house the residuals drying tray. The measurement of residuals weight was performed continuously using a top loading balance (AND HP-22K) and the leaf temperature sensors were used to measure wet bulb, dry bulb and surface temperatures. The moisture content measurement of residuals for the drying tunnel and field experiments were performed using Sartorius MA 30 moisture analyser. Field experiments required the use of a weather monitoring station and experimental sand drying beds. The weather station is used to monitor the weather conditions, however, the weather parameters were stored in the data logger and later downloaded via a laptop. In the field, experiments were performed in open and solar experimental beds as well as field experiments performed without drainage.

Finally, the sample collection, analysis and calculation protocols were discussed. The following two chapters will present and discuss the experimental work produced in this study.

6 Field Drying Experiments

6.1 Introduction

The dewatering of water treatment residuals on sand drying beds produces residuals consisting of 5% solids content in a relatively short time through the process of gravity drainage. The solids concentration of residuals of 5% to 15% produces a mud like suspension. Further drying allows residuals to shrink and crack, becoming more like a solid, with over 50% solids content. Residuals with solids content of between 30% and 50% can be readily removed for final disposal or reuse. This investigation will focus on drying residuals above 5% solids content and up to 50% solids content.

Experimental work included a significant number of field (21 experiments) and drying tunnel experiments (56 experiments). Field experiments were initially performed in both open and solar (covered with glass) drying experimental beds in order to improve the drying time of the residuals. The results of field experimental studies will be presented and discussed in this chapter. Some experiments were performed without gravity drainage (evaporation only) in the field under perspex cover in order to prevent rain from entering into the experiments. This chapter will focus on the experimental work performed in the field and the drying behaviour in both the open and solar experimental beds.

6.2 Open (Normal) Bed Field Experiments

The residuals under investigation were collected directly from the treatment plant thickeners and applied into the experimental sand drying beds. Weather parameters were measured by the weather station, drainage water was collected and measured on a

daily basis, and samples of the residuals were taken on a daily basis and their solids content measured using the moisture analyser. Open bed experiments were exposed to changes in meteorological conditions. The experiments of the open bed were either single or multiple application thickness experiments. Residuals are applied on the sand bed with a typical application depth of 200 to 450 mm (Cheremisinoff, 2002). Residuals are applied layer over layer until the final depth is achieved; however, experience best determines the optimal residuals application depth.

Figure 6.1 shows experiment 13 drying time, drainage time, and daily total rainfall in a typical open bed curve. A large portion of the drainage water was collected in the first two to three days. Cracks start to appear at about 10% solids content (Figure 6.2) and the cracks deepen to the bottom of the cake at about 15%. Around 50% solids content the cake appears to be very dry and many cracks and fragments are formed.

6.2.1 Single Application Experiments

Series of single application experiments were conducted in the field and the depth of experimental applications were 50, 100, 150 and 200mm. Twelve single application thickness experiments were conducted starting from July 1999 until September 2000 for a period of 15 months. The experiments shown in Table 6.1 are for single application thickness. Table 6.1 shows the daily average meteorological conditions except for total rainfall during the drying time of each experiment as well as the application depth of residuals, initial and final solids content, drying time and the total drained water. No surface temperature measurement was undertaken for experiments 4 through 9. Full experimental data of all experiments can be found in the appendices.

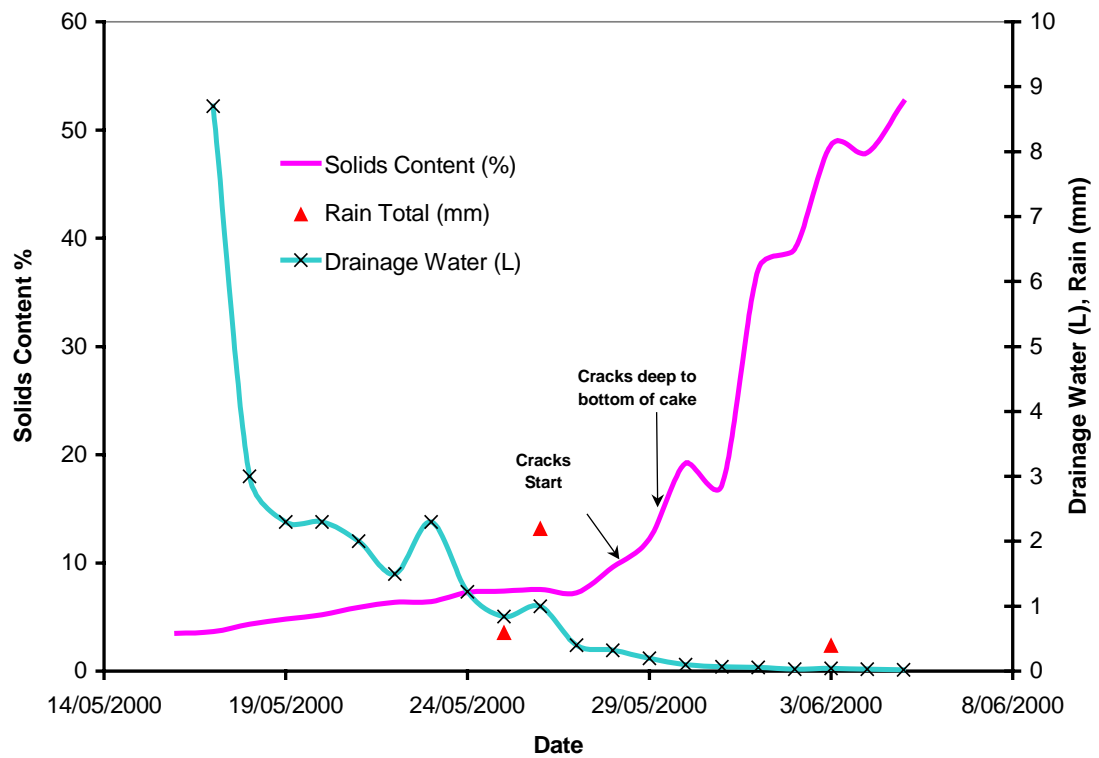


Figure 6.1 Typical curve showing drying time, drainage water, and rainfall



Figure 6.2 Residuals cracked at 10% solids content

6.2.2 Multiple Application Experiments

The liquid residuals are applied intermittently in the sand drying beds in small thicknesses; when the small thickness becomes dry, another layer is applied. However,

multiple applications experiments 10, 17, 18, 19 and 20 were conducted to simulate actual drying bed operation (Table 6.2). The applications were applied on a daily basis; the number of applications and their initial solids content are shown in Table 6.3. The first application experiences a reduction in thickness due to water drainage and evaporation; therefore the second application will be applied on top of the first and this continues until the 200 mm top section of the experimental bed is full. Experiment 10 had an initial application of 100 mm and four subsequent applications of 50 mm. Experiments 17, 19 and 20 had a total of five 50 mm applications whereas experiment 18 had a total of three 100 mm thickness applications.

Table 6.1 Single application experiments

Experiment Number	Application Depth (mm)	Initial Solids Content %	Final Solids Content %	Drying Time (Days)	Relative Humidity Daily Average %	T (°C)	T _{surface} (°C)	Rainfall Total (mm)	Solar Radiation Daily Average (MJ/m ²)	Wind Speed Daily Average (m/s)	Drained Water Total (L)
4	50	1.6	82.8	16	84.6	12.9	-	170.2	6.5	2.0	20.5
5	50	1.7	88.9	11	71.7	12.6	-	11.2	11.0	2.1	11
6	200	3.2	23.1	14	86.8	15.9	-	7.6	10.7	2.0	28.6
7	200	1.2	90.7	10	75	13.6	-	6.8	13.4	2.3	24.8
8	200	2.4	59.6	13	90.9	18	-	13.4	12.6	1.6	33
9	200	4.4	46.6	17	84.5	16.7	-	55.6	16.1	2.0	34
11	150	3.4	66.5	23	91	20.9	19.9	189.2	6.3	1.6	71.0
12	200	1.6	57.2	34	89	17.1	16.0	73.6	5.7	1.5	51.6
13	200	3.5	65	21	70	12.7	10.8	3.2	8.7	3.0	26.5
14	200	1.5	54	27	76	12.2	9.8	29	6.0	2.1	42.4
15	150	2.6	64	22	64	13.7	11.0	19.3	17.4	2.8	26.9
16	100	2.7	92.2	18	72	17.8	16.8	14.1	13.0	2.5	15.5

The multiple application experiments (Table 6.2) vary in their drying time from 21 days to as high as 56 days. The range of the daily average relative humidity for all

experiments is within 5%. The daily average solar radiation intensity varies from 17.7 to 8.2 MJ/m² and the daily average wind speed varies from 1.5 to 2.03 m/s. Substantial rainfall was experienced for all the experiments except for experiment 10. Experiment 10 was conducted in summertime and Experiment 20 was conducted in early winter, which may explain high drying time for Experiment 20. The variations in solar radiation, rainfall and relative humidity also contribute to the variations of drying time.

Table 6.2 Open bed multiple application experiments

Experiment Number	1st Application Thickness (mm)	Total Applications	Subsequent Applications Thickness (mm)	Drying Time (Days)	Relative Humidity Daily Average %	T (°C)	T _{surface} (°C)	Rainfall Total (mm)	Solar Radiation Daily Average (MJ/m ²)	Wind Speed Daily Average (m/s)	Drained Water Total (L)
10	100	5	50	23	84.6	18.4	-	6.4	17.7	2.03	49.5
17	50	5	50	33	89	19.6	18.7	122.2	12.2	1.8	81.2
18	100	3	100	21	84	22.4	20.8	82.6	14.1	1.9	72.4
19	50	5	50	35	87	21.7	20.8	166.4	11.5	1.5	66.7
20	50	5	50	56	85	16.9	15.9	94.8	8.2	1.8	46.2

Table 6.3 Open bed multiple application experiments and their applications initial solids content

Experiment Number	1st Application Solids Content %	2nd Application Solids Content %	3rd Application Solids Content %	4th Application Solids Content %	5th Application Solids Content %	Final Solids Content %
10	2.3	2.8	4.1	2.95	3.1	58.5
17	1.4	4.1	3.4	0.5	3.8	58.4
18	1.5	2.7	1.1	-	-	56.3
19	1.7	2.4	2.4	2.4	2.6	58.5
20	2.6	2.5	2.0	2.4	2.9	51.5

6.3 Solar Bed Experiments

The solar bed acts as a greenhouse heat trap, where the short wavelengths of visible light from the sun pass through a transparent medium and are absorbed, but the longer wavelengths of the infrared re-radiation from the heated objects are unable to pass through that medium. As a result, high surface temperatures compared to ambient were experienced in the solar drying bed (see Table 6.4). In experiments (4, 5, 6, 7 and 8), the solar bed was sealed (see Figure 5.9 in Chapter 5). Table 6.4 shows the daily average meteorological conditions, the application depth, initial and final solid contents, drying time and the daily average surface and cavity temperatures. The drying times of the sealed solar bed experiments were lower than the open bed. Therefore, in subsequent experiments (9, 11, 12, 13 and 14) the bed was equipped with ventilation holes and a wind ventilator (Figure 6.3) in order to improve the drying of residuals in the solar bed. The holes on the sides of the bed and the wind ventilator (no electrical energy was used) assisted the removal of humid air from the cavity for experiments (9, 11, 12, 13 and 14).

Table 6.4 Solar bed single application experiments

Experiment Number	Application Depth (mm)	Initial Solids Content %	Final Solids Content %	Drying Time (Days)	Relative Humidity Daily Average %	T _∞ (°C)	T _{surface} (°C)	T _{cavity} (°C)	Solar Radiation Daily Average (MJ/m ²)	Wind Speed Daily Average (m/s)
4	50	1.6	19.6	25	85	12.9	17.2	16.5	6.5	2.0
5	50	1.7	19.8	11	72	12.6	21.1	18.5	11.0	2.1
6	200	3.2	17.1	14	87	15.9	22.5	20.9	10.7	2.0
7	200	1.2	26.2	18	75	13.6	21.1	19	13.4	2.3
8	200	2.4	30.9	28	91	18	22.4	20.3	12.6	1.6
9	200	3.2	24.9	17	85	16.7	23.5	20.5	16.1	2.0
11	150	3.4	25.1	33	91	20.9	23.6	22.4	6.3	1.6
12	200	1.6	35.0	35	89	17.1	20.0	19.4	5.7	1.5
13	200	3.5	36.6	41	70	12.7	14.3	14.4	8.7	3.0
14	200	1.5	49.3	18	76	12.2	15.3	18.5	6.0	2.1

6.3.1 Solar Bed Single Application Experiments

Table 6.5 shows the conditions of the single application solar bed experiments. The solar bed was sealed for experiments 4, 5, 6, 7 and 8; evaporated water from the residuals surface condensed on the glass cover and collected in the distillate trough. The solar drying bed has been designed in a similar way to that of the solar distillation still (Gharaibeh et al 2003). In experiments 9, 11, 12 and 13 the bed was not sealed (see Table 6.5), however no improvement was observed in the drying time compared to the open bed.

Table 6.5 Solar bed single application experimental conditions

Experiment Number	(25mm) Polystyrene Insulation Layers	Condensate Water (L)	Drained Water (L)	Solar Bed Experimental Conditions
4	Single	0.646	9.5	Sealed
5	Double	0.627	11.9	Sealed
6	Double	2.606	30.9	Sealed
7	Double	1.218	23.7	Sealed
8	None	3.864	33.6	Sealed
9	None	2.105	34.8	Bed has 5 holes (3mm, Dia) in each side of bed and 5 holes at top back
11	Double	1.526	28.7	Bed has 5 holes (3mm, Dia) in each side of bed and 5 holes at top back + air ventilator
12	Double	0.976	38.9	Same as Experiment 11 except the front holes are 25 mm in diameter
13	Double	0.419	31.2	Same as Experiment 11 except the front holes are 25 mm in diameter
14	Double	0.000	39.4	Blind cover, fan heater in front of 25mm holes, other holes on sides blocked except back

The condensate is clean water. Substantial quantities of condensate were collected for the sealed experiments and much less quantities for the ventilated experiments. The

condensate quantities of the ventilated experiments (9, 11, 12 and 13) were significantly less due to enhanced ventilation.

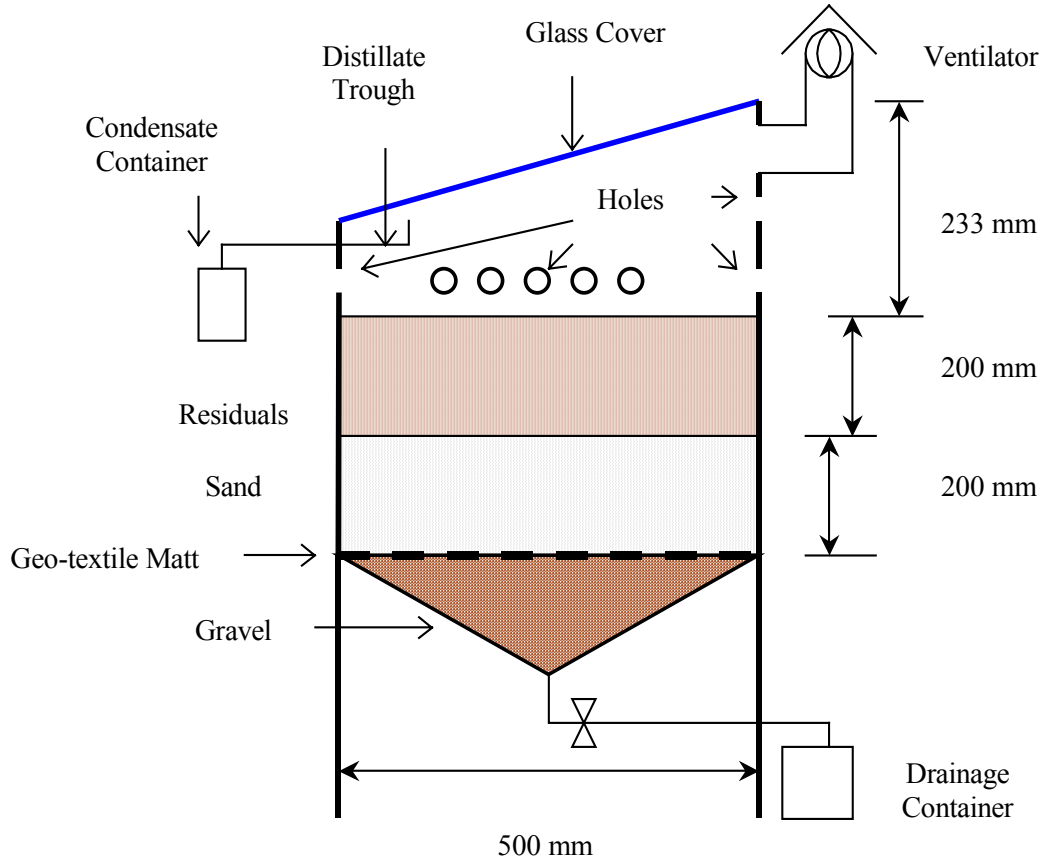


Figure 6.3 The solar bed showing the holes in all sides and the ventilator

In experiment 14, the solar bed was provided with a fan heater blowing air from the front holes of the bed and air exiting from the back via the ventilator. A timer was used to run the fan heater for two hours and to stop for two hours in order to avoid overheating the fan heater. The variations in temperature inside the solar bed cavity can be seen in Figure 6.4 as a result of the fan heater operation. The residuals temperature of the solar bed was higher than the open bed. The forced hot air over the residuals surface supplied heat to evaporate and remove the moisture from the cavity of the bed. The moisture holding capability of air increases with elevated temperatures. A reduction in

drying time from 27 days to 18 days (33%) to reach 50% solids content was achieved in this experiment using the fan heater in the solar bed. The modifications made in the solar bed show that it is important to improve both the heating and mechanical ventilation capabilities of the bed. However, no condensate was observed in experiment 14 as shown in Table 6.5 due to heated air flow. Heating without ventilation does not improve the drying process since the saturated air is not capable of holding more moisture.

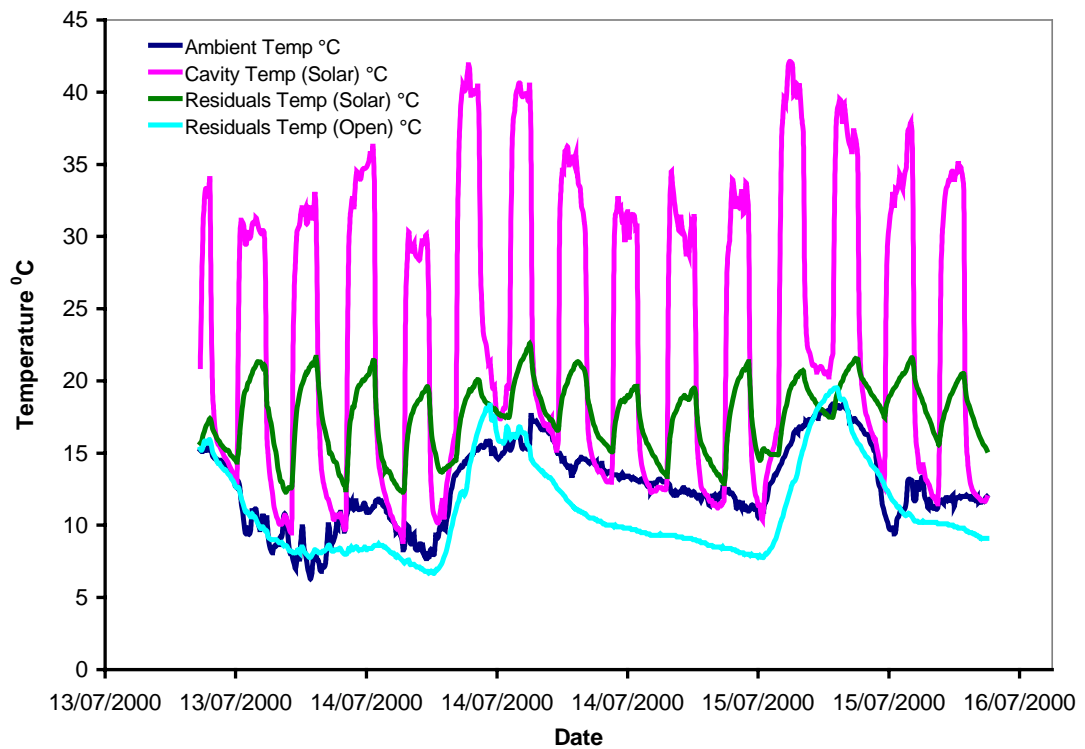


Figure 6.4 The effect of heated air on the temperatures of solar bed cavity and residuals compared to the open bed residuals temperature (Experiment 14)

6.3.2 Solar Bed Multiple Application Experiments

The multiple application experimental conditions are shown in Tables 6.6, 6.7 and 6.8. Experiment 10 was performed in the sealed solar bed; therefore, Table 6.8 shows high amounts of condensate water. Experiments 17 and 18 experienced less condensate since most of the evaporated water escaped from the holes outside the solar bed. The

solar bed was modified further in experiment 19 where the gap for air ventilation is widened (Table 6.8), hence minimising the condensate further. In Experiment 20, the glass cover was laid flat 130 mm above the bed and supported by four metal angular supports of the bed. The glass cover allowed solar radiation to reach the residuals surface whilst preventing rain from entering the bed and therefore no condensate collected under the glass cover. Table 6.7 clearly shows the reduction in residuals surface temperature in Experiment 20 compared to the other four experiments, indicating an increase of evaporative cooling during the drying process. Elevated temperatures of residuals did not help in the drying process without moisture removal from the vicinity of the evaporation surface.

Table 6.6 Solar bed multiple application experiments and their applications initial solids content

Experiment Number	Ist Application Thickness (mm)	Subsequent Applications Thickness (mm)	Total Applications	Ist Application Solids Content %	2nd Application Solids Content %	3rd Application Solids Content %	4th Application Solids Content %	5th Application Solids Content %
10	100	50	5	2.3	2.8	4.1	2.95	3.1
17	50	50	5	1.4	4.1	3.4	0.5	3.8
18	100	100	3	1.5	2.7	1.1	-	-
19	50	50	5	1.7	2.4	2.4	2.4	2.6
20	50	50	5	2.6	2.5	2.0	2.4	2.9

Table 6.7 Weather conditions of the solar bed multiple application experiments

Experiment Number	Final Solids Content %	Drying Time (Days)	Relative Humidity %	T_{∞} ($^{\circ}\text{C}$)	T_{surface} ($^{\circ}\text{C}$)	T_{cavity} ($^{\circ}\text{C}$)	Solar Radiation (MJ/m^2)	Wind Speed (m/s)	Drained Water Total (L)
10	24.2	23	84.6	18.4	26.9	22.7	17.7	2.03	67.0
17	50.8	33	89	20.0	23.3	22.4	13.4	1.7	43.9
18	51.6	21	84	22.4	23.4	24.9	14.1	1.9	60.1
19	51.6	35	87	21.7	18.2	22.0	11.5	1.5	39.8
20	53.1	56	85	16.9	16.5	17.8	8.2	1.8	28.6

Table 6.8 Solar bed multiple application experimental conditions

Experiment Number	(25mm) Polystyrene Insulation Layers	Condensate Water (L)	Drained Water (L)	Solar Bed Experimental Conditions
10	Double	5.817	67.0	Sealed
17	Double	0.268	43.9	Bed has 5 holes (3mm, Dia) in each side of bed and 5 holes at top back, except for front holes (25mm, Dia) + air ventilator.
18	Double	0.299	60.1	Bed has 5 holes (3mm, Dia) in each side of bed and 5 holes at top back, except for front holes (25mm, Dia) + air ventilator.
19	Double	0.139	39.8	All side are open 500mm wide by 50mm high + ventilator.
20	Double	0.000	28.6	No ventilator, glass cover 130mm flat above residuals maximum thickness.

6.4 Comparison of Open and Solar beds Results

6.4.1 Single Application Experiments Results

The comparison of drying rate between the open and solar beds for single application experiments is shown in Table 6.9. In general, the drying rate of the open bed was faster than the passive solar bed. Although the volume of drainage water in both beds was identical, except when there was rain, water drainage was observed to be slower in the solar bed, prolonging the drying time. The average solids content per day of the open bed in Experiments 4 through 8 was much higher, meaning that the drying rate was much faster (Table 6.9). Experiment 6 was interrupted when the glass cover of the solar bed was broken before the end of drying time. The drying rates varied from one experiment to another according to variations in weather conditions, the application thickness and the initial solids content.

The drying rate was improved in experiments 11, 12 and 13 for the solar bed, however was still less than the open bed. The roof ventilator was not effective in removing the humid air from the cavity of the passive solar bed at low or zero wind

speed; therefore, there was no advantage of using the passive solar bed. Active solar bed drying rate (in Experiment 14) improved dramatically using a heat source (fan heater) as was explained earlier.

Table 6.9 Comparison of solar and open beds drying rates for single application experiments

Experiment Number	Open Bed Drying Rate (%/Day)	Solar Bed Drying Rate (%/Day)
4	5.1	0.7
5	7.9	1.6
6	1.4	1.0
7	9.0	1.4
8	4.4	1.0
9	2.5	1.3
11	2.7	0.7
12	1.6	1.0
13	2.9	0.8
14	1.9	2.7
15	2.8	-
16	5.0	-

Drying curves of the single bed experiments 4, 5, 6, 7, and 8 are shown in Figures 6.5 through 6.9 the solar bed was sealed in these experiments. Open bed performed well specifically when the weather was dry or windy. Residuals dry faster in the open bed; however the solar bed did not perform well in these experiments. The figures show clear gaps between the solar and the open bed drying time curves for the same drying time.

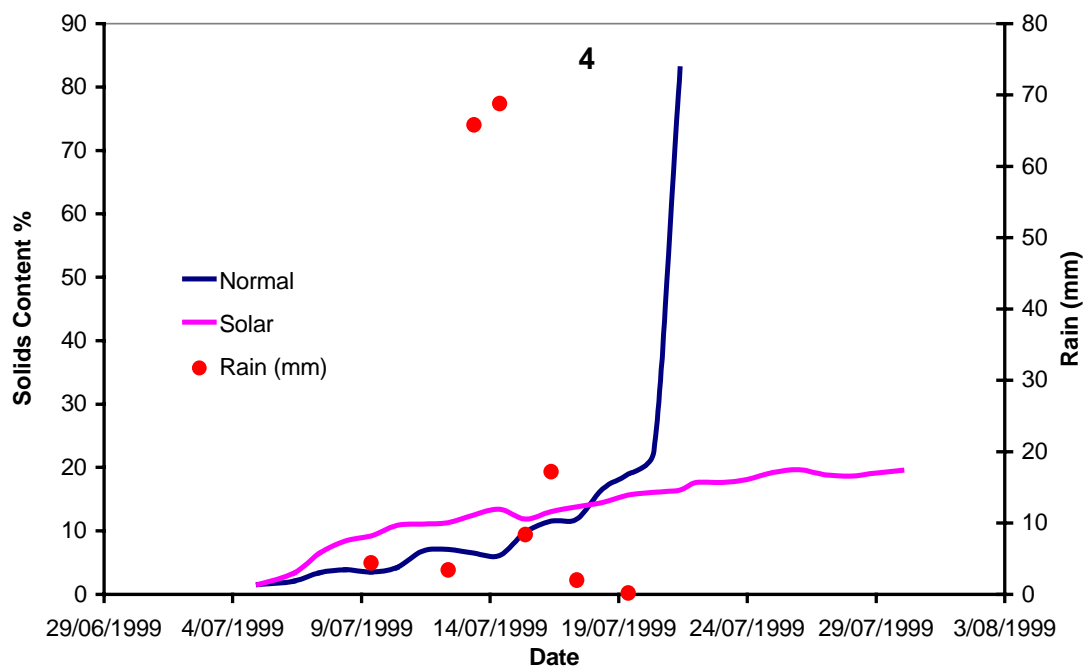


Figure 6.5 Drying of residuals (Experiment 4)

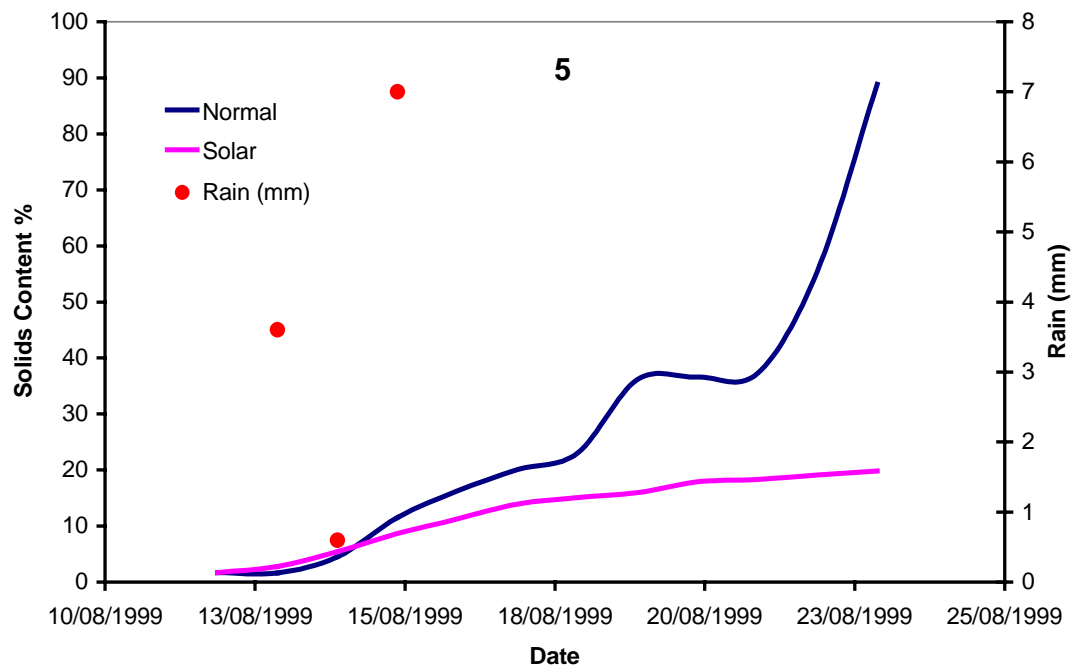


Figure 6.6 Drying of residuals (Experiment 5)

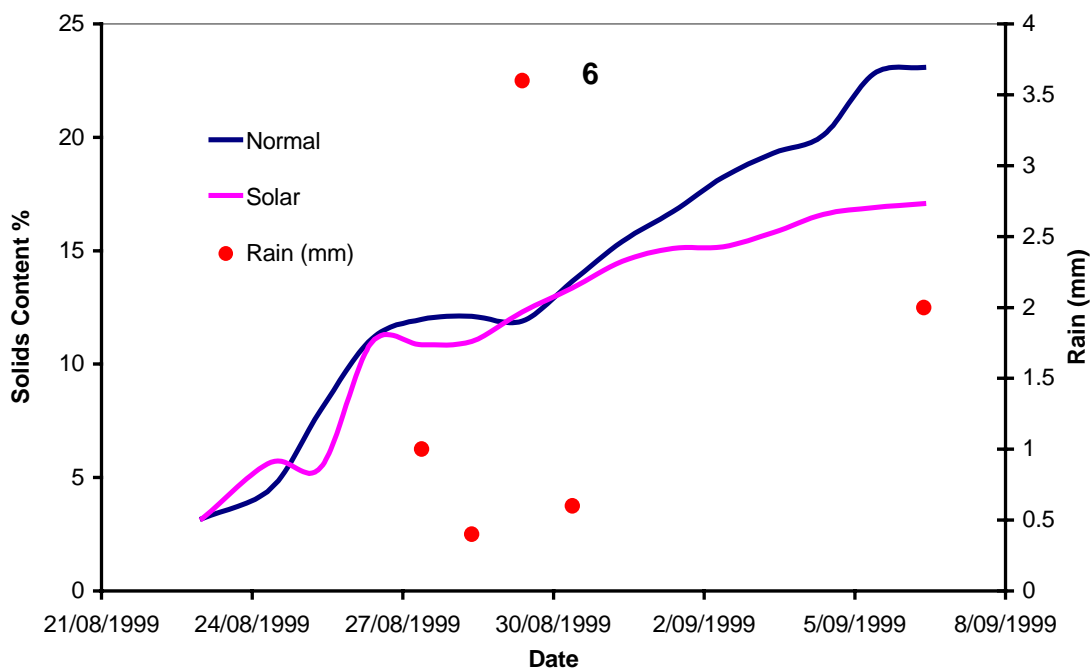


Figure 6.7 Drying of residuals (Experiment 6)

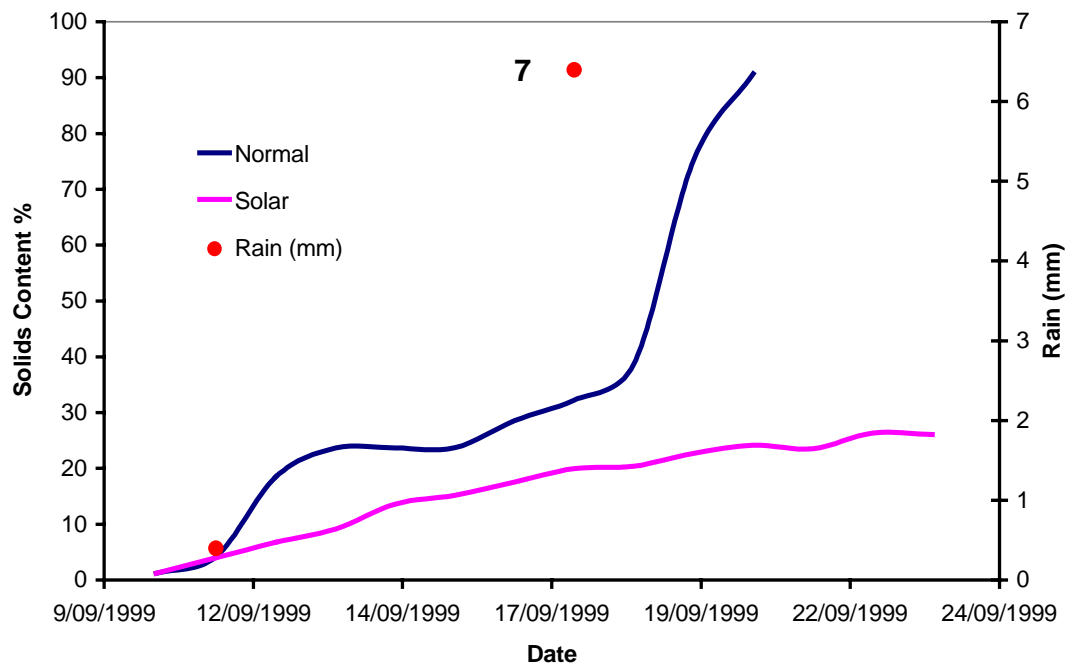


Figure 6.8 Drying of residuals (Experiment 7)

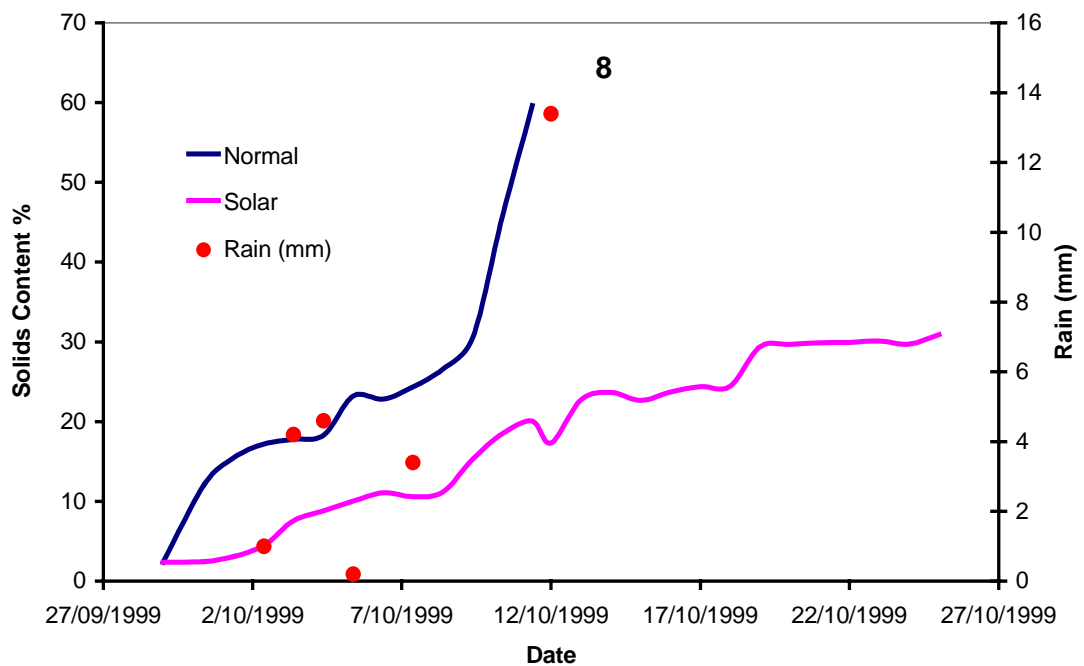


Figure 6.9 Drying of residuals (Experiment 8)

Figures 6.10, 6.11, 6.12, and 6.13 show the drying curves of Experiments 9, 11, 12, and 13. The solar bed was not sealed for these experiments (see Table 6.9) and the drying rate improved in the solar bed. The dips in the curve of the open bed occurred after a rain event; however, the solar bed drying curve dips are smaller because of high humidity in the atmosphere and less sunshine. It can generally be observed that the curve of the solar bed is smoother and flatter than the open bed. The solar bed is unaffected by rain and therefore less fluctuations occur in the drying curve unless residuals in the unsealed experiments were affected by high humidity in the atmosphere.

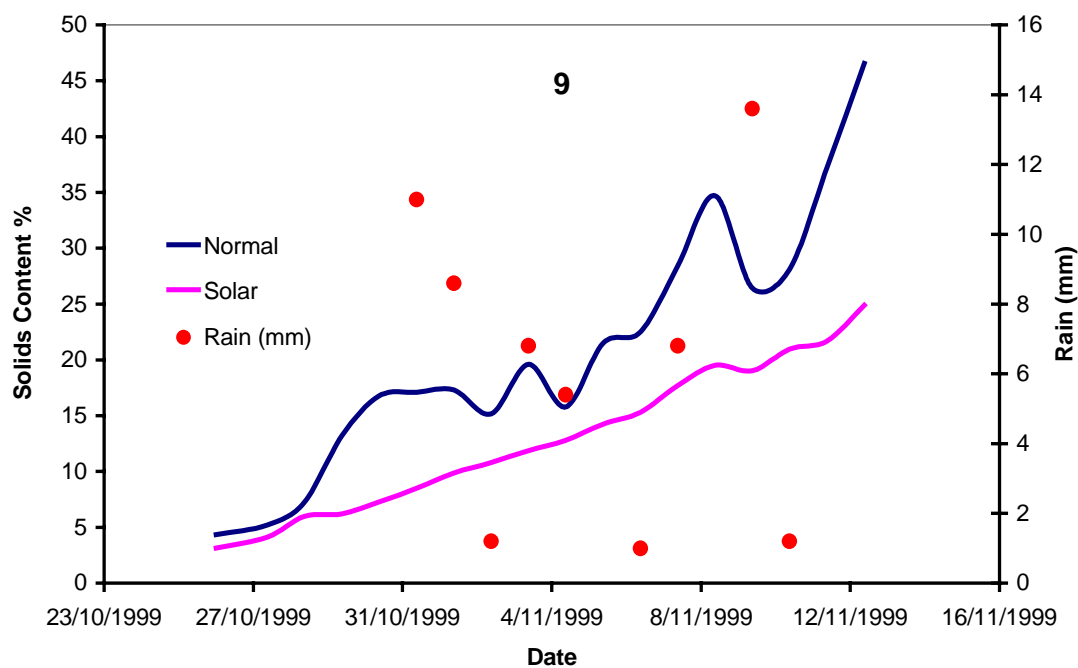


Figure 6.10 Drying of residuals (Experiment 9)

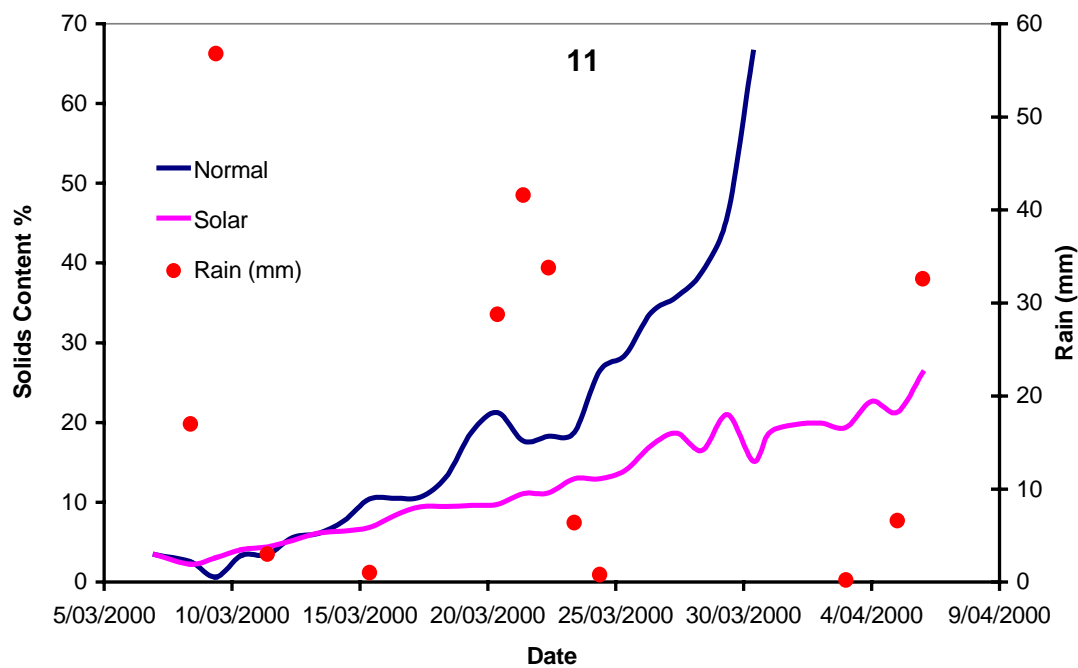


Figure 6.11 Drying of residuals (Experiment 11)

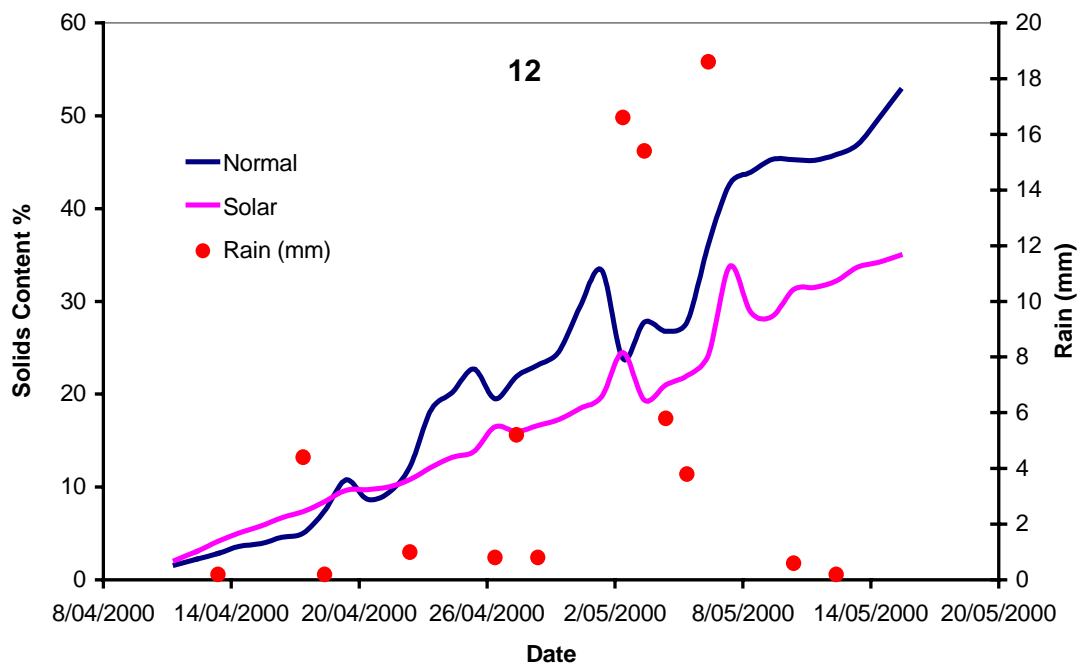


Figure 6.12 Drying of residuals (Experiment 12)

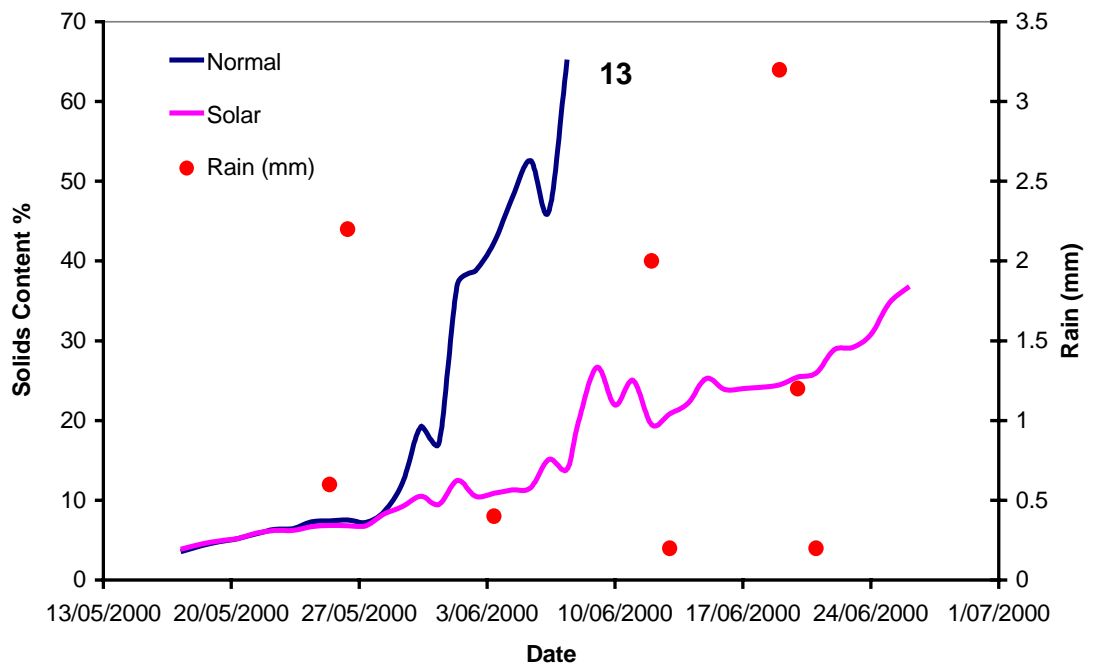


Figure 6.13 Drying of residuals (Experiment 13)

Figure 6.14 shows Experiment 14 where the solar bed was equipped with a fan heater. The curve shows the dramatic improvement of the drying time in the solar bed. In the open bed, the residuals when dried have a dry crust while remain wet deeper in the cake, however in the solar bed and in experiment 14, the residuals remained rubbery in texture. In experiment 14, the cover is non-transparent in order to provide heat only from the hot air of the fan heater and not from direct solar radiation. Direct sunshine and wind effect create a hard crust on the residuals surface, while the deeper cake remains wet. However, the covered solar bed had a fan heater and this has provided the residuals with a steady heated air flow, and this would have created uniform drying conditions. In Figures 16 and 17, no solar bed experiments were performed for technical reasons and therefore only the open bed experiments curves are shown.

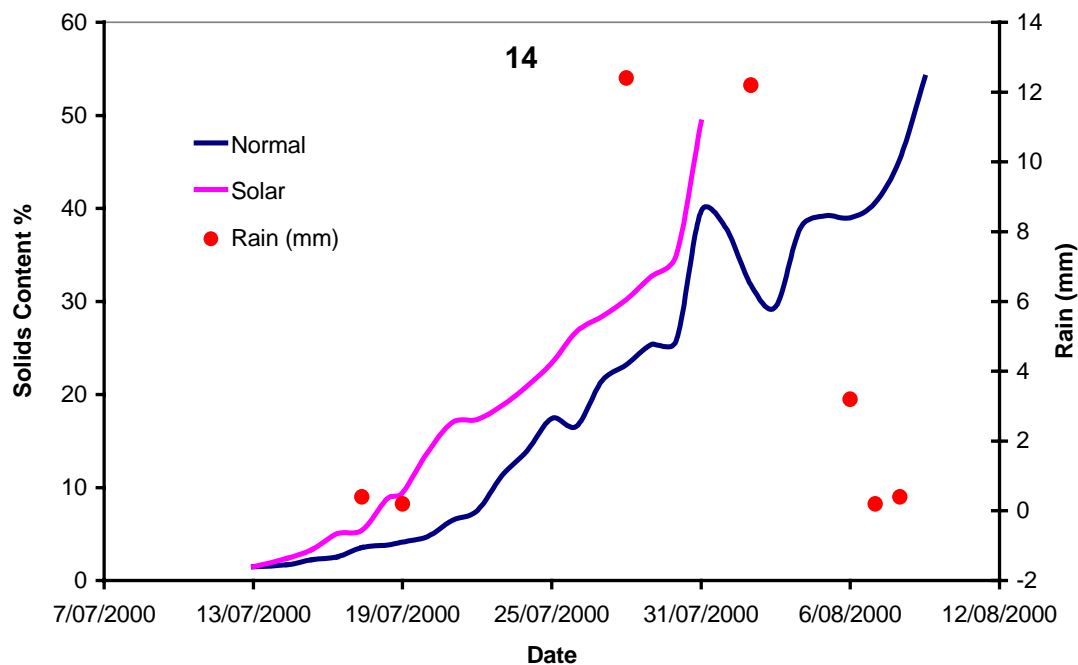


Figure 6.14 Drying of residuals (Experiment 14)

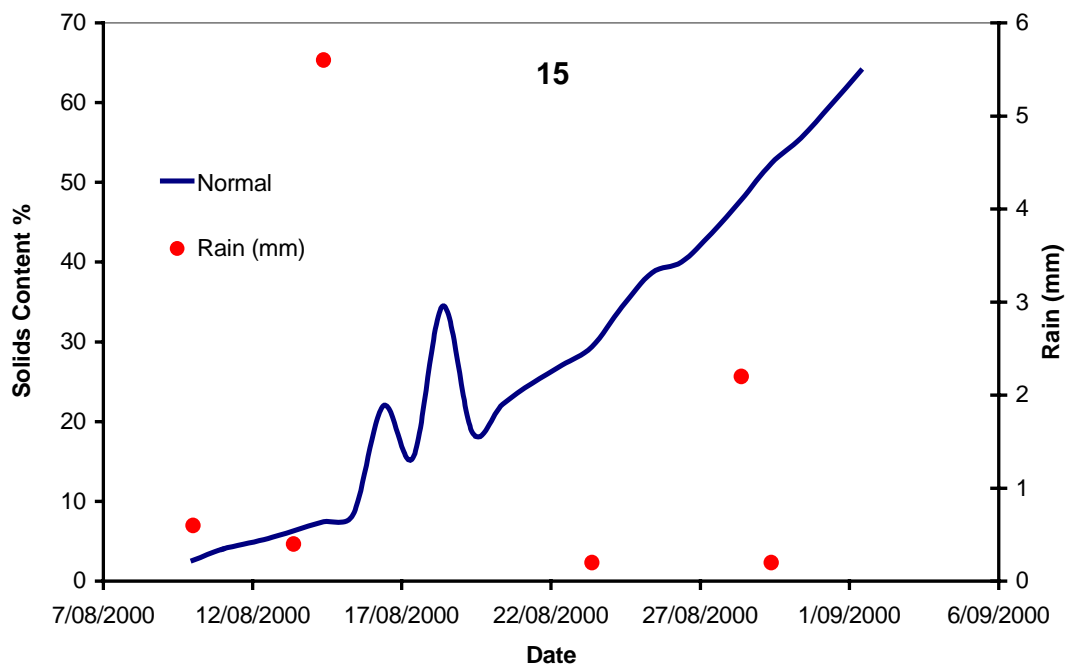


Figure 6.15 Drying of residuals (Experiment 15)

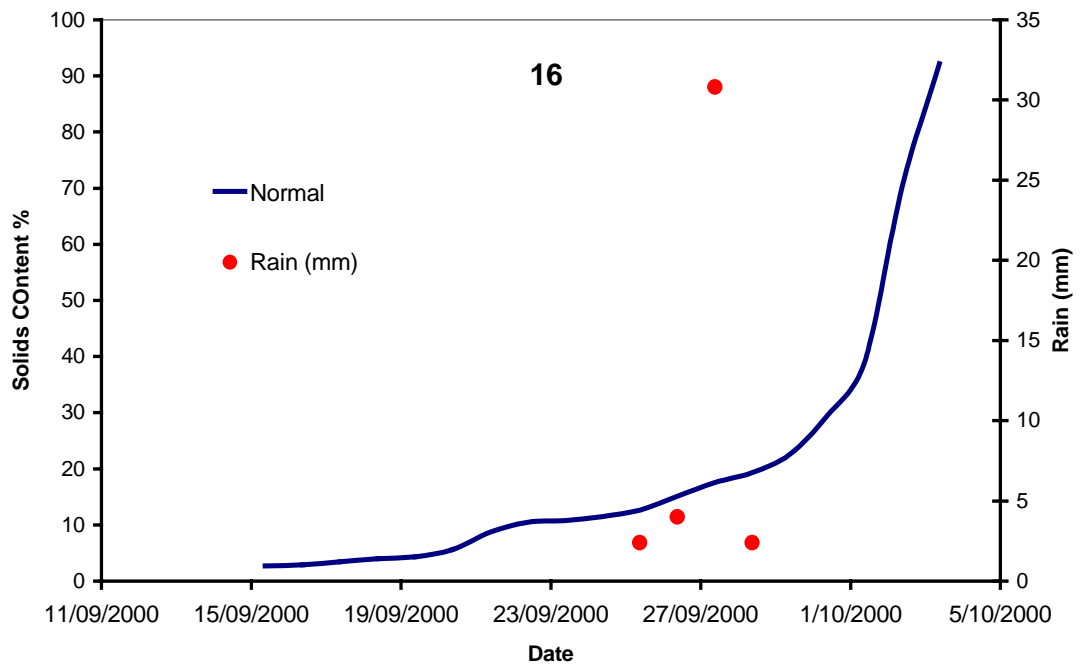


Figure 6.16 Drying of residuals (Experiment 16)

6.4.2 Multiple Application Experiments Results

The drying rate of the open bed is about 60% faster compared to the completely sealed solar bed in Experiment 10. The drying rate of solar bed Experiments 17, 18 and 19 improved dramatically by about 50% but remained less than the drying rate of the open bed experiments (Table 6.10). The modification of the solar bed to ventilate the bed cavity improved the rate of drying. The drying rate of Experiment 20 for both beds was the same, when both beds were open except for the glass cover to prevent rainfall entering through the top of the solar bed. Although the rainfall was substantial during Experiment 20 (Table 6.2), the drying rate of residuals in the open bed recovered quickly when the rain stops. The solar bed had no significant increase in drying during rainy days due to high relative humidity and the absence of sunshine.

Table 6.10 Comparison of solar and open beds drying rates for multiple applications experiments

Experiment Number	Open Bed Drying Rate (%/Day)	Solar Bed Drying Rate (%/Day)
10	2.4	1.0
17	1.7	1.5
18	2.6	2.4
19	1.6	1.4
20	0.9	0.9

The solar bed performance improved in the multiple application experiments, however remained slower than the open bed experiments. Figure 6.17 shows Experiment 10, where the solar bed was sealed. The drying curve of the open bed began to deviate higher than the solar bed at about 10% and then increased sharply when the solids content reached about 15%, whilst the solar bed drying curve continued to rise with a slight slope. Figures 6.18, 6.19, and 6.20 show the drying curves of Experiments

17, 18, and 19; the performance of the solar bed shows progressive improvement since the drying time is closing the gap with the open bed. Figure 21 shows Experiment 20 drying curves, which reveals identical drying times. All multiple application experiments (open and solar) show a peak in the curves after the first application, indicating quick drying of residuals for the small application thickness.

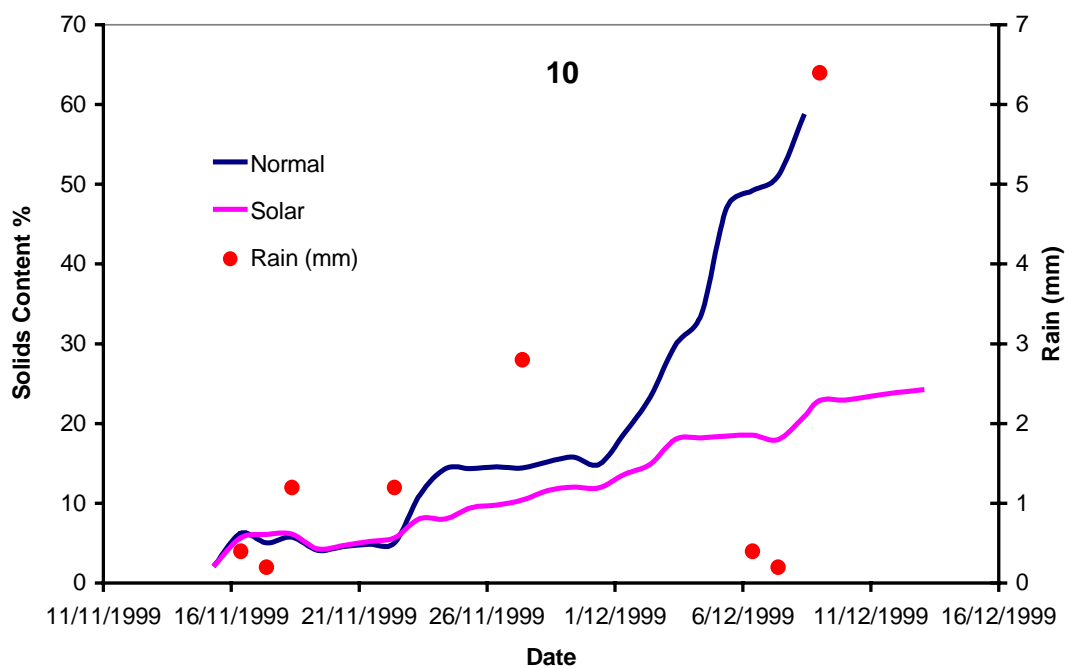


Figure 6.17 Drying of residuals (Experiment 10)

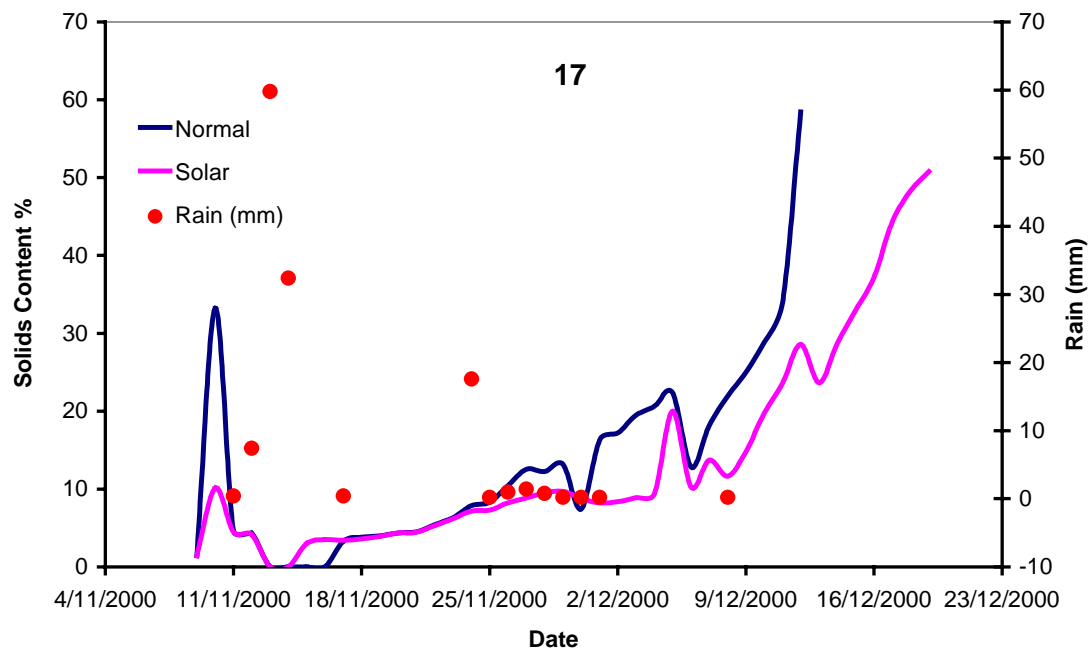


Figure 6.18 Drying of residuals (Experiment 17)

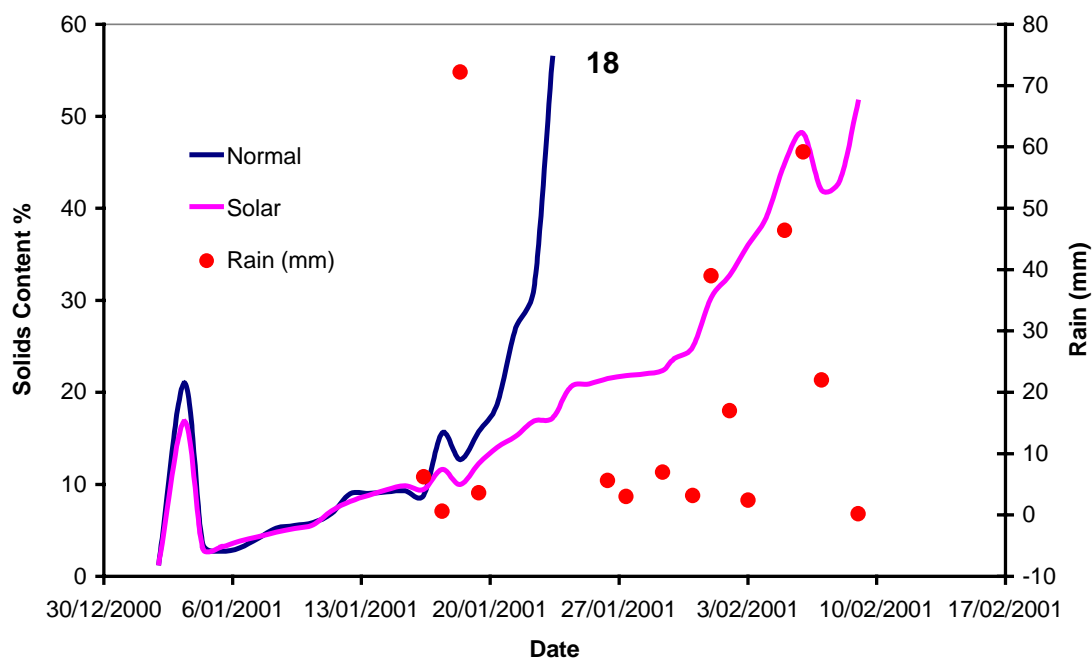


Figure 6.19 Drying of residuals (Experiment 18)

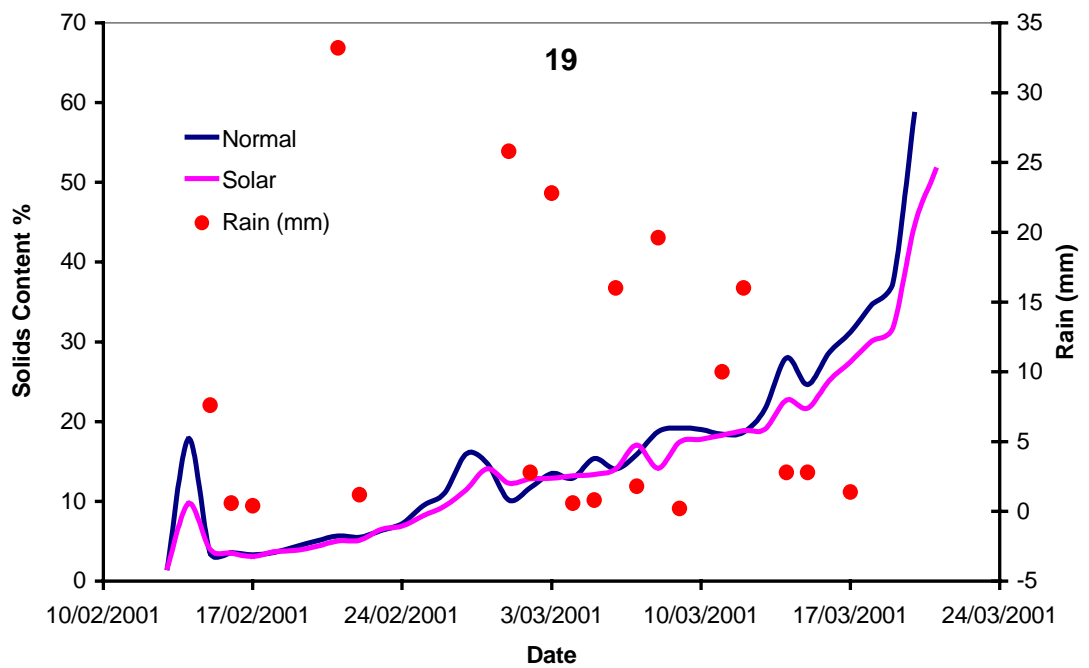


Figure 6.20 Drying of residuals (Experiment 19)

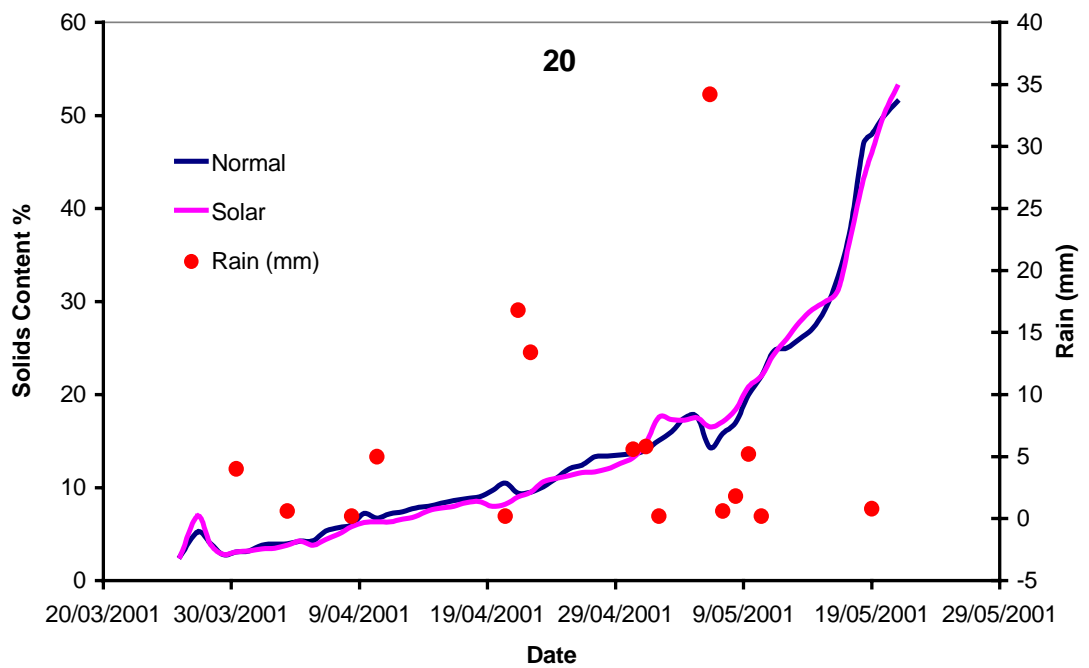


Figure 6.21 Drying of residuals (Experiment 20)

6.5 Field Experiments without Drainage and Rain

The aim of conducting the experiments, shown in Table 6.11, was to study the drying of residuals in the field without the effect of rain and drainage. Four experiments were conducted in the field next to the weather monitoring station starting from March 2002 until November 2002. Table 11 shows the daily average meteorological conditions as well as the application depth of residuals, initial and final solids content and drying time. A plastic tray having dimensions of 495 mm long and 335 mm wide placed under a cover sheet of Perspex (800 mm above the tray) was used for the experiments. The Perspex cover allows solar radiation penetration and prevents the rain from filling up the tray (Figure 6.22). The tray was weighed on a daily basis in order to calculate the daily water evaporation from the residuals and subsequently to calculate the solids content of the residuals.

Table 6.11 Field experiments without drainage

Experiment Number	Application Depth (mm)	Initial Solids Content %	Final Solids Content %	Drying Time (Days)	Relative Humidity %	T _∞ (°C)	T _{surface} (°C)	Solar Radiation (MJ/m ²)	Wind Speed (m/s)
20E	60	10.5	64.4	17	89	20.2	19.6	7.1	1.2
20F1	120	7	51.9	35	92	19.0	18.8	7	1.3
20F2	70	7	50.5	22	92	18.6	18.3	6.3	1.3
20K	120	6.5	79.7	19	70	18.3	17.6	13.4	1.2

Although the meteorological conditions of 20F1 and 20F2 experiments are comparable, the drying time has increased by almost 60%. However, the drying time of experiment 20K was 19 days compared to 17 days for experiment 20E. Although the initial solids content for both experiments are different, the drying rate is almost twice in favour of experiment 20K. The Solar radiation value is almost twice in favour of

experiment 20K and the 19% less relative humidity can influence the drying rate greatly.

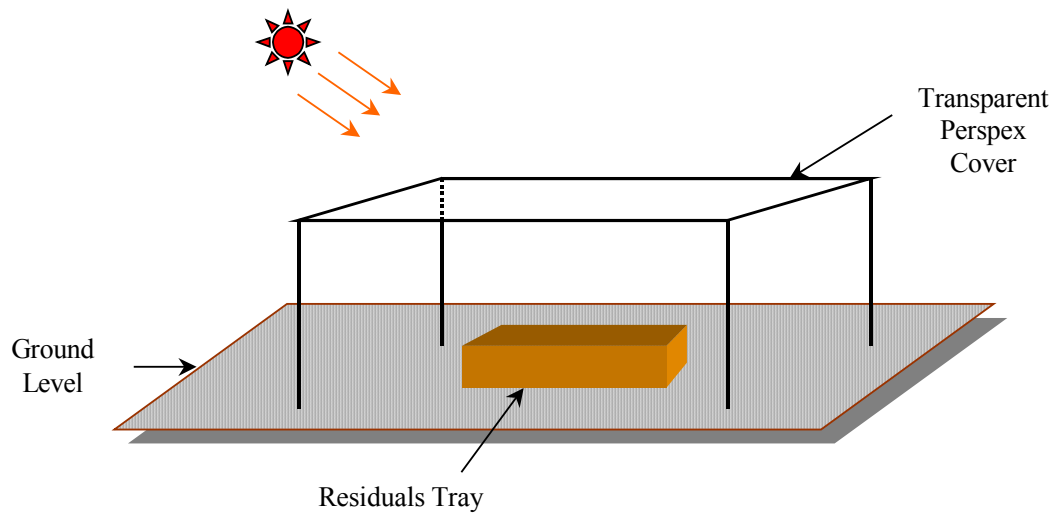


Figure 6.22 The setup of the field experiments performed without drainage and rain

6.6 Summary

The results of residuals field experiments were presented in this chapter. The single application thickness experiments were performed using four different application thicknesses (50, 100, 150 and 200 mm). However, the multiple application thickness experiments were applied in 50 mm or 100 mm applications. The multiple application experiments were conducted to simulate the actual drying bed operation. The field experiments were conducted to simulate the actual drying bed operation. The field experiments were performed in two identical experimental drying beds in size, an open drying bed and a solar drying bed. Although high temperatures were achieved in the cavity of the solar bed, drying time could not be enhanced compared to the experimental open sand drying bed. It appeared that removing the humid air from the cavity of the solar bed was a very important factor for enhancing the drying process. Therefore, the use of a fan heater in the solar bed improved the drying time by 33%

compared to the open bed. The field study revealed no significant advantage with the passive solar drying bed, and was therefore concluded that drying time would not be enhanced in comparison to the conventional sand drying bed. The normal bed drying is better in dry and windy conditions; however, the active solar bed can be the best option in humid and wet climates. Other experiments in the field were performed without drainage and under a perspex cover to allow solar radiation to reach the drying surface of residuals and prevent rain from entering the residuals tray.

In the following chapter (Chapter 7), predictions of the drying tunnel experimental work as well as the model calibration and application will be presented.

7 Calibration and Verification of the Mathematical Model

7.1 Introduction

The model presented in Chapter 4 describes the drying of water treatment plant residuals with the knowledge of meteorological conditions. In order to describe the drying process of residuals, calibration of the model was performed by selecting the most likely suitable inputs that affect the drying process. The mathematical model calibration is the process by which the model parameters are changed until a reasonable match between model output (moisture content or solids content) and observed data is achieved. This chapter will focus on the model calibration and validation with data from experiments performed in a laboratory drying tunnel and the field experimental drying bed. The model output shows good agreement with a set of experimental data performed in the drying tunnel and the field.

7.2 Non-dimensional Heat Transfer Coefficient

Drying results obtained from several residuals drying experiments performed in the drying tunnel were used to develop a non-dimensional heat transfer coefficient expression. A number of experiments data (23 experiments) were used to develop the heat transfer expression and the other experiments data to validate the model. The model explained in Chapter 4 is shown in the following equation:

$$\alpha_s A (G_{direct} \cos \theta + G_{diffuse}) + A \alpha_l \varepsilon_{atmospheric} \sigma T_{sky}^4 + Ah(T_{\infty} - T_{surface}) - A \varepsilon \sigma T_{surface}^4 - h_{fg} m_{solids} \frac{dX}{dt} = \frac{d}{dt} [(m_{solids} c_{solids} + m_{water(i)} c_{water}) T_{surface}] \quad (4.21)$$

In order to predict the moisture content of the residuals at any time t (dX/dt) using equation (7.1), the variables in the equation have to be either measured or obtained from

the literature. Table 7.1 shows the measured model parameters as well as the constants and their assumed values. An attempt was made to calculate the heat transfer coefficient for the water treatment plant residuals by limiting the number of varying parameters. Laboratory experiments were conducted indoors; therefore, the short wave heat radiation can be considered negligible. The heat stored term can be ignored since it is very small. Equation (4.21) can now be reduced, and in terms of heat transfer coefficient, to the following equation:

$$h = \frac{(\varepsilon \sigma T_{surface}^4 - \alpha_l \sigma T_{\infty}^4 + h_{fg} m_{solids} (dX / dt))}{A(T_{\infty} - T_{surface})} \quad (4.23)$$

Equation (4.23) can be used to calculate the heat transfer coefficient assuming both the emissivity and absorptivity values are to be (0.9). These values may change with temperature but the changes are negligible. All other parameters on the right hand side of equation (4.23) can be measured.

In practice, heat transfer coefficient is expressed as a non-dimensional quantity and is usually related to other known non-dimensional numbers. This relationship can be obtained from dimensional analysis. The convective heat transfer coefficient is a strong function of wind speed. Other factors that have influence on the heat transfer coefficient could be the difference in temperature between the residuals and the drying medium (air), relative humidity, the characteristic length and the thickness of the application. Using the Buckingham Pi theorem (Munson et al. 1994) a relationship was formulated to empirically predict the heat transfer coefficient in the following form:

$$Nu = \frac{hL}{k} = \gamma Re^a Gr^b \left(\frac{L}{s} \right)^c RH^d \quad (4.24)$$

Table 7.1 Model parameters

Name	Symbol	Unit	Assumed Values
<i>Measured parameters</i>			
Ambient Temperature	T_{∞}	$^{\circ}\text{C}$	-
Surface Temperature	T_{surface}	$^{\circ}\text{C}$	-
Mass of Water	m_{water}	kg	-
Mass of Solids	m_{solids}	kg	-
<i>Constants</i>			
Absorptivity	α_l	dimensionless	0.9
Emissivity	ε	dimensionless	0.9
Latent Heat of Vaporisation	h_{fg}	J/kg	-

Where γ, a, b, c, d are empirical constants, k is the thermal conductivity of humid air in ($\text{J/m}^2 \cdot \text{K}$), L is the characteristic length of the application of residuals in (m), Nu is the dimensionless Nusselt number $= hL/k$, Re is the Reynolds number $= uL/\nu$, u is the wind speed of air in (m/s), ν is the kinematic viscosity of air in (m^2/s), Gr is the Grashof number $= \beta g L^3 \Delta T / \nu^2$, β is the coefficient of volume expansion $= 1/((T_{\infty} + T_{\text{surface}})/2)$ in (K^{-1}), g is the gravitational acceleration (9.8 m/s^2), ΔT is the temperature difference between the air and the residuals surface temperature in degrees (K), s is the application thickness in (m) and RH is the relative humidity of air expressed in decimal. Taking the logarithm of equation (4.24) then performing a linear regression analysis using Microsoft Excel gives the following expression:

$$\frac{hL}{k} = 890.36 (\text{Re})^{1.192} (Gr)^{-0.927} \left(\frac{L}{s} \right)^{0.0628} (RH)^{-1.997} \quad (4.25)$$

Table 7.2 shows the summary output of the regression analysis performed using MS Excel, which is collected from data points of 23 drying tunnel experiments. The regression model very well explains the proportion of the variation in the dependent

variable, since the coefficient of determination (R^2) has a value of (0.968). The ANOVA table shows that the model is significant having a value less than (0.01). The P-values of the independent variables show that all the variables are significant except for (L/s), which is insignificant. The model shows that the meteorological variables have greater effect on the dependent variable than the geometry of the residuals application. The reason for the insignificance of (L/s) could be due to the small variations in the thickness (s) data of the residuals applications; however, the area for all experiments is the same.

Table 7.2 Regression analysis table

<i>Regression Statistics</i>	
Multiple R	0.984056955
R Square	0.96836809
Adjusted R Square	0.961338777
Standard Error	0.073056951
Observations	32809

ANOVA					
	<i>df</i>	<i>SS</i>	<i>MS</i>	<i>F</i>	<i>Significance F</i>
Regression	4	2.941105776	0.7352764	137.761407	3.08025E-13
Residual	32804	0.096071725	0.0053373		
Total	32808	3.037177501			

	<i>Coefficients</i>	<i>Standard Error</i>	<i>t Stat</i>	<i>P-value</i>	<i>Lower 95%</i>	<i>Upper 95%</i>
Intercept	2.949566238	1.149329387	2.5663367	0.01942421	0.534912928	5.364219548
log(Re)	1.191522609	0.066016784	18.048783	5.6225E-13	1.052826385	1.330218833
log(Gr)	-0.927332338	0.168993536	-5.487383	3.2738E-05	-1.282374858	-0.572289819
log(RH)	-1.996726001	0.735822633	-2.713597	0.01423437	-3.542633184	-0.450818817
log(L/S)	0.062832171	0.066536407	0.9443277	0.35750638	-0.076955742	0.202620083

7.3 Discussion of Results

7.3.1 Drying Tunnel Experiments

The drying tunnel experiments are summarised in (Tables 7.3 and 7.4). The tables show the application thickness for each experiment, wind speed, average air and surface

temperatures, average relative humidity, and the calculated and predicted heat transfer coefficients. The average values of temperatures and relative humidity are the average data values taken over the whole period of a single experiment. The initial solids content for all the experiments vary from 5 to 10% and experiments were stopped when the solids content reached 50%. The drying tunnel, as discussed in Chapter 5, is able to control the wind speed using a variable speed fan; however, the temperature and relative humidity vary during any given experiment. The variations in relative humidity can be as low as 8% in experiments 36 and 37, and as high as 50% in experiment 46. The air temperature variations were as high as 22 °C for experiment 14 and as low as 4 °C for experiment 36. The error in temperature measurement is ± 0.1 °C, which will result in about 1% error in relative humidity measurement, since relative humidity is calculated from the dry and wet bulb temperatures (see Chapter 5). The drying experiments were conducted with variations in air temperature and relative humidity, and only wind speed was controlled. The model is able to predict the moisture content, and hence the drying time using the variations in the weather conditions.

Residuals surface cracks start at 10% solids content; a clear hard crust is formed at 15%. Cracks are about 15-20 mm deep when the initial application depth of the residuals is 50 mm. Figure 7.1 shows the crack formation over the course of the residuals drying process. The cracks are up to 40 mm wide in a 200 mm by 200 mm tray. The cracks reach the bottom of the tray when the solids content is about 20% and at 30%, the dry residuals become fragmented with wet and dry fragments. The fragments (about 15 mm in thickness) become isolated and appear very dry at 50% solids content. Drying from 8% to 15% solids content, the residuals application loose 45% of the moisture, however drying from 8% to 50% solids content accounts for 84% moisture loss.

Table 7.3 Summary of the laboratory drying tunnel experiments (8-38)

Exp	Wind	Thickness	Relative	Air	Surface	Heat Transfer	Heat Transfer
	Speed		Humidity	Temp	Temp	Coefficient	Coefficient
No.	(m/s)	(mm)	%	(°C)	(°C)	(Equation 4.23)	(predicted)
						(W/m ² .K)	(W/m ² .K)
34	1	10	80	22.4	17.1	9.9	8.7
15	1	20	77	21.4	14.4	7.7	6.8
27	1	40	70	25.4	15.4	4.7	5.9
28	1	60	74	25.5	16.4	7.3	5.6
33	1	60	72	29.5	18.5	4.4	5.1
10	1	80	72	22.8	18.1	13.2	11.6
35	2	10	81	22	16.3	16.2	18.3
16	2	20	73	22.3	13.7	12.7	14.1
26	2	40	68	25.8	15.9	12.5	14.5
29	2	60	77	25.8	17.7	13.2	13.4
12	2	80	71	25.4	18.6	15.1	16.9
14	2	80	82	25	18.7	10.5	13.1
36	3	10	82	21.5	16.1	25.2	27.6
17	3	20	70	21	12.7	29.9	27.8
25	3	40	71	25.3	16.6	26.8	23.9
30	3	60	73	27.3	19.8	28.4	25.7
9	3	80	66	26.8	20.2	37.0	35.4
37	4	10	76	23.9	17.6	45.8	43.5
18	4	20	69	20.7	12.2	43.9	41.1
24	4	40	65	23.5	14	45.4	42.5
31	4	60	72	28.3	23.7	63.9	61.0
13	4	80	75	25	18.2	42.8	40.1
38	5	10	78	24.5	16.4	35.7	38.5
19	5	20	70	21.4	12.3	44.8	43.7
23	5	40	69	21.4	14.1	53.4	53.2
32	5	60	73	24.7	18.3	56.3	53.9
8	5	80	67	26.3	21.1	65.7	67.5
20	7	20	68	25.7	14.9	63.1	61.5
22	7	40	65	25.4	14.5	62.2	64.2
21	7	60	65	25.9	15	68.1	65.1
11	7	80	57	29.3	19.8	58.5	60.9

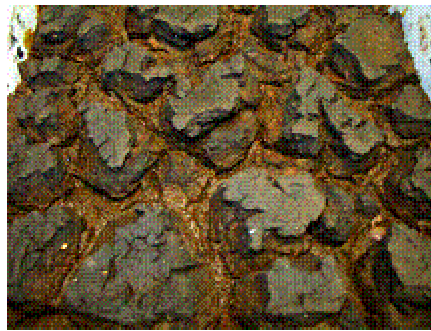
Table 7.4 Summary of the laboratory drying tunnel experiments (39-63)

Exp	Wind	Thickness	Relative	Air	Surface	Heat Transfer	Heat Transfer
No.	Speed	(mm)	Humidity	Temp	Temp	Coefficient	Coefficient
	(m/s)		%	(⁰ C)	(⁰ C)	(Equation 4.23)	(Predicted)
						(W/m ² .K)	(W/m ² .K)
39	2	10	72.1	20.0	15.5	13.7	15
40	2	10	66.3	18.8	14.1	16.9	17.7
41	2	10	83	23.4	19.5	12.5	15.1
42	2	10	86.7	24.1	20.4	12.3	13
43	2	10	59.7	32.3	22.7	13.4	13.9
44	2	10	73.3	32.5	26.5	10.3	11.4
45	4	10	73.5	29.0	23.5	29.3	31.8
46	4	10	87.2	24.4	22.1	29.6	32.2
47	6	10	76.7	24.9	20.7	39.3	43.1
48	6	10	53.6	31.3	21.5	43.4	40.8
49	2	40	88.2	27.1	24.1	18.0	21.3
50	2	40	56	30.9	21.1	22.2	23.5
51	4	40	79.6	25.8	22.5	44.4	45.5
52	4	40	60.4	28.1	21.6	45.0	43.8
53	6	40	80.5	22.9	20.1	58.4	58.6
54	6	40	65	29.4	22.7	52.3	52.7
55	2	80	77.3	28.6	23.7	22.7	23.2
56	2	80	44.5	36.0	23.9	24.3	26.6
57	4	80	70.2	28.9	24.5	56.2	57.1
58	4	80	61	32.1	24.7	39.0	38.8
59	6	80	79.6	26.0	22.7	63.2	64.6
60	6	80	63.8	31.2	24.3	61.8	65.7
61	6	60	69.8	24.9	19.9	61.1	63.1
62	6	20	68.5	23.0	19.0	57.7	59.4
63	6	10	61	26.6	21.1	47.1	51.2

Figures (7.2, 7.3, 7.4, 7.5 and 7.6) show the experiments used for verification of the model. The predicted and experimental solids content curves are plotted versus drying time for these drying tunnel experiments. It is apparent that solids content increases continuously with drying time. Analysis of all obtained graphs show that results of calculations obtained from the model very well correlated with experimental data (the lowest correlation coefficient amounted to 0.93).



8%



15%



30%



50%

Figure 7.1 Residuals at four different solids content

From the prediction graphs, deviation mainly occurs at the end of the drying period. The dry crust creates high resistance for the moisture movement within the residuals. The shrinkage and cracking of residuals occurred simultaneously during drying (Tao et al. 2005). Above 15% solids content, cracks and shrinkage create temperature variations within the body of the application, hence affecting temperature measurement and therefore the prediction of the model.

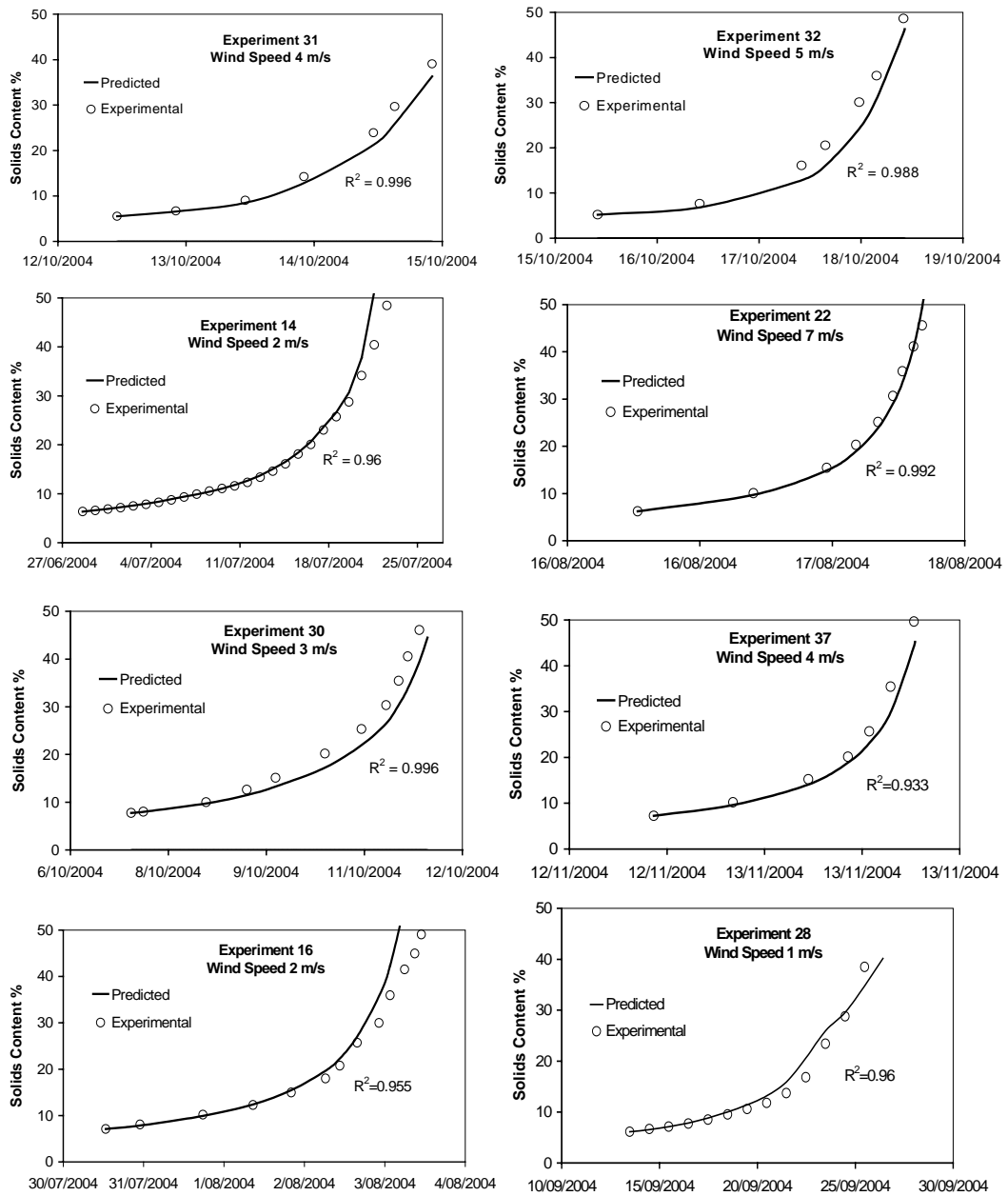


Figure 7.2 Laboratory drying tunnel experiments (14, 16, 22, 28, 30, 31, 32, 37)

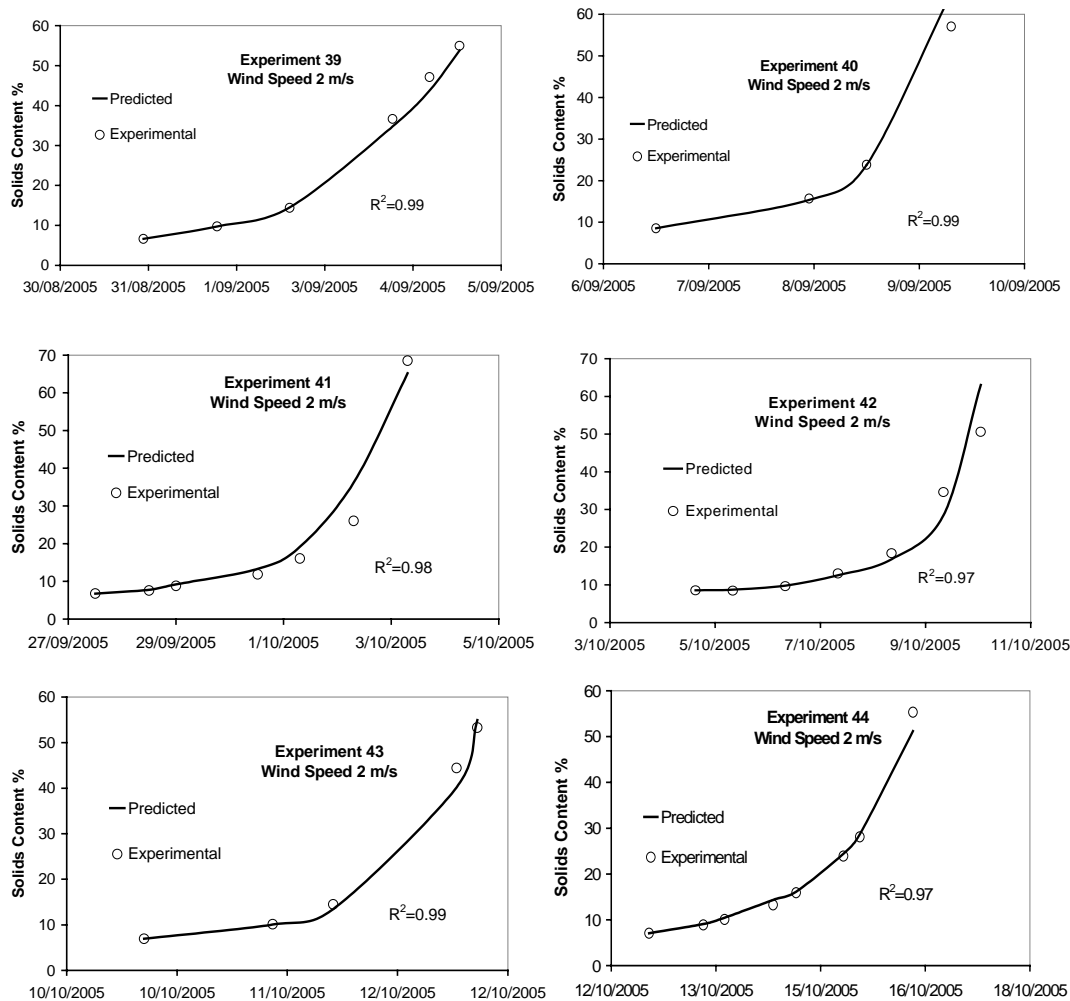


Figure 7.3 Laboratory drying tunnel experiments (39-44)

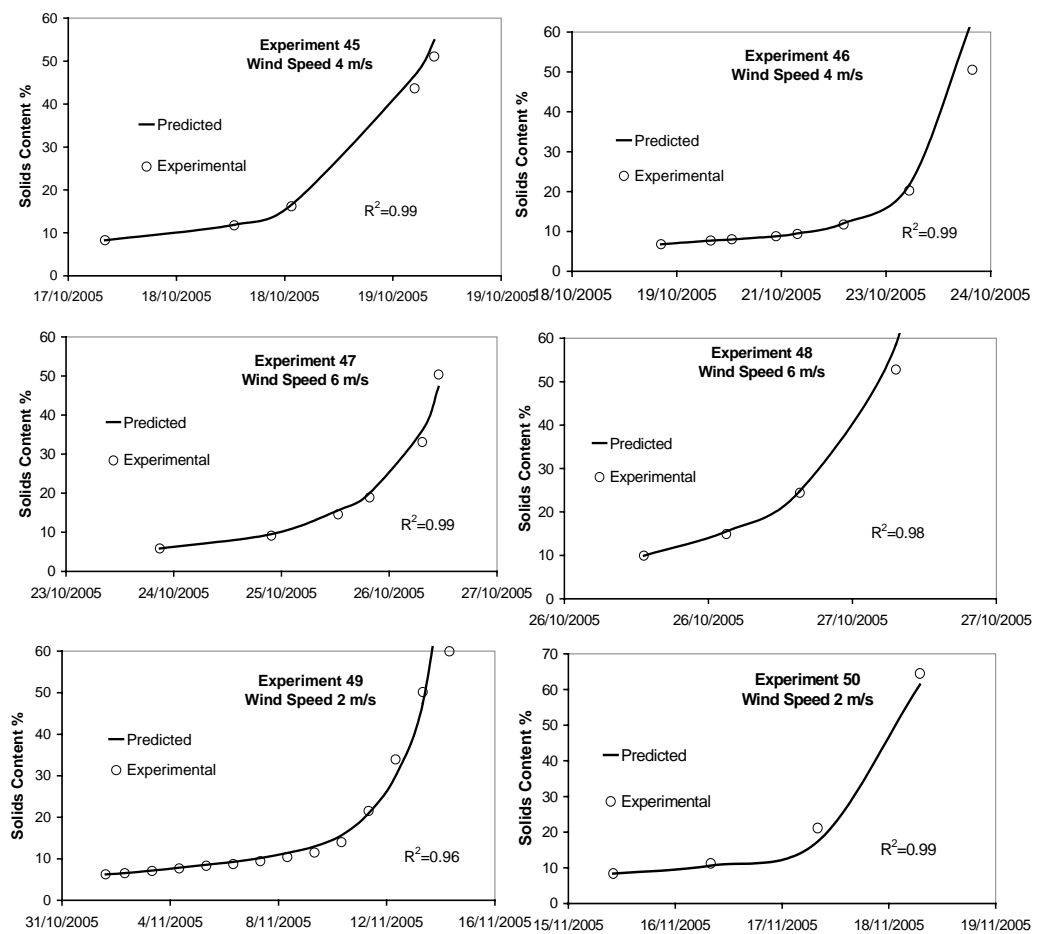


Figure 7.4 Laboratory drying tunnel experiments (45-50)

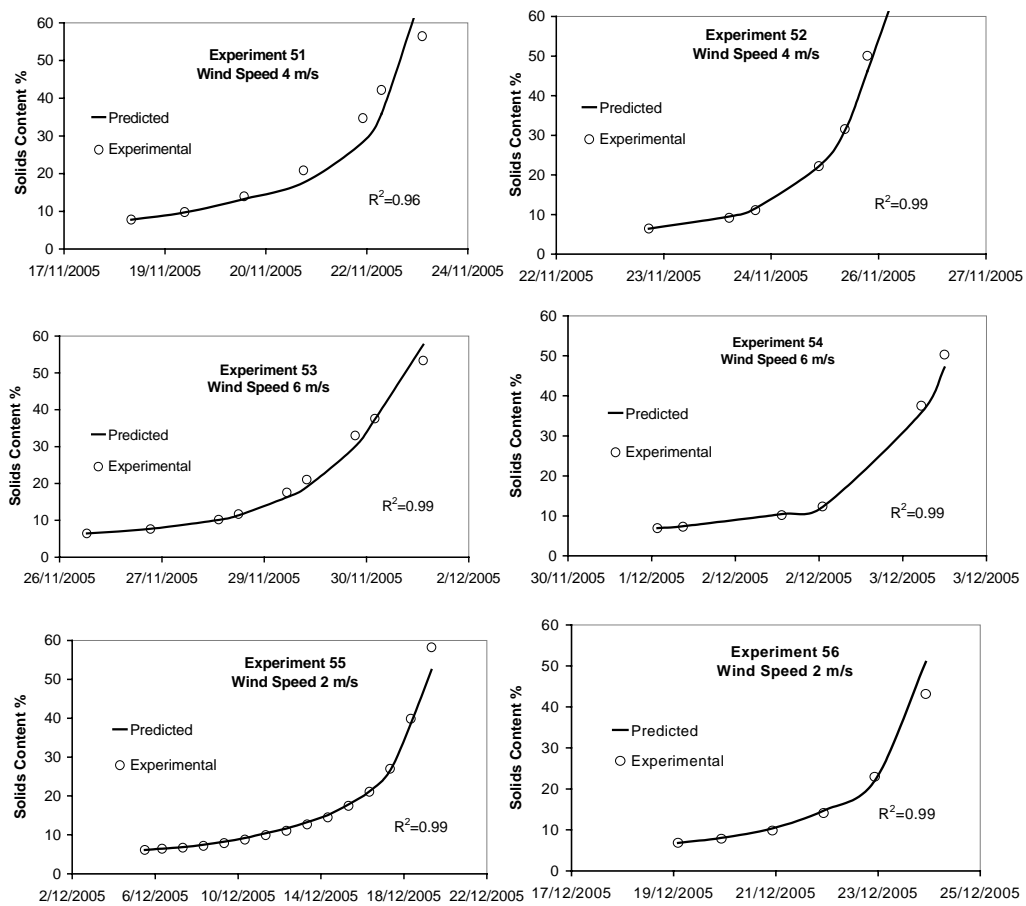


Figure 7.5 Laboratory drying tunnel experiments (51-56)

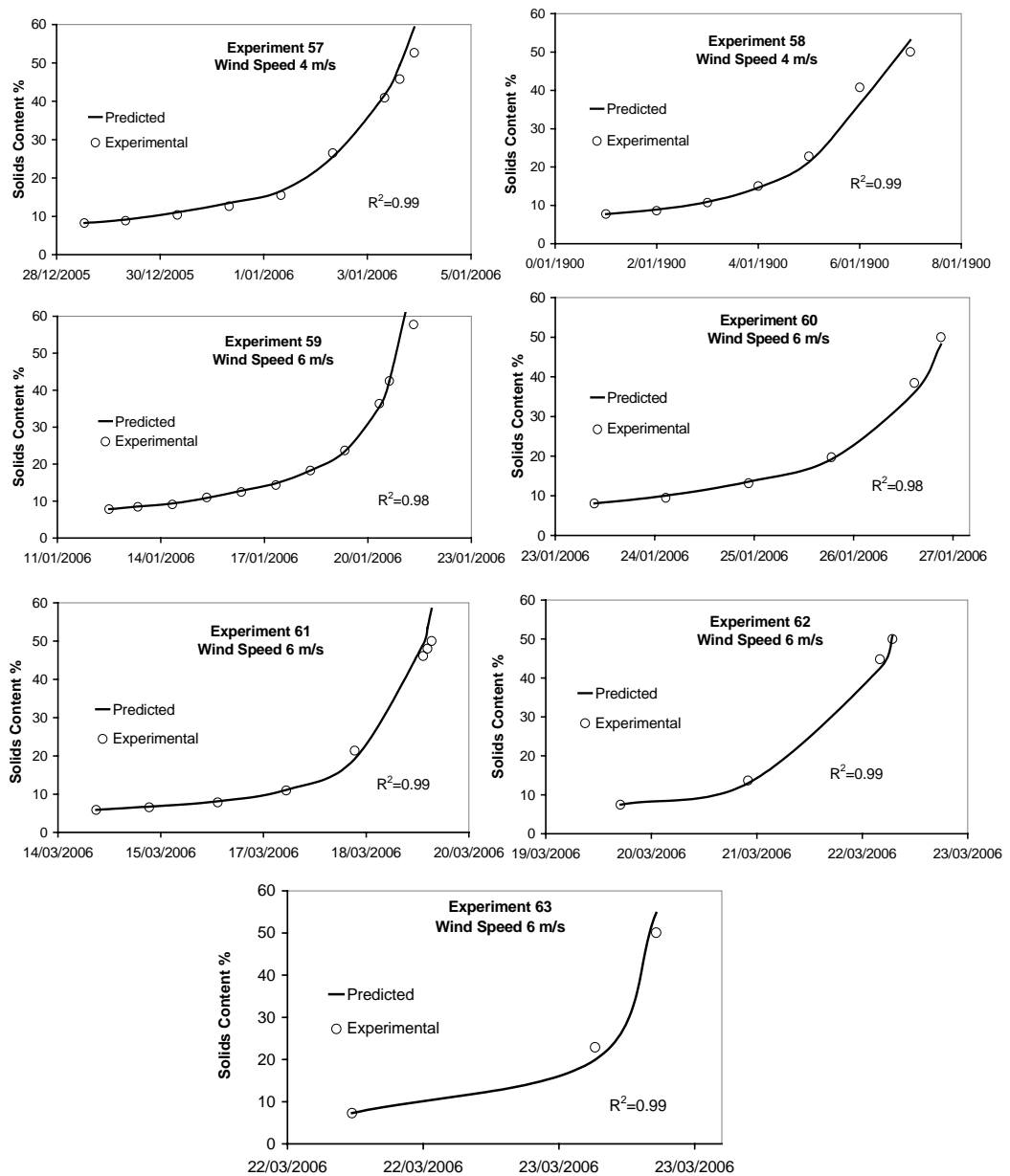


Figure 7.6 Laboratory drying tunnel experiments (57-63)

7.3.2 Field Experiments

7.3.2.1 Single Application Field Experiments

Six experiments were conducted in a sand drying bed. The moisture content with respect to time is calculated using equation 4.21 for these experiments. The wind speed values are corrected for measurement height using the empirical power-law wind profile ($u_{ref} = u(z_{ref}/z)^{0.31}$) (Hsu and Meindl 1994). Where z, z_{ref} are the heights above the ground surface and at reference height in (m) respectively and u, u_{ref} are the wind speed and wind speed at reference level in (m/s) respectively. The drainage and rainwater are included in the mass balance equation for the experimental sand drying bed using the following equation:

$$\begin{aligned} \frac{dX}{dt} = & \frac{1}{h_{fg} m_{solids}} \left(\alpha_s A (G_{direct} \cos \theta + G_{diffuse}) + A \alpha_l \varepsilon_{atmospheric} \sigma T_{sky}^4 \right) \\ & + \frac{d}{dt} \left(\frac{m_{drained}}{m_{solids}} \right) + \frac{d}{dt} \left(\frac{m_{rain}}{m_{solids}} \right) \end{aligned} \quad (7.1)$$

In order to calculate the moisture content for the single application field experiments, equation 7.1 is used. Unlike the laboratory drying tunnel experiments, the field experiments were exposed to direct sunshine and rainfall as well as fluctuations in ambient temperature, wind speed and relative humidity. Figure 7.7 show the predicted and experimental results for field experiments 11, 12, 13 and 14. The plots show dips and peaks due to high rainfall during the course of the experiments. The deep cracks in the residuals surface allow rainwater to easily find its way to be drained through the sand bed layer without being absorbed by the residuals. Therefore, the dips in these curves soon recover when the rain stops within a day or two and depending on the weather conditions.

The drying curves of Figure 7.7 show good agreement between the predicted and experimental results up to 30% solids content. However, in experiment 13, the prediction and experimental graphs deviate between 15% and 40% solids content but the gap becomes less at the end of the drying period in which the model gives a satisfactory prediction of 44% predicted and 46% experimental ($R^2=0.904$). Above 30% solids content, all experiments drying curves deviate from experimental results due to unpredictable drying patterns and temperature measurements. In experiment 14, the dip in the predicted curve, which is caused by rain, has a slight shift due to late accumulative measurement of drainage water from the sand drying bed. The coefficient of determination (R^2) varies from 0.805 for experiment 11 and as high as 0.97 for experiment 16 as shown in Figure 7.7.

7.3.2.2 Multiple Application Field Experiments

In practice, residuals are applied on the sand drying bed continuously. Residuals are discharged on the sand drying beds via several PVC pipes around the bed (Figure 7.8). Residuals are spread over the sand, which overlies a filter system of gravel and drain pipes. When the bed is covered with around 20-30 mm in application thickness, the residuals are left to dry before another layer is applied. In practice, 200-300 mm of final residuals thickness is applied in the bed before it is cleaned. Experiments 17, 18, 19 and 20 are multiple applications conducted to simulate actual bed operation in practice. The applications were applied on a daily basis until the 200 mm top section of the experimental bed is full (explained in chapter 6). Equation 7.1 is applied to predict the moisture content with respect to time. The thickness term s in the heat transfer equation 4.25 is updated for each daily application.

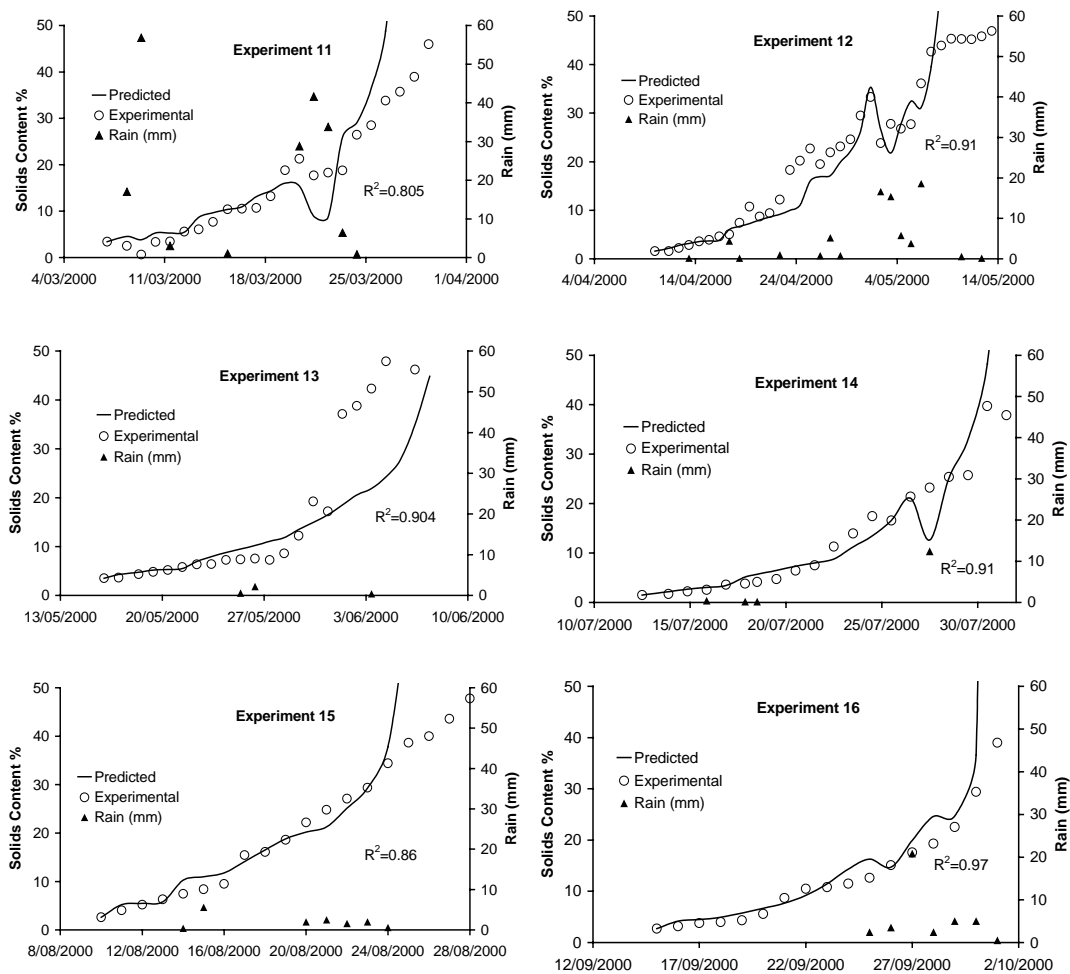


Figure 7.7 Single application thickness field experiments



Figure 7.8 Residuals pumped out into the sand drying bed

The plots of the four experiments are shown in Figure 7.9. There is good agreement between predicted and experimental curves except for experiment 17 ($R^2 = 0.88$) in which the predicted curve deviates from experimental; however, they agree at the end of the drying time above 20% solids content. High and continuous rainfall occurs below 20% in experiment 19, which might have contributed to the error in the measurement of solids content since the residuals are still reasonably wet. The fluctuations seen in the drying curves for experiments 18 and 20 coincide with rainfall, however, good coefficient of determination 0.984 and 0.97 can be observed. Rain does not greatly affect the drying of residuals; this is evident that the curve recovers soon after the rain stops. However, the overall drying period is affected with extended rain periods.

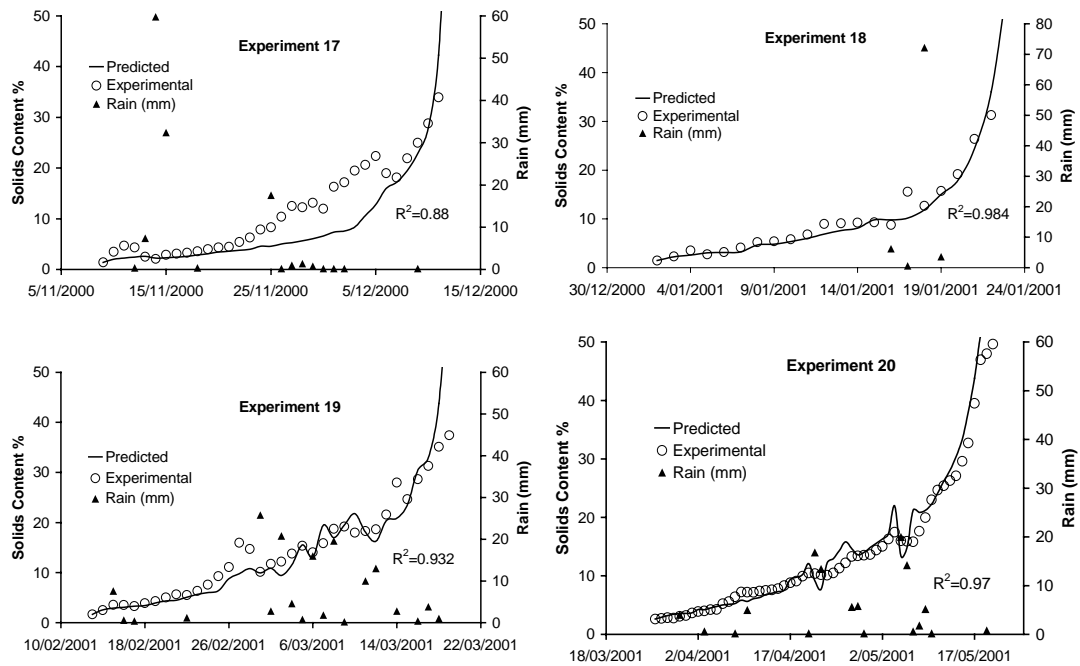


Figure 7.9 Multiple application field experiments

7.3.2.3 Field Experiments without Drainage and Rain

The aim of conducting these experiments was to study the drying of residuals in the field without the effect of rain and drainage. Four experiments were conducted in the field next to the weather monitoring station. A plastic tray having dimensions of 495 mm long and 335 mm wide, placed under a cover sheet of Perspex (800 mm above the tray), was used for the experiments. The Perspex cover allows solar radiation penetration and prevents rain from filling up the tray. The tray was weighed on a daily basis at an exact time (8:00 am) to calculate the daily water evaporation from the residuals and subsequently to calculate the solids content of the residuals.

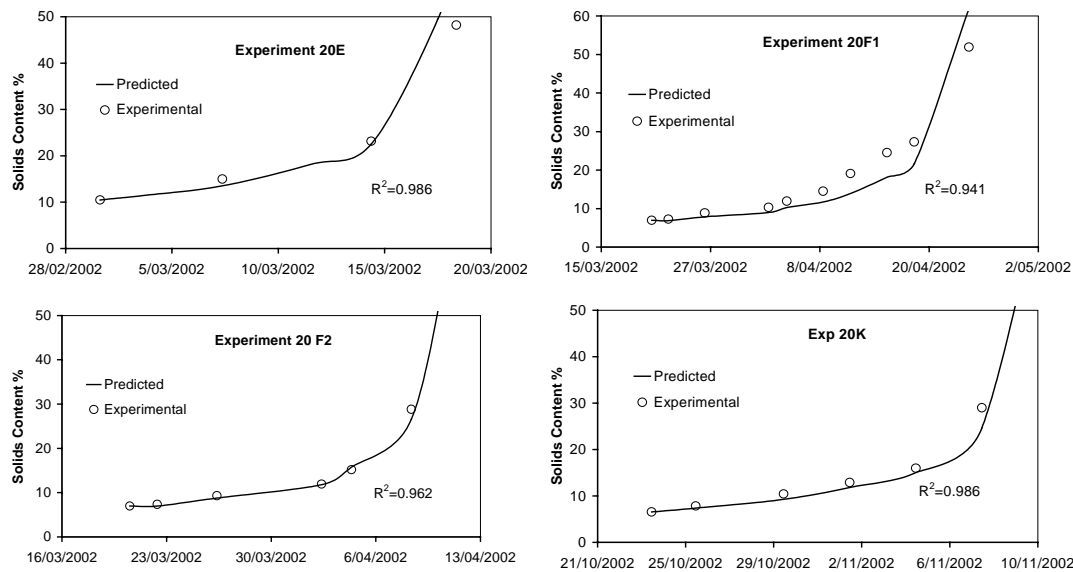


Figure 7.10 Single application field experiments (without drainage and rain)

Equation 4.21 was used to predict the moisture content for the four experiments. The predicted and experimental results show good agreement as shown in Figure 7.10. No dips in the curves due to rain since the cover prevented rain from wetting the residuals. Experiments 20F2 and 20K show good agreement; small deviations occur at the end of

the drying time in Experiment 20E whereas the prediction has slight deviations from the experimental results. Since the (R^2) is higher than 0.94 in this set of experiments, then, the uncertainty in prediction seems to be much less in the covered experiments which makes the model more applicable to be used under these conditions.

7.4 Summary

In this chapter, the mathematical model was calibrated and validated with data from experiments performed in the laboratory drying tunnel and the field experimental drying bed. A heat transfer coefficient correlation was formulated using dimensional analysis. The drying tunnel experiments were used in the prediction of the heat transfer coefficient correlation with the knowledge of weather parameters. A set of drying tunnel experiments were used to verify the model as well as other experiments performed in the field. The predictions using the model gave good agreement with experimental work in the drying tunnel and the field experiments. The coefficient of determination (R^2) is greater than 0.93 for the drying tunnel experiments, however it greater than 0.8 for the single application thickness experiments and greater than 0.88 for the multiple application thickness experiments. The model predicts the drying time even better in the field experiments without drainage and rain with a 0.94 coefficient of determination. The ANOVA table results indicate that the weather parameters were more significant than the physical dimensions of the residuals application. However, the significance of weather parameters will be thoroughly examined in the following chapter.

8 Sensitivity Analysis

8.1 Introduction

This chapter determines the most sensitive meteorological parameter on the residuals drying model output. Sensitivity analyses in engineering systems are employed to verify how input parameters of a specific engineering problem influence the state functions (i.e. displacements, stresses, temperatures) (Kaminski, 2003). The relation between varied input and output is measured by different sensitivity measures that are the basis for the model validation and optimisation. Economically, residuals should be reduced before final disposal or reuse. Therefore, it is important to successfully predict the drying process of residuals. Uncertainty in the drying process happens as a result of changing weather conditions and hence unpredictable drying time. Therefore, simulation can be a valuable approach in modelling and solving problems. The weather conditions vary widely and unpredictably from place to place and through time. Knowledge of probability distributions is important to applying simulation successfully.

Monte Carlo Simulation is a technique that helps to reduce the uncertainty involved in estimating future outcomes. Monte Carlo Simulation can be applied to complex non-linear models or used to evaluate the accuracy and performance of other models. This technique converts uncertainties in input variables of a model into probability distributions. By combining the distributions and randomly selecting values from them, it recalculates the simulated model many times and brings out the probability of the output. Different types of probability distributions can be assigned to the inputs of the model. When the distribution is unknown, the one that represents the best fit could be chosen. On the other hand, Monte Carlo analysis does not require that the probability

density functions be defined for all input parameters (Hayse, 2000). Monte Carlo Simulation generates the output as a range instead of a fixed value and shows how likely the output value is to occur in the range. The normal distribution has the best fit for the weather parameters data used in the sensitivity analysis (Table 8.1); however, normal distribution is observed in many natural phenomena.

Table 8.1 Model variables showing their probability distribution functions

Parameter	Distribution	Range	Mean	Standard Deviation
Thickness (m)	Normal	0.01-0.20	0.04	0.004
Ambient Temperature ($^{\circ}\text{C}$)	Normal	18.00-35.00	25.30	2.53
Wind Speed (m/s)	Normal	0.50-7.00	3.00	0.30
Relative Humidity (Decimal)	Normal	0.05-1.00	0.712	0.071
Solar Radiation (MJ/m^2)	Normal	0.00-25.00	12.00	1.20

For this study, the model has been solved using Microsoft Excel and Crystal Ball software (an Excel-based application) from Decisioneering, Inc. to perform simulation, analysis, and reporting. Sensitivity analysis will be performed firstly by varying the parameters one at a time and having all others at standard or base values; and secondly by examining combinations of changes using Crystal Ball software. Crystal Ball is based on the Monte Carlo simulation, which randomly generates values from the probability distributions for the uncertain variables by using those values for the spreadsheet cell.

Many researchers have used sensitivity analysis to optimise predictions for a model, relative importance of variables, risk, and uncertainty. Krzykacz-Hausmann (2005) used Monte Carlo simulation to study the effect of model input variables subject to aleatory uncertainty (random behaviour) on the results of a complex model. In optimising a solar tunnel dryer, Hossain et al (2005) found that the design geometry is

sensitive to costs of major construction materials, solar radiation, and air velocity. Cannon and McKendry (2002) performed a study where they applied graphical sensitivity analysis to artificial neural networks; the technique is illustrated using a real-world, long-range climate prediction example. Wallis and Griffiths (1997) simulated weather parameters from weather records for agricultural models.

The model developed in Chapter 4 is a descriptive model, used to explain the behaviour of the ferric chloride residuals' drying process. Weather parameters create uncertainty in the prediction of the drying process; it is important to know the relative importance of weather parameters on the output of the model. The relative importance of several variables was determined by Sinicio et al (1997) in a model for simulating aeration of stored wheat. In this chapter, variance-based sensitivity analysis will be used to determine the input variables variances and their influence on the model output. The sensitivity analysis procedure has been adopted from (Evans and Olson, 1998), (Mun, 2004), and (Chan et al. 1997). A schematic representation of the procedure is shown in Figure 8.1.

8.2 Selection of Parameters

Each parameter of the model affects the model output differently; therefore, we need to identify the most influential parameter on the model output. Weather parameters interact with one another. The selected parameters that influence the model output are ambient temperature, relative humidity, wind speed, solar radiation, and application thickness. Table 8.2 shows the various parameters and their upper and lower ranges as well as their measurement accuracies. The above-mentioned parameters and their effect on the drying of water treatment residuals will be discussed.

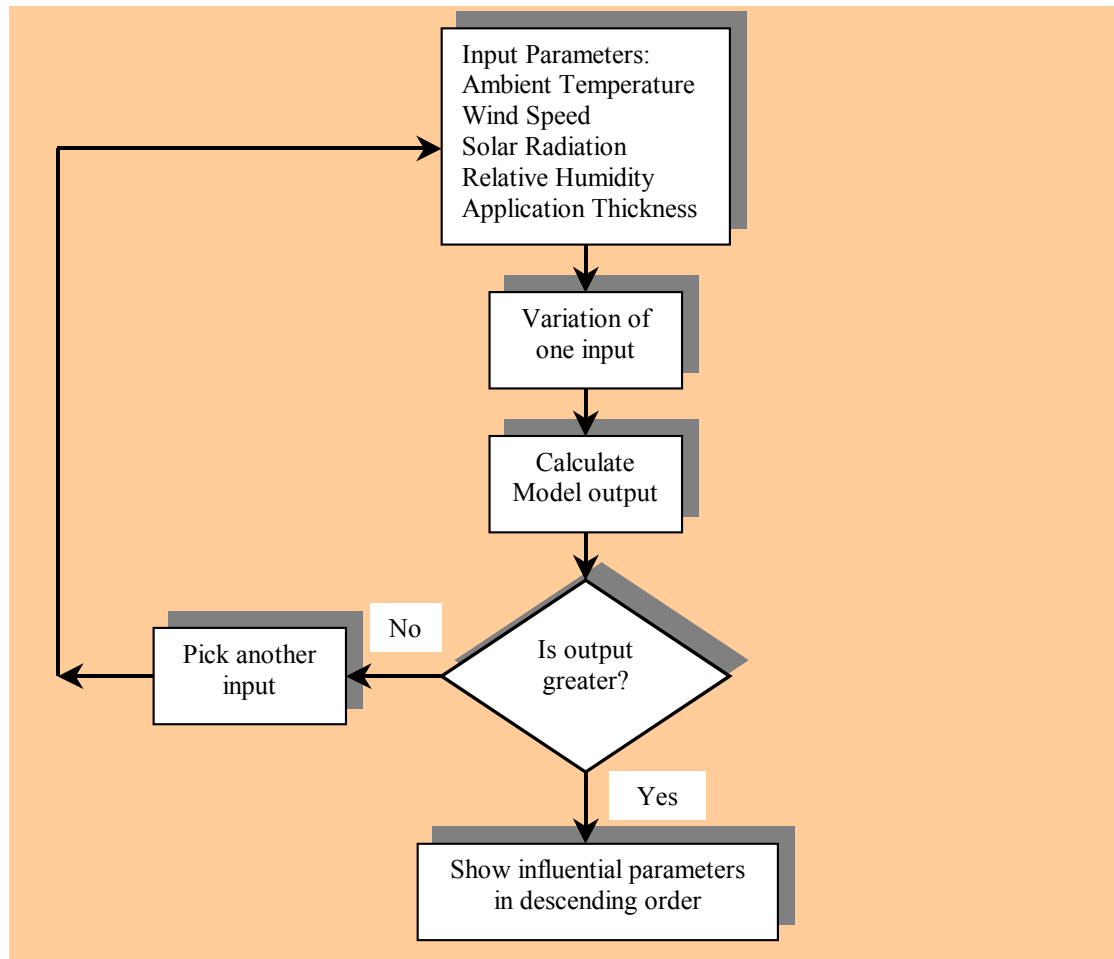


Figure 8.1 A schematic overview of the procedure for sensitivity analysis

8.2.1 Relative Humidity

Relative humidity variations depend upon the climatic condition of the region. Relative humidity can reach 100% in extremely humid regions, and as low as a few percentage points in arid regions. During the current study, average relative humidity was around 65%; the variations were between 25% and 100%. Relative humidity is a very important parameter in the drying process; very high (or close to saturation) relative humidity reduces the drying rate to minimum. However, very low relative humidity improves drying dramatically. For example, drying of residuals in a green house dryer can increase relative humidity if it does not have sufficient ventilation.

Table 8.2 Model parameters showing their lower and upper ranges

Parameters	Lower Range	Upper Range	Measuring Accuracy
Ambient Temperature ($^{\circ}\text{C}$)	15.0	35.0	± 0.1 $^{\circ}\text{C}$
Relative Humidity (%)	5	100	$\pm 2\%$ (over the full range)
Wind Speed (m/s)	0.5	7.0	$<\pm 2\%$ (over the full range) (0-55 m/s)
Solar Radiation (MJ/m^2)	0.0	25.0	$\pm 5\%$ (over the full range) (0-2000 W/m^2)
Application Thickness (m)	0.010	0.200	-

8.2.2 Wind Speed

Solar energy strikes the surface of the earth at different angles, and because of the curvature of its surface, warms different regions at different rates. Variations in temperature and atmospheric pressure are the driving force for air movement on the surface of the earth. This movement of air is called wind speed, and has a great impact on local climates and hence on the drying process. The average outdoor wind speed was 5.5 m/s during this study and thus the variations in wind speed for the drying tunnel were chosen to be 1 to 7 m/s. A velocity boundary layer develops whenever there is a fluid flow over a surface and a thermal boundary layer develops if the fluid free stream and surface temperatures differ. The thermal boundary layer becomes small with higher wind speeds and smaller with low wind speeds. Therefore, wind speed can affect the drying process greatly since it has a great influence on the heat transfer coefficient.

8.2.3 Ambient Temperature

The ambient temperature varies depending on the weather conditions of the area where the drying takes place. In some parts of the world temperature can drop well below freezing point, whereas in hot climates it can reach as high as 50 $^{\circ}\text{C}$. In the area

where this study was taken, the normal variation of ambient temperature varies seasonally from 15 °C to 35 °C. The vapour pressure of the air increases exponentially with increasing temperature; vapour pressure at 15 °C is about 3.3 times less than that at 35 °C. Therefore, it is important to consider higher temperatures in any dryer design.

8.2.4 Solar Radiation

The earth's atmosphere reflects 30% of the total incoming solar radiation of 5.4 million Exa-Joules (10^{18} joules) from the sun (Boyle et al. 2003). The extraterrestrial solar irradiation striking the surface of the earth depends on the geographic latitude, as well as the time of day and year (Incropera and DeWitt, 1996). It may be determined from the following expression:

$$G_{incident} = S_{constant} f \cos \theta \quad (8.1)$$

$G_{incident}$ Incident solar radiation (W/m²)

$S_{constant}$ The solar radiation constant (1353 W/m²)

θ Angle of incidence

f Correction factor to account for the eccentricity of the earth's orbit about the sun ($0.97 \leq f \leq 1.03$)

The weather station measured the incident solar radiation $G_{incident}$ while performing the field drying experiments. The average solar radiation measured during the time of field experiments was 12 MJ/m²; therefore, the range of 0 to 25 has been selected for the variation of this parameter. Solar radiation provides the drying material with the energy to evaporate moisture. When solar radiation strikes the surface of the earth the air heats up as well. The variations of solar radiation intensity happen during the day and from one season to another. The cloud cover during daytime, as well as dust

particles and pollution, can reduce solar radiation to the minimum and hence affects the drying significantly.

8.2.5 Application Thickness

The effect of application thickness on the drying of residuals has been considered in development of the model. In any drying process, it is advised to minimise the thickness of the drying material in order to reduce the drying time. The operation of residuals drying beds is optimised by the application thickness of residuals. Normally, residuals are applied in a rotational sequence around the bed in order to spread the residuals evenly. A small thickness is applied (around 10 mm) and left to dry after this initial layer another layer is applied in order to facilitate the drainage through the cracks. The thickness of the drying experiments of the field and drying tunnel ranges between 0.01 to 0.2 metres. Applying a thick layer of residuals prolongs the drying process and may induce odour problems. The effect of the thickness drying process will be assessed in this chapter in order to find out its sensitivity on the forecast compared to the other parameters.

8.3 The Effect of Model Parameters

The effect of the variations of input parameters on the model output will be calculated and discussed. The base values of the input parameters will be selected, then one input variable will be varied between the lower and upper limits and the other parameters will be kept at the base values. The base value is the starting point when a single parameter is varied between the lower and upper range; however, the other parameters are kept constant at their base value. The area of the evaporation surface selected is 0.0709 m² in a six minutes time frame as an example; however, any value

can be selected. The model output is the change of moisture content with respect to time (dX/dt). The moisture content will be transformed to drying rate for easy comparisons.

Table 8.3 shows the base values of the parameters used in the sensitivity analysis and parameter identification. The calculations in the sensitivity analysis for all the parameters are performed within 6-minute intervals. The sensitivity of a parameter is the slope of the curve fitted to the change of output versus the change of input (Lamoureux et al. 2006).

Table 8.3 Base values of various parameters used in sensitivity analysis and parameter identification

Parameters	Base Value	Range
Ambient Temperature ($^{\circ}\text{C}$)	27.3	18.0-35.0
Relative Humidity (%)	73	5-100
Wind Speed (m/s)	3	0.5-7.0
Solar Radiation (MJ/m^2)	12	0-25.0
Application Thickness (m)	0.060	0.010-0.200
Surface Temperature ($^{\circ}\text{C}$)	17.7	-

8.3.1 Effect of Relative Humidity

Figure 8.2 shows a power curve increase of the drying rate with the reduction of relative humidity. Reducing the air holding capability of moisture improves the drying process; therefore, the curve shows that reducing the relative humidity below 25% could result in a sharp increase in drying rate. By reducing relative humidity from 75% to 25%, the drying rate increases 6.2 times. In a study describing the transport phenomena involved in some vegetables drying, Aversa et al (2007) presented a theoretical model where they found that by reducing relative humidity from 75 to 25% the drying rate increased 4.4 times.

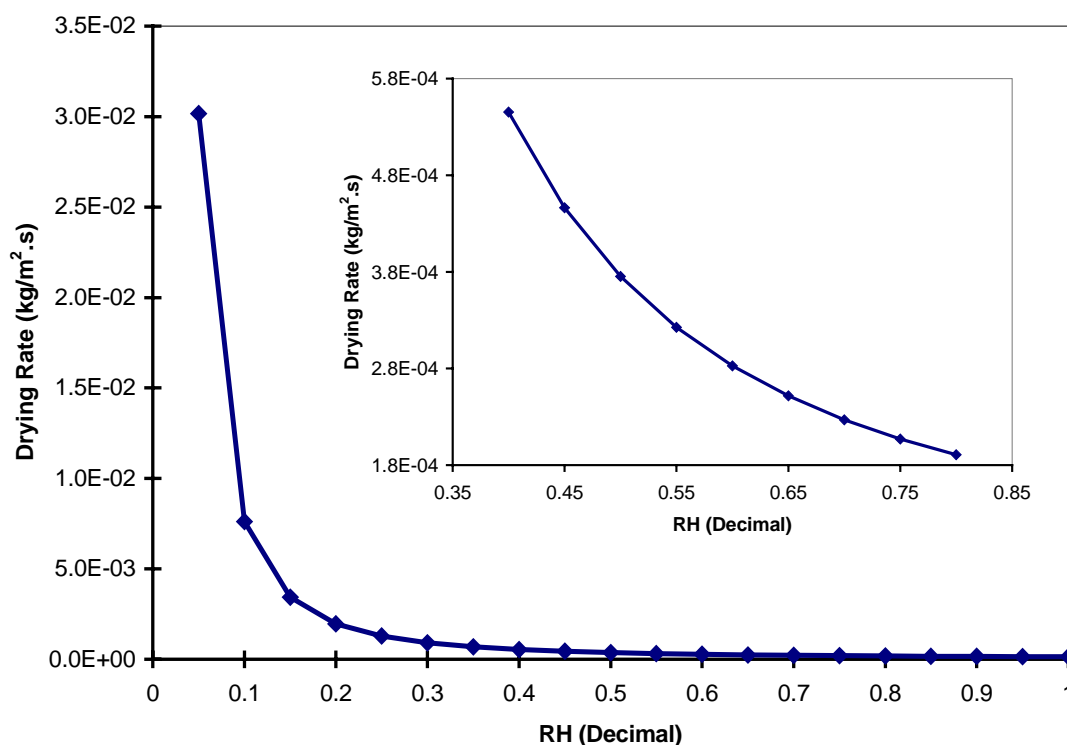


Figure 8.2 The effect of relative humidity on drying rate

8.3.2 Effect of Wind Speed

A wind speed increase of 1 m/s resulted in a 64% increase in drying rate. With increased wind speed, the thermal boundary layer over the drying surface becomes small, which improves the heat transfer which in turn increases the evaporation rate of water vapour away from the surface. The effect of wind speed on the thin-layer drying of figs has been studied by Babalis and Belessiotis (2004); they found that an increase in wind speed of 1 m/s decreased drying time by 83%. Inazu et al (2003) studied the effect of air velocity on fresh Japanese noodle drying and found that by increasing the wind speed 1 m/s, while keeping the relative humidity at 70% and the temperature 40 °C, the drying time reduced by almost 83%. However, Doymaz (2004) found that the increase of 1 m/s wind speed reduced drying time by 40% in a convective air drying of thin layer carrots.

8.3.3 Effect of Ambient Temperature

The drying rate increases 64% by increasing temperature from 18 to 35 °C; when temperature increases by one degree, the drying rate increases 3.8%. The higher the air temperature, the more moisture it can absorb, providing absolute humidity is kept constant therefore increasing the drying rate of the material. In a study of the effect of different pre-treatments on the convective drying of apple slices, Schultz et al (2007) found that drying time was reduced by 42% when temperature increased from 60 to 80 °C at 3 m/s wind speed. In another study of the drying of dill and parsley leaves (Doymaz et al. 2006) a reduction of 53% in drying time was achieved by increasing the temperature from 50 to 70 °C at 1.1 m/s wind speed. Togrul (2006) and Mohamed et al (2005) performed similar drying studies and studied the effect of temperature on food drying. It is clear from these studies that different drying products have different drying behaviour.

8.3.4 Effect of Solar Radiation

Drying rate increases linearly with the increase in solar radiation. The Solar radiation increase from 0 to 25 MJ/m² results in 65% increase in drying rate or for every 1 MJ/m² 2.6% increase of drying rate. Solar radiation supplies the drying product with energy required to evaporate moisture; therefore direct solar energy is utilised in solar dryers of food products as well as other varieties of applications. Sacilik et al (2006), in a solar tunnel dryer, achieved a drying time reduction of 26.9% of organic tomato in comparison to open sun drying. The authors did not specify the drying conditions in the dryer for this specific reduction in drying time.

8.3.5 Effect of Application Thickness

The drying rate is inversely proportional to the application thickness of residuals. An increase of 20 times in the application thickness gives around 12.8% reduction in drying rate or a reduction of 0.68% in drying rate for every 10 mm increase in application thickness. A reduction in drying time of 3.5 times has been achieved by 4 times reduction in the thickness of grape leather (pestil) (Maskan et al. 2002). At 60 °C and 0.82 m/s wind speed, Sankat and Castaigne (2004) achieved 7.7 times reduction in drying time of banana by 4 times reduction in thickness. The effect of the drying material's thickness is due to the internal resistance to moisture transport within the internal structure. Therefore, the higher the resistance the higher the effect and different materials have different internal resistances.

8.4 Sensitive Parameters

A Monte Carlo simulation of 20000 trials was performed using Crystal Ball software for the model parameters shown in Table 8.3 considering their lower and upper ranges. To ensure a high level of accuracy, at least 10000 trials should be used (Crystal Ball 7.3 user manual, 2007). The simulation uses the model calculated in an Excel spreadsheet to run the trials with a slightly different input each time, according to their selected distributions, calculating the output. Figure 8.7 displays the forecast results as vertical columns that correspond to the frequency counts of the display range as a cumulative frequency distribution. The frequency chart (Figure 8.7) shows the degree of uncertainty in the drying rate, namely the range of the obtained 20,000 values for drying rate and how often it occurs.

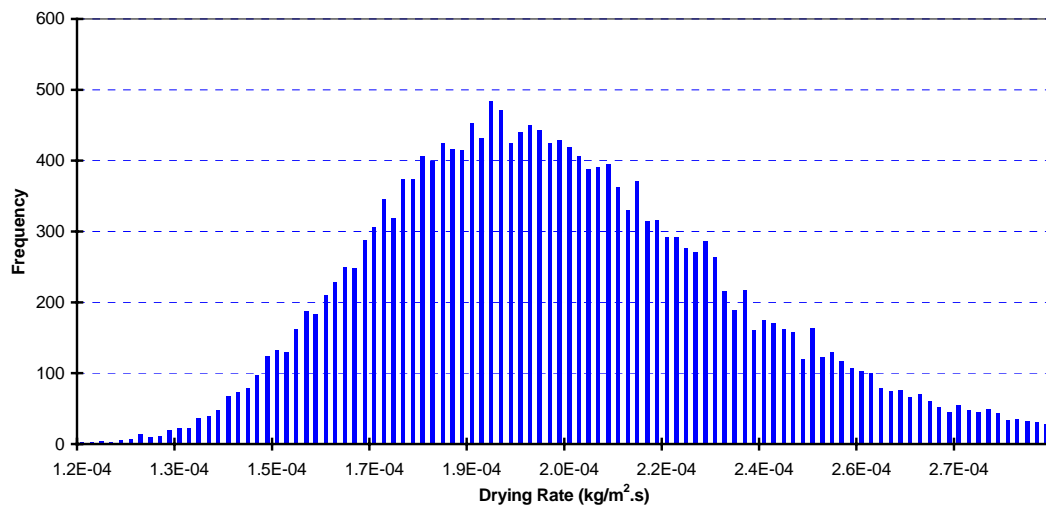


Figure 8.3 Frequency chart for the sensitivity analysis trials

Simulation statistics (Table 8.4) reveal that the forecast values are most likely to happen around the mean and median values since they have high frequency occurrence (Figure 8.3). The standard deviation is a measure of risk or simply a measure of dispersion about the mean forecast. The probability that the true mean of the forecast is the estimated mean (plus or minus the mean standard error) is approximately 68% (Crystal Ball 7.3 reference manual, 2007). Therefore, the simulation provides good accuracy since the mean standard error is very small. The distribution is moderately skewed (0.86) and highly peaked (kurtosis 4.7), which indicate that the forecast has a high probability of occurrence towards the higher end of the distribution (right hand side of Figure 8.3). The variance value is very small, which indicates that the values are close to the mean.

Table 8.4 Summary of the statistics report

Statistics	Value
Trials	20000
Mean	0.000202578
Median	0.000198613
Standard Deviation	0.000034390
Variance	0.000000001
Skewness	0.86
Kurtosis	4.70
Coeff. of Variability	0.17
Range Minimum	0.000104545
Range Maximum	0.000448404
Range Width	0.000343859
Mean Std. Error	0.000000243

Ostwald and McLaren (2004) defined the percentile as the point below which a stated percentage of observations lie. Table 8.5 shows the percentiles of evaporated water with 100% probability that a minimum of (0.0001045 kg/m².s) drying rate will be achieved. Therefore, for the given weather conditions in Table 8.3, there are a 50% probability to achieve (0.0001986 kg/m².s) drying rate. Risk arises from a wide range of potential outcomes; therefore, the variability of weather parameters can influence the span in drying times of residuals. Wide variations in drying times and delays in drying of residuals involve a risk associated with the cost of final disposal or reuse.

8.5 Discussion of Results

Crystal Ball calculates sensitivity by computing rank correlation coefficients between every assumption and the forecast. Figure 8.4 shows the input variables measured by rank correlation. Figure 8.5 shows the input variables and their percentage contribution to the target forecast, which is the drying rate. The correlation coefficients in Figure 8.4 provide a measure of the degree to which assumptions and the forecast change together; the larger the absolute value of the correlation coefficient, the greater

the sensitivity. The percentages shown in Figure 8.5 are calculated by dividing the squares of each coefficient by the sum of all the squares to ensure a sum of 1 and converting each normalised value to a percentage. The percentage contribution to variance chart could be easier to interpret than the correlation coefficients chart.

Table 8.5 Percentiles for the evaporated water

Percentile	Drying Rate (kg/m².s)
100%	0.0001045
90%	0.0001632
80%	0.0001740
70%	0.0001828
60%	0.0001908
50%	0.0001986
40%	0.0002069
30%	0.0002160
20%	0.0002285
10%	0.0002473
0%	0.0004484

The sensitivity chart ranks the assumptions from the most important, which is relative humidity, to the least important in the model, being the application thickness. Both assumptions, relative humidity and application thickness, have negative correlation coefficients, hence reducing the drying rate by increasing relative humidity and application thickness and vice versa. The second highest important assumption is wind speed, followed by ambient temperature and then solar radiation. These three assumptions have positive correlation coefficients, which is a clear indication of their physical effect on the drying rate. The interactions of the weather parameters could have mixed effects; in wet days, relative humidity is high, solar radiation is low, ambient

temperature relatively lower, and even if it is windy, wind will not affect the drying process much.

Figures 8.4 and 8.5 clearly illustrate the effect of the various parameters on the target forecast. Whilst the relative humidity has the greatest influence on the target forecast, the least influential parameter remains the application thickness. Relative humidity and application thickness both have a negative influence on the target forecast (drying rate), however all the other parameters have a positive influence. Researchers continue to study the influence of weather parameters including relative humidity on the drying process. For example, when investigating the drying time of food, Liu et al (1997) found that the drying air humidity has the greatest impact upon drying time. The changes in humidity can also be related to the drying of water treatment residuals, in a fluidised drying bed. Shin et al (2000) found that the equilibrium moisture ratio of residuals was more sensitively dependent on relative humidity than the temperature of drying air. Qui et al (1998) revealed in a model for estimation of evaporation from a soil surface that the dry soil surface temperature, the drying soil surface temperature, and air temperature were the most sensitive input parameters than the solar radiation.

Figure 8.6 shows results from several parameters on a single graph. This allows easy comparison of the relative impacts of these parameters when varied over their realistic ranges, and these ranges are communicated by the horizontal span of the lines. In order to maximise the drying rate, the application thickness and the relative humidity have to be kept to a minimum, whilst on the other hand the other parameters should be maximised. A natural increase of some weather conditions, such as solar radiation and ambient temperature, allow a reduction of relative humidity if the absolute humidity remained constant. Therefore, the sensitivity analysis revealed good information using the model to better utilise weather conditions in drying design of residuals.

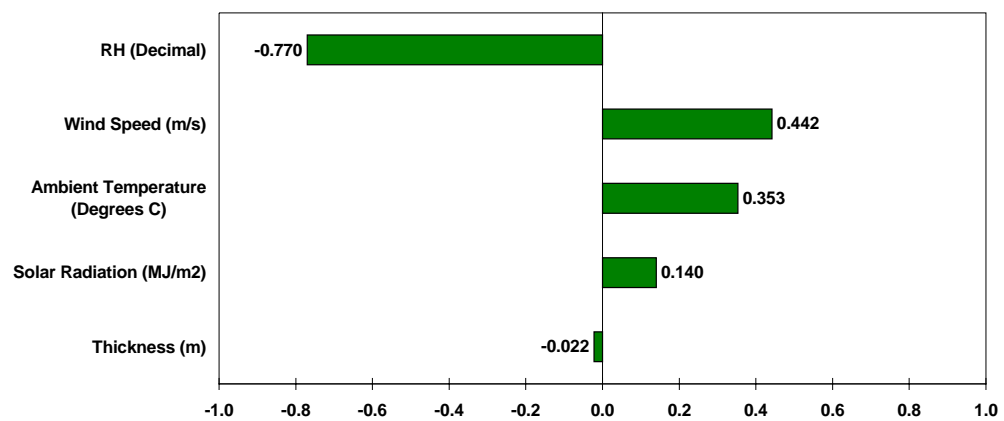


Figure 8.4 Input variables measured by rank correlation

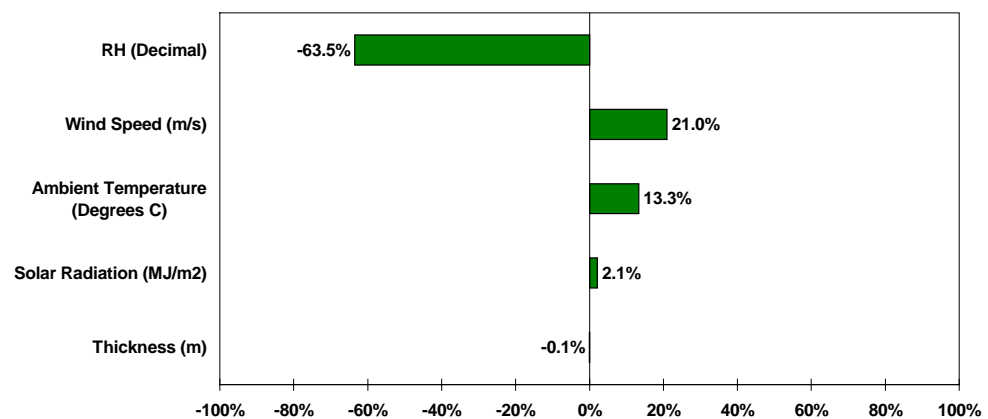


Figure 8.5 Input variables and their percentage contribution to the target forecast

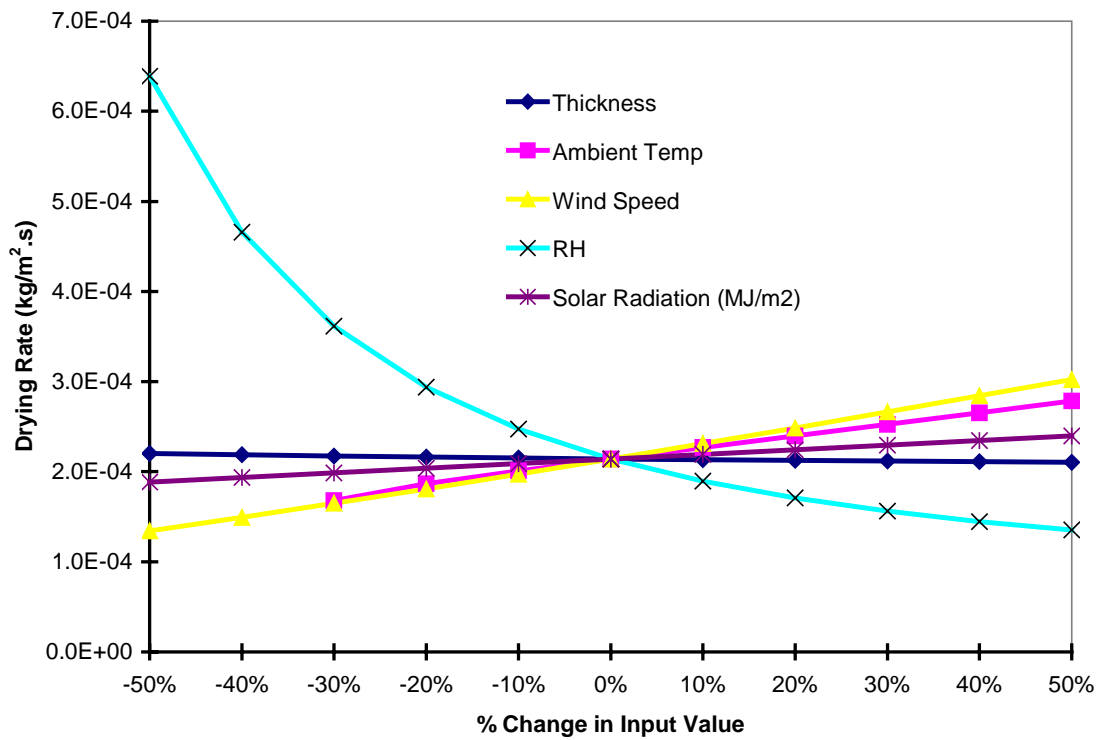


Figure 8.6 Spider plot for the multiple input parameters for the output variable

Sensitivity analysis is often performed in order to give a guide for optimum design and construction; in this case, it is important to discuss its implications on the drying of residuals in drying beds or thermal and mechanical dryers. The factors influencing the residuals drying process are design parameters and meteorological conditions. The design parameters are the orientation of the drying bed (could be a solar dryer), insulation of the dryer, glazing of the solar collector and the thermal properties of the materials of construction. Moreover, the meteorological conditions influencing the drying process are mainly solar radiation, ambient temperature, relative humidity and wind speed. Since the most sensitive parameter is relative humidity, it would be important to dry the air rather than increasing the other parameters in a solar or thermal dryer. Leonard et al. (2005) found that the influence of ambient temperature was highest on the drying kinetics, followed by wind speed and relative humidity for one type of

residuals, whilst the latter variables have the same order of influence, but opposite effect, for a second type of residuals. Sensitivity to climate conditions help in the selection of production locations and for optimising greenhouse design while drying tomatoes (Cooman and Schrevers, (2007). However, performing sensitivity analysis in a natural convection solar dryer, Bala and Woods (1995) found that the design geometry is not very sensitive to material or fixed costs but grain capacity of the dryer was more sensitive. Sensitivity analysis is a powerful tool when applied for the design and construction of dryers in order to minimise materials of construction, land usage and maximize the dryer output.

8.6 Summary

A variance-based sensitivity analysis has been used to find the most influential input variables on the residuals drying model output. The application thickness and weather parameters, namely wind speed, relative humidity, ambient temperature, and solar radiation were varied one at a time, between their realistic ranges, to study their effect on the model output. Crystal Ball software, which is based on Monte Carlo simulation, was used to study the relative importance of all the parameters on the model output. The published research showed that the meteorological parameters have mixed effects on the drying of various products. It was found that the most sensitive parameter was relative humidity and the least sensitive parameter was application thickness. Reducing relative humidity from 75% to 25%, the drying rate increased 6.2 times. However, when the ambient temperature increased 1 °C, 3.8% reduction in drying time was achieved for the residuals. For the effect of wind speed, an increase of 1 m/s wind speed resulted in a 64% increase in the drying of residuals. A solar radiation increase of 1 MJ/m² resulted in a 2.6% increase in drying rate. The results of the sensitivity analysis

provide an in depth physical meaning for the model to be used appropriately in the design of the residuals drying process. In the following chapter, a proposed solar drying bed design will be presented in order to save energy and land use for the residuals drying process before final disposal or reuse.

9 Solar Drying of Residuals

9.1 Introduction

Solar drying is a technology suitable for producing dried material of certain water content at an economical price. The potential is to accelerate the drying of the water treatment plant residuals to a manageable level keeping in mind minimisation of adverse environmental issues. The boundary conditions of a solar drying design are mainly the quantity of sludge produced, the local meteorological conditions, and the available sources of energy. The advantages of accelerated residuals drying process are reduction of time for final disposal or reuse, reduction in the area used for drying and the reduction of the health hazards of handling the residuals.

Residuals drying process has two major effective factors; drainage and evaporation. Drainage in a conventional sand drying bed might last a few days until the sand is clogged with the fine particles and/or all of the free water has drained away. Further dewatering occurs by evaporation, which depends on unpredictable weather conditions. The use of solar drying technology is required to dry residuals in order to achieve a target of 45-50% dry solids faster than normal drying techniques.

This chapter is divided into four parts. The first describes various types of solar drying technologies of residuals. The second part is concerned with orientation of the solar collector and optimising the tilt angle to maximise the collector gain. The third part uses theoretical design equations in order to size the collector and the drying chamber. Finally, the solar dryer heat balance equations will be presented and a new

model is developed to predict the moisture content in the solar dryer as well as some predictions for various weather conditions.

9.2 Solar Drying Technologies of Residuals

There are several applications around the world using solar technology such as solar distillation stills (passive and active). Solar collectors are used to heat air entering a packed bed in a food batch dryer, wood drying through the use of a collector funnel equipped with a belt conveyor, a drying chamber, a chimney and finally, a reverse flat plate absorber used in a cabinet drier to dry various types of crops. One other notable application has been the solar drying of residuals.

Conventional sand drying beds use available solar energy in the drying of residuals. Wet weather prolongs the drying time and therefore there is a need for accelerated drying techniques in modern societies with the increase in demand for clean drinking water. Limited attempts were undertaken in the past to dry sewage residuals using active solar drying technologies. Cornwell and Vandermeiden (1999) reasoned that the main advantages of the active solar drying beds are the low maintenance cost and ease of cleaning.

The greenhouse type solar dryers have recently been popular. Seginer and Bux (2006) developed a prediction model for greenhouse solar sewage residuals dryer as a function of meteorological conditions and control actions (residuals mixing, ventilation and air mixing). Another follow-up study (Seginer et al. 2007) was performed to optimise the previous study and found that there was sufficient economic incentive for residuals solar drying. Salihoglu et al (2007) conducted a study in open and covered

(greenhouse type) solar residuals drying beds constructed in pilot scale for experimental purposes; they achieved 40% reduction in the disposed residuals quantity compared to the open bed.

Several sewage residuals drying studies have been reported in the literature such as (Luboschik, 1999), (Hossam et al. 1990), (El-Ariny and Miller, 1984) and Shannon et al (2004). The average evaporated water reported in these studies ranges from 2 to 17 kg/m²/day. However, Shannon et al (2004) achieved a maximum of 30 kg/m²/day with temperatures up to 65⁰C, however no wind speed results were provided.

In previous research studies, experiments were performed on sewage residuals and there was one study reported on solar drying of water treatment plant residuals (Gharaibeh et al. 2003). Experiments were performed to compare the drying of residuals in open versus solar drying beds. The solar drying bed was provided with a fan heater blowing hot air inside the cavity of the bed to simulate an air solar collector. A reduction in drying time from 27 days to 18 days to reach 50% solids content was achieved.

9.3 Theoretical Analysis

The basic resource for all solar energy systems is the sun. Knowledge of the quantity and quality of solar energy available at a specific location is of prime importance for the design of any solar energy system. Although solar radiation is relatively constant outside the earth's atmosphere, local climate influences can cause wide variations in available solar radiation on the earth's surface from one place to

another. In addition, the relative motion of the sun with respect to the earth will allow surfaces with different orientations to intercept different amounts of solar energy.

The most common flat-plate collectors consist of a dark metal plate, covered with one or two sheets of glass that absorb heat. The heat is transferred to air or water, called carrier fluids, that flows past the back of the plate. This heat may be used directly or it may be transferred to another medium. Flat-plate collectors typically heat carrier fluids to temperatures of up to 93°C. The efficiency of such collectors varies from 20 to 80 percent.

9.3.1 Orientation of Solar Collector

In order to design a solar dryer, it is important know the available solar energy in the local area as well as its latitude. From the data provided by the Australian Bureau of Meteorology, the average incident solar radiation in the Wollongong area is as low as 5 MJ/m² in winter and as high as 32 MJ/m² and the latitude is (-34.58°). The solar altitude angle *ALT* above the horizon is calculated using the following equation:

$$ALT = \sin^{-1}[\cos(DEC)\cos(LAT)\cos(HOUR) + \sin(DEC)\sin(LAT)] \quad (9.1)$$

Where,

DEC Solar declination angle (degrees)

LAT Latitude of particular site of interest (degrees)

HOUR Hour angle, number of hours between solar noon and the time of interest multiplied by 15°/hr (noon = 0°)

The solar declination angle *DEC* can be calculated from the following equation (Spencer, 1971):

$$\begin{aligned} DEC = & 0.006918 - 0.399912 \cos(Y) + 0.070257 \sin(Y) \\ & - 0.006758 \cos(2Y) + 0.000907 \sin(2Y) \\ & - 0.002697 \cos(3Y) + 0.00148 \sin(3Y) \end{aligned} \quad (9.2)$$

Where,

Y The fractional year in radians

The fractional year term is calculated from the following equation:

$$Y = \frac{2\pi}{365}(DAY - 1) \quad (9.3)$$

Where,

DAY The number of days of the calculated from January 1

The incident angle for given latitude (in the southern hemisphere) can be calculated using the following equation (Duffie and Beckman, 1991):

$$INC = \cos^{-1} \left[\cos(DEC) \cos(LAT + TILT) \cos(HOUR) \right. \\ \left. + \sin(DEC) \sin(LAT + TILT) \right] \quad (9.4)$$

Where,

$TILT$ The tilt angle (Degrees)

In the northern hemisphere, equation (9.4) becomes:

$$INC = \cos^{-1} \left[\cos(DEC) \cos(LAT - TILT) \cos(HOUR) \right. \\ \left. + \sin(DEC) \sin(LAT - TILT) \right] \quad (9.5)$$

Figure 9.1 shows the design angles calculated using equations (9.1), (9.2) and (9.4). The solar altitude angle ALT for Wollongong ranges between 32° in winter and 78° in summer. The maximum gain of incident solar radiation on a collector surface happens when the incident angle is 0° (perpendicular on the collector surface), which can be calculated from the following expression:

$$Q_{gained} = Q_{solar} \cos(INC) \quad (9.6)$$

The optimum tilt angle of the solar collector can be found by maximising the solar radiation gain over the whole year; the average monthly incident solar radiation for the Wollongong area is shown in Figure 9.2. The optimum tilt angle for given latitude and a

given day of the year can be simply shown in the following equation (Atomstromfreie Website, 2007):

$$TILT = LAT - DEC \quad (9.7)$$

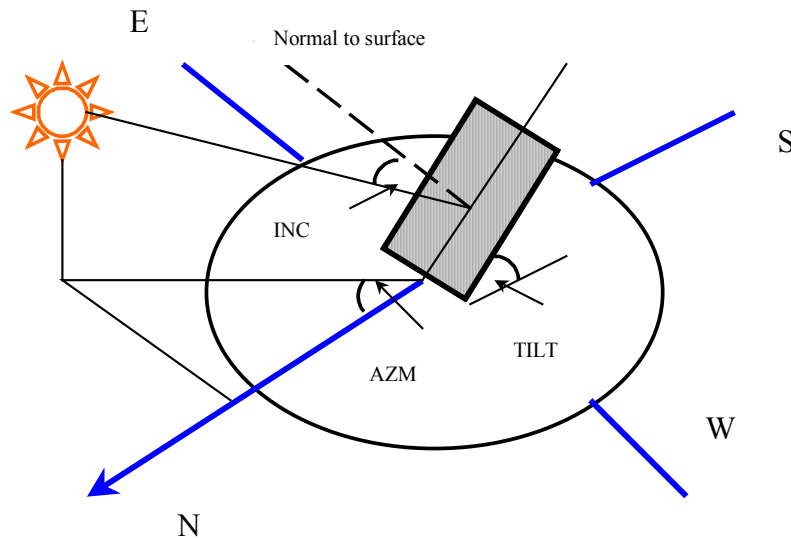


Figure 9.1 Tilted surface facing solar radiation and the corresponding design angles

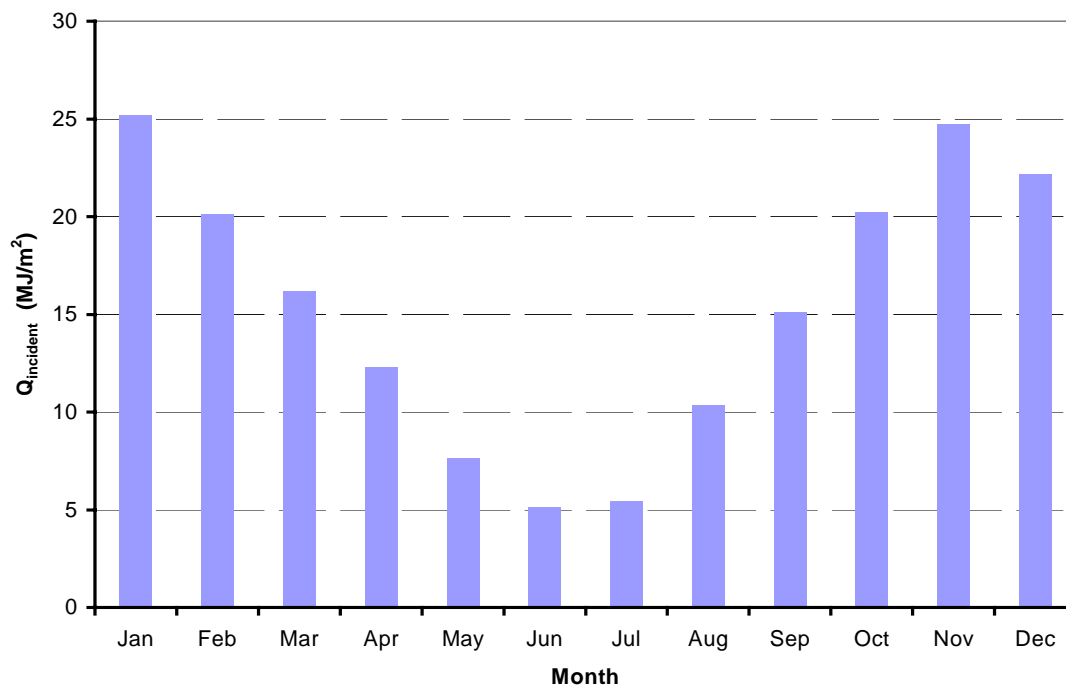


Figure 9.2 Monthly average incident solar radiation for Wollongong

The optimum tilt angle of a flat plate collector in the southern hemisphere is taken as the absolute value of equation (9.7). Figure 9.3 shows the optimum tilt angles for latitudes (-34.58°) and (34.58°) . The monthly average incident solar radiation data from Figure 9.2 together with equation (9.6) can be used to find the optimum tilt angle using MS Excel solver, which maximises the incident solar radiation gain over the entire year. The optimum *TILT* angle has been found to be 27.9° for Wollongong (Figure 9.4).

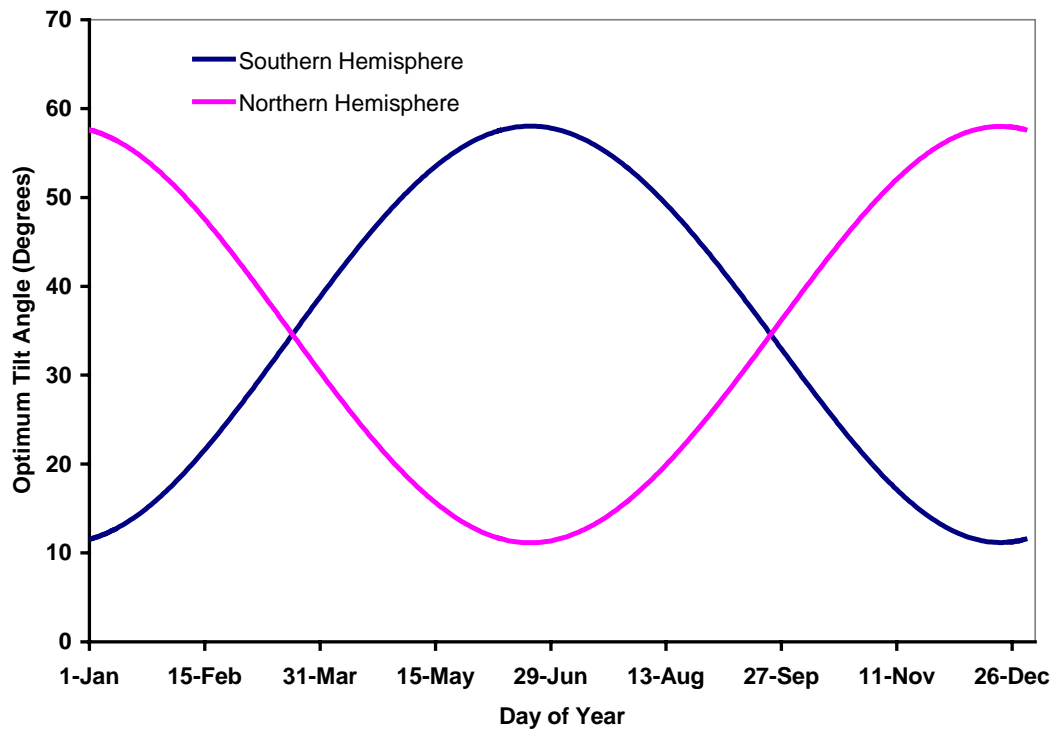


Figure 9.3 Optimum tilt angles for latitudes (-34.58°) and (34.58°)

9.3.2 Theoretical Considerations

Consider a residuals application to be dried in a solar dryer having water mass (m_{water}) calculated from the following equation (Exell, 1980):

$$m_{water} = \frac{m_{residuals} (X_{wet,initial} - X_{wet,final})}{(100 - X_{wet,final})} \quad (9.8)$$

Where,

$m_{residuals}$ Mass of residuals (kg)

m_{water} Mass of water (kg)

$X_{wet,initial}$ Initial moisture content, wet basis (%)

$X_{wet,final}$ Final moisture content, wet basis (%)

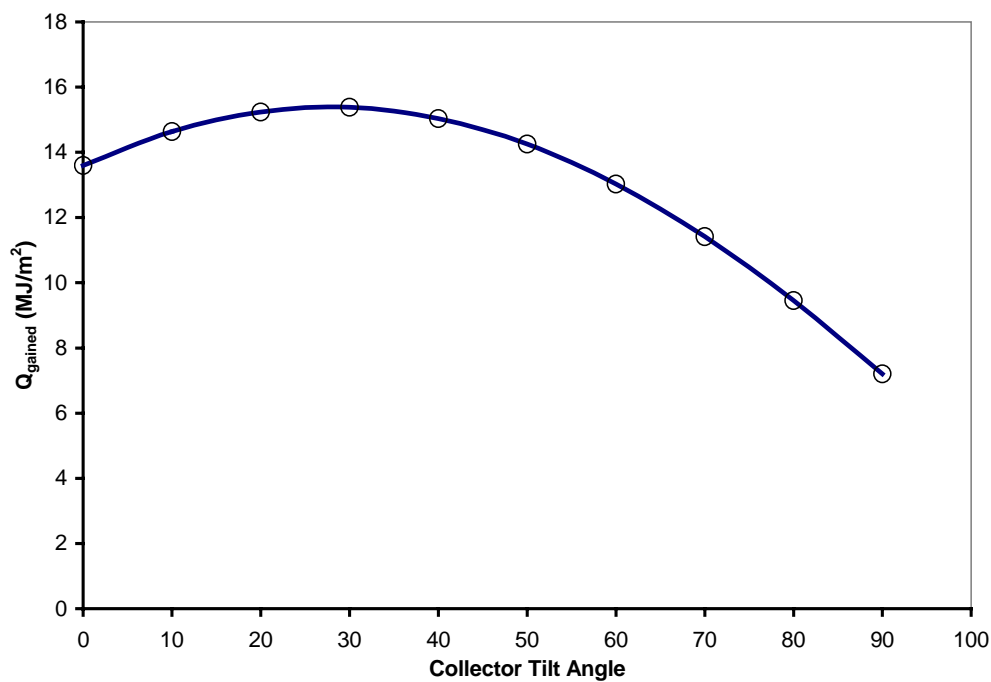


Figure 9.4 The optimum solar collector tilt angle for Wollongong area

The heat required to evaporate water from the residuals can be calculated from the following equation:

$$Q = h_{fg} m_{water} \quad (9.9)$$

Where,

h_{fg} The latent heat of vaporisation (J/kg)

Inserting equation (9.8) in equation (9.9) gives:

$$Q = h_{fg} \left[\frac{m_{residuals} (X_{wet,initial} - X_{wet,final})}{(100 - X_{wet,final})} \right] \quad (9.10)$$

The sensible heat is much smaller than the latent heat and hence can be ignored. Figure 9.5 shows a schematic of the solar dryer in order to be used for residuals drying, which consists of a solar air collector, a fan and the drying chamber. The thermal efficiency of a solar collector is defined as the ratio of the useful thermal energy to the total incident solar radiation averaged over the same time interval. The efficiency of a solar collector is expressed in the following equation (Morrison, 2001):

$$\eta = \frac{Q_{gained}}{Q_{incident}} \quad (9.11)$$

Where,

η The efficiency of a solar collector

Q_{gained} The rate of heat gained (W)

$Q_{incident}$ The rate of heat incident (W)

The rate of heat incident is shown in the following equation:

$$Q_{incident} = G_{solar} A_{collector} \quad (9.12)$$

Where,

G_{solar} Incident solar radiation (W/m²)

$A_{collector}$ The area of the solar collector (m²)

Substituting equation (9.12) in equation (9.11) gives:

$$\eta = \frac{Q_{gained}}{G_{solar} A_{collector}} \quad (9.13)$$

The steady state thermal performance of a solar collector is expressed by the Hottel-Whillier-Bliss equation (Duffie and Beckman, 1991):

$$\eta = \frac{Q_{\text{gained}}}{G_{\text{solar}} A_{\text{collector}}} = F_{\text{Removal}} (\tau \alpha) - F_{\text{Removal}} U_{\text{Lost}} \frac{(T_{\text{air},\text{in}} - T_{\text{air},\text{out}})}{G_{\text{solar}}} \quad (9.14)$$

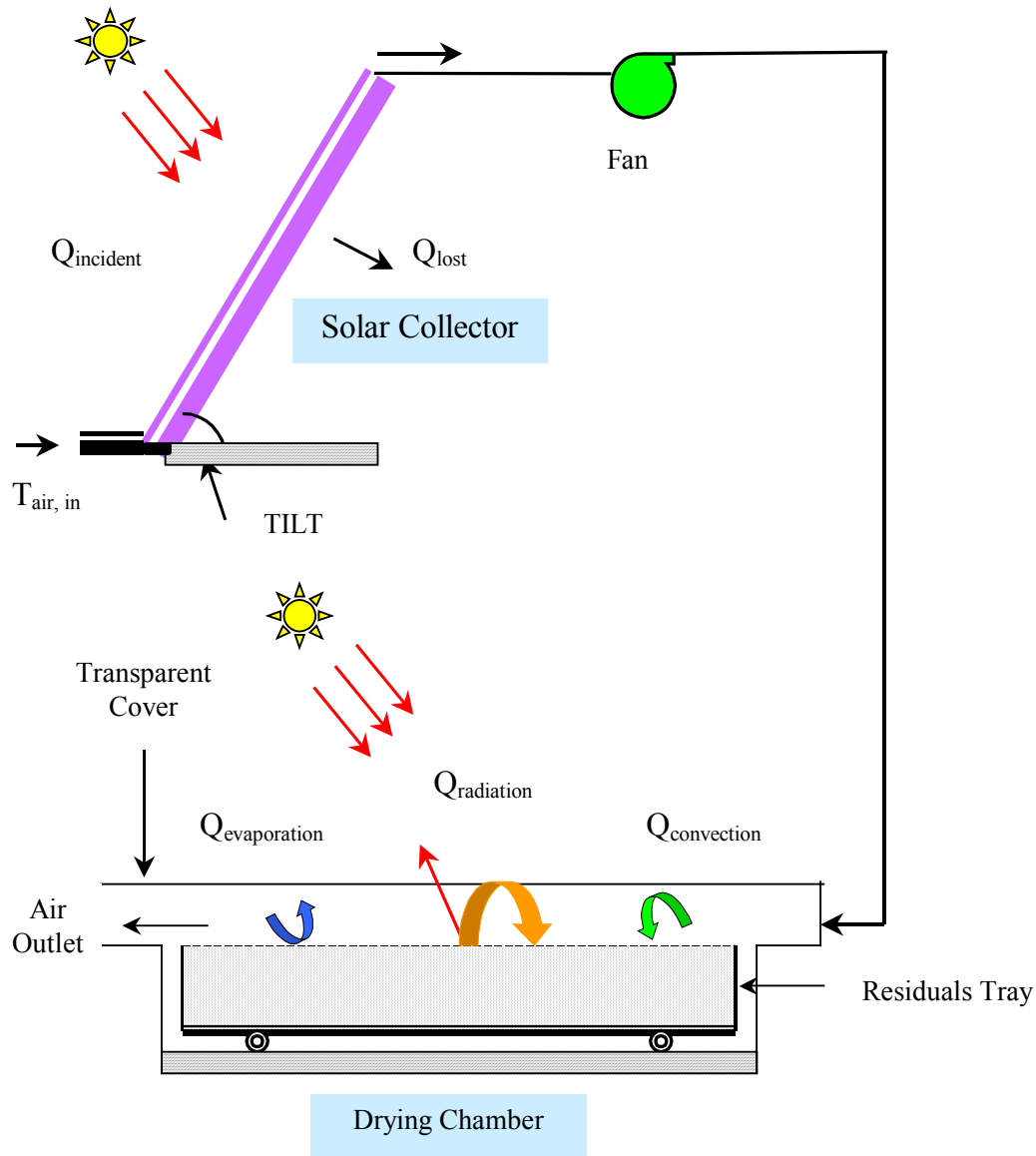


Figure 9.5 A diagram showing the flat plate solar collector and the drying chamber

Where,

F_{Removal} The collector heat removal factor (dimensionless)

U_{lost} The overall heat lost coefficient ($\text{W}/\text{m}^2 \cdot \text{K}$)

τ Transmission coefficient of glazing

α Absorption coefficient of the absorber plate

$T_{air,out}$ Temperature of air collector outlet (K)

$T_{air,in}$ Temperature of air collector inlet (K)

The rate of heat gained by the collector can be estimated by means of the amount of heat carried away in the air passing through it that is:

$$Q_{gained} = m_f c_{air} (T_{air,out} - T_{air,in}) \quad (9.15)$$

Where,

m_f The mass flow rate of air through the collector (kg/s)

c_{air} Specific heat of air (J/kg.K)

Some of the heat gained by the collector will be lost through the walls of the duct and the fan before entering the drying chamber. The heat loss can be minimised if the air duct is well insulated. The rate of heat lost through the length of the air duct and the fan can be estimated from the following equation:

$$Q_{lost} = m_f c_{air} (T_{DryingChamber,in} - T_{air,out}) \quad (9.16)$$

Where,

$T_{DryingChamber,in}$ Temperature of drying chamber inlet (K)

Q_{lost} The rate of heat lost from the duct (W)

Therefore, the rate of heat entering the drying chamber would be:

$$Q_{DryingChamber} = m_f c_{air} (T_{DryingChamber,in} - T_{air,in}) \quad (9.17)$$

Combining equations (9.13) and (9.17) gives:

$$A_{collector} G_{solar} \eta_{collector} = m_f c_{air} (T_{DryingChamber,in} - T_{air,in}) \quad (9.18)$$

Equation (9.18) can be written in terms of the collector air outlet temperature as follows:

$$T_{DryingChamber,in} = \frac{A_{collector} G_{solar} \eta_{collector}}{m_f c_{air}} + T_{air,in} \quad (9.19)$$

The heat and mechanical losses from the duct can be estimated using equations (9.20) up to equation (9.25). The pressure drop in the full length of the air duct in a fully developed flow can be calculated from the following equation (Incropera and DeWitt, 1996):

$$\Delta p = f \frac{\rho_{Density} u^2}{2D} (x_2 - x_1) \quad (9.20)$$

Where,

Δp Pressure drop (kg/m.s²) (Pascals)

f Friction factor (dimensionless)

$\rho_{Density}$ The air density (kg/m³)

u Wind speed (m/s)

D Duct diameter (m)

x_1, x_2 The axial positions (m)

For laminar flow, the friction factor can be calculated from:

$$f = \frac{64}{Re} \quad (9.21)$$

Where,

Re The Reynolds number (dimensionless)

The Reynolds number can be calculated from the following expression:

$$Re = \frac{4m_f}{\pi \mu D} \quad (9.22)$$

Where,

μ Dynamic viscosity (kg/s.m)

For turbulent flow, the friction factor can be calculated from the following two equations:

$$f = 0.316 \text{Re}^{-1/4}, \text{Re} \leq 2 \times 10^4 \quad (9.23)$$

$$f = 0.184 \text{Re}^{-1/5}, \text{Re} \geq 2 \times 10^4 \quad (9.24)$$

The power required to overcome the resistance to flow associated with the pressure drop of equation (9.20) can be calculated using the mechanical energy equation:

$$W = \frac{\Delta p V_{\text{flowrate}}}{\eta_{\text{pump}}} \quad (9.25)$$

Where,

W The total power output (W)

η_{pump} The efficiency of the pump (dimensionless)

Q_{flowrate} Volumetric flow rate (m^3/s)

The volumetric flow rate of air through the collector can be calculated using the universal gas law:

$$PV = \frac{m_{\text{dryair}}}{N} RT_{\infty} \quad (9.26)$$

Where,

P The atmospheric pressure in $\text{kg}/\text{m} \cdot \text{s}^2$ (Pascal)

V Volume of air (m^3)

m_{dryair} Mass of dry air (kg)

N Air molecular weight (29 $\text{kg}/\text{kg-mole}$)

R Universal gas constant ($8314 \text{ kg} \cdot \text{m}^2/\text{s}^2 \cdot \text{kg-mole} \cdot \text{K}$)

T_{∞} The ambient temperature of air (K)

Assuming an application $0.5 \times 0.5 \text{ m}$ and a thickness of 0.2 m , the application weight would be about 50 kg . The residuals are to be dried from initial moisture content

95% to 50% final moisture content (wet basis). Therefore, the amount of water to be extracted from 50 kg of residuals is 45 kg calculated from equation (9.8). Assuming 15 kg of water to be evaporated from the residuals per day, therefore, the latent heat required for evaporation is 37.5 MJ. From equation (9.15), the mass flow rate of the air (m_f) through the collector would be 0.038 kg/s, assuming the design parameters Q_{gained} 37.5 MJ, $T_{air,in}$ 15 °C or 288 K, $T_{air,out}$ 65 °C or 338 K, c_{air} 1006 J/kg.K. If the temperature drops by 10 °C in the duct, the heat losses calculated from equation (9.16) will be 352.1 W. The average annual solar radiation in Wollongong is 15 MJ/m²/Day (Bureau of Meteorology). Assuming flat plate collector efficiency of 60%, and in order to compensate for the heat loss, the collector area would be 5.3 m² using equation (9.18). In order to achieve a wind speed of 3 m/s in the drying chamber, it is required to estimate the boundary layer thickness above the drying tray. The boundary layer thickness is 0.17 m calculated from the following equation for turbulent flow:

$$\delta = 0.37x Re^{-1/5} \quad (9.27)$$

Where,

δ The boundary layer thickness (m)

x The axial distance along the length of the drying chamber (m)

Therefore, the height of the gap above the tray can be 0.2 m and the volumetric flow rate is 0.03 m³/s calculated from equation (9.26).

9.4 Solar Dryer Design

The fan blows the air inside the drying chamber between the transparent cover and the drying tray along the length of the tray (Figure 9.6). The air enters the chamber at temperature $T_{air,0}$ and reduces over the full length of the drying tray since heat is used up in the drying process of the residuals. The energy balance on the air flowing through a small length Δx can be written as follows:

$$W_t D_t m_f c_{air} T_{air}|_x - W_t D_t m_f c_{air} T_{air}|_{x+\Delta x} + W_t \Delta x q_{added} = 0 \quad (9.28)$$

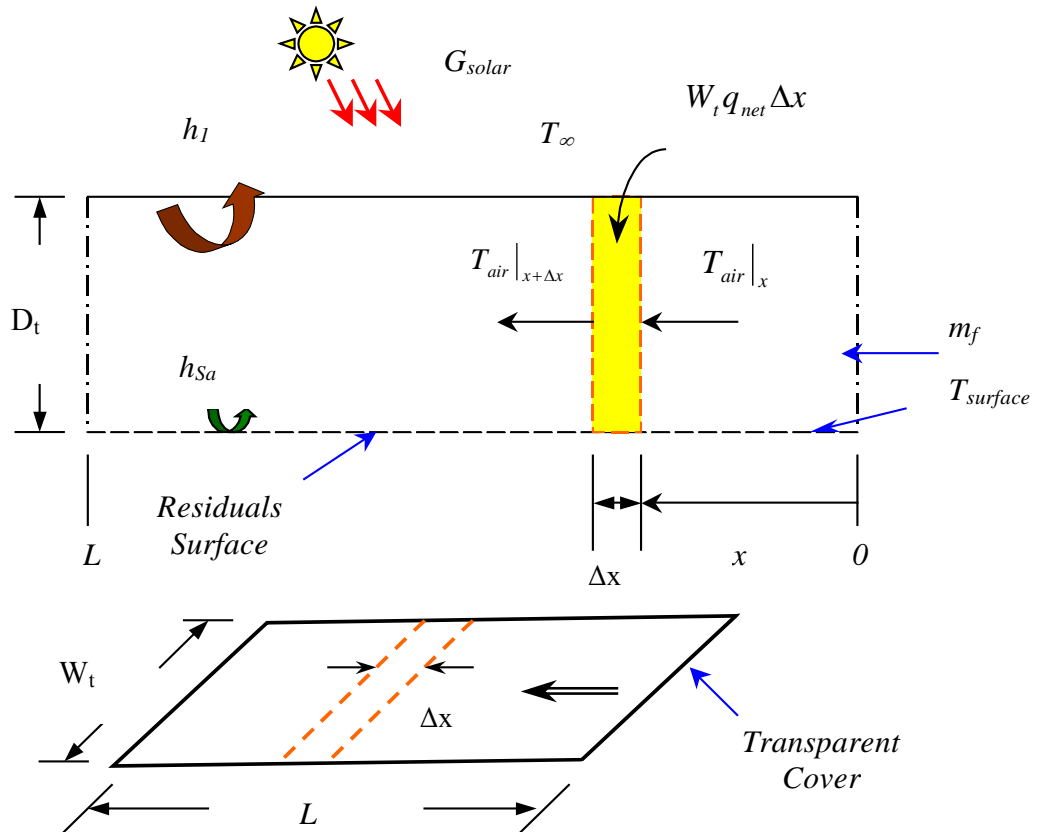


Figure 9.6 Heat balances for the residuals surface, airflow and transparent cover

Where,

W_t	The breadth of the drying chamber (m)
D_t	The height of the gap of the drying chamber (m)
c_{air}	Specific heat of air (J/kg.K)
m_f	The mass flow rate of air through the drying chamber (kg/s)
T_{air}	Temperature of air inside the drying chamber (K)
q_{net}	The net heat flux (W/m ²)

Dividing equation (9.28) by $W_t \Delta x$ and taking the limit as Δx approaches zero (Duffie and Beckman, 1991), (Smitabhindu et al. 2008), equation (9.28) can be written:

$$D_t m_f c_{air} \frac{dT_{air}}{dx} - q_{added} = 0 \quad (9.29)$$

The net heat (added and removed) in the small differential thickness Δx is the sum of the convective and evaporative heat fluxes, therefore, equation (9.29) can be written in the following expanded form:

$$D_t m_f c_{air} \frac{dT_{air}}{dx} = h_{Sa} (T_{surface} - T_{air}) - h_1 (T_{air} - T_{\infty}) + 0.016 h_{Sa} [p_{saturated}(T_{surface}) - RH \times p_{saturated}(T_{air})] \quad (9.30)$$

Where,

T_{∞}	The ambient temperature of the outside air (K)
T_{air}	Temperature of air inside the drying chamber (K)
$T_{surface}$	The surface temperature of residuals (K)
$p_{saturated}$	Partial pressure of saturated vapour at the given temperature (kg/m.s ²)
RH	Relative humidity (decimal)
h_{Sa}	Surface to air convective heat transfer coefficient (W/m ² .K)
h_1	Overall heat transfer coefficient from flowing air to ambient (W/m ² .K)

The partial vapour pressure has an exponential relationship, which is too complex to solve. It is given in the following expression:

$$P_{saturated} = 611 \times 10^{\left(\frac{7.5T_{\infty}}{237.7+T_{\infty}}\right)} \quad (4.13)$$

Where,

T_{∞} Ambient temperature in degrees ($^{\circ}\text{C}$)

Therefore, the partial vapour pressure can be linearised (Gain and Tiwari, 2004) for a small range of temperature between 25 and 55 $^{\circ}\text{C}$:

$$P_{saturated}(T) = R_1 T + R_2 \quad (9.31)$$

Where,

R_1, R_2 Constants

Substituting equation (9.31) into equation (9.30) and simplifying, equation (9.30) can be written as follows:

$$D_t \rho_{air} u c_{air} \frac{dT_{air}}{dx} = h_{Sa} (T_{surface} - T_{air}) - h_1 (T_{air} - T_{\infty}) + 0.016 h_{Sa} [(R_1 (T_{surface}) + R_2) - RH (R_1 (T_{air}) + R_2)] \quad (9.32)$$

Where,

ρ_{air} The density of air (kg/m^3)

u The air speed in the drying chamber above the tray (m/s)

Equation (9.32) can be rearranged to give a form of first order differential equation:

$$\frac{d(T_{air})}{dx} + a T_{air} = f(t) \quad (9.33)$$

The time dependent derivative is given in the following equation:

$$f(t) = \frac{(1 + 0.016 R_1) h_{Sa} T_{surface} + h_1 T_{\infty} + (1 - RH) 0.016 h_{Sa} R_2}{D_t \rho_{air} u c_{air}} \quad (9.34)$$

The coefficient a of equation (9.33) is given in the following expression:

$$a = \frac{h_1 + (1 + 0.016RHR_1)h_{sa}}{D_t \rho_{air} u c_{air}} \quad (9.35)$$

The solution of equation (9.33) for the average value of $\overline{f(t)}$ with the initial temperature of the air entering the drying chamber is given in the following equation:

$$T_{air} = \frac{\overline{f(t)}}{a} (1 - e^{-ax}) + T_{air,0} e^{-ax} \quad (9.36)$$

Where,

$T_{air,0}$ The initial air temperature entering the chamber at $x = 0$ (K)

Equation (9.29) can be used to estimate the air outlet temperature at $x = L$ and then integrated from zero to L in order to find the average value of the flowing air temperature inside the drying chamber above the tray:

$$T_{air,average} = \frac{1}{L} \int_0^L T_{air} dx = \frac{\overline{f(t)}}{a} \left(1 - \frac{1 - e^{-aL}}{aL} \right) + T_{air,0} \frac{1 - e^{-aL}}{aL} \quad (9.37)$$

The drying model developed in Chapter 4 is shown in the following equation:

$$\alpha_s A (G_{direct} \cos \theta + G_{diffuse}) + A \alpha_l \varepsilon_{atmospheric} \sigma T_{sky}^4 + Ah(T_{\infty} - T_{surface}) - A \varepsilon \sigma T_{surface}^4 - h_{fg} m_{solids} \frac{dX}{dt} = \frac{d}{dt} [(m_{solids} c_{solids} + m_{water(i)} c_{water}) T_{surface}] \quad (4.21)$$

The useful energy gained from the collector becomes the input energy for the drying chamber (Tiwari et al, 1997), which is given by:

$$m_f c_{air} (T_{air,0} - T_{\infty}) = m_f c_{air} (T_{air,average} - T_{surface}) \quad (9.38)$$

The transparent cover will act as a heat trap (greenhouse effect) in the drying chamber. The cover can back radiate about 83% of the reradiated heat from the surface of residuals (Hardy, 2003), therefore, The long wave radiation term reradiated from the residuals surface can be multiplied by 0.17 in equation (4.21). When drying occurs in an enclosure, the average flowing air temperature replaces the sky temperature as

expressed by Cengel (1997). Solving equation (9.38) for the surface temperature and substituting in equation (4.21) gives:

$$\alpha_s A G_{solar} + A \alpha_l \sigma T_{air,average}^4 + Ah(T_{air,0} - T_\infty) - 0.17 A \varepsilon \sigma (T_{air,0} - T_\infty)^4 - h_{fg} m_{solids} \frac{dX}{dt} = \frac{d}{dt} [(m_{solids} c_{solids} + m_{water(i)} c_{water}) (T_{air,0} - T_\infty)] \quad (9.39)$$

The moisture content of the residuals in the drying tray of the solar dryer can then be calculated from equation (9.39) using the finite difference technique explained in chapter 4. The design parameters and input values used in the calculation are shown in Table 9.1.

Table 9.1 Design parameters for the solar dryer and input values used for modelling

Parameter	Symbol	Values	Units
The breadth of the drying chamber	W_t	0.5	m
The depth of the drying chamber	D_t	0.2	m
Length of drying chamber	L	0.5	m
Surface to air heat transfer coefficient	h_{sa}	17	$W/m^2.K$
Overall heat transfer coefficient from flowing air to ambient	h_1	6	$W/m^2.K$
Mass flow rate of air	m_f	0.038	kg/s
Specific heat of air	c_{air}	1006	J/kg.K
Relative humidity	RH	0.5-0.8	-
Incident solar radiation	G_{solar}	460	W/m^2
Wind Speed	u	3	m/s
Air density	ρ_{air}	1.069	kg/m^3
Ambient Temperature	T_∞	25	0C
Surface absorbance (short wave)	α_s	0.9	-
Surface absorbance (long wave)	α_l	0.9	-
Constant, equation (9.31)	R_1	407.9	-
Constant, equation (9.31)	R_2	-8234.3	-

The drying time can be predicted from equation (9.39) for different ambient relative humidity values (50%-80%) with average air temperature 55 0C inside the drying

chamber calculated from equation (9.37), total daily solar radiation 15 MJ/m^2 and wind speed 3 m/s inside the drying chamber (Figure 9.7).

The drying time can be predicted from equation (9.39) for different temperature values inside the drying chamber ($40\text{-}55^\circ\text{C}$) with ambient relative humidity 80% , total daily solar radiation 15 MJ/m^2 and wind speed 3 m/s inside the drying chamber (Figure 9.8). Figure 9.9 shows predictions (equation 9.39) for different wind speed values $2\text{-}5 \text{ m/s}$ inside the drying chamber assuming air temperature of 55°C , 80% relative humidity and 15 MJ/m^2 total daily solar radiation.

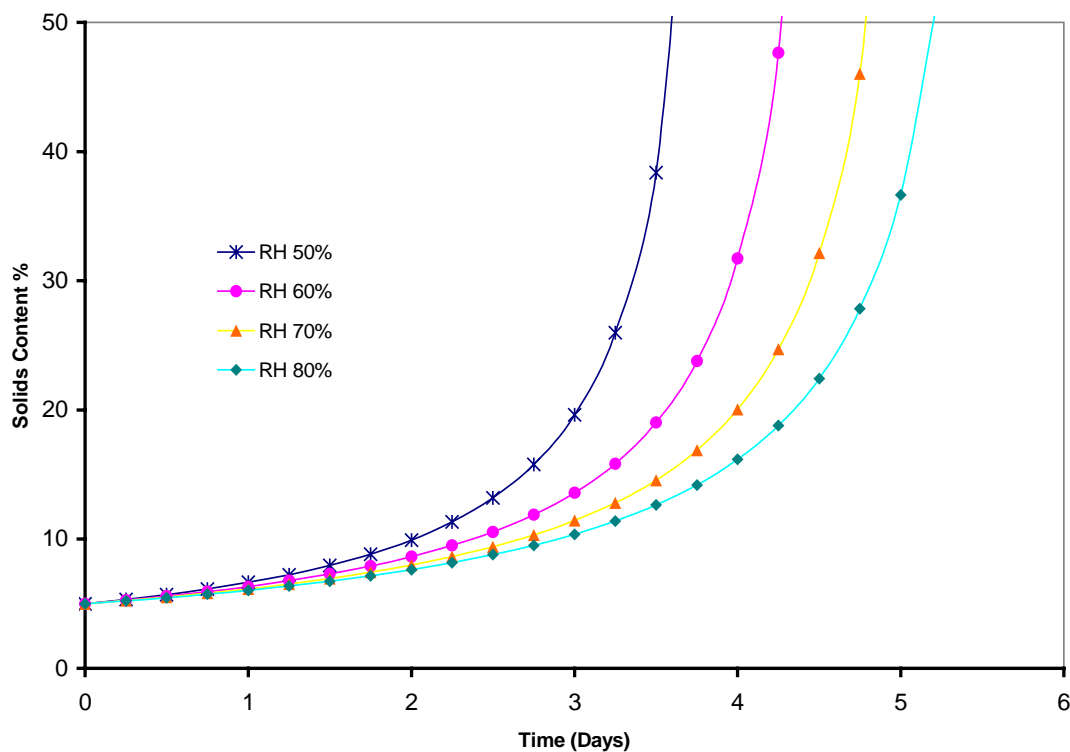


Figure 9.7 Drying predictions for different relative humidity values $50\%\text{-}80\%$ (at 3 m/s and 55°C)

The predictions show that the lowest influential parameter is the average air temperature on the drying time and the highest is relative humidity. The change of ambient relative humidity 50% to 80% results in 6% change of the drying air relative

humidity calculated from the psychrometric chart. Therefore, the 6% relative humidity reduction results in 31% in drying time (Figure 9.7). Wind speed increase from 2 to 5 m/s results in 30% reduction in drying time, however, the temperature increase of 15 °C results in 16% reduction in drying time. The influence order of these parameters on drying time is comparable with the sensitivity analysis results of chapter 8.

The prediction of equation 9.39 has been compared with that of equation 4.21 in Figure 9.10 using experimental data from experiment 20F2 (chapter 7). The prediction of equation 9.39 shows a drying time reduction of ten times for the parameters values shown in Table 9.2. The drying time is reduced dramatically by increasing the air flow temperature to 40 °C and drying air relative humidity (26.6%).

Table 9.2 Parameters and average daily values used for drying time prediction of experiment 20F2

Parameter	Symbol	Ambient Air Values	Drying Chamber Values	Units
The area of the tray	A	-	0.167	m ²
The thickness of application	s	-	0.07	m
Length of drying chamber	L	-	0.495	m
Wind Speed (Air Flow)	u	1.3	1.3	m/s
Relative humidity	RH	0.91	0.266	-
Incident solar radiation	G _{solar}	9.4	-	J/m ²
Ambient Temperature	T _∞	18.6	-	°C
Average air temperature in drying chamber	T _{air,average}	-	40	°C
Initial solids content	SC	-	6.98	%

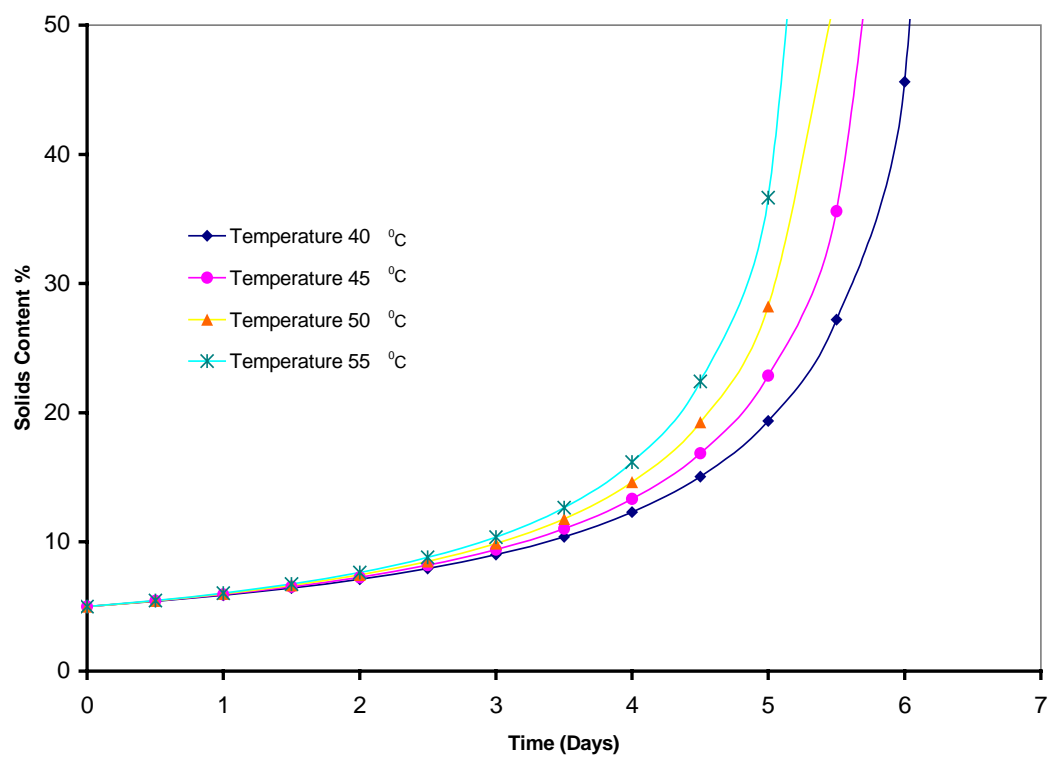


Figure 9.8 The drying prediction for different air temperature values 40⁰ C-55⁰ C (at 3 m/s and 80%)

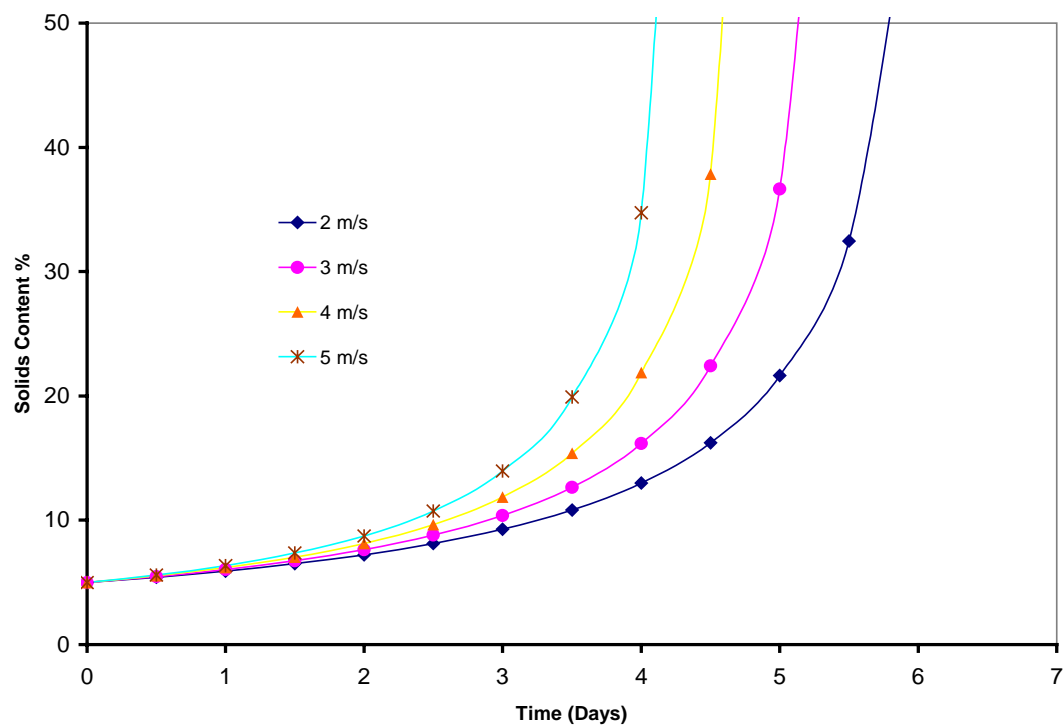


Figure 9.9 The drying prediction for different wind speed values 2-5 m/s (at 80% and 55⁰ C)

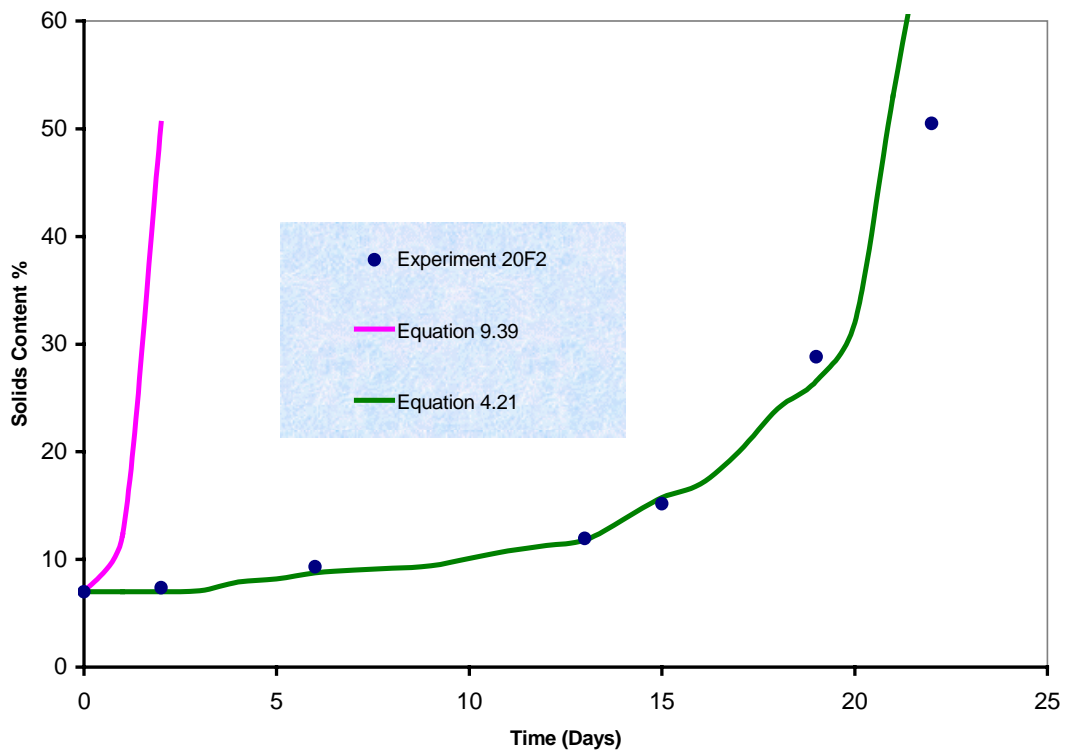


Figure 9.10 Drying predictions of experiment 20F2 using equations (4.21 and 9.39)

9.5 Summary

A mathematical model of the drying of water treatment residuals in a solar dryer has been developed. The optimum solar air collector area and tilt angle has been found based on the available incident solar radiation. A newly developed drying model has been developed using heat balance approach. The drying model was used to estimate the moisture content of the residuals in the drying tray. The solar dryer is expected to be able to evaporate as high as $36 \text{ kg/m}^2/\text{day}$. Drying curves were presented to compare the drying time with different meteorological conditions. The solar dryer is expected to save energy as well as drying bed area and time depending on the local meteorological conditions.

10 Conclusions and Recommendations

10.1 Introduction

The drying and reuse/disposal of water treatment residuals remains an ongoing problem in environmental engineering due to increasing demand on high quality drinking water and increasing waste reuse/disposal problems. Rising demands on clean and safe drinking water have increased the amount of residuals. This in itself has created another problem; namely how best to reuse/dispose of these residuals. Reuse or disposal of water treatment plant residuals could not be economically feasible unless their quantities are reduced. However, reduction of residuals is highly regarded in order to save time in handling of residuals with minimal cost and limited land usage. Residuals are conventionally dried in lagoons and sand drying beds that are open to the atmosphere (A consumer's guide to drinking water, 2006). Weather is a major factor in the drying of residuals, which may take from days to a few months depending upon the conditions. The influence of meteorological conditions on the drying time of residuals is of considerable interest and practical importance.

The overall objectives of this research were to study the drying process of the water treatment plant residuals and to develop a new drying model, which takes into account the effect of meteorological conditions on the drying of residuals. Furthermore, this research aimed to find the most sensitive meteorological parameters on the drying process and to design a solar dryer in order to accelerate the residuals drying process.

A comprehensive review of the literature showed that there were attempts to model the drying process of sewage residuals (Vaxelaire et al. 2000b), (Vaxelaire and Puiggali, 2002), (Reyes et al. 2004) and (Leonard et al. 2005). The review revealed that these

studies focused on diffusion and empirical models. However, Vaxelaire et al (2000b) used the three meteorological parameters (temperature, relative humidity, air velocity) as a single parameter, which is the drying potential defined by Strumillo and Kudra (1986), to explain in an empirical model the drying kinetics of sewage residuals. The drying models of the water treatment residuals have been limited to the empirical models developed by (Clark, 1970), (Lo, 1971), (Rolan, 1980) and (Cornwell and Vandermeijden, 1999). In this research, a new model has been developed to predict the drying of water treatment residuals with the knowledge of changing meteorological parameters.

The purpose of this chapter is to conclude the findings of this study regarding the effect of meteorological parameters on the drying process of residuals. The results of this research are summarised and finally the recommendations for future work are presented based on the limitations of this study.

10.2 Conclusions

10.2.1 Mathematical Modelling of Water Treatment Residuals

A new drying model has been developed using steady-state heat balance approach. Heat balance has been applied to a control volume of residuals, taking into account the heat transfer by radiation, convection and evaporation. A convective heat transfer coefficient was formulated using dimensional analysis. Performing linear regression analysis of the logarithmically transformed data obtained from 23 drying tunnel experiments ($R^2=0.968$), the coefficients of the heat transfer coefficient relationship were determined. The newly developed model (equation 4.21) predicts the change of

moisture content with respect to time and this can then be transformed into solids content versus time (equation 4.29). A finite difference technique has been used in the cumulative moisture content calculation of time intervals in order to achieve the desired moisture content with the knowledge of weather parameters.

10.2.2 Results

10.2.2.1 Laboratory Drying Tunnel Experiments

A total of (56) drying experiments were performed in the laboratory drying tunnel. The drying time for these experiments varied from one to 25 days depending upon variable weather conditions. In these experiments, the residuals start to crack at 10% solids content. For an application depth of 50 mm, the cracks are about 15-20 mm of the cake depth at 15% solids content. At 50% solids content and for a 50 mm application thickness, the residuals appear dry and fragmented (about 15 mm in thickness). The moisture loss accounts for about 45% when residuals dry from 8% to 15% solids content and about 84% in the solids content range of 8% to 50%. The mathematical model was verified using data of the experiments performed in the drying tunnel (33 drying experiments).

The model output (equation 4.21) shows good agreement with a set of experimental data performed in the drying tunnel ($R^2 > 0.93$). The drying curves slightly deviate from the experimental results above 30% solids content that would be attributed to cracks and shrinkage of the application surface and unpredictable drying patterns. The ANOVA table shows that the model is significant having a value less than (0.01). However, the ANOVA results indicate that the weather parameters were more significant than the physical dimensions of the residuals application (thickness and surface area).

10.2.2.2 Field Experimental Drying Beds

The field drying experiments were performed in two identical beds normal (open) drying bed and solar bed (covered with glass) in order to compare the drying behaviour of residuals. In the experiments of the open bed, the data analysis indicated that the drying process curves have two distinct slopes (stages). The first stage occurs when the solids content is less than 15% and the second occurs when the solids content is greater than 15%. The rate of drying is faster in the first stage. The rate of drying is significantly affected by wind speed, relative humidity and rainfall. Wind speed appeared to show a significant effect on the drying time, this effect appears to be more pronounced in the second stage. Dips in the drying curve were observed due to rain events. The dips in the drying curve, however, recover when rain stops within a day or two. The mathematical model predictions show good agreement ($r^2 > 0.8$) with the field experiments of the open drying bed.

The glass covered passive solar drying bed was designed in a similar way to that of the solar distillation still. Despite the fact that very high temperatures were achieved in the cavity of the passive solar bed, drying time could not be enhanced compared to the experimental open drying bed. Removal of the humid air from the cavity of the passive solar bed was a very important factor for enhancing the drying process. Further modifications have been performed for the passive solar bed in order to improve its performance. A wind ventilator was used together with ventilation holes in order to remove moist air from the cavity of the drying bed. The performance has been improved as a result; however, the drying time remained longer than that of the open bed. Finally, when using a fan heater the solar drying bed achieved a reduction of 33% in the drying time compared to the open bed.

10.2.2.3 Sensitivity Analysis

It is of particular interest to understand the most sensitive weather parameters to the drying process of the water treatment residuals. Crystal Ball software, which is based on Monte Carlo simulation, was used to examine the relative importance of all the weather parameters on the mathematical model output. The application thickness and the weather parameters, namely wind speed, relative humidity, ambient temperature and solar radiation were varied one at a time, between their realistic ranges, in order to study their effect on the model output.

It was found that the most sensitive parameter was relative humidity followed by wind speed, ambient temperature, and solar radiation whilst the least sensitive parameter was application thickness. This agrees with the findings of Shin et al (2000) where the drying rate of the water treatment residuals in a fluidised bed dryer was highly influenced by relative humidity rather than the temperature of the drying air. In this study, however, by reducing relative humidity from 75% to 25%, the drying rate increases 6.2 times. The other meteorological parameters, namely wind speed, ambient temperature and solar radiation were less sensitive to the model output. The wind speed increase of 1 m/s, results in a 64% increase in drying rate of residuals. The temperature increase of one degree increases the drying rate of residuals by 3.8%. The solar radiation increase of 1 MJ/m² achieved a 2.6% increase of residuals drying rate.

10.2.2.4 New Active Solar Drying Bed Design

The residuals drying model (equation 4.21) has been modified to predict the drying of residuals in a newly designed active solar bed. The active solar drying bed has been sized for the local meteorological conditions of Wollongong. The tilt angle of the solar collector tilt angle has been optimised using MS Excel solver by maximising the solar radiation gained heat over the whole year, it has been found to be (27.9⁰). The optimum

solar air collector area has been found, for a given residuals application, based on the available incident solar radiation. The modified drying model (equation 9.39) was used to estimate the moisture content of the residuals in the residuals drying tray. For a given application of residuals, the model (equation 9.39) predicted a drying rate of 36 kg/m²/day for dry residuals of up to 50% solids content (wet basis). This is significantly higher than what previous researchers in the sewage solar drying studies have achieved. Luboschik (1999) achieved 2 kg/m²/day, however, Shannon et al (2004) achieved as high as 30 kg/m²/day.

10.2.3 Benefits

The model and methodology presented in this thesis will enable design engineers to predict the drying time of residuals as well as optimising the size of the residuals drying beds. The model enables design engineers to predict the drying process of water treatment residuals with the knowledge of weather parameters. Successful prediction of the residuals drying time helps water treatment facilities with their maintenance scheduling. The benefits of the solar design enable water treatment facilities in their day-to-day operation with the ease of cleaning and low maintenance costs. Other operational benefits could be the reduction of time for final reuse or disposal as well as reduction in space used for the drying beds. The use of active solar beds is of good advantage in reducing the drying time. Moreover, and during rain periods, delays resulting from residuals rewetting in the drying beds can be avoided.

The benefits of applying this study to the residuals drying of the Illawarra Water Treatment Plant:

- The treatment process can be optimised in order to minimise the quantity of residuals generated from the plant.

- An optimum depth of residuals bed can be achieved in the thickeners. The quantity and frequency of the residuals pumped out from the thickeners to the drying beds can be minimised. Drying time can be minimised by applying lower moisture content residuals into the drying beds.
- In the design of the drying beds, the meteorological conditions should be considered particularly the wind direction and solar radiation predominance.
- Although higher capital cost could be involved, the beds can be covered in order to prevent rain from rewetting the residuals. Transparent bed covers (i.e. greenhouse type) with good ventilation can dramatically improve the drying of residuals.
- As residuals dries a hard crust forms on the surface, which inhibits the moisture diffusion of water vapour to the atmosphere. Therefore, mixing of residuals enhances the drying process.
- Monitoring of weather conditions together with the mathematical model can be employed to predict the drying of residuals successfully. In order to achieve that task, meteorological parameters can be entered as inputs in a computer program to facilitate the use of the model by the operators.

Applying the mathematical model and the solar bed design in chapter 9 could lead to environmental, social and financial benefits. The benefits for the environment enable the reduction of greenhouse emissions by using solar energy in the drying of residuals. Accelerated drying process using solar energy minimises nuisance odour problems for any type of residuals. Drying diminishes residuals volume making the transport cost lower and hence less carbon dioxide emissions to the atmosphere from vehicles. Accelerated residuals drying process require less land area, which is a sustainable

practice and should be encouraged by local and national authorities. The beneficial use of residuals is of great benefit to the society and the environment.

It should be pointed out that the residuals of the Illawarra Water Treatment Plant are not disposed of in a landfill; however, they are used by a local company as a soil conditioner for agricultural use.

10.3 Recommendations for future work

This research presents a new approach in the experimental and theoretical modelling of the drying process of residuals. However, opportunity exists to conduct further studies:

- Experiments used in this dissertation can be employed in future studies as a basis to assess the drying conditions of other types of potable water treatment residuals (i.e. alum) as well as sewage or similar industrial residuals. Constituents and properties of materials affect their drying behaviour. Since ferric chloride residuals particle size increases with reduced moisture content; therefore, other types of residuals drying could be investigated and hence the heat transfer coefficient (equation 4.25) could be modified.
- Only the wind speed was controlled in the drying tunnel of this study; therefore, the experiments could be performed in a controlled environment (environmental chamber) in order to study the effect of changing relative humidity as well as the other meteorological parameters.
- The level of uncertainty associated with the measurement of the residuals surface temperature, specifically at the dry period above 30% solids content,

using the leaf temperature sensor can be improved by more advanced technique of measurement such as infrared thermometer. The error in surface temperature measurement affects greatly the prediction of the model, which affects the highest influential parameter that is relative humidity.

- The experimental work has been performed in small drying beds in the field experiments as well as the drying tunnel. The model successfully predicts a given application of residuals, however, applications in a large bed could be difficult to predict. Therefore, scale up (25 m^2) of the experimental work using a pilot plant could give more insight into the residuals drying process.
- The active solar dryer could be built in order to verify the modified drying model (equation 9.39), and hence further analysis on the drying rate for the constant and falling rate periods could be done. On the other hand, the solar collector can be improved by using a solar tracking system in order to maximise the solar radiation gain in the dryer.
- Drying experiments in this study dealt with drying of residuals above 5% solids content where large quantity of free water is drained. The drying model developed in this study (equation 4.21) is concerned with the evaporation part since drainage can lead to blinding of the sand in the drying bed. However, the model can be improved by including the drainage part.
- Sensitivity analysis found that the application thickness was the least sensitive parameter. Larger application thicknesses could be investigated, however, it is not recommended from operational point of view to have applications larger than 500 mm.

References

- A consumer's guide to drinking water, (2006), The Cooperative Research Centre for Water Quality and Treatment (Australia's national drinking water research centre). <<http://www.waterquality.crc.org.au/consumers/consumer.pdf>>. Viewed: 14 August 2006.
- A Special Focus on Australian Natives, (2007), <http://www.scottsaustralia.com.au/Need_Help/Australian_Natives>. Viewed: 4 August 2007.
- Ait Mohamed, L., Kouhila, M., Jamali, A., Lahsasni, S., Kechaou, N. and Mahrouz, M. (2005), *Single Layer Solar Drying Behaviour of Citrus Aurantium Leaves under Forced Convection*, Energy Conversion and Management, Volume 46, pp. 1473–1483.
- Albertson, O. E., Burris, B. E., Reed, S. C., Semon, J. A., Smith, Jr., J. E. and Wallace, A. T., (1991), *Dewatering Municipal Wastewater Sludges*, Noyes Data Corporation, New Jersey, USA.
- Aldeeb, A. A., Qasim, S. R., Puppala, A. J. and Anderson C. F. (2003), *Physical and Engineering Properties of Treatment Plant Residuals and Disposal*, American Water Works Association Journal, Volume 95(8), pp. 127-137.
- Anen, M. V. and Dharmappa, H. B. (1997), A Survey of Water Treatment Plants in New South Wales, Water, November/December issue, pp. 15-18.
- Ashman, M. R. and Puri, G. (2002), *Essential Soil Science*, Blackwell Science Ltd., UK.
- Atomstromfreie Website, (2007), *Solar Radiation Estimation and Site Analysis*, <<http://www.pvresources.com/en/location.php>>. Viewed: 15 Nov. 2007.
- Aversa, M, Curcio, S., Calabro', V. and Iorio, G. (2007), *An Analysis of the Transport Phenomena Occurring During Food Drying Process*, Journal of Food Engineering, Volume 78, pp. 922–932.
- Babalis, S. J. and Belessiotis, V. G. (2004), *Influence of the Drying Conditions on the Drying Constants and Moisture Diffusivity During the Thin-Layer Drying of Figs*, Journal of Food Engineering, Volume 65, pp. 449–458.
- Bala, B. K. and Woods, J. L. (1995), *Optimisation of Natural Convection Solar Drying Systems*, Energy, Volume 20(4), pp. 285-294.
- Berdahl, P. and Martin, M. (1984), *Emissivity of Clear Skies*, Solar Energy, Volume 32, No. 5, pp. 663-664.

- Boudhrioua, N., Bonazzi, C. and Daudin, J. D. (2003), *Estimation of Moisture Diffusivity in Gelatin-Starch Gels Using Time-Dependent Concentration-Distance Curves at Constant Temperature*, Food Chemistry, Volume 82, pp. 139-149.
- Boyle, G., Everett, B. and Ramage, J. (2003), *Energy Systems and Sustainability*, Oxford University Press, Glasgow, UK.
- Broughton, D. B. (1945), *The Drying of Solids (Prediction of Critical Moisture Content)*, Industrial and Engineering Chemistry, Volume 37, pp. 1184-1185.
- Brutsaert, W. (1982), *Evaporation into the Atmosphere*, D. Reidel Publishing Company, USA.
- Calvert, J. B. (2003), *Fans and Wind Power*,
<<http://www.du.edu/~jcalvert/tech/fluids/fan.htm>>. Viewed: 17 November 2007.
- Cannon, A. J. and McKendry, I. G. (2002), *A Graphical Sensitivity Analysis for Statistical Climate Models: Application to Indian Monsoon Rainfall Prediction by Artificial Neural Networks and Multiple Linear Regression Models*, International Journal of Climatology, Volume 22, pp. 1687-1708.
- Carslaw, H. S. and Jaeger, J. C. (1986), *Conduction of Heat in Solids*, Oxford [Oxfordshire]: Clarendon Press; New York, USA: Oxford University Press, London, England.
- Ceaglske, N. H. and Hougen, D. A. (1937), *The Drying of Granular Solids*, Transactions, American Institute of Chemical Engineers, Volume 33, pp. 283-312.
- Cengel, Y. A. (1997), *Introduction to Thermodynamics and Heat Transfer*, The McGraw-Hill Companies, Inc., USA.
- Cengel, Y. A. and Boles, M. A. (2006), *Thermodynamics: An Engineering Approach*, Fifth Edition, McGraw-Hill Companies, Inc., New York, USA.
- Chan, K., Saltelli, A. and Tarantola, S. (1997), *Sensitivity Analysis of Model Output: Variance-Based Methods Make the Difference*, Proceedings of the 1997 Winter Simulation Conference, Italy, pp. 261-268.
- Chen, G., Yue, P. L. and Mujumdar, A. S. (2002), *Sludge Dewatering and Drying*, Drying Technology, Volume 20, Nos. 4&5, pp. 883-916.
- Chen, P. and Pei, C. T. (1989), *A Mathematical Model of Drying Processes*, International Journal of Heat and Mass Transfer, Volume 32, No. 2, pp. 297-310.
- Chen, X. D., Lin, S. X. Q., Chen, G. (2002), *On the Ratio of Heat to Mass Transfer Coefficient for Water Evaporation and its Impact upon Drying Modelling*, International Journal of Heat and Mass Transfer, Volume 45, pp. 4369-4372.
- Cheremisinoff, N. P. (2002), *Handbook of Water and Wastewater Treatment Technologies*, Butterworth-Heinemann, Woburn, Massachusetts, USA.

- Cheremisinoff, P. N. (1994), *Sludge Management and Disposal*, Prentice Hall, USA.
- Chu, C. P. and Lee, D. J. (April 1999), *Moisture Distribution in Sludge: Effects of Polymer Conditioning*, Journal of Environmental Engineering, pp. 340-345.
- Clark E. E. (1969), *The Drying of Water Treatment Waste Solids*, Source Control of Water treatment Waste Solids (D. D. Adrian, J. H. Nebiker) Report No. EVE 13-69-1, Department of Civil Engineering, University of Massachusetts, Amherst, Massachusetts, USA.
- Clark, E. E. (1971), *Water Treatment Sludge Drying and Drainage on Sand Beds*, University of Massachusetts, Civil Engineering, PhD Thesis.
- Cooman, A. and Schrevens, E. (2007), *Sensitivity of the Tomgro Model to Solar Radiation Intensity, Air Temperature and Carbon Dioxide Concentration*, Biosystems Engineering, Volume 96(2), pp. 249-255.
- Cornwell, D. A. and Vandermeyden, C. (1999), *Sizing Residuals Drying Beds*, American Water Works Association Journal, Volume 91, No. 11, pp. 94-105.
- Cornwell, D. A., Bishop, M. M., Gould, R. G. and Vandermeyden, C. (1987), *Water Treatment Plant Waste Management*, AWWA Research Foundation and American Water Works Association, Denver, Colorado, U. S. A.
- Crank, J. (1975), *The Mathematics of Diffusion*, Oxford, [Eng]: Clarendon Press, London, England.
- Crittenden J. C., Trussell, R. R., Hand, D. W., Howe, K. J. and Tchobanoglous, G. (2005), *Water Treatment: Principles and Design*, 2nd Edition, John Wiley & Sons Inc., USA.
- Crystal Ball 7.3 Reference Manual. (2007),
<<http://www.crystalball.com/support/documentation/CB7%20Reference%20Manual.pdf>>. Viewed: 19 October 2007.
- Crystal Ball 7.3 User Manual. (2007),
<<http://www.crystalball.com/support/documentation/CB7%20User%20Manual.pdf>>. Viewed: 19 October 2007.
- Dharmappa, H. B., Prasanthi, H., Krishna, M. U. and Xiao, Y. (1997), *Estimation of Empirical Coefficients of A Granular Filtration Model*, Water Research, Volume 31, No. 5, pp. 1083-1091.
- Dicorato, M., Forte, G. and Trovato, M. (2008), *Environmental-Constrained Energy Planning using Energy-Efficiency and Distributed-Generation Facilities*, Renewable Energy, Volume 33, pp. 1297-1313.
- Doymaz, I. and Tugrul, N. and Pala, M. (2006), *Drying Characteristics of Dill and Parsley Leaves*, Journal of Food Engineering, Volume 77, pp. 559-565.

- Doymaz, I. (2004), *Convective Air Drying Characteristics of Thin Layer Carrots*, Journal of Food Engineering, Volume 61, pp. 359–364.
- Doymaz, I., Tugrul, N. and Pala, M. (2006), *Drying characteristics of dill and parsley leaves*, Journal of Food Engineering, Volume 77, pp. 559–565.
- Duffie, J. A. and Beckman, W. A. (1991), *Solar Engineering of Thermal Processes*, Second Edition, Wiley, New York, USA.
- Eaton, A. d., Clesceri, L. S. and Greenberg, A. E. (1995), *Standard Methods for the Examination of Water and Wastewater*, 19th Edition, American Public Health Association, Washington D.C., USA.
- El-Ariny, A. S. and Miller, H. I. (1984), *Utilization of Solar Energy for Sludge Drying Beds*, Journal of Solar Energy Engineering, Volume 106, pp. 351-357.
- El-Haggar S. M. and Awn A. A. (1993), *Optimum Conditions for a Solar Still and its use for a Greenhouse using the Nutrient Film Technique*, Desalination, Volume 94, pp. 55-68.
- Elliott, H. A., Dempsey, B. A., Hamilton, D. W. and DeWolfe, J. R. (1990), *Land Application of Water Treatment Sludges: Impact and Management*, AWWA Research Foundation and American Water Works Association.
- EPA. (2003), <http://www.epa.sa.gov.au/pdfs/epwq_report.pdf>. Viewed: 26 July 2007.
- Evans, J. R. and Olson, D. L. (1998), *Introduction to Simulation and Risk Analysis*, Prentice Hall, Inc., Upper Saddle River, New Jersey, USA.
- Exell, R. H. B. (1980), *Grain Drying*, Sunworld, Volume 4, November 6.
- Fabrou, L. (1998), *Illawarra Water Treatment Plant Process Handbook*, OTV, Paris, France.
- Facts and Figures: Water use. (2003), <http://www.unesco.org/water/iyfw2/water_use.shtml>. Viewed: 14 August 2006.
- Gain, D. and Tiwari, G. N. (2004), *Effect of Greenhouse on Crop Drying Under Natural and Forced Convection II. Thermal Modelling and Experimental Validation*, Energy Conversion & Management, Volume 45, pp. 2777-2793.
- Gardner, W. R. and Hillel, D. I. (1962), *The relation of external evaporative conditions to the drying of soils*, Journal of Geophysical Research, Volume 67, No. 11, pp. 4319-4325.
- Gharaibeh, A. and Craig, K. (1999), *Removal of Manganese from Drinking Water using a Modified Treatment Process*, Second Annual New South Wales Water Industry

Operators Conference, 30th September – 1st October, Penrith Panthers, Penrith, NSW, Australia.

Gharaibeh, A., Sivakumar, M. and Dharmappa, H. (2003), *Drying of Water Treatment Plant Residuals*, 7th Annual Environmental Research Conference, Proceeding of EERE 2003 Conference, The Cumberland, Marysville, VIC, Australia.

Gharaibeh, A., Sivakumar, M., and Dharmappa, H. B. (2001), *The effect of meteorological conditions on residuals drying*, The Proceedings of 19th Federal Convention, AWA, Canberra, ACT, Australia.

Ghoneym A. and Ileri A. (1997), *Software to Analyse Solar Stills and an Experimental Study on the Effects of the Cover*, Desalination, Volume 114, pp. 37-44.

Gilliland, E. R. and Sherwood, T. K. (1933), *The Drying of Solids-VI (Diffusion Equation for the Period of Constant Drying Rate)*, Industrial and Engineering Chemistry, Volume 25, No. 10, pp. 1134-1136.

Gogus, F. and Maskan, M. (2006), *Air Drying Characteristics of Solid Waste (pomace) of Olive Oil Processing*, Journal of Food Engineering, Volume 72, pp. 378-382.

Goswami, Y., Kreith, F. and Kreider, J. F. (2000), *Principles of Solar Engineering*, Taylor & Francis, Philadelphia, PA, USA.

Hardy, J. T. (2003), *Climate Change: Causes, Effects, and Solution*, John Wiley & Sons, Ltd. USA.

Haseltine, T. R. (1951), *Measurement of Sludge Drying Bed Performance*, Sewage and Industrial Wastes, Volume 23, No. 9, pp. 1065.

Hayse, J. W. (2000), Using Monte Carlo Analysis in Ecological Risk Assessments, <<http://web.ead.anl.gov/ecorisk/issue/pdf/montecarlo.pdf>>. Viewed: 23 October 2007.

Henderson, S. M. (1952), *A Basic Concept of Equilibrium Moisture*, Agricultural Engineering, January, pp. 29-32.

Henderson, S. M. and Perry, R. L. (1955), *Agricultural Process Engineering*, John Wiley & Sons, USA.

Hossain, M. A., Woods, J. L. and Bala, B. K. (2005), *Optimisation of Solar Tunnel Drier for Drying of Chilli without Colour Loss*, Renewable Energy, Volume 30, pp. 729-742.

Hossam, A. A., Saad, S. G., Mitwally, H. H., Saad, L. M. and Noufal, L. (1990), *Solar Energy for Sludge Drying in Alexandria Metropolitan Area: Case Study in Egypt*, Water Science Technology, Volume 22, No. 12, pp. 193-204.

- Hougen, D. A., McCauley, H. J. and Marshall, W. R. (1940), *Limitations of Diffusion Equations in Drying*, Transactions, American Institute of Chemical Engineers, Volume 36, pp. 183-209.
- Hsu, S. A. and Meindl, E. A. (1994), *Determination of the Power-Law Wind Profile Exponent under Near-Neutral Stability Conditions at Sea*, Applied Meteorology, Volume 33, pp. 757-765.
- Illawarra Water Quality Report. (1992), Sydney Water, Sydney, Australia.
- Inazu, T., Iwasaki, K. and Furuta T. (2003), *Effect of air velocity on fresh Japanese noodle (Udon) drying*, Lebensm.-Wiss. U.-Technol., Swiss Society of Food Science and Technology, Volume 36, pp. 277–280.
- Incropera, F. P. and Dewitt, D. P. (1996), *Fundamentals of Heat and Mass Transfer*, Forth Edition, John Wiley & Sons, USA.
- Kadam, D. M. and Samuel, D. V. K. (2006), *Convective Flat-plate Solar Heat Collector for Cauliflower Drying*, Biosystems Engineering, Volume 93, No. 2, pp. 189-198.
- Kaminski, M. (2003), *Sensitivity Analysis of Homogenized Characteristics for some Elastic Composites*, Computer Methods in Applied Mechanics and Engineering, Volume 192, No. (16-18), pp.1973-2005.
- Keey, R. B. (1972), *Drying: Principles and Practice*, Pergamon, New York, USA.
- Keey, R. B., Langrish, T. A. and Walker, J. C. (2000). *Kiln-Drying of Lumber*, Springer, Berlin, Germany.
- Kerkhof, P. J. A. M. and Coumans, W. J. (2002), *Drying: a fascinating unit operation*, Chemical Engineering Journal, Volume 86, pp. 1-2.
- Kreider J. F., Hoogendoorn C. J. and Kreith F. (1989), *Solar Design Components, Systems, Economics*, Hemisphere Publishing Corporation, New York, USA.
- Krzykacz-Hausmann, B. (2005), *Sensitivity Analysis of Monte Carlo Estimates from Computer Models in the Presence of Epistemic and Aleatory Uncertainty*, Los Alamos National Laboratory, <<http://library.lanl.gov/>>, pp. 71-80. Viewed 4 November 2007.
- Lamoureux, J., Tiersch, T. R. and Hall, S. G. (2006), *Sensitivity Analysis of the Pond Heating and Temperature Regulation (PHATR) Model*, Aquacultural Engineering, Volume 34, pp. 117-130.
- Lee, D. J. (1996), *Moisture distribution and Removal Efficiency of Waste Activated Sludges*, Water Science and Technology, Volume 33, No. 12, pp. 269-272.
- Leite, J. B., Mancini, M.C. and Borges, S.V. (2007), *Effect of Drying Temperature on the Quality of Dried Bananas cv. prata and d'a'gua*, LWT, Swiss Society of Food Science and Technology, Volume 40, pp. 319–323.

- Leonard, A., Blacher, S., Marchot, P., Pirard, J. P. and Crine, M. (2005), *Convective Drying of Wastewater Sludges: Influence of Air Temperature, superficial Velocity, and Humidity on the Kinetics*, *Drying Technology*, Volume 23, pp. 1667-1679.
- Letterman, R. D. (1991), *Filtration Strategies to Meet the Surface Water Treatment Rule*, Denver, CO: American Water Works Association, USA.
- Liu, H., Zhou, L. and Hayakawa, K. (1997), *Sensitivity Analysis for Hygrostress Crack Formation in Cylindrical Food During Drying*, *Journal of Food Science*, Volume 62, No. 3, pp. 447-450.
- Lo, Kuuang-Mei. (1971), *Digital Computer Simulation of Water and Wastewater Sludge Dewatering on Sand Beds*, University of Massachusetts, Civil Engineering, PhD. Thesis, Amherst, Massachusetts, Publisher: University Microfilms, A XEROX Company, Ann Arbor, Michigan, USA.
- Luboschik, U. (1999), *Solar Sludge Drying-Based on the IST Process*, *Renewable Energy*, Volume 16, pp. 785-788.
- Mahdi J. T. and Smith B. E. (1994), *Solar Distillation of Water using a V-Trough Solar Concentrator with a Wick-Type Solar Still*, *Renewable Energy*, Volume 5, No. 1, pp. 520-523.
- Manuals of British practice in water pollution control. (1981), *Unit processes: Sewage sludge 2: conditioning, dewatering and thermal drying / The Institute of Water Pollution Control*, Maidstone, Kent: The Institute of Water Pollution Control.
- Marklund, S. (1990), *dewatering of Sludge by Natural Methods*, *Water Science Technology*, Volume 22, Nos. (3&4), pp. 239-246.
- Marklund, S. (1990), *dewatering of Sludge by Natural Methods*, *Water Science Technology*, Volume 22, Nos. 3/4, pp. 239-246.
- Maskan, A., Kaya, S. and Maskan, M. (2002), *Hot Air and Sun Drying of Grape Leather (Pestil)*, *Journal of Food Engineering*, Volume 54, pp. 81-88.
- McAdams, W. H. (1954), *Heat Transmission*, Third Edition, McGraw-Hill, New York, USA.
- McCabe, W. L. and Smith J. C. (2000). *Unit Operations of Chemical Engineering*, Sixth Edition, McGraw-Hill, Inc., USA.
- McKenzie, K. A. (1992), *Equilibrium Moisture Content Measurement for Drying Operations*, *Measurement + Control*, Volume 25, pp. 109-110.
- Miller, S. (1999), *The Need to Improve De-Watering Technologies*, *Water*, January/February.

- Mohammad M. A., Soliman S. H., Abdel-Salam M. S. and Hussein H. M. S. (1995), *Experimental and Financial Investigation of Asymmetrical Solar Stills with Different Insulation*, Applied Energy, Volume 52, pp. 265-271.
- Moller, U. K. (1983), *Water binding*, (Carberry B. C. and England A. J. Jr. (Editors)), Sludge Characteristics and behaviour, Proceedings of the NATO Advanced Study Institute on Sludge Characteristics and Behaviour, University of Delaware, Newark, USA, July 17-26, 1979, Martinus Nijhoff Publishers, The Hague, The Netherlands. pp. 182-194.
- Morrison, G. L. Solar Collectors. In: Gordon, J. (Editor). (2001), *Solar Energy: The State of the Art*, James & James (Science Publisher), London, UK.
- Mujumdar, A. S. (1987), *Handbook of Industrial Drying*, Marcel Dekker, Inc., New York, USA.
- Mun, J. (2004), *Applied Risk Analysis: Moving Beyond Uncertainty in Business*, John Wiley & Sons, Inc., Hoboken, New Jersey, USA.
- Munson, B. R., Young, D. F. and Okiishi, T. H. (1994). *Fundamentals of Fluid Mechanics*, 2nd Ed., John Wiley & Sons, Inc., USA.
- Murray, F. W. (1967), *On the Computation of Saturation Vapour Pressure*, Journal of Applied Meteorology, Volume 6, pp. 203-204.
- Nebiker, J. H. (1967), *The drying of Wastewater Sludge in the Open Air*, Journal of the Water pollution Control Federation, Volume 39, No. 4, pp. 608-626.
- Novak, J. T. and Montgomery, G. E. (February 1975), *Chemical Sludge Dewatering on Sand Beds*, Journal of the Environmental Engineering Division, pp. 1-14.
- Ostwald, P. F. and McLaren T. S. (2004), *Cost Analysis and Estimating for Engineering and Management*, Pearson Prentice Hall, NJ, USA.
- Palanz, B. (1984), *Analysis of Solar-dehumidifying Drying*, International Journal of Heat and Mass Transfer, Volume 27, No. 5, pp. 647.
- Penman, H. L. (1948), *Natural evaporation from open water, bare soil and grass*, Proceedings of the Royal Society, London, Series A, 7, Volume 193, pp. 120-146.
- Perry, R., and Green, D. (1997), *Perry's Chemical Engineers' Handbook*, Seventh Edition, McGraw-Hill, Inc., New York, USA.
- Porta M. A., Chargoy N. and Fernandez J. L. (1997), *Extreme Operating Conditions in Shallow Solar Stills*, Solar Energy, Volume 61, No. 4, pp. 279-286.
- Prasad B. and Tiwari G. N. (1996), *Analysis of Double Effect Active Solar Distillation*, Energy Conversion Management, Volume 37, No. 11, pp. 1647-1656.

- Pratoto, A., Daguenet, M. and Zeghmatti, B. (1997), *Sizing Solar-Assisted Natural Rubber Dryers*, Solar Energy, Volume 61, No. 4, pp. 287-291.
- Qui, G. Y., Yano T. and Momii, K. (1998), *An Improved Methodology to Measure Evaporation from Bare Soil based on Comparison of Surface Temperature with a Dry Soil Surface*, Journal of Hydrology, Volume 210, pp. 93-105.
- Quon, J. E. and Tamblyn, T. A. (1965), *Intensity of Radiation and Rate of Sludge Drying*, Journal of the Sanitary Engineering Division, Proceedings of the American Society of Civil Engineering, Volume 91, No. SA2, pp. 17-31.
- Reardon, C. (2005), *Your Home Technical Manual*,
<http://www.yourhome.gov.au/technical/fs32.htm>. Viewed: 15 June 2007.
- Reimers, R. S. and Englands, A. J. Jr. (1983), *Interaction with Heavy Metals*, (Carberry B. C. and Englands A. J. Jr. (Editors)), Sludge Characteristics and behaviour, Proceedings of the NATO Advanced Study Institute on Sludge Characteristics and Behaviour, University of Delaware, Newark, USA, July 17-26, 1979, Martinus Nijhoff Publishers, The Hague, The Netherlands. pp. 235-279.
- Reyes, A., Eckholt, M., Toroncoso, F. and Efremov, G. (2004), *Drying Kinetics of Sludge from a Wastewater Treatment Plant*, Drying Technology, Volume 22, No. 9, pp. 2135-2150.
- Rolan, A. T. (1980), *Determination of Design Loading for Sand Drying Beds*, Journal North Carolina Section, AWWA and North Carolina WPCA, Volume L5, No. 1, pp. 25.
- Ruiz, T., Wisniewski, C., Kaosol, T. and Persin, F. (2007), *Influence of Organic Content in Dewatering and Shrinkage of Urban Residual Sludge Under Controlled Atmospheric Drying*, Trans IChemE, Process Safety and Environmental Protection, Volume 85, No. B1, pp. 104-110.
- Sacilik, K., Keskin, R. and Elicin, A. K. (2006), *Mathematical Modelling of Solar Tunnel Drying of Thin Layer Organic Tomato*, Journal of Food Engineering, Volume 73, pp. 231-238.
- Salihoglu, N. K., Pinarli, V. and Salihoglu, G. (2007), *Solar drying in sludge management in Turkey*, Renewable Energy, Volume 32, pp. 1661-1675.
- Sankata, C. K. and Castaigneb, F. (2004), *Foaming and Drying Behaviour of Ripe Bananas*, Swiss Society of Food Science and Technology, Volume 37, pp. 517-525.
- Schultz, E.L., Mazzuco, M.M., Machado, R.A.F., Bolzan, A., Quadri, M.B. and Quadri, M.G.N. (2007), *Effect of Pre-treatments on Drying, Density and Shrinkage of Apple Slices*, Journal of Food Engineering, Volume 78, pp. 1103-1110.
- Scotts Australia. (2007), *A Special Focus on Australian Natives*,
http://www.scottsaustralia.com.au/Need_Help/Australian_Natives. Viewed: 4 August 2007.

- Seginer, I. and Bux, M. (2006), *Modeling Solar Drying Rate of Wastewater Sludge*, Drying Technology, Volume 24, pp. 1353–1363.
- Seginer, I., Ioslovich, I. and Bux, M. (2007), *Optimal Control of Solar Sludge Dryers*, Drying Technology, Volume 25, pp. 401–415.
- Shannon, R., Nathan, S. and Luboschik, V. (2004), *Solar Sludge Drying*, WaterWorks, December issue, pp. 38-43.
- Sherwood, T. K. (1929), *The Drying of Solids-I*, Industrial and Engineering Chemistry, Volume 21, No. 1, pp. 12-16.
- Sherwood, T. K. (1929), *The Drying of Solids-II*, Industrial and Engineering Chemistry, Volume 21, No. 10, pp. 976-980.
- Sherwood, T. K. (1930), *The Drying of Solids-III (Mechanism of the Drying of Pulp and Paper)*, Industrial and Engineering Chemistry, Volume 22, No. 2, pp. 132-136.
- Sherwood, T. K. (1932), *The Drying of Solids-IV (Application of Diffusion Equations)*, Industrial and Engineering Chemistry, Volume 24, No. 3, pp. 307-310.
- Sherwood, T. K. (1936), *The Air Drying of Solids*, Chemical Engineering Congress of the World Power Conference, London, England, pp. 150-168.
- Sherwood, T. K. and Comings, E. W. (1933), *The Drying of Solids-V (Mechanisms of Drying of Clays)*, Industrial and Engineering Chemistry, Volume 25, No. 3, pp. 311-315.
- Shin, Y., Kim, H. and Chun, H. (2000), *Drying of Water Treatment Process Sludge in a Fluidised Bed Dryer*, Korean Journal of Chemical Engineering, Volume 17, No. 1, pp. 22-26.
- Sinicio, R., Muir, W. E. and Jayas, D. S. (1997), *Sensitivity Analysis of a Mathematical Model to Simulate Aeration of Wheat Stored in Brazil*, Postharvest Biology and Technology, Volume 11, pp. 107-122.
- Smitabhindu, R., Janjai, S. and Chankong, V. (2008), *Optimisation of a Solar-Assisted Drying System for Drying Bananas*, Renewable Energy, Volume 33, pp. 1523-1531.
- Smith, J. M., Van Ness, H. C. and Abbott, M. M. (1996), *Introduction to Chemical Engineering Thermodynamics*, Fifth Edition, The McGraw-Hill Companies, Inc.
- Smollen, M. (1990), *Evaluation of Municipal Sludge Drying and Dewatering with Respect to Sludge Volume Reduction*, Water Science Technology, Volume 22, No. 12, pp. 153-161.
- Spellman, F. R. (1997), *Dewatering Biosolids*, CRC Press. Old Dominion University, Norfolk, Virginia, USA.

- Spencer, J. W. (1971), *Fourier Series Representation of the Position of the Sun*, Search, Volume 2, No. 5, pp. 172.
- Strumillo, C. and Kudra, T. (1986), *Drying: Principles, Applications and Design*, Topics in Chemical Engineering (Volume 3), Gordon and Breach Science Publishers, Switzerland.
- Suneja S., Tiwari G. N. and Rai S. N. (1997), *Parametric Study of an Inverted Absorber Double-Effect Solar Distillation System*, Desalination, Volume 109, pp. 177-186.
- Swami, S. B., Das, S. K. and Maiti B. (2007), *Convective Hot Air Drying and Quality Characteristics of Bori: A traditional Indian nugget prepared from black gram pulse batter*, Journal of Food Engineering, Volume 79, pp. 225–233.
- Swamy, C. B. (2006), Particle Size Distribution of Water Treatment Plant Residuals, <<http://aiche.confex.com/aiche/s06/techprogram/P37320.HTM>>. Viewed: 3 August 2007.
- Tao, T., Peng, X. F. and Lee, D. J. (2005), *Structure of Crack in Thermally Dried Sludge Cake*, Drying Technology, Volume 23, pp. 1555-1568.
- Tao, T., Peng, X. F. and Lee, D. J. (2005), *Thermal Drying of Wastewater Sludge: Change in Drying Area Owing to Volume Shrinkage and Crack Development*, Drying Technology, Volume 23, pp. 669-682.
- Tiwari G. N., Kumar S., Sharma P. B. and Emran Khan M. (1996), *Instantaneous Thermal Efficiency of an Active Solar Still*, Applied Thermal Engineering, Volume 16, No. 2, pp. 189-192.
- Tog˘rul, H. (2006), *Suitable Drying Model for Infrared Drying of Carrot*, Journal of Food Engineering, Volume 77, pp. 610–619.
- Tsang, K. R. and Vesilind, P. A., (1990), *Moisture Distribution in Sludges*, Water Science Technology, Volume 22, No. 12, pp. 135-142.
- Vaxelaire, J. and Puiggali, J. R. (2002), *Analysis of the Drying of Residual Sludge: From the Experiment to the Simulation of a Belt Dryer*, Drying Technology, Volume 20, Nos. (4&5), pp. 989–1008.
- Vaxelaire, J., Bongiovanni, J. M. and Puiggali, J. R. (1999). *Mechanical Dewatering and Thermal Drying of Residual Sludge*, Environmental Technology, Volume 20, pp. 29-36.
- Vaxelaire, J., Bongiovanni, J. M., Mousques, P. and Puiggali, J. R. (2000b), *Thermal Drying of Residual Sludge*, Water Research, Volume 34, No. 17, pp. 4318-4323.
- Vesilind P. A., Hartman G. C., Skene E. T. (1986), *Sludge Management & Disposal for the Practicing Engineer*, Lewis Publishers, Inc.

- Walker, J. C., Butterfield, B. G., Langrish, T. A., Harris, J. M. and Uprichard, J. M. (1993). *Primary Wood Processing*. Chapman and Hall, London, UK.
- Wallis, T. W. R. and Griffiths, J. F. (1997), *Simulated Meteorological Input for Agricultural Models*, Agricultural and Forest Meteorology, Volume 88, pp. 241-258.
- Water for life: Making it happens. (2005),
<http://www.who.int/water_sanitation_health/waterforlife.pdf>. Viewed: 14 August 2006.
- Water in the Future. (2006), Consumer's Guide to Drinking Water,
<<http://www.waterquality.crc.org.au/consumers/Consumersp16.htm>>. Viewed: 22 May 2008.
- Water Treatment Handbook (Sixth Edition). (1991), Degremont, Lavoisier Publishing, Paris, France.
- Watmuff, J. H., Charters, W. W. S., and Proctor, D. (1977), *Solar and Wind Induced External Coefficients for Solar Collectors*, COMPLES, No. 2, pp. 56.
- Welty, J. R., Wicks, C. E., and Wilson, R. E. (1984), *Fundamentals of Momentum, Heat, and Mass Transfer*, Third Edition, Wiley, New York, USA.
- Wright, D. A., Frost, J. P., Patterson¹, D. C. and Kilpatrick, D. J. (2001), *Development of a Model to predict Drying Rates of Cut Ryegrass*, Journal of Agricultural Engineering Research, Volume 79, No. 1, pp. 23-35.
- Youngman, M. J., Kulasiri, G. D., Woodhead, I. M. and Buchan, G. D. (1999), *Use of a Combined Constant Rate and Diffusion Model to Simulate Kiln-Drying of Pinus radiata Timber*, Silva Fennica, Volume 33, No. 4, pp 317-325.
- Yuan, C. and Weng, C. (2003), *Sludge Dewatering by Electrokinetic Technique: Effect of Processing Time and Potential Gradient*, Advances in Environmental Research, Volume 7, pp. 727-732.
- Zaki G. M., Rodhwan A. M. and Balbeid A. O. (1993), Analysis of Assisted Coupled Solar Stills, Solar Energy, Volume 51, No. 4, pp. 277-288.

Appendices

Sample experimental data points are shown for all experiments due to space limitation; however, complete data files are available on a CD upon request.

Appendix A: Drying Tunnel Experiments

Experiment 8					Experiment 9				
Date/Time	Residuals Temp °C	Dry Bulb Temp °C	Wet Bulb Temp °C	Moisture Weight Loss (grams)	Date/Time	Residuals Temp °C	Dry Bulb Temp °C	Wet Bulb Temp °C	Moisture Weight Loss (grams)
17/03/2004 14:18	21.8	25.6	22.2	6483	24/03/2004 12:30	24.2	24.7	21.8	6156
17/03/2004 14:24	22.3	25.6	22.3	6463	24/03/2004 12:36	26.3	24.7	21.4	6156
17/03/2004 14:30	27.3	25.4	21.5	6463	24/03/2004 12:42	28.1	25.5	20.5	6116
17/03/2004 14:36	29.3	25.8	20.5	6463	24/03/2004 12:48	27.1	25.9	20.8	6116
17/03/2004 14:42	28.5	26.2	21.3	6443	24/03/2004 12:54	26.3	26.1	21	6096
17/03/2004 14:48	27.8	26.7	21.7	6423	24/03/2004 13:00	25.6	26.3	21.2	6096
17/03/2004 14:54	27	27	22.2	6423	24/03/2004 13:06	25	26.2	21.1	6076
17/03/2004 15:00	26.5	26.9	22.2	6423	24/03/2004 13:12	24.5	26.2	21.1	6076
17/03/2004 15:06	26	27.4	22.4	6403	24/03/2004 13:18	24.2	27.1	21.4	6076
17/03/2004 15:12	25.6	28	23	6403	24/03/2004 13:24	23.7	27	21.6	6076
17/03/2004 15:18	25.3	28.7	23.6	6383	24/03/2004 13:30	23.5	26.8	21.5	6076
17/03/2004 15:24	25	28.8	23.7	6383	24/03/2004 13:36	23.3	26.8	21.6	6056
17/03/2004 15:30	24.8	28.6	23.7	6383	24/03/2004 13:42	23.1	26.7	21.4	6056
17/03/2004 15:36	24.7	28.6	23.7	6363	24/03/2004 13:48	22.7	26.5	21.3	6056
17/03/2004 15:42	24.5	28.4	23.5	6363	24/03/2004 13:54	22.5	26.6	21.3	6056
17/03/2004 15:48	24.4	28.4	23.5	6363	24/03/2004 14:00	22.4	26.4	21.2	6036

Experiment 10					Experiment 11				
Date/Time	Residuals Temp °C	Dry Bulb Temp °C	Wet Bulb Temp °C	Moisture Weight Loss (grams)	Date/Time	Residuals Temp °C	Dry Bulb Temp °C	Wet Bulb Temp °C	Moisture Weight Loss (grams)
2/04/2004 7:54	22.4	22.6	20.4	6387	27/04/2004 15:06	22.7	23	21.4	6491
2/04/2004 8:00	18	21.4	19.8	6387	27/04/2004 15:12	20.1	23.7	20.7	6491
2/04/2004 8:06	17.6	20.2	18.7	6387	27/04/2004 15:18	19.4	26.9	19.4	6471
2/04/2004 8:12	17.5	19.5	18.1	6387	27/04/2004 15:24	19.1	27.7	19.7	6471
2/04/2004 8:18	17.4	19.5	17.8	6367	27/04/2004 15:30	18.8	28.2	19.9	6471
2/04/2004 8:24	17.3	19.6	17.7	6367	27/04/2004 15:36	18.6	28.7	20.3	6471
2/04/2004 8:30	17.3	19.6	17.7	6367	27/04/2004 15:42	18.5	28.8	21.6	6431
2/04/2004 8:36	17.3	19.8	17.7	6367	27/04/2004 15:48	18.5	28.8	22.6	6431
2/04/2004 8:42	17.3	20	17.8	6347	27/04/2004 15:54	18.4	28.9	23.1	6431
2/04/2004 8:48	17.3	19.9	17.9	6347	27/04/2004 16:00	18.3	28.9	23.1	6431
2/04/2004 8:54	17.3	20.3	18	6347	27/04/2004 16:06	18.3	29	22.7	6431
2/04/2004 9:00	17.4	20.3	18.1	6347	27/04/2004 16:12	18.1	29.1	22.4	6411
2/04/2004 9:06	17.4	20.5	18.3	6347	27/04/2004 16:18	18.1	29.2	22.2	6411
2/04/2004 9:12	17.5	20.5	18.4	6347	27/04/2004 16:24	18	29.1	22.2	6411
2/04/2004 9:18	17.5	20.6	18.4	6347	27/04/2004 16:30	18	29.2	22.2	6391
2/04/2004 9:24	17.5	20.5	18.5	6347	27/04/2004 16:36	18	29.2	22.1	6391

Experiment 12					Experiment 13				
Date/Time	Residuals Temp °C	Dry Bulb Temp °C	Wet Bulb Temp °C	Moisture Weight Loss (grams)	Date/Time	Residuals Temp °C	Dry Bulb Temp °C	Wet Bulb Temp °C	Moisture Weight Loss (grams)
20/05/2004 15:30	22.2	22.6	17.4	6614	8/06/2004 13:30	20.4	21.1	18.6	6654
20/05/2004 15:36	21.9	22.9	17.6	6614	8/06/2004 13:36	20	23.1	19.9	6654
20/05/2004 15:42	20.4	22.8	17.6	6594	8/06/2004 13:42	19.3	23.7	20.5	6654
20/05/2004 15:48	19.7	24.8	18.3	6574	8/06/2004 13:48	18.7	23.9	20.7	6654
20/05/2004 15:54	19.3	27.3	19.8	6574	8/06/2004 13:54	18.5	24.1	21.1	6634
20/05/2004 16:00	18.9	28.6	20.6	6554	8/06/2004 14:00	18.3	24.3	20.6	6634
20/05/2004 16:06	19.3	31.4	22.1	6554	8/06/2004 14:06	18	24.5	20.7	6634
20/05/2004 16:12	19.6	32.4	23.3	6554	8/06/2004 14:12	17.8	24.7	21.1	6634
20/05/2004 16:18	19.7	32.2	23.6	6554	8/06/2004 14:18	17.9	25.8	22.1	6634
20/05/2004 16:24	19.3	29.8	22.5	6554	8/06/2004 14:24	18.2	26.2	22.6	6634
20/05/2004 16:30	19.6	32.6	23.4	6534	8/06/2004 14:30	18.5	26.4	23.1	6614
20/05/2004 16:36	19.7	32.7	23.7	6534	8/06/2004 14:36	18.5	26.5	23.3	6594
20/05/2004 16:42	19.5	29.7	22.9	6534	8/06/2004 14:42	18.6	26.7	23.4	6594
20/05/2004 16:48	19.5	32.3	23	6534	8/06/2004 14:48	18.6	26.8	23.4	6594
20/05/2004 16:54	19.7	32.5	23.5	6534	8/06/2004 14:54	18.6	26.8	23.5	6594
20/05/2004 17:00	19.6	31	23.2	6514	8/06/2004 15:00	18.7	26.9	23.5	6594

Experiment 14					Experiment 15				
Date/Time	Residuals Temp °C	Dry Bulb Temp °C	Wet Bulb Temp °C	Moisture Weight Loss (grams)	Date/Time	Residuals Temp °C	Dry Bulb Temp °C	Wet Bulb Temp °C	Moisture Weight Loss (grams)
28/06/2004 14:18	18.3	20.1	17.2	6885	23/07/2004 9:00	17.2	18.2	15.4	1503
28/06/2004 14:24	17.1	23.9	19.5	6885	23/07/2004 9:06	16.8	20	16.9	1503
28/06/2004 14:30	16.8	23.5	19.8	6885	23/07/2004 9:12	16.6	20.4	17.7	1503
28/06/2004 14:36	16.9	23.5	19.8	6885	23/07/2004 9:18	16.2	20.3	17.9	1503
28/06/2004 14:42	16.7	23.4	19.8	6885	23/07/2004 9:24	16	20.4	17.9	1503
28/06/2004 14:48	16.5	23.5	19.8	6885	23/07/2004 9:30	15.9	20.3	17.9	1483
28/06/2004 14:54	16.1	23.6	19.9	6885	23/07/2004 9:36	15.8	20.3	17.8	1483
28/06/2004 15:00	16	24.1	20.5	6885	23/07/2004 9:42	15.6	20.4	17.9	1483
28/06/2004 15:06	16	25.8	22.3	6885	23/07/2004 9:48	15.4	20.4	17.9	1483
28/06/2004 15:12	16.1	25.9	22.8	6885	23/07/2004 9:54	15.3	20.5	18.1	1483
28/06/2004 15:18	16.2	26.2	23.2	6865	23/07/2004 10:00	15.3	20.4	18.1	1483
28/06/2004 15:24	16.5	26.2	23.3	6865	23/07/2004 10:06	15.2	20.5	18	1483
28/06/2004 15:30	16.7	26.4	23.4	6865	23/07/2004 10:12	15.2	20.6	18.2	1483
28/06/2004 15:36	16.8	26.2	23.3	6865	23/07/2004 10:18	15.2	20.7	18.3	1483
28/06/2004 15:42	16.9	26.4	23.5	6865	23/07/2004 10:24	15.1	20.8	18.3	1483
28/06/2004 15:48	17	26.7	23.6	6865	23/07/2004 10:30	15.1	20.9	18.5	1463

Experiment 16					Experiment 17				
Date/Time	Residuals Temp °C	Dry Bulb Temp °C	Wet Bulb Temp °C	Moisture Weight Loss (grams)	Date/Time	Residuals Temp °C	Dry Bulb Temp °C	Wet Bulb Temp °C	Moisture Weight Loss (grams)
30/07/2004 12:42	19.8	21.1	19.4	1520	4/08/2004 9:06	15.2	15.5	13.7	1580
30/07/2004 12:48	16.5	22.1	18.8	1520	4/08/2004 9:12	14.5	18	14.4	1580
30/07/2004 12:54	16.2	23.1	19.3	1520	4/08/2004 9:18	13.9	18.6	15.3	1580
30/07/2004 13:00	16	23.4	19.6	1520	4/08/2004 9:24	13.5	18.9	15.4	1580
30/07/2004 13:06	16	23.4	19.6	1520	4/08/2004 9:30	13.1	18.9	15.6	1580
30/07/2004 13:12	15.8	23.5	19.7	1520	4/08/2004 9:36	12.9	19.1	15.8	1580
30/07/2004 13:18	15.7	23.7	19.8	1500	4/08/2004 9:42	12.7	19.3	15.9	1580
30/07/2004 13:24	15.5	23.7	19.9	1500	4/08/2004 9:48	12.5	19.3	16	1560
30/07/2004 13:30	15.4	23.8	20	1500	4/08/2004 9:54	12.3	19.3	16	1560
30/07/2004 13:36	15.3	23.7	20.1	1500	4/08/2004 10:00	12.2	19.6	16.1	1560
30/07/2004 13:42	15.3	23.8	20.1	1500	4/08/2004 10:06	12.1	19.7	16.2	1560
30/07/2004 13:48	15.2	23.9	20.3	1480	4/08/2004 10:12	12.1	19.8	16.2	1540
30/07/2004 13:54	15.2	24	20.3	1480	4/08/2004 10:18	12.1	19.7	16.2	1540
30/07/2004 14:00	15.2	24.2	20.4	1480	4/08/2004 10:24	12.1	19.8	16.2	1540
30/07/2004 14:06	15.2	24.2	20.5	1480	4/08/2004 10:30	12	19.6	16.1	1540
30/07/2004 14:12	15.2	24.2	20.5	1480	4/08/2004 10:36	12	19.6	16.1	1540

Experiment 18					Experiment 19				
Date/Time	Residuals Temp °C	Dry Bulb Temp °C	Wet Bulb Temp °C	Moisture Weight Loss (grams)	Date/Time	Residuals Temp °C	Dry Bulb Temp °C	Wet Bulb Temp °C	Moisture Weight Loss (grams)
6/08/2004 8:30	16	16.5	14.8	1544	9/08/2004 8:54	17.1	17.6	15.4	1621
6/08/2004 8:36	11.5	17.5	14.7	1544	9/08/2004 9:00	17	17.6	15.4	1621
6/08/2004 8:42	9.5	18.6	15.3	1544	9/08/2004 9:06	17	17.5	15.4	1621
6/08/2004 8:48	9.9	18.8	15.4	1524	9/08/2004 9:12	17	17.5	15.4	1621
6/08/2004 8:54	10	18.8	15.4	1524	9/08/2004 9:18	17	17.5	15.4	1621
6/08/2004 9:00	10.1	18.8	15.5	1524	9/08/2004 9:24	17	17.4	15.4	1601
6/08/2004 9:06	10.4	18.9	15.5	1524	9/08/2004 9:30	17	17.5	15.4	1601
6/08/2004 9:12	10.6	19	15.7	1524	9/08/2004 9:36	17	17.5	15.4	1601
6/08/2004 9:18	10.7	19.2	15.9	1524	9/08/2004 9:42	17.4	17.6	15.4	1581
6/08/2004 9:24	10.7	19.2	16	1504	9/08/2004 9:48	17.2	19	15.7	1581
6/08/2004 9:30	10.8	19.4	16	1504	9/08/2004 9:54	16.4	20.2	16.5	1581
6/08/2004 9:36	10.9	19.4	16	1504	9/08/2004 10:00	15.7	20.4	16.9	1581
6/08/2004 9:42	11.1	19.4	16	1504	9/08/2004 10:06	15.2	20.5	17	1581
6/08/2004 9:48	11.2	19.5	16.1	1484	9/08/2004 10:12	14.8	20.6	17	1581
6/08/2004 9:54	11.2	19.5	16.2	1484	9/08/2004 10:18	14.4	20.8	17.1	1561
6/08/2004 10:00	11.3	19.7	16.3	1484	9/08/2004 10:24	14.2	21	17.3	1561

Experiment 20					Experiment 21				
Date/Time	Residuals Temp °C	Dry Bulb Temp °C	Wet Bulb Temp °C	Moisture Weight Loss (grams)	Date/Time	Residuals Temp °C	Dry Bulb Temp °C	Wet Bulb Temp °C	Moisture Weight Loss (grams)
11/08/2004 12:00	17.4	18.1	16.1	1593	12/08/2004 11:36	18.1	19.3	16.9	4007
11/08/2004 12:06	16	21.6	17.4	1593	12/08/2004 11:42	16.6	22.3	18.2	3987
11/08/2004 12:12	15.7	23.1	19.1	1533	12/08/2004 11:48	15.9	24	19.8	3987
11/08/2004 12:18	15.3	23.6	19.6	1513	12/08/2004 11:54	15.3	24.5	20.4	3987
11/08/2004 12:24	15.1	23.9	20	1493	12/08/2004 12:00	15.1	24.6	20.5	3987
11/08/2004 12:30	14.9	24.2	20.4	1473	12/08/2004 12:06	14.9	24.9	20.6	3967
11/08/2004 12:36	14.6	24.6	20.5	1473	12/08/2004 12:12	14.5	25	20.6	3967
11/08/2004 12:42	14.5	24.7	20.6	1433	12/08/2004 12:18	14.5	25.1	21	3967
11/08/2004 12:48	14.5	24.9	20.9	1433	12/08/2004 12:24	14.4	25.3	21.2	3967
11/08/2004 12:54	14.5	25	21.2	1433	12/08/2004 12:30	14.4	25.4	21.3	3947
11/08/2004 13:00	14.5	25.3	21.3	1413	12/08/2004 12:36	14.4	25.4	21.3	3927
11/08/2004 13:06	14.5	25.4	21.4	1393	12/08/2004 12:42	14.3	25.4	21.3	3907
11/08/2004 13:12	14.5	25.4	21.4	1393	12/08/2004 12:48	14.3	25.6	21.3	3907
11/08/2004 13:18	14.5	25.6	21.5	1393	12/08/2004 12:54	14.3	25.7	21.4	3907
11/08/2004 13:24	14.5	25.8	21.5	1373	12/08/2004 13:00	14.3	25.6	21.4	3907
11/08/2004 13:30	14.6	26.1	21.8	1373	12/08/2004 13:06	14.3	25.8	21.5	3887

Experiment 22					Experiment 23				
Date/Time	Residuals Temp °C	Dry Bulb Temp °C	Wet Bulb Temp °C	Moisture Weight Loss (grams)	Date/Time	Residuals Temp °C	Dry Bulb Temp °C	Wet Bulb Temp °C	Moisture Weight Loss (grams)
16/08/2004 11:18	16.2	16.6	14.6	2709	18/08/2004 11:36	17.4	18.6	16.2	2831
16/08/2004 11:24	16	16.7	14.8	2669	18/08/2004 11:42	16.4	20	16.3	2831
16/08/2004 11:30	11.4	20.4	16.7	2649	18/08/2004 11:48	15.9	20.2	16.7	2831
16/08/2004 11:36	11.8	22.1	18.5	2649	18/08/2004 11:54	15.4	20.3	16.8	2811
16/08/2004 11:42	12.1	22.8	18.9	2629	18/08/2004 12:00	15.2	20.3	16.8	2811
16/08/2004 11:48	12.2	23.3	19.3	2629	18/08/2004 12:06	15.1	20.3	16.9	2811
16/08/2004 11:54	12.5	23.8	19.5	2629	18/08/2004 12:12	15	20.3	17	2791
16/08/2004 12:00	12.8	24	19.7	2609	18/08/2004 12:18	14.9	20.5	17	2791
16/08/2004 12:06	12.9	24.3	20.1	2609	18/08/2004 12:24	14.7	20.7	17	2791
16/08/2004 12:12	13	24.5	20.3	2589	18/08/2004 12:30	14.6	20.7	17.1	2771
16/08/2004 12:18	13.3	24.7	20.3	2589	18/08/2004 12:36	14.6	20.8	17.2	2771
16/08/2004 12:24	13.5	25	20.3	2569	18/08/2004 12:42	14.5	21	17.3	2771
16/08/2004 12:30	13.6	25.2	20.4	2569	18/08/2004 12:48	14.5	21	17.4	2771
16/08/2004 12:36	13.7	25.3	20.4	2549	18/08/2004 12:54	14.5	21	17.5	2751
16/08/2004 12:42	13.8	25.4	20.4	2549	18/08/2004 13:00	14.5	21	17.5	2751
16/08/2004 12:48	14.1	25.6	20.4	2549	18/08/2004 13:06	14.4	21.1	17.5	2751

Experiment 24					Experiment 25				
Date/Time	Residuals Temp °C	Dry Bulb Temp °C	Wet Bulb Temp °C	Moisture Weight Loss (grams)	Date/Time	Residuals Temp °C	Dry Bulb Temp °C	Wet Bulb Temp °C	Moisture Weight Loss (grams)
21/08/2004 8:48	17.9	18.2	15.9	2872	23/08/2004 13:00	20.1	22.4	20.5	2849
21/08/2004 8:54	17.9	18.3	15.9	2872	23/08/2004 13:06	18.4	25.5	20.8	2829
21/08/2004 9:00	17.9	18.3	15.9	2872	23/08/2004 13:12	18.2	26	21.4	2829
21/08/2004 9:06	17.8	19.7	15.8	2852	23/08/2004 13:18	18	26.4	21.7	2829
21/08/2004 9:12	17.3	20.8	16.4	2832	23/08/2004 13:24	17.8	26.4	21.8	2829
21/08/2004 9:18	16.8	21.2	16.9	2832	23/08/2004 13:30	17.8	26.6	22	2829
21/08/2004 9:24	16.3	21.5	17.1	2832	23/08/2004 13:36	17.7	26.7	22.1	2809
21/08/2004 9:30	16	21.7	17.5	2812	23/08/2004 13:42	17.6	26.9	22.2	2809
21/08/2004 9:36	15.7	22.1	17.6	2812	23/08/2004 13:48	17.6	27	22.3	2789
21/08/2004 9:42	15.4	22.1	17.8	2812	23/08/2004 13:54	17.6	27.1	22.4	2789
21/08/2004 9:48	15.3	22.2	17.9	2812	23/08/2004 14:00	17.5	27.1	22.4	2789
21/08/2004 9:54	15.1	22.1	17.9	2812	23/08/2004 14:06	17.6	27.2	22.5	2769
21/08/2004 10:00	15	22.3	18	2792	23/08/2004 14:12	17.5	27.4	22.6	2769
21/08/2004 10:06	14.8	22.4	18	2792	23/08/2004 14:18	17.6	27.5	22.7	2769
21/08/2004 10:12	14.5	22.6	18.2	2772	23/08/2004 14:24	17.5	27.6	22.9	2769
21/08/2004 10:18	14.5	22.6	18.3	2772	23/08/2004 14:30	17.5	27.6	23.1	2769

Experiment 26					Experiment 27				
Date/Time	Residuals Temp °C	Dry Bulb Temp °C	Wet Bulb Temp °C	Moisture Weight Loss (grams)	Date/Time	Residuals Temp °C	Dry Bulb Temp °C	Wet Bulb Temp °C	Moisture Weight Loss (grams)
27/08/2004 12:30	23.8	25.6	22.6	2738	2/09/2004 9:06	17.6	18.6	16.3	2744
27/08/2004 12:36	21	27.9	22.8	2718	2/09/2004 9:12	18.3	18.7	16.3	2744
27/08/2004 12:42	20.5	29.4	23.6	2718	2/09/2004 9:18	18.3	18.6	16.3	2744
27/08/2004 12:48	20.3	29.7	24	2718	2/09/2004 9:24	18.3	18.6	16.4	2744
27/08/2004 12:54	20	29.7	24.2	2718	2/09/2004 9:30	18.4	18.7	16.4	2744
27/08/2004 13:00	19.7	29.9	24.3	2698	2/09/2004 9:36	18.4	18.7	16.3	2724
27/08/2004 13:06	19.6	30	24.4	2698	2/09/2004 9:42	18.5	18.8	16.3	2724
27/08/2004 13:12	19.5	30.1	24.4	2698	2/09/2004 9:48	18.5	18.8	16.4	2724
27/08/2004 13:18	19.3	30	24.4	2698	2/09/2004 9:54	18.5	18.8	16.5	2724
27/08/2004 13:24	19.3	30.2	24.5	2698	2/09/2004 10:00	18.6	18.9	16.5	2724
27/08/2004 13:30	19.2	30.2	24.6	2698	2/09/2004 10:06	18.6	19	16.6	2704
27/08/2004 13:36	19	30.2	24.5	2698	2/09/2004 10:12	18.7	19	16.7	2704
27/08/2004 13:42	18.8	30.2	24.5	2698	2/09/2004 10:18	18.7	19.1	16.8	2704
27/08/2004 13:48	18.8	30.2	24.5	2698	2/09/2004 10:24	18.8	19.1	16.8	2704
27/08/2004 13:54	18.7	30.1	24.5	2678	2/09/2004 10:30	18.8	19.2	16.8	2704
27/08/2004 14:00	18.7	30.2	24.5	2678	2/09/2004 10:36	18.9	19.2	16.9	2704

Experiment 28					Experiment 29				
Date/Time	Residuals Temp °C	Dry Bulb Temp °C	Wet Bulb Temp °C	Moisture Weight Loss (grams)	Date/Time	Residuals Temp °C	Dry Bulb Temp °C	Wet Bulb Temp °C	Moisture Weight Loss (grams)
13/09/2004 11:30	19.1	19.3	17	4093	27/09/2004 11:12	20	21.9	19.6	3998
13/09/2004 11:36	19.5	23.9	18.8	4093	27/09/2004 11:18	18.5	21.9	19.4	3998
13/09/2004 11:42	19	24.8	20.1	4093	27/09/2004 11:24	18.3	22	19.6	3978
13/09/2004 11:48	18.6	25.1	20.8	4093	27/09/2004 11:30	18.1	22.1	19.6	3978
13/09/2004 11:54	18.4	25.1	21.3	4073	27/09/2004 11:36	17.9	22.3	19.7	3978
13/09/2004 12:00	18.1	25.1	21.3	4073	27/09/2004 11:42	17.8	22.4	19.8	3958
13/09/2004 12:06	17.8	25.3	21.4	4073	27/09/2004 11:48	17.8	22.5	20	3958
13/09/2004 12:12	17.7	25.3	21.5	4053	27/09/2004 11:54	17.8	22.6	20.1	3958
13/09/2004 12:18	17.6	25.3	21.5	4053	27/09/2004 12:00	17.7	22.7	20.3	3958
13/09/2004 12:24	17.5	25.3	21.5	4053	27/09/2004 12:06	17.8	22.8	20.3	3958
13/09/2004 12:30	17.3	25.6	21.6	4053	27/09/2004 12:12	17.7	22.9	20.3	3958
13/09/2004 12:36	17.1	25.8	21.8	4053	27/09/2004 12:18	17.7	23	20.4	3958
13/09/2004 12:42	17	25.5	21.7	4053	27/09/2004 12:24	17.7	23	20.4	3958
13/09/2004 12:48	17	25.7	21.9	4053	27/09/2004 12:30	17.7	23	20.4	3958
13/09/2004 12:54	16.9	26	22.2	4053	27/09/2004 12:36	17.7	23.2	20.4	3958
13/09/2004 13:00	16.8	26.3	22.3	4053	27/09/2004 12:42	17.6	23.2	20.5	3938

Experiment 30					Experiment 31				
Date/Time	Residuals Temp °C	Dry Bulb Temp °C	Wet Bulb Temp °C	Moisture Weight Loss (grams)	Date/Time	Residuals Temp °C	Dry Bulb Temp °C	Wet Bulb Temp °C	Moisture Weight Loss (grams)
7/10/2004 10:18	21.6	23.6	20.3	4353	12/10/2004 11:06	25.7	26.4	24	4451
7/10/2004 10:24	20.6	25.7	21.5	4353	12/10/2004 11:12	25.7	26.4	23.2	4431
7/10/2004 10:30	19.8	26.1	22.2	4353	12/10/2004 11:18	25.1	26.6	22.4	4431
7/10/2004 10:36	19.4	26.3	22.3	4353	12/10/2004 11:24	24.1	26.8	22.6	4431
7/10/2004 10:42	19	26.6	22.4	4353	12/10/2004 11:30	23.3	26.9	22.8	4411
7/10/2004 10:48	18.7	26.7	22.8	4353	12/10/2004 11:36	22.6	27.1	23	4391
7/10/2004 10:54	18.6	27	22.8	4333	12/10/2004 11:42	22.1	27.1	23.1	4391
7/10/2004 11:00	18.5	27.2	23	4333	12/10/2004 11:48	21.7	27.2	23.2	4391
7/10/2004 11:06	18.4	27.4	23.2	4333	12/10/2004 11:54	21.3	27.3	23.2	4391
7/10/2004 11:12	18.4	27.5	23.3	4333	12/10/2004 12:00	21.1	27.4	23.2	4371
7/10/2004 11:18	18.4	27.6	23.3	4313	12/10/2004 12:06	20.7	27.4	23.3	4371
7/10/2004 11:24	18.3	27.7	23.2	4313	12/10/2004 12:12	20.6	27.5	23.3	4351
7/10/2004 11:30	18.4	27.7	23.5	4313	12/10/2004 12:18	20.4	27.6	23.4	4351
7/10/2004 11:36	18.4	27.8	23.6	4313	12/10/2004 12:24	20.2	27.7	23.5	4331
7/10/2004 11:42	18.4	27.9	24	4313	12/10/2004 12:30	20.1	27.8	23.6	4331
7/10/2004 11:48	18.4	28	24.2	4313	12/10/2004 12:36	19.9	27.8	23.6	4311

Experiment 32					Experiment 33				
Date/Time	Residuals Temp °C	Dry Bulb Temp °C	Wet Bulb Temp °C	Moisture Weight Loss (grams)	Date/Time	Residuals Temp °C	Dry Bulb Temp °C	Wet Bulb Temp °C	Moisture Weight Loss (grams)
15/10/2004 10:00	22.4	23	19.6	4255	18/10/2004 11:36	19.6	24.8	21.2	4312
15/10/2004 10:06	20.9	23.2	19.5	4255	18/10/2004 11:42	19.5	27.2	22.7	4312
15/10/2004 10:12	19.6	23.5	19.6	4255	18/10/2004 11:48	19.5	27.6	23.5	4312
15/10/2004 10:18	18.8	23.5	19.7	4235	18/10/2004 11:54	19.4	27.7	23.8	4312
15/10/2004 10:24	18.2	23.7	19.7	4235	18/10/2004 12:00	19.3	27.8	24.1	4312
15/10/2004 10:30	17.8	23.7	19.8	4235	18/10/2004 12:06	19.3	27.8	24.3	4312
15/10/2004 10:36	17.5	23.8	19.9	4235	18/10/2004 12:12	19.2	27.8	24.3	4312
15/10/2004 10:42	17.2	23.9	20	4215	18/10/2004 12:18	19.1	28	24.3	4292
15/10/2004 10:48	16.9	23.8	19.9	4215	18/10/2004 12:24	19	27.9	24.4	4292
15/10/2004 10:54	16.8	23.8	19.9	4215	18/10/2004 12:30	18.9	27.9	24.4	4292
15/10/2004 11:00	16.6	23.9	19.9	4195	18/10/2004 12:36	18.8	28	24.4	4292
15/10/2004 11:06	16.4	23.9	20.1	4195	18/10/2004 12:42	18.8	27.8	24.3	4292
15/10/2004 11:12	16.2	23.9	20.2	4175	18/10/2004 12:48	18.8	27.9	24.4	4292
15/10/2004 11:18	16.1	24	20.3	4175	18/10/2004 12:54	18.7	27.8	24.3	4292
15/10/2004 11:24	16	24	20.3	4155	18/10/2004 13:00	18.7	27.9	24.3	4292
15/10/2004 11:30	16	24.2	20.4	4135	18/10/2004 13:06	18.7	27.9	24.3	4292

Experiment 34					Experiment 35				
Date/Time	Residuals Temp °C	Dry Bulb Temp °C	Wet Bulb Temp °C	Moisture Weight Loss (grams)	Date/Time	Residuals Temp °C	Dry Bulb Temp °C	Wet Bulb Temp °C	Moisture Weight Loss (grams)
3/11/2004 15:24	23.2	22.8	19.6	875	7/11/2004 10:42	21.5	22.4	19.7	1022
3/11/2004 15:30	22.4	22.8	19.4	875	7/11/2004 10:48	20.3	22.6	19.6	1022
3/11/2004 15:36	21.1	22.9	19.5	875	7/11/2004 10:54	19.5	22.6	19.6	1002
3/11/2004 15:42	19.9	22.9	19.5	875	7/11/2004 11:00	18.9	22.8	19.7	1002
3/11/2004 15:48	19	23.1	19.6	875	7/11/2004 11:06	18.3	22.9	19.8	1002
3/11/2004 15:54	18.2	23.1	19.6	855	7/11/2004 11:12	17.8	23	19.9	982
3/11/2004 16:00	17.6	23.1	19.7	855	7/11/2004 11:18	17.6	23	20.1	982
3/11/2004 16:06	17	23.3	19.7	835	7/11/2004 11:24	17.2	23.2	20.3	982
3/11/2004 16:12	16.6	23.3	19.8	835	7/11/2004 11:30	17.2	23.2	20.3	982
3/11/2004 16:18	16.3	23.3	19.8	835	7/11/2004 11:36	17.4	23.4	20.4	982
3/11/2004 16:24	16	23.3	19.8	835	7/11/2004 11:42	17.4	23.4	20.4	982
3/11/2004 16:30	15.8	23.5	19.9	835	7/11/2004 11:48	17.6	23.6	20.5	982
3/11/2004 16:36	15.6	23.4	19.9	835	7/11/2004 11:54	17.6	23.6	20.5	982
3/11/2004 16:42	15.4	23.5	20	835	7/11/2004 12:00	17.6	23.6	20.5	982
3/11/2004 16:48	15.3	23.5	20.1	835	7/11/2004 12:06	17.7	23.7	20.6	982
3/11/2004 16:54	15.3	23.6	20.2	835	7/11/2004 12:12	17.7	23.7	20.6	962

Experiment 36					Experiment 37				
Date/Time	Residuals Temp °C	Dry Bulb Temp °C	Wet Bulb Temp °C	Moisture Weight Loss (grams)	Date/Time	Residuals Temp °C	Dry Bulb Temp °C	Wet Bulb Temp °C	Moisture Weight Loss (grams)
10/11/2004 9:00	19.3	19.6	17.8	1011	12/11/2004 13:06	20.4	24	21.4	1030
10/11/2004 9:06	18.9	19.6	17.8	1011	12/11/2004 13:12	19.6	24	21.4	1030
10/11/2004 9:12	18.3	19.7	17.8	1011	12/11/2004 13:18	19	24.1	21.4	1030
10/11/2004 9:18	17.7	19.8	17.9	991	12/11/2004 13:24	18.6	24.2	21.5	1010
10/11/2004 9:24	17.3	19.9	18	991	12/11/2004 13:30	18.4	24.3	21.5	1010
10/11/2004 9:30	17	19.9	18	991	12/11/2004 13:36	18.2	24.3	21.5	1010
10/11/2004 9:36	16.8	20	18.1	991	12/11/2004 13:42	18	24.3	21.6	1010
10/11/2004 9:42	16.6	20.1	18.2	971	12/11/2004 13:48	17.9	24.4	21.6	990
10/11/2004 9:48	16.5	20.3	18.5	971	12/11/2004 13:54	18	24.5	21.6	990
10/11/2004 9:54	16.5	20.3	18.6	971	12/11/2004 14:00	18	24.5	21.7	990
10/11/2004 10:00	16.4	20.5	18.6	971	12/11/2004 14:06	18.2	24.7	21.8	990
10/11/2004 10:06	16.3	20.6	18.6	971	12/11/2004 14:12	18.2	24.7	21.9	990
10/11/2004 10:12	16.3	20.7	18.7	971	12/11/2004 14:18	18.3	24.8	22	990
10/11/2004 10:18	16.3	20.8	18.7	971	12/11/2004 14:24	18.3	24.8	22	990
10/11/2004 10:24	16.3	20.8	18.8	971	12/11/2004 14:30	18.5	25	22.1	970
10/11/2004 10:30	16.3	20.9	18.8	971	12/11/2004 14:36	18.5	25	22.2	970

Experiment 38					Experiment 39				
Date/Time	Residuals Temp °C	Dry Bulb Temp °C	Wet Bulb Temp °C	Moisture Weight Loss (grams)	Date/Time	Residuals Temp °C	Dry Bulb Temp °C	Wet Bulb Temp °C	Moisture Weight Loss (grams)
15/11/2004 8:48	20.8	21.9	18.8	1042	31/08/2005 12:42	18.6	23.9	23.9	992
15/11/2004 8:54	19.6	22.1	19.1	1042	31/08/2005 12:48	18.5	23.9	24	992
15/11/2004 9:00	18.3	22.3	19.3	1042	31/08/2005 12:54	17.2	23.4	21.5	992
15/11/2004 9:06	17.3	22.4	19.4	1042	31/08/2005 13:00	18.3	23.6	18.9	992
15/11/2004 9:12	16.6	22.4	19.5	1042	31/08/2005 13:06	18.3	23.5	19.2	992
15/11/2004 9:18	16.1	22.5	19.5	1042	31/08/2005 13:12	17.2	23.2	19.3	992
15/11/2004 9:24	15.8	22.6	19.6	1022	31/08/2005 13:18	18.4	23.5	19.3	992
15/11/2004 9:30	15.5	22.7	19.6	1022	31/08/2005 13:24	17.3	23.3	19.4	992
15/11/2004 9:36	15.4	22.7	19.7	1022	31/08/2005 13:30	18.2	23.5	19.4	972
15/11/2004 9:42	15.3	22.8	19.7	1022	31/08/2005 13:36	17.8	23.2	19.5	972
15/11/2004 9:48	15.2	22.8	19.8	1022	31/08/2005 13:42	17	23	19.5	972
15/11/2004 9:54	15.2	22.9	19.8	1002	31/08/2005 13:48	17.8	23.1	19.3	972
15/11/2004 10:00	15.1	23	19.8	1002	31/08/2005 13:54	18.3	23.6	19.4	972
15/11/2004 10:06	15.1	23.1	19.9	1002	31/08/2005 14:00	17.5	23.2	19.5	972
15/11/2004 10:12	15.1	23.1	19.9	1002	31/08/2005 14:06	17.9	23.4	19.4	972
15/11/2004 10:18	15.1	23.1	20	1002	31/08/2005 14:12	18.3	23.5	19.5	972

Experiment 40					Experiment 41				
Date/Time	Residuals Temp °C	Dry Bulb Temp °C	Wet Bulb Temp °C	Moisture Weight Loss (grams)	Date/Time	Residuals Temp °C	Dry Bulb Temp °C	Wet Bulb Temp °C	Moisture Weight Loss (grams)
6/09/2005 12:00	13.6	17.9	19.2	861	27/09/2005 12:00	22.1	24.5	24	4240
6/09/2005 12:06	13.6	18.1	18.1	861	27/09/2005 12:06	21	24.1	20.6	4220
6/09/2005 12:12	13.7	18.2	17.2	861	27/09/2005 12:12	21.3	24.3	20.9	4220
6/09/2005 12:18	13.8	18.3	16.5	841	27/09/2005 12:18	21.8	24.5	21.3	4200
6/09/2005 12:24	13.8	18.4	16	821	27/09/2005 12:24	21.7	24.6	21.7	4200
6/09/2005 12:30	13.8	18.4	15.6	821	27/09/2005 12:30	20.8	24.1	21.8	4200
6/09/2005 12:36	13.9	18.5	15.3	821	27/09/2005 12:36	21.8	24.6	22	4200
6/09/2005 12:42	13.9	18.5	15.1	781	27/09/2005 12:42	21.8	24.7	22.2	4180
6/09/2005 12:48	14	18.6	15	781	27/09/2005 12:48	20.8	24.3	22.3	4180
6/09/2005 12:54	14	18.8	14.9	781	27/09/2005 12:54	21.6	24.7	22.3	4180
6/09/2005 13:00	14.1	18.8	14.8	781	27/09/2005 13:00	21.4	24.7	22.4	4180
6/09/2005 13:06	14.2	18.9	14.8	781	27/09/2005 13:06	20.5	24.1	22.2	4180
6/09/2005 13:12	14.2	19	14.7	781	27/09/2005 13:12	21.6	24.8	22.2	4180
6/09/2005 13:18	14.3	19	14.8	761	27/09/2005 13:18	21.4	24.8	22.3	4180
6/09/2005 13:24	14.3	19.1	14.7	761	27/09/2005 13:24	20.3	24.2	22.2	4180
6/09/2005 13:30	14.4	19.1	14.8	761	27/09/2005 13:30	21.4	24.8	22.2	4180

Experiment 42					Experiment 43				
Date/Time	Residuals Temp °C	Dry Bulb Temp °C	Wet Bulb Temp °C	Moisture Weight Loss (grams)	Date/Time	Residuals Temp °C	Dry Bulb Temp °C	Wet Bulb Temp °C	Moisture Weight Loss (grams)
4/10/2005 15:00	18.7	24.1	21.9	4220	10/10/2005 14:54	18.5	30.6	29.9	4140
4/10/2005 15:06	22	25.6	21.6	4220	10/10/2005 15:00	18.6	30.9	27.9	4140
4/10/2005 15:12	22.4	25.9	22.3	4220	10/10/2005 15:06	18.8	31.1	25.6	4140
4/10/2005 15:18	23	26	23	4220	10/10/2005 15:12	19.1	31.4	24.4	4100
4/10/2005 15:24	23.4	26.1	23.5	4220	10/10/2005 15:18	21	32.4	23.9	4080
4/10/2005 15:30	23.5	26.1	24	4220	10/10/2005 15:24	22.1	33.1	24.1	4060
4/10/2005 15:36	23.2	25.9	24	4220	10/10/2005 15:30	22.4	33.3	24.3	4060
4/10/2005 15:42	23.8	26.1	24.3	4220	10/10/2005 15:36	22.6	33.5	24.5	4060
4/10/2005 15:48	23.4	26	24.5	4220	10/10/2005 15:42	22.7	33.6	24.7	4040
4/10/2005 15:54	23.7	25.9	24.5	4220	10/10/2005 15:48	22.9	33.6	24.9	4040
4/10/2005 16:00	23.8	26	24.8	4220	10/10/2005 15:54	23	33.7	25	4040
4/10/2005 16:06	23.7	25.9	24.8	4220	10/10/2005 16:00	22	33.5	25	4040
4/10/2005 16:12	24	26	24.9	4220	10/10/2005 16:06	23	33.8	24.9	4040
4/10/2005 16:18	23.9	25.9	24.9	4220	10/10/2005 16:12	22.9	33.8	25.1	4040
4/10/2005 16:24	23.8	25.9	25	4220	10/10/2005 16:18	22.7	33.7	25	4040
4/10/2005 16:30	24.1	25.9	25	4220	10/10/2005 16:24	22.9	33.8	25.1	4040

Experiment 44					Experiment 45				
Date/Time	Residuals Temp °C	Dry Bulb Temp °C	Wet Bulb Temp °C	Moisture Weight Loss (grams)	Date/Time	Residuals Temp °C	Dry Bulb Temp °C	Wet Bulb Temp °C	Moisture Weight Loss (grams)
12/10/2005 13:00	19.2	29.1	29.1	4220	17/10/2005 14:30	19.4	27.9	26.6	4240
12/10/2005 13:06	19.5	30	22.6	4220	17/10/2005 14:36	19.8	28.2	24.5	4240
12/10/2005 13:12	20.7	30.6	20.5	4200	17/10/2005 14:42	22.2	29.6	24.2	4220
12/10/2005 13:18	24.3	32.1	21.6	4200	17/10/2005 14:48	22.7	29.9	24.3	4200
12/10/2005 13:24	24.7	32.3	22.7	4200	17/10/2005 14:54	23.1	30.1	24.4	4180
12/10/2005 13:30	25.1	32.4	23.6	4180	17/10/2005 15:00	23.5	30.2	24.6	4180
12/10/2005 13:36	25.4	32.6	24.4	4180	17/10/2005 15:06	23.8	30.3	24.8	4180
12/10/2005 13:42	24.6	32.4	24.9	4180	17/10/2005 15:12	23.5	30.2	24.8	4160
12/10/2005 13:48	25.1	32.4	25.3	4180	17/10/2005 15:18	23.6	30.3	24.9	4160
12/10/2005 13:54	24.2	32	25.5	4180	17/10/2005 15:24	23.9	30.4	25	4160
12/10/2005 14:00	24.6	32.2	25.6	4180	17/10/2005 15:30	23.7	30.3	25.1	4160
12/10/2005 14:06	24.6	32.2	25.8	4180	17/10/2005 15:36	24.1	30.5	25.1	4160
12/10/2005 14:12	24.7	32.2	26	4160	17/10/2005 15:42	24.3	30.6	25.3	4160
12/10/2005 14:18	24.8	32.2	26.1	4160	17/10/2005 15:48	24.1	30.6	25.4	4140
12/10/2005 14:24	24.6	32.2	26.2	4160	17/10/2005 15:54	24.2	30.6	25.4	4140
12/10/2005 14:30	24.6	32.1	26.2	4160	17/10/2005 16:00	24	30.5	25.5	4140

Experiment 46					Experiment 47				
Date/Time	Residuals Temp °C	Dry Bulb Temp °C	Wet Bulb Temp °C	Moisture Weight Loss (grams)	Date/Time	Residuals Temp °C	Dry Bulb Temp °C	Wet Bulb Temp °C	Moisture Weight Loss (grams)
19/10/2005 13:30	20	28.1	25.4	4300	24/10/2005 11:54	20.2	23.5	23	4280
19/10/2005 13:36	20	28.6	22.6	4300	24/10/2005 12:00	20.4	23.7	22.1	4280
19/10/2005 13:42	20.1	28.8	22.3	4300	24/10/2005 12:06	20.5	23.9	21.8	4260
19/10/2005 13:48	20.2	29	22	4220	24/10/2005 12:12	20.7	24.1	21.6	4260
19/10/2005 13:54	20	28.2	21.8	4220	24/10/2005 12:18	21	24.2	21.5	4260
19/10/2005 14:00	18.8	25	21.1	4200	24/10/2005 12:24	21.5	24.5	21.6	4260
19/10/2005 14:06	18.7	24.8	20.7	4200	24/10/2005 12:30	22.3	25.1	21.9	4260
19/10/2005 14:12	19.2	25.1	20.5	4200	24/10/2005 12:36	22.6	25.3	22.2	4240
19/10/2005 14:18	20	25.9	20.6	4200	24/10/2005 12:42	22.9	25.3	22.6	4240
19/10/2005 14:24	20.1	25.9	20.7	4200	24/10/2005 12:48	23.2	25.4	22.8	4240
19/10/2005 14:30	20.1	26	20.8	4180	24/10/2005 12:54	23.3	25.3	23.1	4220
19/10/2005 14:36	20.2	26	20.9	4180	24/10/2005 13:00	23.4	25.4	23.3	4220
19/10/2005 14:42	20.3	25.9	20.9	4180	24/10/2005 13:06	23.3	25.2	23.4	4220
19/10/2005 14:48	20.4	25.9	21	4180	24/10/2005 13:12	23	24.9	23.4	4220
19/10/2005 14:54	20	25.6	21	4180	24/10/2005 13:18	23	25.2	23.3	4220
19/10/2005 15:00	20.3	25.8	21	4180	24/10/2005 13:24	23	25.2	23.3	4220

Experiment 48					Experiment 49				
Date/Time	Residuals Temp °C	Dry Bulb Temp °C	Wet Bulb Temp °C	Moisture Weight Loss (grams)	Date/Time	Residuals Temp °C	Dry Bulb Temp °C	Wet Bulb Temp °C	Moisture Weight Loss (grams)
26/10/2005 14:54	18.5	27.2	26.8	4200	1/11/2005 14:48	21.7	25.8	25.2	6360
26/10/2005 15:00	19	29.8	25.9	4200	1/11/2005 14:54	22.9	26.7	23.6	6360
26/10/2005 15:06	19.6	31.2	24.2	4200	1/11/2005 15:00	24.3	27.6	23.9	6360
26/10/2005 15:12	20	31.6	23.5	4160	1/11/2005 15:06	24.7	27.8	24.2	6320
26/10/2005 15:18	20.8	32.3	23.2	4160	1/11/2005 15:12	24.8	27.9	24.5	6300
26/10/2005 15:24	21.1	32.8	23.1	4140	1/11/2005 15:18	24.8	28	24.7	6300
26/10/2005 15:30	21.3	33	23.2	4140	1/11/2005 15:24	24.6	28.1	24.9	6300
26/10/2005 15:36	21.5	33.2	23.2	4140	1/11/2005 15:30	24.6	28.1	25	6300
26/10/2005 15:42	21.4	33.3	23.2	4120	1/11/2005 15:36	24.3	28	25.1	6300
26/10/2005 15:48	21.6	33.4	23.3	4120	1/11/2005 15:42	24.2	27.9	25	6300
26/10/2005 15:54	21.6	33.3	23.4	4120	1/11/2005 15:48	24.5	28.1	25.1	6300
26/10/2005 16:00	21.5	33.2	23.4	4120	1/11/2005 15:54	24.8	28.2	25.3	6300
26/10/2005 16:06	21.6	33.5	23.4	4100	1/11/2005 16:00	25	28.3	25.4	6280
26/10/2005 16:12	21.9	33.7	23.5	4100	1/11/2005 16:06	24.5	28.1	25.5	6280
26/10/2005 16:18	22.4	33.8	23.9	4100	1/11/2005 16:12	24.8	28.3	25.5	6280
26/10/2005 16:24	22.3	33.7	24.2	4080	1/11/2005 16:18	25	28.3	25.6	6280

Experiment 50					Experiment 51				
Date/Time	Residuals Temp °C	Dry Bulb Temp °C	Wet Bulb Temp °C	Moisture Weight Loss (grams)	Date/Time	Residuals Temp °C	Dry Bulb Temp °C	Wet Bulb Temp °C	Moisture Weight Loss (grams)
15/11/2005 10:06	21.5	29.9	25.4	6020	18/11/2005 10:24	16.1	22.7	22.5	6120
15/11/2005 10:12	22	30.6	22.2	6020	18/11/2005 10:30	16.2	22.9	21.1	6120
15/11/2005 10:18	22.2	30.9	21.9	6020	18/11/2005 10:36	16.3	23.2	20.3	6120
15/11/2005 10:24	22.3	31	22	6020	18/11/2005 10:42	16.5	23.3	19.8	6100
15/11/2005 10:30	22.4	31.2	22.2	5980	18/11/2005 10:48	16.8	23.6	19.6	6100
15/11/2005 10:36	22.5	31.4	22.4	5980	18/11/2005 10:54	18.1	24.6	19.7	6080
15/11/2005 10:42	22.6	31.5	22.6	5960	18/11/2005 11:00	18.5	24.8	19.8	6080
15/11/2005 10:48	22.8	31.7	22.8	5960	18/11/2005 11:06	18.6	25.1	19.9	6060
15/11/2005 10:54	22.9	31.8	23	5960	18/11/2005 11:12	18.8	25.2	20	6060
15/11/2005 11:00	23	32	23.2	5960	18/11/2005 11:18	19.1	25.3	20	6060
15/11/2005 11:06	23.2	32.2	23.4	5960	18/11/2005 11:24	19.1	25.4	20.1	6060
15/11/2005 11:12	23.3	32.3	23.5	5960	18/11/2005 11:30	19.1	25.3	20.1	6040
15/11/2005 11:18	23.3	32.3	23.7	5940	18/11/2005 11:36	19	25.3	20	6040
15/11/2005 11:24	23.4	32.4	23.8	5940	18/11/2005 11:42	19.5	25.6	20.1	6040
15/11/2005 11:30	23.3	32.4	24	5940	18/11/2005 11:48	19.8	25.8	20.3	6040
15/11/2005 11:36	23.4	32.5	24	5940	18/11/2005 11:54	21	26.1	20.5	6020

Experiment 52					Experiment 53				
Date/Time	Residuals Temp °C	Dry Bulb Temp °C	Wet Bulb Temp °C	Moisture Weight Loss (grams)	Date/Time	Residuals Temp °C	Dry Bulb Temp °C	Wet Bulb Temp °C	Moisture Weight Loss (grams)
23/11/2005 10:24	20.3	27.4	26.4	6100	26/11/2005 9:36	21.2	23.1	23.1	6280
23/11/2005 10:30	20.5	27.9	24	6100	26/11/2005 9:42	21.3	23.3	22.5	6280
23/11/2005 10:36	20.5	28.1	23.2	6040	26/11/2005 9:48	21.4	23.3	22.1	6260
23/11/2005 10:42	20.6	28.2	22.9	6040	26/11/2005 9:54	21.5	23.3	21.9	6240
23/11/2005 10:48	20.6	28.2	22.6	6020	26/11/2005 10:00	21.6	23.4	21.8	6240
23/11/2005 10:54	20.7	28.2	22.5	6020	26/11/2005 10:06	21.4	23.3	21.7	6220
23/11/2005 11:00	20.8	28.3	22.3	6020	26/11/2005 10:12	21.2	23.1	21.6	6220
23/11/2005 11:06	20.8	28.3	22.2	6000	26/11/2005 10:18	20.8	22.8	21.5	6220
23/11/2005 11:12	20.8	28.3	22.1	6000	26/11/2005 10:24	20.8	23	21.3	6220
23/11/2005 11:18	20.9	28.4	22.1	6000	26/11/2005 10:30	21	23.4	21.3	6220
23/11/2005 11:24	21	28.5	22	6000	26/11/2005 10:36	21.2	23.6	21.2	6220
23/11/2005 11:30	21.1	28.7	22	5980	26/11/2005 10:42	21.5	23.8	21.2	6220
23/11/2005 11:36	21.2	28.7	22	5980	26/11/2005 10:48	21.4	23.7	21.2	6220
23/11/2005 11:42	21.3	28.8	22	5980	26/11/2005 10:54	21.4	23.7	21.2	6200
23/11/2005 11:48	21.5	28.8	22	5980	26/11/2005 11:00	21.1	23.4	21.2	6200
23/11/2005 11:54	21.5	28.9	22	5980	26/11/2005 11:06	21.3	23.6	21.1	6200

Experiment 54					Experiment 55				
Date/Time	Residuals Temp °C	Dry Bulb Temp °C	Wet Bulb Temp °C	Moisture Weight Loss (grams)	Date/Time	Residuals Temp °C	Dry Bulb Temp °C	Wet Bulb Temp °C	Moisture Weight Loss (grams)
1/12/2005 10:36	21	23.5	23.1	6140	5/12/2005 12:00	24.4	29.7	28.3	9520
1/12/2005 10:42	21.7	25.9	23.5	6140	5/12/2005 12:06	24.3	29.6	27.6	9500
1/12/2005 10:48	22	26.5	22.3	6140	5/12/2005 12:12	24.5	29.8	27.4	9500
1/12/2005 10:54	22.2	26.7	22.3	6120	5/12/2005 12:18	24.5	29.8	27.3	9500
1/12/2005 11:00	22.3	27	22.4	6120	5/12/2005 12:24	24.7	29.8	27.1	9500
1/12/2005 11:06	22.5	27.1	22.5	6120	5/12/2005 12:30	24.8	30	27	9480
1/12/2005 11:12	22.6	27.3	22.6	6100	5/12/2005 12:36	25	30.1	27	9480
1/12/2005 11:18	22.8	27.5	22.7	6100	5/12/2005 12:42	25.1	30.1	27	9480
1/12/2005 11:24	23	27.7	22.8	6100	5/12/2005 12:48	25.2	30.2	26.9	9480
1/12/2005 11:30	23.1	27.9	23	6080	5/12/2005 12:54	25.2	30.3	26.9	9480
1/12/2005 11:36	23.3	28.1	23.1	6080	5/12/2005 13:00	25.3	30.3	26.8	9480
1/12/2005 11:42	23.4	28.2	23.3	6060	5/12/2005 13:06	25.3	30.4	26.8	9480
1/12/2005 11:48	23.6	28.4	23.4	6060	5/12/2005 13:12	25.5	30.5	26.8	9480
1/12/2005 11:54	23.7	28.5	23.6	6060	5/12/2005 13:18	25.5	30.6	26.8	9480
1/12/2005 12:00	23.8	28.7	23.7	6060	5/12/2005 13:24	25.4	30.6	26.8	9460
1/12/2005 12:06	23.9	28.8	23.8	6060	5/12/2005 13:30	25.3	30.6	26.8	9460

Experiment 56					Experiment 57				
Date/Time	Residuals Temp °C	Dry Bulb Temp °C	Wet Bulb Temp °C	Moisture Weight Loss (grams)	Date/Time	Residuals Temp °C	Dry Bulb Temp °C	Wet Bulb Temp °C	Moisture Weight Loss (grams)
19/12/2005 11:42	19.8	31.8	28.9	9680	28/12/2005 12:54	22.7	27.5	27.5	9300
19/12/2005 11:48	20.1	32.7	28.3	9660	28/12/2005 13:00	22.7	27.6	28.3	9300
19/12/2005 11:54	20.2	33	27.3	9640	28/12/2005 13:06	23	27.9	27.6	9300
19/12/2005 12:00	20.2	33.2	26.6	9640	28/12/2005 13:12	23.2	28	27.2	9280
19/12/2005 12:06	20.3	33.4	26.2	9640	28/12/2005 13:18	23.5	28.2	26.8	9280
19/12/2005 12:12	20.5	33.6	25.8	9620	28/12/2005 13:24	24.3	28.8	26.6	9280
19/12/2005 12:18	20.5	33.7	25.5	9620	28/12/2005 13:30	25.1	29.3	26.6	9280
19/12/2005 12:24	20.6	33.9	25.3	9620	28/12/2005 13:36	25.5	29.6	26.6	9280
19/12/2005 12:30	20.8	34	25.1	9620	28/12/2005 13:42	25.8	29.7	26.7	9280
19/12/2005 12:36	20.9	34.2	25	9620	28/12/2005 13:48	26	29.8	26.7	9280
19/12/2005 12:42	21	34.3	24.9	9600	28/12/2005 13:54	26.3	29.9	26.8	9280
19/12/2005 12:48	21.2	34.5	24.8	9600	28/12/2005 14:00	26.5	30	26.9	9280
19/12/2005 12:54	21.3	34.5	24.7	9600	28/12/2005 14:06	26.7	30	27	9260
19/12/2005 13:00	21.5	34.6	24.7	9600	28/12/2005 14:12	26.6	29.8	27	9260
19/12/2005 13:06	21.5	34.7	24.6	9600	28/12/2005 14:18	26.8	30	27.1	9260
19/12/2005 13:12	20.8	34.2	24.5	9580	28/12/2005 14:24	27	30.1	27.1	9260

Experiment 58					Experiment 59				
Date/Time	Residuals Temp °C	Dry Bulb Temp °C	Wet Bulb Temp °C	Moisture Weight Loss (grams)	Date/Time	Residuals Temp °C	Dry Bulb Temp °C	Wet Bulb Temp °C	Moisture Weight Loss (grams)
6/01/2006 11:06	22.1	28.2	25.4	9240	12/01/2006 12:00	22.2	26.4	26.2	8320
6/01/2006 11:12	21.6	28.5	22.9	9240	12/01/2006 12:06	22.3	26.6	25.8	8320
6/01/2006 11:18	21.6	28.7	22.9	9240	12/01/2006 12:12	22.3	26.7	25.3	8320
6/01/2006 11:24	21.5	28.9	22.8	9240	12/01/2006 12:18	22.4	26.7	24.9	8300
6/01/2006 11:30	21.5	29	22.8	9240	12/01/2006 12:24	22.5	26.8	24.6	8300
6/01/2006 11:36	21.4	29.2	22.7	9240	12/01/2006 12:30	22.5	26.8	24.5	8280
6/01/2006 11:42	21.4	29.3	22.7	9240	12/01/2006 12:36	22.6	26.9	24.3	8280
6/01/2006 11:48	21.4	29.4	22.7	9240	12/01/2006 12:42	22.7	27	24.2	8280
6/01/2006 11:54	21.4	29.4	22.7	9240	12/01/2006 12:48	22.7	26.9	24.1	8260
6/01/2006 12:00	21.4	29.5	22.7	9220	12/01/2006 12:54	22.8	27	24	8260
6/01/2006 12:06	21.4	29.5	22.7	9220	12/01/2006 13:00	22.9	27	24	8260
6/01/2006 12:12	21.5	29.6	22.8	9220	12/01/2006 13:06	23	27.1	24	8260
6/01/2006 12:18	21.5	29.6	22.8	9220	12/01/2006 13:12	23.1	27.1	24	8260
6/01/2006 12:24	21.5	29.7	22.8	9220	12/01/2006 13:18	23.1	27.2	23.9	8260
6/01/2006 12:30	21.5	29.8	22.8	9220	12/01/2006 13:24	23.1	27.1	24	8260
6/01/2006 12:36	21.6	30.2	22.9	9220	12/01/2006 13:30	23.2	27.2	23.9	8260

Experiment 60					Experiment 61				
Date/Time	Residuals Temp °C	Dry Bulb Temp °C	Wet Bulb Temp °C	Moisture Weight Loss (grams)	Date/Time	Residuals Temp °C	Dry Bulb Temp °C	Wet Bulb Temp °C	Moisture Weight Loss (grams)
23/01/2006 11:18	23.4	30.7	27.9	8320	14/03/2006 13:24	20.8	26.1	25.2	7420
23/01/2006 11:24	23.6	31	26	8320	14/03/2006 13:30	20.9	26.2	23.3	7420
23/01/2006 11:30	23.9	31.2	25.7	8320	14/03/2006 13:36	21	26.2	22.9	7420
23/01/2006 11:36	24.1	31.5	25.6	8300	14/03/2006 13:42	21	26.4	22.6	7400
23/01/2006 11:42	24.2	31.5	25.5	8300	14/03/2006 13:48	21	26.3	22.4	7400
23/01/2006 11:48	24.4	31.8	25.4	8300	14/03/2006 13:54	21	26.3	22.3	7400
23/01/2006 11:54	24.5	31.9	25.3	8280	14/03/2006 14:00	21	26.4	22.2	7380
23/01/2006 12:00	24.6	32	25.3	8280	14/03/2006 14:06	21	26.3	22.1	7380
23/01/2006 12:06	24.8	32.2	25.3	8280	14/03/2006 14:12	21	26.4	22	7380
23/01/2006 12:12	24.9	32.3	25.3	8280	14/03/2006 14:18	21	26.4	22	7380
23/01/2006 12:18	25	32.6	25.3	8260	14/03/2006 14:24	21	26.3	21.9	7360
23/01/2006 12:24	25.2	32.6	25.4	8260	14/03/2006 14:30	21.1	26.3	21.9	7360
23/01/2006 12:30	25.3	32.8	25.4	8260	14/03/2006 14:36	21.1	26.4	21.9	7360
23/01/2006 12:36	25.4	32.8	25.5	8260	14/03/2006 14:42	21.1	26.3	21.8	7360
23/01/2006 12:42	25.5	32.9	25.5	8260	14/03/2006 14:48	21.1	26.2	21.8	7360
23/01/2006 12:48	25.7	33	25.6	8260	14/03/2006 14:54	21.2	26.2	21.8	7360

Experiment 62					Experiment 63				
Date/Time	Residuals Temp °C	Dry Bulb Temp °C	Wet Bulb Temp °C	Moisture Weight Loss (grams)	Date/Time	Residuals Temp °C	Dry Bulb Temp °C	Wet Bulb Temp °C	Moisture Weight Loss (grams)
20/03/2006 8:48	19.8	24.5	24.3	5420	22/03/2006 10:30	19.7	22.6	21.8	4100
20/03/2006 8:54	19	24.7	24.5	5400	22/03/2006 10:36	18.8	22.7	21.7	4100
20/03/2006 9:00	19	24.8	23.5	5400	22/03/2006 10:42	18.9	22.7	20.9	4100
20/03/2006 9:06	19	24.7	22.8	5360	22/03/2006 10:48	18.9	22.8	20.4	4100
20/03/2006 9:12	19	24.7	22.2	5360	22/03/2006 10:54	18.9	22.9	20	4080
20/03/2006 9:18	19	24.6	21.8	5340	22/03/2006 11:00	18.9	22.8	19.7	4080
20/03/2006 9:24	19	24.7	21.4	5340	22/03/2006 11:06	18.9	22.9	19.5	4080
20/03/2006 9:30	19	24.6	21.1	5340	22/03/2006 11:12	19	22.9	19.4	4080
20/03/2006 9:36	19	24.6	20.9	5340	22/03/2006 11:18	19	23	19.3	4060
20/03/2006 9:42	19	24.5	20.7	5320	22/03/2006 11:24	19	23	19.2	4060
20/03/2006 9:48	19	24.6	20.5	5320	22/03/2006 11:30	19	23.1	19.2	4060
20/03/2006 9:54	19	24.5	20.3	5320	22/03/2006 11:36	19	23.1	19.2	4060
20/03/2006 10:00	19	24.5	20.2	5320	22/03/2006 11:42	19	23.1	19.2	4040
20/03/2006 10:06	19	24.6	20.1	5320	22/03/2006 11:48	19	23.2	19.2	4040
20/03/2006 10:12	19	24.5	20	5300	22/03/2006 11:54	19.1	23.3	19.2	4020
20/03/2006 10:18	18.9	24.5	20	5300	22/03/2006 12:00	19.2	23.4	19.2	4020

Appendix B: Open and Solar Drying Beds Experiments

Experiment 4									
Date/Time	RH Hourly %	Air Temp Hourly °C	Solar Bed Glass Cover Temp °C	Open Bed Residuals Temp °C	Rain (6 min) mm	Rain Daily mm	Wind Speed Hourly (km/h)	Solar Radiation (KJ/m ²)	Solar Radiation Daily Total (MJ/m ²)
7/07/1999 8:48			22.6	14.6					
7/07/1999 8:54			24.8	15.3					
7/07/1999 9:00	62	14.2	23.3	15.6			3	70	9
7/07/1999 9:06			23.8	16.1					
7/07/1999 9:12			24.2	16.5					
7/07/1999 9:18			22.9	16.7					
7/07/1999 9:24			20.8	16.6					
7/07/1999 9:30			19.5	16.5					

Experiment 5									
Date/Time	RH Hourly %	Air Temp Hourly °C	Solar Bed Glass Cover Temp °C	Open Bed Residuals Temp °C	Rain (6 min) mm	Rain Daily mm	Wind Speed Hourly (km/h)	Solar Radiation (KJ/m²)	Solar Radiation Daily Total (MJ/m²)
31/07/1999 8:48			26.7	21.5					
31/07/1999 8:54			26.1	21.9					
31/07/1999 9:00	57	13.6	26.3	21.9			12	90	8
31/07/1999 9:06			25.7	22.3					
31/07/1999 9:12			26.6	23.4					
31/07/1999 9:18			27	24.5					
31/07/1999 9:24			26.8	25.4					
31/07/1999 9:30			27.5	26.1					
Experiment 6									
Date/Time	RH Hourly %	Air Temp Hourly °C	Solar Bed Glass Cover Temp °C	Open Bed Residuals Temp °C	Rain (6 min) mm	Rain Daily mm	Wind Speed Hourly (km/h)	Solar Radiation (KJ/m²)	Solar Radiation Daily Total (MJ/m²)
24/08/1999 8:24			19.6	14.2					
24/08/1999 8:30			22.6	14.7					
24/08/1999 8:36			25.1	15.1					
24/08/1999 8:42			27.5	15.5					
24/08/1999 8:48			27.2	15.8					
24/08/1999 8:54			28.8	16.3					
24/08/1999 9:00	78	15.6	30.7	16.9			4	110	9.5
24/08/1999 9:06			32.5	17.6					

Experiment 7									
Date/Time	RH Hourly %	Air Temp Hourly °C	Solar Bed Glass Cover Temp °C	Open Bed Residuals Temp °C	Rain (6 min) mm	Rain Daily mm	Wind Speed Hourly (km/h)	Solar Radiation (KJ/m²)	Solar Radiation Daily Total (MJ/m²)
17/09/1999 0:42			15.1	17.1					
17/09/1999 0:48			15.1	17.1	0.2				
17/09/1999 0:54			15	16.9	0.2				
17/09/1999 1:00	84	16	14.8	16.7	0.2		26		
17/09/1999 1:06			14.6	16.6	0.4				
17/09/1999 1:12			14.5	16.5	0.4				
17/09/1999 1:18			14.6	16.4					
17/09/1999 1:24			14.6	16.4					

Experiment 8									
Date/Time	RH Hourly %	Air Temp Hourly °C	Solar Bed Glass Cover Temp °C	Open Bed Residuals Temp °C	Rain (6 min) mm	Rain Daily mm	Wind Speed Hourly (km/h)	Solar Radiation (KJ/m²)	Solar Radiation Daily Total (MJ/m²)
3/10/1999 8:30			16.6	17.5	0.2				
3/10/1999 8:36			16.6	17.5	0.2				
3/10/1999 8:42			16.6	17.5					
3/10/1999 8:48			16.9	17.5	0.2				
3/10/1999 8:54			17.6	17.8	0.2				
3/10/1999 9:00	100	16.6	17.9	18	0.2	4.2		20	13.1
3/10/1999 9:06			18.1	18.1					
3/10/1999 9:12			18.3	18.4	0.2				

Experiment 9									
Date/Time	RH Hourly %	Air Temp Hourly °C	Solar Bed Glass Cover Temp °C	Open Bed Residuals Temp °C	Rain (6 min) mm	Rain Daily mm	Wind Speed Hourly (km/h)	Solar Radiation (KJ/m²)	Solar Radiation Daily Total (MJ/m²)
27/10/1999 8:18			28.5	24.7					
27/10/1999 8:24			29.7	25					
27/10/1999 8:30			31	25.7					
27/10/1999 8:36			30.5	26.2					
27/10/1999 8:42			32.1	26.8					
27/10/1999 8:48			30.9	27.5					
27/10/1999 8:54			30.9	28.3					
27/10/1999 9:00	46	20.9	32	29.1				210	15.4

Experiment 10									
Date/Time	RH Hourly %	Air Temp Hourly °C	Solar Bed Glass Cover Temp °C	Open Bed Residuals Temp °C	Rain (6 min) mm	Rain Daily mm	Wind Speed Hourly (km/h)	Solar Radiation (KJ/m²)	Solar Radiation Daily Total (MJ/m²)
16/11/1999 0:48			17	21.4					
16/11/1999 0:54			17	21.3					
16/11/1999 1:00	70	16.6	16.9	21.3			3		
16/11/1999 1:06			16.8	21.2					
16/11/1999 1:12			16.8	21.1					
16/11/1999 1:18			16.8	21.1					
16/11/1999 1:24			16.8	21					
16/11/1999 1:30			16.8	20.9					

Experiment 11										
Date/Time	RH Hourly %	Air Temp °C	Cavity Temp (Solar Bed) °C	Residuals Temp (Solar Bed) °C	Rain (6 min) mm	Rain Daily mm	Wind Hourly (km/h)	Radiation Sample Hourly (KJ/m²)	Radiation Daily Total (MJ/m²)	Residuals Temp (Open Bed) °C
7/03/2000 10:42		21.7	21.9	22.4						22.5
7/03/2000 10:48		21.8	22	22.5						22.5
7/03/2000 10:54		21.9	22.3	23						22.9
7/03/2000 11:00	83	22.1	22.5	23.3			10	100		23.2
7/03/2000 11:06		22.1	22.6	23.6						23.4
7/03/2000 11:12		22.3	22.8	24						23.6
7/03/2000 11:18		22.6	23.3	25.1						24.5
Experiment 12										
Date/Time	RH Hourly %	Air Temp °C	Cavity Temp (Solar Bed) °C	Residuals Temp (Solar Bed) °C	Rain (6 min) mm	Rain Daily mm	Wind Hourly (km/h)	Radiation Sample Hourly (KJ/m²)	Radiation Daily Total (MJ/m²)	Residuals Temp (Open Bed) °C
13/04/2000 8:48		18.1	24.1	20						16.7
13/04/2000 8:54		18.3	25	20.2						17
13/04/2000 9:00	100	18.6	26	20.6		0.2		100	8.1	17.2
13/04/2000 9:06		19	27.3	21.1						17.5
13/04/2000 9:12		19.4	29.1	21.7						17.8
13/04/2000 9:18		19.9	29.5	22.1						18.1
13/04/2000 9:24		20	29.2	22.5						18.4

Experiment 13										
Date/Time	RH Hourly %	Air Temp °C	Cavity Temp (Solar Bed) °C	Residuals Temp (Solar Bed) °C	Rain (6 min) mm	Rain Daily mm	Wind Hourly (km/h)	Radiation Sample Hourly (KJ/m²)	Radiation Daily Total (MJ/m²)	Residuals Temp (Open Bed) °C
13/06/2000 18:42	93	11	9.1	12.5						10.1
13/06/2000 18:48		10.6	8.6	12.3						9.9
13/06/2000 18:54		10.1	8.2	12.1						9.7
13/06/2000 19:00		9.7	7.8	11.9			1			9.5
13/06/2000 19:06		9.6	7.7	11.7						9.3
13/06/2000 19:12		9.4	7.5	11.6						9.1
13/06/2000 19:18		9.6	7.4	11.5						9
Experiment 14										
Date/Time	RH Hourly %	Air Temp °C	Cavity Temp (Solar Bed) °C	Residuals Temp (Solar Bed) °C	Rain (6 min) mm	Rain Daily mm	Wind Hourly (km/h)	Radiation Sample Hourly (KJ/m²)	Radiation Daily Total (MJ/m²)	Residuals Temp (Open Bed) °C
14/07/2000 9:00	62	13.5	16.7	14.5			4	90	8.4	11.1
14/07/2000 9:06		13.7	30.1	15.5						11.5
14/07/2000 9:12		13.8	35.3	16.5						11.7
14/07/2000 9:18		14	38.1	17.1						12.1
14/07/2000 9:24		14	39.8	17.7						12.3
14/07/2000 9:30		14.1	40.5	18.1						12.3
14/07/2000 9:36		14.4	40.1	18.4						12.1

Experiment 15										
Date/Time	RH Hourly %	Air Temp °C	Cavity Temp (Solar Bed) °C	Residuals Temp (Solar Bed) °C	Rain (6 min) mm	Rain Daily mm	Wind Hourly (km/h)	Radiation Sample Hourly (KJ/m²)	Radiation Daily Total (MJ/m²)	Residuals Temp (Open Bed) °C
11/08/2000 3:36		9.7								7.9
11/08/2000 3:42		9.6								7.8
11/08/2000 3:48		9.5								7.8
11/08/2000 3:54		9.8								7.8
11/08/2000 4:00	60	9.8					14			7.8
11/08/2000 4:06		9.9								7.8
11/08/2000 4:12		10								7.8
Experiment 16										
Date/Time	RH Hourly %	Air Temp °C	Cavity Temp (Solar Bed) °C	Residuals Temp (Solar Bed) °C	Rain (6 min) mm	Rain Daily mm	Wind Hourly (km/h)	Radiation Sample Hourly (KJ/m²)	Radiation Daily Total (MJ/m²)	Residuals Temp (Open Bed) °C
19/09/2000 9:00	45	19.8					5	150	16.1	16.2
19/09/2000 9:06		20.3								16.4
19/09/2000 9:12		20.1								16.8
19/09/2000 9:18		20.3								17.2
19/09/2000 9:24		20.7								17.5
19/09/2000 9:30		20.9								17.9
19/09/2000 9:36		21.1								18.2

Experiment 17										
Date/Time	RH Hourly %	Air Temp °C	Cavity Temp (Solar Bed) °C	Residuals Temp (Solar Bed) °C	Rain (6 min) mm	Rain Daily mm	Wind Hourly (km/h)	Radiation Sample Hourly (KJ/m²)	Radiation Daily Total (MJ/m²)	Residuals Temp (Open Bed) °C
9/11/2000 22:54		17.5	16.7	17						15.2
9/11/2000 23:00	78	17.4	16.6	17			5			15.2
9/11/2000 23:06		17.4	16.6	17						15.1
9/11/2000 23:12		17.4	16.6	17						15.1
9/11/2000 23:18		17.5	16.7	17						15.2
9/11/2000 23:24		17.3	16.6	17.2						15.1
9/11/2000 23:30		16.8	16.3	17.1						15
Experiment 18										
Date/Time	RH Hourly %	Air Temp °C	Cavity Temp (Solar Bed) °C	Residuals Temp (Solar Bed) °C	Rain (6 min) mm	Rain Daily mm	Wind Hourly (km/h)	Radiation Sample Hourly (KJ/m²)	Radiation Daily Total (MJ/m²)	Residuals Temp (Open Bed) °C
3/01/2001 9:42		29.4	35.2	37						30.1
3/01/2001 9:48		29.2	35	37.8						29.8
3/01/2001 9:54		29.5	35.6	38.5						30.2
3/01/2001 10:00	59	29.8	35.7	38.8			11	220		30.4
3/01/2001 10:06		29.6	35.7	39.3						30.4
3/01/2001 10:12		29.4	35.6	39.6						30.3
3/01/2001 10:18		30.2	36.8	40.1						31.3

Experiment 19										
Date/Time	RH Hourly %	Air Temp °C	Cavity Temp (Solar Bed) °C	Residuals Temp (Solar Bed) °C	Rain (6 min) mm	Rain Daily mm	Wind Hourly (km/h)	Radiation Sample Hourly (KJ/m²)	Radiation Daily Total (MJ/m²)	Residuals Temp (Open Bed) °C
13/02/2001 10:30		31.7	34.5	31.2						28.4
13/02/2001 10:36		31.9	32.5	31						24.9
13/02/2001 10:42		32.9	34	33						26.1
13/02/2001 10:48		33.1	35.6	36.4						27.4
13/02/2001 10:54		32.9	36	37.2						27.1
13/02/2001 11:00	64	33.1	37.3	38.2			5	230		29.7
13/02/2001 11:06		33.7	37.1	38.6						35.2
Experiment 20										
Date/Time	RH Hourly %	Air Temp °C	Cavity Temp (Solar Bed) °C	Residuals Temp (Solar Bed) °C	Rain (6 min) mm	Rain Daily mm	Wind Hourly (km/h)	Radiation Sample Hourly (KJ/m²)	Radiation Daily Total (MJ/m²)	Residuals Temp (Open Bed) °C
30/03/2001 5:42		15.6	15	16.6	1.4					15.8
30/03/2001 5:48		15.5	15	16.6	0.6					15.8
30/03/2001 5:54		15.5	15	16.6	0.2					15.7
30/03/2001 6:00	100	15.5	15	16.6			3			15.8
30/03/2001 6:06		15.5	15	16.6						15.7
30/03/2001 6:12		15.7	15.1	16.6						15.7
30/03/2001 6:18		15.7	15.2	16.5	0.2					15.7

Appendix C: Field Experiments (Under Perspex Cover) and without Drainage

Experiment 20E								
Date/Time	RH Hourly %	Air Temp °C	Rain (6 min) mm	Rain Daily mm	Wind Hourly (km/h)	Radiation Sample Hourly (KJ/m ²)	Radiation Daily Total (MJ/m ²)	Residuals Temp °C
2/03/2002 8:54		22.3						21.2
2/03/2002 9:00	73	22.9			3	130	16.2	21.5
2/03/2002 9:06		23.1						21.8
2/03/2002 9:12		23						22
2/03/2002 9:18		22.4						22
2/03/2002 9:24		22.1						21.9
2/03/2002 9:30		22.1						21.7
2/03/2002 9:36		22.7						21.8

Experiment 20F1								
Date/Time	RH Hourly %	Air Temp °C	Rain (6 min) mm	Rain Daily mm	Wind Hourly (km/h)	Radiation Sample Hourly (KJ/m²)	Radiation Daily Total (MJ/m²)	Residuals Temp °C
22/03/2002 11:42		19.7						19
22/03/2002 11:48		19.8						19
22/03/2002 11:54		19.9						19
22/03/2002 12:00	72	19.8			3	40		19
22/03/2002 12:06		19.8						19
22/03/2002 12:12		19.7						18.9
22/03/2002 12:18		19.9						19
22/03/2002 12:24		21.5						19
Experiment 20F2								
Date/Time	RH Hourly %	Air Temp °C	Rain (6 min) mm	Rain Daily mm	Wind Hourly (km/h)	Radiation Sample Hourly (KJ/m²)	Radiation Daily Total (MJ/m²)	Residuals Temp °C
22/03/2002 8:54		20.1						17.4
22/03/2002 9:00	77	20		12.6	6	160	4.3	17.8
22/03/2002 9:06		20						18.1
22/03/2002 9:12		19.8						18.4
22/03/2002 9:18		19.6						18.5
22/03/2002 9:24		19.4						18.6
22/03/2002 9:30		19.4						18.7
22/03/2002 9:36		19.5						18.8

Experiment 20K

Date/Time	RH Hourly %	Air Temp °C	Rain (6 min) mm	Rain Daily mm	Wind Hourly (km/h)	Radiation Sample Hourly (KJ/m²)	Radiation Daily Total (MJ/m²)	Residuals Temp °C
23/10/2002 6:00	47	21.3				10		19.8
23/10/2002 6:06		19.9						18.8
23/10/2002 6:12		19						18.4
23/10/2002 6:18		18.8						18.2
23/10/2002 6:24		18.8						18.3
23/10/2002 6:30		19.1						18.6
23/10/2002 6:36		19						18.1
23/10/2002 6:42		18.9						18.1